

AD 687324

AD

USAAVLABS TECHNICAL REPORT 68-46

**PASSIVE HELICOPTER ROTOR ISOLATION
USING THE KAMAN DYNAMIC ANTIRESONANT
VIBRATION ISOLATOR (DAVI)**

By

Erich P. Schuett

December 1968



**U. S. ARMY AVIATION MATERIEL LABORATORIES
FORT EUSTIS, VIRGINIA**

**CONTRACT DA 44-177-AMC-420(T)
KAMAN AIRCRAFT
DIVISION OF KAMAN CORPORATION
BLOOMFIELD, CONNECTICUT**

*This document has been approved
for public release and sale; its
distribution is unlimited.*



Reproduced by the
CLEARINGHOUSE
for Federal Scientific & Technical
Information Springfield Va 22151

176



DEPARTMENT OF THE ARMY
U. S. ARMY AVIATION MATERIEL LABORATORIES
FORT EUSTIS, VIRGINIA 23604

This contract was initiated to assess the feasibility of helicopter rotor isolation using the Dynamic Antiresonant Vibration Isolator (DAVI). Feasibility of rotor isolation was demonstrated for "statistical" helicopters ranging from 2,000 pounds to 100,000 pounds as well as for a 20,000-pound compound helicopter with an operational rotor speed range of 15 percent. The DAVI, a very simple passive mechanical isolator, exhibits high static stiffness while simultaneously offering an antiresonant frequency which may be tuned to be coincident with the η/rev frequency of excitation, where η is the number of rotor blades. Effective isolation is predicted for all three translational and rotational directions, with the associated weight penalty varying from .33 percent to 1.61 percent of aircraft gross weight for the configurations considered.

This report has been reviewed by the U. S. Army Aviation Materiel Laboratories and is considered to be technically sound.

Task 1F125901A13903
Contract DA 44-177-AMC-420(T)
USAAVLABS Technical Report 68-46
December 1968

PASSIVE HELICOPTER ROTOR ISOLATION
USING THE KAMAN DYNAMIC ANTIRESONANT
VIBRATION ISOLATOR (DAVI)

Final Report

Kaman Aircraft Report No. R-710

By

Erich P. Schuett

Prepared by

Kaman Aircraft
Division of Kaman Corporation
Bloomfield, Connecticut

For

U. S. ARMY AVIATION MATERIEL LABORATORIES
FORT EUSTIS, VIRGINIA

This document has been approved
for public release and sale; its
distribution is unlimited.

ABSTRACT

This report contains the analysis and results of a study to determine the feasibility of rotor isolation employing the Dynamic Antiresonant Vibration Isolator (DAVI).

The theoretical analysis was conducted employing a two-dimensional DAVI for lateral and vertical isolation with conventional isolation in the longitudinal direction. Steady-state and transient inputs were analyzed. The steady-state analysis includes all six degrees of freedom of the upper body and of the lower isolated body of the helicopter.

Statistical data and excitation frequency criteria were established to study the effects and to determine the feasibility of rotor isolation for a range of statistical aircraft ranging from 2000 pounds to 100,000 pounds. Also discussed are the effects of rotor isolation on control motions, crash loads, mechanical instability, and system reliability.

Results of this feasibility study show that rotor isolation employing the DAVI is feasible. Isolation is feasible at the predominant frequency (N/rev) and all its multiples up to $4N/\text{rev}$. Low static deflection and a minimum weight penalty are some of the features of the DAVI system.

FOREWORD

This research program for the study of a helicopter rotor/transmission isolation system was performed by Kaman Aircraft, Division of Kaman Corporation, Bloomfield, Connecticut, under Contract DA 44-177-AMC-420(T) for the U. S. Army Aviation Materiel Laboratories (USAAVLABS), Fort Eustis, Virginia

The program was conducted under the technical direction of Mr. J. McGarvey, Contracting Officer's Representative, USAAVLABS.

Principal Kaman personnel in this program were Messrs. E. Schuett, Project Engineer; W. G. Flannelly, Assistant Chief of Vibrations Research and the inventor of the Dynamic Antiresonant Vibration Isolator (DAVI); R. C. Anderson, Research Engineer; and R. Metzger, Research Technician. The work was done under the direction of Mr. R. Jones, Chief of Vibrations Research. Mr. A. Berman, Chief of Engineering Analysis, with his staff was responsible for the programming effort.

TABLE OF CONTENTS

	<u>Page</u>
ABSTRACT.	iii
FOREWORD.	v
LIST OF ILLUSTRATIONS	viii
LIST OF TABLES.	xv
LIST OF SYMBOLS	xvii
INTRODUCTION.	1
THE PROBLEM.	1
THE PROPOSED SOLUTION.	1
THEORETICAL ANALYSIS.	3
STEADY-STATE EQUATIONS	3
CONFIGURATIONS	13
ROTOR ISOLATION OF HELICOPTER.	26
ROTOR ISOLATION OF COMPOUND HELICOPTERS.	61
TRANSIENT EQUATIONS.	69
MECHANICAL INSTABILITY.	88
CRASH LOADS	90
CONTROL MOTIONS	91
MISALIGNMENT CONSIDERATIONS AND ROTOR RESPONSES	92
RELIABILITY ANALYSIS.	93
ASSUMPTIONS AND DEFINITIONS.	93
FAILURE MODES AND EFFECTS ANALYSIS	95
RELIABILITY ANALYSIS	97
CONCLUSIONS	99
RECOMMENDATIONS	101
REFERENCES CITED.	102
APPENDIX - STATISTICAL DATA	105
DISTRIBUTION.	154

LIST OF ILLUSTRATIONS

<u>Figure</u>		<u>Page</u>
1	Diagram of Two-Body System.	4
2	DAVI Schematic.	5
3	12-X-12 Two-Body Solution Matrix.	8
4	Diagram of Rigid-Body System.	9
5	6-X-6 Rigid Body Solution Matrix.	10
6	Variation of DAVI Weight With Static Deflection for Four-Bladed, 2300-Pound Helicopter.	15
7	Vertical Effectivity at N/rev Versus Vertical Distance From DAVI Isolator to Upper-Body Center of Gravity for Case 20 HS.	30
8	Vertical Effectivity at N/rev Versus Horizontal Distance From Upper-Body Center of Gravity to Rigid-Body Center of Gravity for Case 20 HS . . .	31
9	Vertical Effectivity for Case 1 HS Versus Frequency	36
10	Lateral Effectivity for Case 1 HS Versus Frequency	37
11	Roll Effectivity for Case 1 HS Versus Frequency	38
12	Longitudinal Effectivity for Case 1 HS Versus Frequency.	39
13	Pitch Effectivity for Case 1 HS Versus Frequency	40
14	Vertical Effectivity for Case 12 HS Versus Frequency	41
15	Lateral Effectivity for Case 12 HS Versus Frequency	42
16	Roll Effectivity for Case 12 HS Versus Frequency	43
17	Longitudinal Effectivity for Case 12 HS Versus Frequency.	44

LIST OF ILLUSTRATIONS (Continued)

<u>Figure</u>		<u>Page</u>
18	Pitch Effectivity for Case 12 HS Versus Frequency	45
19	Vertical Effectivity for Case 14 HS Versus Frequency	48
20	Lateral Effectivity for Case 14 HS Versus Frequency	49
21	Roll Effectivity for Case 14 HS Versus Frequency	50
22	Longitudinal Effectivity for Case 14 HS Versus Frequency.	51
23	Pitch Effectivity for Case 14 HS Versus Frequency	52
24	Vertical Effectivity for Case 25 HS Versus Frequency.	53
25	Lateral Effectivity for Case 25 HS Versus Frequency.	54
26	Roll Effectivity for Case 25 HS Versus Frequency	55
27	Longitudinal Effectivity for Case 25 HS Versus Frequency.	56
28	Pitch Effectivity for Case 25 HS Versus Frequency	57
29	Vertical Effectivity at the Tuned Frequency for Several Damping Rates for Case 14 HS Versus Frequency.	58
30	Change in Vertical Effectivity at Tuned Frequency Versus Change in Lower Body Mass for Case 4 HS.	59
31	Vertical Effectivities at the Tuned Frequency for Several DAVI Arrangements for Case 17 HS.	60

LIST OF ILLUSTRATIONS (Continued)

<u>Figure</u>		<u>Page</u>
32	Vertical Effectivity for the Compound Helicopter for Case 28 CS Versus Frequency. . .	64
33	Longitudinal Effectivity for the Compound Helicopter for Case 28 CS Versus Frequency. . .	65
34	Pitch Effectivity for the Compound Helicopter for Case 28 CS Versus Frequency	66
35	Roll Effectivity for the Compound Helicopter for Case 28 CS Versus Frequency	67
36	Lateral Effectivity for the Compound Helicopter for Case 28 CS Versus Frequency	68
37	Schematic of DAVI Installation for Transient Analysis.	69
38	Transient Deflection Envelope for a 1-Second $\frac{1}{2} \sin^2$ Input for Case 38 CT Versus Time. . . .	74
39	Transient Deflection Envelope for a 1-Second Ramp Input for Case 38 CT Versus Time	75
40	Transient Deflection Envelope for a 0.8-Second $\frac{1}{2} \sin^2$ Input for Case 38 CT Versus Time. . . .	76
41	Transient Deflection Envelope for a 0.8-Second Ramp Input for Case 38 CT Versus Time	77
42	Transient Response to a $-0.5 \text{ g } \frac{1}{2} \sin^2$, 0.6-Second Input for Case 38 CT Versus Time . .	78
43	Transient Response to a $3.0 \text{ g } \frac{1}{2} \sin^2$, 0.6-Second Input for Case 38 CT Versus Time . .	79
44	Transient Response Envelope for a 0.6-Second Ramp Input for Case 38 CT Versus Time	80
45	Transient Response to a $3.0 \text{ g } \frac{1}{2} \sin^2$, 1.0-Second Input for Case 34 HT Versus Time . .	81
46	Transient Response to a $-0.5 \text{ g } \frac{1}{2} \sin^2$, 1.0-Second Input for Case 34 HT Versus Time . .	82

LIST OF ILLUSTRATIONS (Continued)

<u>Figure</u>		<u>Page</u>
47	Transient Response Envelope for a 1.0-Second Ramp Input for Case 34 HT Versus Time.	83
48	Transient Response Envelope for a 0.8-Second $\frac{1}{2} \sin^2$ Input for Case 34 HT Versus Time	84
49	Transient Response Envelope for a 0.8-Second Ramp Input for Case 34 HT Versus Time.	85
50	Transient Response Envelope for a 0.6-Second $\frac{1}{2} \sin^2$ Input for Case 34 HT Versus Time	86
51	Transient Response Envelope for a 0.6-Second Ramp Input for Case 34 HT Versus Time.	87
52	Two-Dimensional DAVI	94
53	Statistical Rotor RPM for a Range of Helicopter Gross Weights	108
54	Statistical Rotor Weights for a Range of Helicopter Gross Weights	109
55	Statistical Rotor-Transmission Weights for a Range of Helicopter Gross Weights.	110
56	Statistical Rotor-Engine-Transmission Weights for a Range of Helicopter Cross Weights.	111
57	Statistical Roll Inertia of Rotor Plus Transmission Upper Body for a Range of Helicopter Gross Weights	112
58	Statistical Pitch Inertia of Rotor Plus Transmission Upper Body for a Range of Helicopter Gross Weights	113
59	Statistical Yaw Inertia of Rotor Plus Transmission Upper Body for a Range of Helicopter Gross Weights	114
60	Statistical Roll Inertia of Rotor Plus Engine Plus Transmission Upper Body for a Range of Helicopter Gross Weights	115

LIST OF ILLUSTRATIONS (Continued)

<u>Figure</u>		<u>Page</u>
61	Statistical Pitch Inertia of Rotor Plus Engine Plus Transmission Upper Body for a Range of Helicopter Gross Weights.	116
62	Statistical Yaw Inertia of Rotor Plus Engine Plus Transmission Upper Body for a Range of Helicopter Gross Weights.	117
63	Statistical Roll Inertia of Helicopter for a Range of Helicopter Gross Weights	118
64	Statistical Pitch Inertia of Helicopter for a Range of Helicopter Gross Weights	119
65	Statistical Yaw Inertia of Helicopter for a Range of Helicopter Gross Weights	120
66	Compound Helicopter Rotor RPM Versus a Range of Compound Helicopter Gross Weights.	122
67	Compound Helicopter Rotor Plus Transmission Upper Body Weight Versus a Range of Compound Helicopter Gross Weights.	123
68	Compound Helicopter Rotor Plus Engine Plus Transmission Upper Body Weight Versus Compound Helicopter Gross Weight	124
69	Roll Inertia of Compound Helicopter Rotor Plus Transmission Upper Body for a Range of Compound Helicopter Gross Weights.	125
70	Pitch Inertia of Compound Helicopter Rotor Plus Transmission Upper Body for a Range of Compound Helicopter Gross Weights	126
71	Yaw Inertia of Compound Helicopter Rotor Plus Transmission Upper Body for a Range of Compound Helicopter Gross Weights.	127
72	Roll Inertia of Compound Helicopter Rotor Plus Engine Plus Transmission Upper Body for a Range of Gross Weights.	128

LIST OF ILLUSTRATIONS (Continued)

<u>Figure</u>		<u>Page</u>
73	Pitch Inertia of Compound Helicopter Rotor Plus Engine Plus Transmission Upper Body for a Range of Gross Weights.	129
74	Yaw Inertia of Compound Helicopter Rotor Plus Engine Plus Transmission Upper Body for a Range of Gross Weights.	130
75	Roll Inertia of Compound Helicopter for a Range of Gross Weights.	131
76	Pitch Inertia of Compound Helicopter for a Range of Gross Weights.	132
77	Yaw Inertia of Compound Helicopter for a Range of Gross Weights.	133
78	General Location of Centers of Gravity and Point of Excitation	134
79	Vertical Distance From Vehicle Center of Gravity to Upper Body Center of Gravity and Point of Excitation for a Range of Gross Weights	137
80	Longitudinal Distance From Vehicle Center of Gravity to Upper Body Center of Gravity for a Range of Gross Weights.	137
81	Roll Inertia of Lower Body for Rotor Plus Transmission Configuration for a Range of Helicopter Gross Weights.	138
82	Pitch Inertia of Lower Body for Rotor Plus Transmission Configuration for a Range of Helicopter Gross Weights.	139
83	Yaw Inertia of Lower Body for Rotor Plus Transmission Configuration for a Range of Helicopter Gross Weights.	140
84	Roll Inertia of Lower Body for Rotor Plus Engine Plus Transmission Configuration for a Range of Helicopter Gross Weights	141

LIST OF ILLUSTRATIONS (Continued)

<u>Figure</u>		<u>Page</u>
85	Pitch Inertia of Lower Body for Rotor Plus Engine Plus Transmission Configuration for a Range of Helicopter Gross Weights.	142
86	Yaw Inertia of Lower Body for Rotor Plus Engine Plus Transmission Configuration for a Range of Helicopter Gross Weights.	143
87	Roll Inertia of Lower Body for Rotor Plus Transmission Configuration for a Range of Compound Helicopter Gross Weights.	144
88	Pitch Inertia of Lower Body for Rotor Plus Engine Configuration for a Range of Compound Helicopter Gross Weights	145
89	Yaw Inertia of Lower Body for Rotor Plus Transmission Configuration for a Range of Compound Helicopter Gross Weights.	146
90	Roll Inertia of Lower Body for Rotor Plus Engine Plus Transmission Configuration for a Range of Compound Helicopter Gross Weights.	147
91	Pitch Inertia of Lower Body for Rotor Plus Engine Plus Transmission Configuration for a Range of Compound Helicopter Gross Weights	148
92	Yaw Inertia of Lower Body for Rotor Plus Engine Plus Transmission Configuration for a Range of Compound Helicopter Gross Weights.	149
93	Normalized Excitation Criteria	153

LIST OF TABLES

<u>Table</u>		<u>Page</u>
I	CASE AND CONFIGURATION IDENTIFICATION.	16
II	DAVI DESIGN DETAILS AND STATIC DEFLECTION VERSUS CONFIGURATIONS.	17
III	VERTICAL LOCATION OF ISOLATORS FOR FOUR-DAVI INSTALLATION	18
IV	LONGITUDINAL LOCATION OF ISOLATORS FOR FOUR- DAVI INSTALLATION.	19
V	LATERAL LOCATION OF ISOLATORS FOR FOUR-DAVI INSTALLATION	20
VI	LOCATION OF POINT OF EXCITATION FOR ALL CONFIGURATIONS	21
VII	SUMMARY OF GROSS WEIGHT, MASS, AND PREDOMINANT FREQUENCIES VERSUS CONFIGURATIONS.	22
VIII	SUMMARY OF AIRCRAFT AND UPPER BODY INERTIA VERSUS CONFIGURATION	23
IX	VARIATION OF DAVI WEIGHT WITH STATIC DEFLECTION	24
X	NATURAL FREQUENCIES OF COUPLED DAVI ROTOR ISOLATION SYSTEM	25
XI	EFFECTIVITY AT 1/REV	27
XII	EFFECTIVITY AT N/REV	28
XIII	EFFECTIVITY AT 2N/REV.	32
XIV	EFFECTIVITY AT 3N/REV.	33
XV	EFFECTIVITY AT 4N/REV.	34
XVI	NORMALIZED ACCELERATION FOR THE VERTICAL EXCITATION ONLY.	35

LIST OF TABLES (Continued)

<u>Table</u>		<u>Page</u>
XVII	RANGE EFFECTIVITIES FOR THE VARIOUS COMPOUND HELICOPTER CONFIGURATIONS.	62
XVIII	ANTIRESONANT EFFECTIVITIES AT N/REV FOR THE COMPOUND HELICOPTER CASES	63
XIX	NORMALIZED ACCELERATION FOR COMPOUND HELICOPTER (VERTICAL ONLY).	63
XX	SUMMARY OF STEADY AND VIBRATORY TRANSIENT DEFLECTIONS FOR A $1/2 \sin^2$ INPUT.	72
XXI	SUMMARY OF STEADY AND VIBRATORY TRANSIENT DEFLECTIONS FOR A RAMP INPUT.	72
XXII	SUMMARY OF MAXIMUM STEADY DEFLECTIONS AND PITCHING MOTIONS FOR A $1/2 \sin^2$ AND RAMP INPUT	73
XXIII	CENTERS OF MECHANICAL INSTABILITY	89
XXIV	FAILURE MODES AND EFFECTS ANALYSIS.	96
XXV	EFFECTS SUMMARY	98
XXVI	EXCITATION CRITERIA NORMALIZED ON N-HARMONIC.	152

LIST OF SYMBOLS

a	Distance from the center of the hub to the lag hinge
A_i	$K_{\theta_i} + j\omega C_{\theta_i}$
b	Distance from the lag hinge to the center of gravity of the blade
B_i	$K_{x_i} + j\omega C_{x_i}$
C_{θ_i}	Vertical and lateral damping rate at DAVI (i)
C_{x_i}	Longitudinal damping rate at DAVI (i)
D	Dissipation function
E_α	Pitch effectivity
E_x	Longitudinal effectivity
E_z	Vertical effectivity
E_y	Lateral effectivity
E_ϕ	Roll effectivity
E_ψ	Yaw effectivity
F_x	Longitudinal excitation force
F_y	Lateral excitation force
F_z	Vertical excitation force
I_{ax}	Roll inertia of upper body
I_{ay}	Pitch inertia of upper body
I_{az}	Yaw inertia of upper body
I_{rx}	Roll inertia of lower body
I_{ry}	Pitch inertia of lower body
I_{rz}	Yaw inertia of lower body
I_{sx}	Roll inertia of aircraft

LIST OF SYMBOLS (Continued)

I_{s_y}	Pitch inertia of aircraft
I_{s_z}	Yaw inertia of aircraft
I_{RT_x}	Roll inertia of rotor plus transmission upper body
I_{RT_y}	Pitch inertia of rotor plus transmission upper body
I_{RT_z}	Yaw inertia of rotor plus transmission upper body
I_{RET_x}	Roll inertia of rotor plus engine plus transmission upper body
I_{RET_y}	Pitch inertia of rotor plus engine plus transmission upper body
I_{RET_z}	Yaw inertia of rotor plus engine plus transmission upper body
I_{FRT_x}	Roll inertia of fuselage plus engine lower body
I_{FRT_y}	Pitch inertia of fuselage plus engine lower body
I_{FRT_z}	Yaw inertia of fuselage plus engine lower body
I_{FRT_y}	Roll inertia of fuselage lower body
I_{FRT_y}	Pitch inertia of fuselage lower body
I_{FRT_z}	Yaw inertia of fuselage lower body
I_b	Inertia of the blade about the lag hinge
I_{D_i}	DAVI bar inertia
K_{D_i}	Vertical and lateral spring rate at DAVI (i)
K_{L_i}	Longitudinal spring rate at DAVI (i)
m_b	Mass of the rotor blade
m_{D_i}	Inertia bar mass of DAVI (i)
m_L	Lower body mass

LIST OF SYMBOLS (Continued)

m_R	Upper body mass
m_s	Mass of aircraft
M_{Ai}	$[m_{oi}(\frac{R_i}{r_i})(1 - \frac{R_i}{r_i}) - \frac{I_{oi}}{r_i^2}]$
M_{Ci}	$[m_{oi}(\frac{R_i}{r_i})^2 + \frac{I_{oi}}{r_i^2}]$
M_{Ki}	$[m_{oi}(1 - \frac{R_i}{r_i})^2 + \frac{I_{oi}}{r_i^2}]$
M_x	Roll moment at point of excitation
M_y	Pitch moment at point of excitation
M_z	Yaw moment at point of excitation
r_i	Distance between pivots on inertia bar of DAVI (i)
R_i	Cx distance of inertia bar of DAVI (i) from input pivot
T	Kinetic Energy
V	Potential Energy
W	Work
x_r	Longitudinal translation of lower body cg
x_{ri}	Longitudinal distance from lower body cg to DAVI (i)
x_{ri}	Longitudinal translation of lower body at DAVI (i)
x_u	Longitudinal translation of upper body cg
x_{ui}	Longitudinal distance from upper body cg to DAVI (i)
x_{ui}	Longitudinal translation of upper body at DAVI (i)
y_{oi}	Lateral translation of inertia bar at DAVI (i)
y_r	Lateral translation of lower body cg

LIST OF SYMBOLS (Continued)

Y_{L_i}	Lateral distance from lower body cg to DAVI (i)
y_{F_i}	Lateral translation of lower body at DAVI (i)
y_A	Lateral translation of upper body cg
Y_{U_i}	Lateral distance from upper body cg to DAVI (i)
y_{U_i}	Lateral translation of upper body at DAVI (i)
z_{D_i}	Vertical translation of inertia bar at DAVI (i)
z_L	Vertical translation of lower body cg
Z_{F_i}	Vertical distance from lower body cg to DAVI (i)
z_L	Vertical translation of lower body at DAVI (i)
z_U	Vertical translation of upper body cg
Z_{U_i}	Vertical distance from upper body cg to DAVI (i)
z_{U_i}	Vertical translation of upper body at DAVI (i)
α_{D_i}	Angular deflection of inertia bar of DAVI (i) for vertical isolation
α_L	Pitching motion about lower body cg
α_U	Pitching motion about upper body cg
α_S	Pitching motion about aircraft cg
S_i	Motion across DAVI (i)
θ_L	Rolling motion about lower body cg
θ_U	Rolling motion about upper body cg
θ_S	Rolling motion about aircraft cg
μ	$\frac{m_a}{m_s + m_a}$
ψ_{D_i}	Angular deflection of inertia bar of DAVI (i) for lateral isolation

LIST OF SYMBOLS (Continued)

ψ_F	Yawing motion about lower body cg
ψ_R	Yawing motion about upper body cg
ψ_s	Yawing motion about aircraft cg

INTRODUCTION

THE PROBLEM

Outstanding engineering achievements have brought about remarkable advances in rotary-wing state of the art; however, fundamental problems still persist. One of these problems is the high level of rotor induced vibration. The aerodynamic forces, which derive their energy from the air reacting upon the rotating blades, are transmitted to the rotor hub as shearing forces in both the vertical and in-plane directions; they may be evidenced as high-level vibration upon the fuselage. The nature of these forces is such as to produce an input at the hub at a frequency that is an integral multiple of the number of blades in the rotor system. Thus, the hub of a 3-bladed rotor would "feel" a periodic force of 3/rev, 6/rev, 9/rev, etc., in the vertical and in-plane directions. A 1/rev force input at the hub would also result for any unequal alternating or steady force; however, this is generally a function of blade track or unbalance, and it can be substantially reduced.

The primary consequences of high-level rotor-induced vibration are the reduction in performance and mission readiness of current inventory helicopters and the possible limitation in advancement of the high-speed and compound helicopter programs. Adequate reduction of vibration levels would indeed reduce much of the present logistic and maintenance personnel demands.

THE PROPOSED SOLUTION

Two approaches can be taken to reduce helicopter vibration. One approach concerns itself with the source of the problem, namely, the periodic aerodynamic forces. Research is presently pursued in finding ways and means of reducing the periodic excitations. Another approach to reduce helicopter vibration is rotor isolation, which is the proposed solution of this study. Production helicopters are flying today which have various configurations of rotor isolation, yet none of these vehicles exhibits isolation in the vertical direction. One of the early published research studies was conducted by C. E. Theobald, Jr., and R. Jones in 1956 and 1957 at Kaman Aircraft for Wright Air Development Center (Reference 1). The analysis of Theobald and Jones determined that by using a conventional mounting system (springs and dampers),

"the dominant harmonic, that is 2/rev, 3/rev, 4/rev, etc., depending upon the number of blades considered, could be isolated in the longitudinal, pitch, lateral, and roll directions. However, in the vertical direction, for a helicopter having a 4-bladed rotor or less, other than a conventional mounting system must be used". Isolation in the vertical direction has indeed been a difficult task to accomplish because of the conflicting requirements of control mechanism (small deflection across isolator) and soft-spring, low-frequency conventional isolation (large deflection across isolator). This study will attempt to establish the feasibility of rotor isolation in all 3 translational and rotational modes of motion.

In 1963, W. G. Flannelly of Kaman Aircraft invented the DAVI (Dynamic Antiresonant Vibration Isolator). This passive device, which counteracts spring forces with inertia forces, possesses low-frequency isolation capability with low static deflection. Results of DAVI analytical studies and laboratory testing have demonstrated the feasibility and capability of the DAVI as an effective means that can be employed for mitigation of the vibration problem. References 2 and 3 describe and illustrate some of the basic concepts, analysis, and testing of the DAVI. It is this type of isolator, DAVI, which will be employed throughout this study to determine the feasibility of rotor isolation.

THEORETICAL ANALYSIS

STEADY-STATE EQUATIONS

The analysis for the system, illustrated in Figure 1, includes all six degrees of freedom for each body. The energies of the isolation system illustrated can be written as follows:

$$\begin{aligned} T = & \frac{1}{2} m_R \dot{z}_R^2 + \frac{1}{2} m_R \dot{x}_R^2 + \frac{1}{2} m_R \dot{y}_R^2 + \frac{1}{2} m_F \dot{z}_F^2 + \frac{1}{2} m_F \dot{x}_F^2 + \frac{1}{2} m_F \dot{y}_F^2 \\ & + \frac{1}{2} \sum_{i=1}^n m_{o_i} \dot{z}_{o_i}^2 + \frac{1}{2} \sum_{i=1}^n m_{o_i} \dot{y}_{o_i}^2 + \frac{1}{2} \sum_{i=1}^n I_{o_i} \dot{\alpha}_{o_i}^2 + \frac{1}{2} \sum_{i=1}^n I_{o_i} \dot{\psi}_{o_i}^2 + \frac{1}{2} I_{R_z} \dot{\psi}_R^2 \\ & + \frac{1}{2} I_{R_x} \dot{\theta}_R^2 + \frac{1}{2} I_{R_y} \dot{\alpha}_R^2 + \frac{1}{2} I_{F_z} \dot{\psi}_F^2 + \frac{1}{2} I_{F_x} \dot{\theta}_F^2 + \frac{1}{2} I_{F_y} \dot{\alpha}_F^2 \end{aligned} \quad (1)$$

$$V = \frac{1}{2} \sum_{i=1}^n K_{o_i} (z_{F_i} - z_{R_i})^2 + \frac{1}{2} \sum_{i=1}^n K_{o_i} (y_{F_i} - y_{R_i})^2 + \frac{1}{2} \sum_{i=1}^n K_{x_i} (x_{F_i} - x_{R_i})^2 \quad (2)$$

$$D = \frac{1}{2} \sum_{i=1}^n C_{o_i} (\dot{z}_{F_i} - \dot{z}_{R_i})^2 + \frac{1}{2} \sum_{i=1}^n C_{o_i} (\dot{y}_{F_i} - \dot{y}_{R_i})^2 + \frac{1}{2} \sum_{i=1}^n C_{x_i} (\dot{x}_{F_i} - \dot{x}_{R_i})^2 \quad (3)$$

The Lagrangian equation is

$$\frac{d}{dt} \frac{\partial T}{\partial \dot{q}_R} - \frac{\partial T}{\partial q_R} + \frac{\partial V}{\partial q_R} + \frac{\partial D}{\partial \dot{q}_R} = Q_R \quad (4)$$

However,

$$\frac{\partial T}{\partial q_R} = 0$$

The equation can be rewritten

$$\frac{d}{dt} \frac{\partial T}{\partial \dot{q}_R} + \frac{\partial V}{\partial q_R} + \frac{\partial D}{\partial \dot{q}_R} = Q_R \quad (5)$$

and the right-hand side of the equation becomes

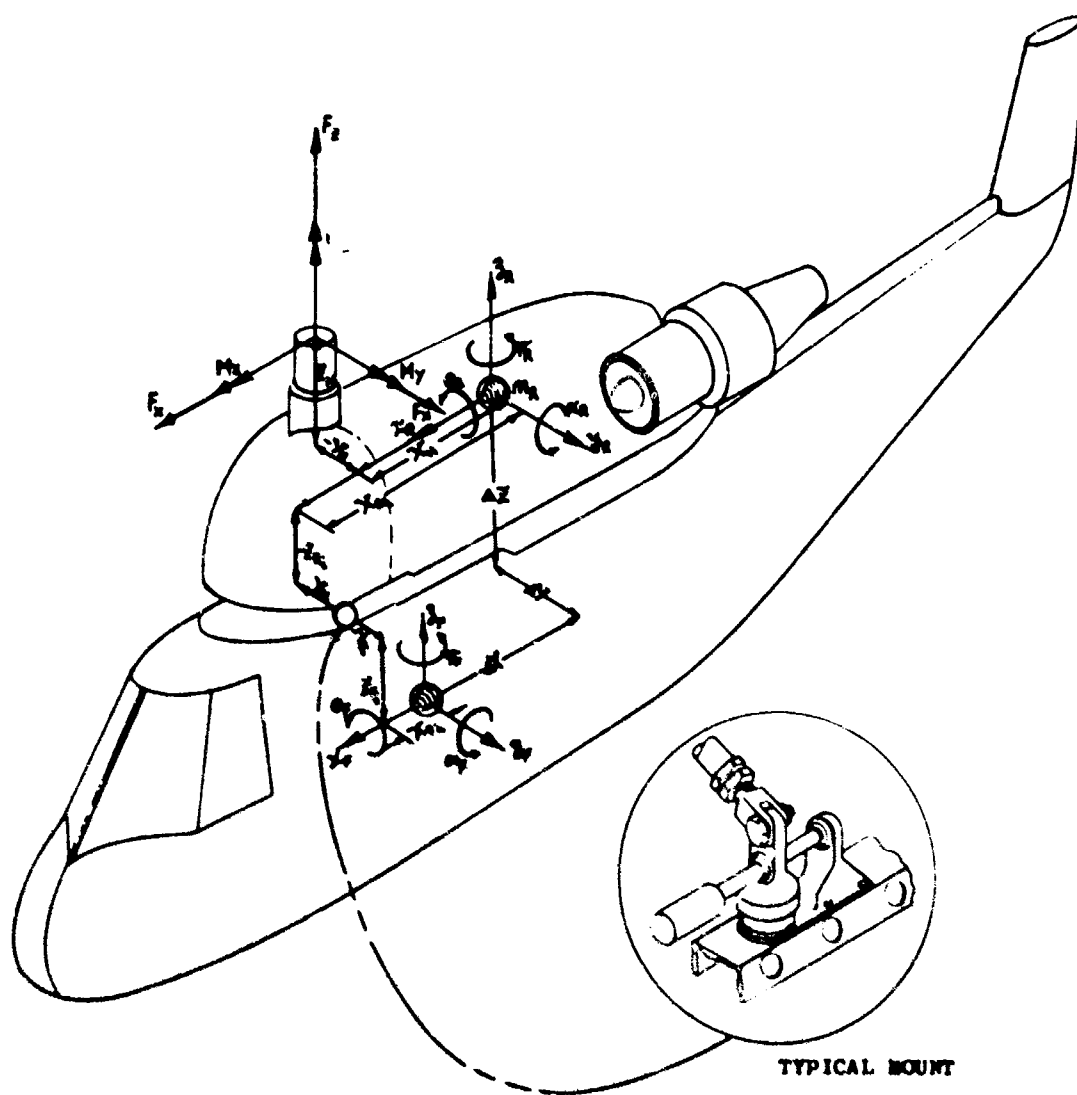


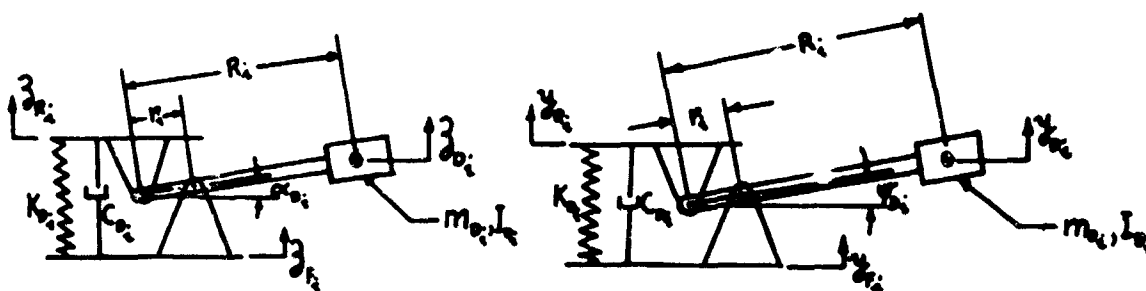
Figure 1. Diagram of Two-Body System.

$$Q_k = \frac{\partial W}{\partial Q_k}$$

where

$$W = F_x x_H + F_y y_H + F_z z_H + M_x \theta_R + M_y \alpha_R + M_z \psi_R \quad (6)$$

This analysis contains two-dimensional DAVI isolation. The DAVI terms for the vertical and lateral directions come from



(a)

(b)

Figure 2. DAVI Schematic.

$$\alpha_{D_i} = \frac{z_{B_i} - z_{D_i}}{R_i} \quad (7)$$

$$z_{D_i} = z_{B_i} + R_i \alpha_{D_i}$$

$$z_{D_i} = z_{B_i} \left(1 - \frac{R_i}{r_i}\right) + z_{F_i} \left(\frac{R_i}{r_i}\right) \quad (8)$$

Also

$$\psi_{D_i} = \frac{y_{B_i} - y_{D_i}}{r_i} \quad (9)$$

$$y_{D_i} = y_{B_i} + R_i \psi_{D_i}$$

$$y_{D_i} = y_{B_i} \left(1 - \frac{R_i}{r_i}\right) + y_{F_i} \left(\frac{R_i}{r_i}\right) \quad (10)$$

But

$$z_{R_i} = z_R + Y_{R_i} \theta_R - X_{R_i} \alpha_R \quad (11)$$

$$y_{R_i} = y_R + X_{R_i} \psi_R - Z_{R_i} \theta_R \quad (12)$$

$$x_{R_i} = x_R - Y_{R_i} \psi_R + Z_{R_i} \alpha_R \quad (13)$$

$$z_{F_i} = z_F + Y_{F_i} \theta_F - X_{F_i} \alpha_F \quad (14)$$

$$y_{F_i} = y_F + X_{F_i} \psi_F - Z_{F_i} \theta_F \quad (15)$$

$$x_{F_i} = x_F - Y_{F_i} \psi_F + Z_{F_i} \alpha_F \quad (16)$$

Also

$$x_H = x_R - Y_H \psi_R + Z_H \alpha_R \quad (17)$$

$$y_H = y_R + X_H \psi_R - Z_H \theta_R \quad (18)$$

$$z_H = z_R + Y_H \theta_R - X_H \alpha_R \quad (19)$$

And let

$$M_{A_i} = \left[m_{o_i} \left(\frac{R_i}{r_i} \right) \left(1 - \frac{R_i}{r_i} \right) - \frac{I_{o_i}}{r_i^2} \right] \quad (20)$$

$$M_{R_i} = \left[m_{o_i} \left(1 - \frac{R_i}{r_i} \right)^2 + \frac{I_{o_i}}{r_i^2} \right] \quad (21)$$

$$M_{c_i} = \left[m_{o_i} \left(\frac{R_i}{r_i} \right)^2 + \frac{I_{o_i}}{r_i^2} \right] \quad (22)$$

$$A_i = K_{o_i} + j\omega C_{o_i} \quad (23)$$

$$B_i = K_{x_i} + j\omega C_{x_i} \quad (24)$$

Substituting the foregoing expressions, performing the appropriate mathematical operations, and assuming a solution of $e^{i\omega t}$, the solution matrix is obtained and presented in Figure 3. Similarly, the solution matrix for the unisolated system, illustrated in Figure 4, is presented in Figure 5. Both solution matrices were then programmed for the IBM Model 360-40 G computer.

It is therefore possible to obtain responses of the rigid system (unisolated) in the 3 translational and 3 rotational modes. Likewise, for the isolated case, as illustrated in Figure 1, it is possible to obtain the 6 responses of the upper body as well as the 6 responses of the lower body. As described in the appendix of this report, headed "Statistical Data", both the isolated two-body system and the unisolated rigid-body system are equivalent in weight, total system center of gravity, and aircraft inertia. In addition, the point of excitation, the hub, is the same in both aircraft with the same forces and moments applied. Thus, a comparison of the responses of the isolated vehicle and the unisolated vehicles can be made.

The rigid-body solution matrix is a conventional six-degree-of-freedom system. If the matrix is rewritten as

$$[A_1]q_m = [B_1] \quad (25)$$

where

- A_1 - Left-hand side of 6-x-6 rigid-body matrix,
- q_m - Generalized coordinates of 6-x-6 matrix,
- B_1 - Right-hand side of 6-x-6 matrix,

the generalized coordinates of the rigid-body system can be calculated as follows:

$$q_m = [A_1]^{-1}[B_1] \quad (26)$$

As illustrated in Figure 1, passive DAVI-type isolators are installed between the upper body and the lower body of the aircraft. The two upper-body configurations studied are:

- (1) RT - Rotor plus transmission, and
- (2) RET - Rotor plus engine plus transmission.

Therefore, in the presentation of data, (RT) and (RET) are used as subscripts to define the particular configuration

[illegible]

Figure 3. 12-X-12 Two-Body Solution Matrix.

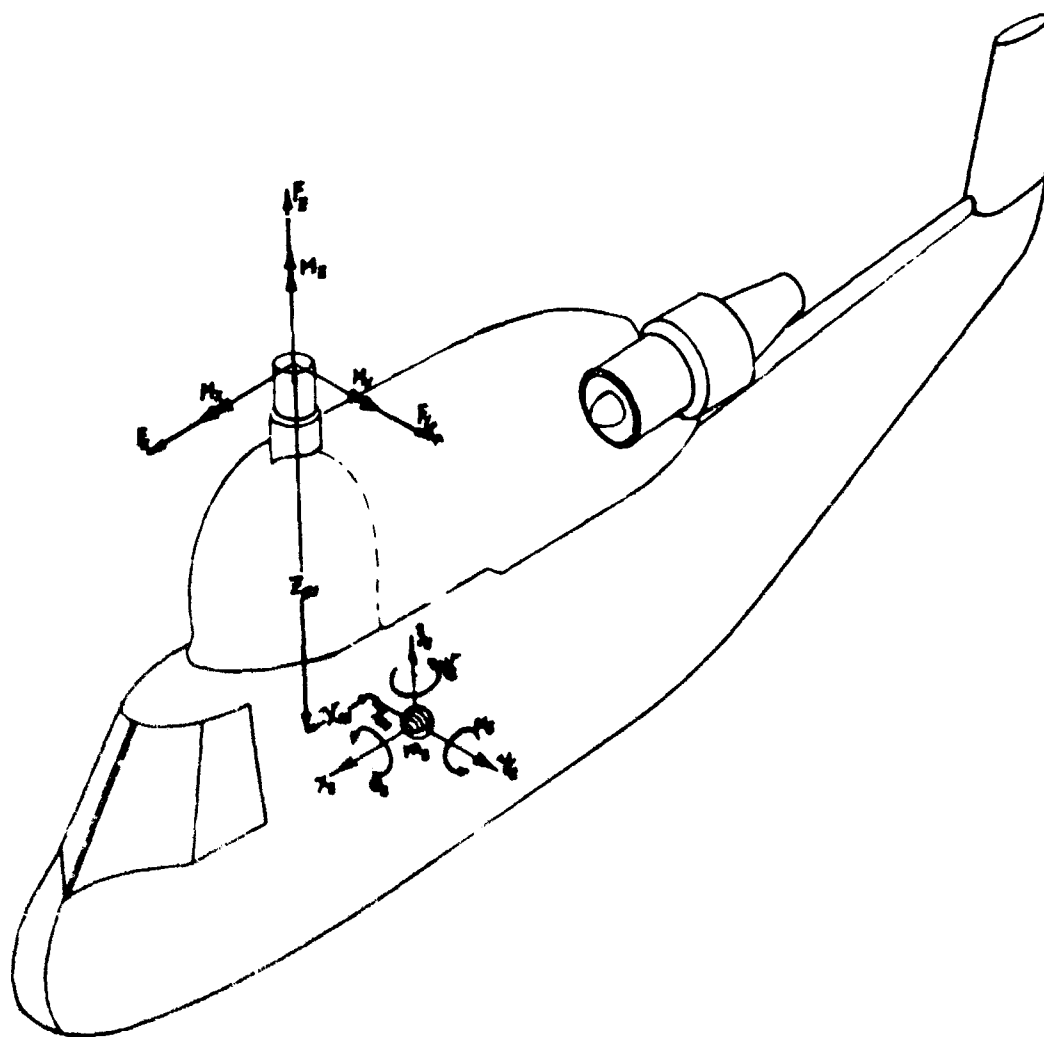


Figure 4. Diagram of Rigid-Body System.

$m_3 \omega^2$	0	0	0	0	0	1	0	0	0	0	0	F_x
$-m_3 \omega^2$	0	0	0	0	0	0	0	0	1	0	0	F_y
0	0	$-m_3 \omega^2$	0	0	0	0	1	0	0	0	0	F_z
0	0	0	0	$-I_{3y} \omega^2$	0	0	$-X_{SH}$	0	0	1	0	M_x
0	0	0	0	0	$-I_{3x} \omega^2$	0	Y_{SH}	0	1	0	0	M_y
0	0	0	0	0	0	$-X_{SH}$	0	0	0	0	1	M_z

=

X_3	Y_3	Z_3	α_3	θ_3	ψ_3
-------	-------	-------	------------	------------	----------

Figure 5. 6-X-6 Rigid-Body Solution Matrix.

studied. The corresponding lower bodies are for:

- (1) Fuselage plus engine, and
- (2) Fuselage only.

The two configurations investigated represent a change in upper and lower body weight, inertia, and center-of-gravity locations; and the results reflect the change in response to these variations.

There are (1) number of DAVI's located with reference to the upper-body center of gravity at dimensions X_{a_i} , Y_{a_i} , and Z_{a_i} with a spring rate of K_{a_i} , mass of m_{a_i} , DAVI-bar inertia of I_{a_i} and design ratio of R_i/r_i and ρ_i/r_i^2 . Since the DAVI considered for this study is a two-dimensional isolator providing isolation in the vertical and lateral directions, conventional isolation was included in the longitudinal direction using a spring of rate K_{x_i} . The effects of damping were included for the DAVI with a damping rate constant of C_{a_i} and for the conventional isolator of constant C_{x_i} .

When the equations were programmed for the computer, the number of isolators was limited to 10. It is believed that no more than 10 isolators would be required for any proposed helicopter isolation.

If the coupled response matrix of Figure 3 is rewritten as

$$[A_z] q_{m_i} = [B_z] \quad (27)$$

then the generalized coordinates of the system can be written as

$$q_{m_i} = [A_z]^{-1} [B_z] \quad (28)$$

These generalized coordinates are the translational and rotational motions about the respective center of gravity of each body. The purpose of this study, however, is to determine the feasibility of isolating the lower body; therefore, of concern is the response of the lower body and how this response compares to the response of unisolated vehicle. Since the center of gravity of the unisolated helicopter and the total system center of gravity of the isolated helicopter are identical, the responses of both systems were calculated at this point to obtain the effectivity. It is this effectivity which is presented in the results of this study.

The lower body responses of the isolated helicopter at the system center of gravity are as follows:

$$\chi_{F_3} = \chi_F + \alpha_F \Delta Z_F - \psi_F \Delta Y_F \quad (29)$$

$$y_{F_3} = y_F - \theta_F \Delta Z_F + \psi_F \Delta X_F \quad (30)$$

$$z_{F_3} = z_F - \alpha_F \Delta X_F + \theta_F \Delta Y_F \quad (31)$$

$$\alpha_{F_3} = \alpha_F \quad (32)$$

$$\theta_{F_3} = \theta_F \quad (33)$$

$$\psi_{F_3} = \psi_F \quad (34)$$

The effectivity of the system is defined as the ratio of the response of the rigid system over the response of the isolated system at the same point. Effectivity (E) is a non-dimensional ratio and can be written as

$$E_x = \frac{\chi_s}{\chi_{F_3}} \quad (35)$$

$$E_y = \frac{y_s}{y_{F_3}} \quad (36)$$

$$E_z = \frac{z_s}{z_{F_3}} \quad (37)$$

$$E_\alpha = \frac{\alpha_s}{\alpha_{F_3}} \quad (38)$$

$$E_\theta = \frac{\theta_s}{\theta_{F_3}} \quad (39)$$

$$E_\psi = \frac{\psi_s}{\psi_{F_3}} \quad (40)$$

The subscripts x , y , z , α , ϕ and ψ identify the effectivity in the three translational and three rotational motions respectively.

The computer was employed in calculating the natural frequencies of the system which are printed out for every configuration studied.

CONFIGURATIONS

There are 26 helicopter cases ranging in gross weight from 2000 pounds to 100,000 pounds and 6 compound cases, all at a gross weight of 20,000 pounds. Therefore, there are 32 cases to be studied under steady-state excitations. To establish a method of identification, the following code was introduced:

Code:	H	- Helicopter
	C	- Compound Helicopter
	S	- Steady-State Condition
	T	- Transient Condition
	RT	- Rotor Plus Transmission Upper Body
	RET	- Rotor Plus Engine Plus Transmission Upper Body

There are an additional 6 cases which will be studied under transient inputs. Therefore, the total number of basic cases is 38. A summary of these cases is presented in Table I. Table II summarizes the DAVI details and presents the static deflection of the system as well as the DAVI weight for each configuration. Tables III, IV, V, and VI present the isolator locations and the point of excitation, namely, the hub.

Tables VII and VIII are summaries of pertinent mass and inertia data describing the configurations studied. As is evidenced from the data shown, some assumptions were made regarding the hub location.

For the configurations dealing with rotor and transmission as the upper body, the hub lines up with the cg's of the upper body and lower body and, therefore, with the rigid body. Where the upper body is defined by the rotor plus engine plus transmission, the arrangement is as follows. The hub still lines up with the rigid-body cg; however, the upper-body cg and the lower-body cg are both offset from the rigid-body cg.

The rigid-body response for any one case will not alter. The rigid-body system, with the three forces applied at the hub (no moments were applied), will not yield any yaw response because the hub is lined up with the center of gravity. Therefore, the results will present only five effectivenesses instead of six.

Unless otherwise specified, four isolators were used. These four isolators were located below the hub with their centerline, normal to the x-y plane, in line with the vertical axis of the hub.

One of the goals of this study was to achieve very low static deflections in the system. As will be noted in Table II, the static deflection for practically all configurations is less than .1 inch. In obtaining these low static deflections, compromises were made reflecting the DAVI inertia bar weights. In some cases, the DAVI exceeded 1.0 percent of the helicopter weight. A typical variation of DAVI weight and static deflection is presented in Table IX, where R/r and ρ/r^2 are held constant.

Figure 6 presents a variation of DAVI weights with static deflection for a four-bladed, 2300-pound helicopter. The weight variation was plotted for five values of the non-dimensional design ratio R/r . This figure clearly illustrates the tremendous weight variation obtainable due to the flexibility of the DAVI design parameters. The DAVI system weight, as exemplified here, ranges from 0.1 percent to 6.6 percent of the gross weight of the helicopter. Most practical DAVI system weights, utilizing the two-dimensional DAVI for rotor isolation, will be about 1.5 percent or less of the helicopter gross weight. Because of the great design flexibility of the DAVI, it is not possible at this time to develop a semi-empirical formula to calculate DAVI weight as a function of gross weight.

The higher the DAVI spring rate and the lower the DAVI static deflection, the higher the inertia force required to oppose the spring force. Thus, as is demonstrated in Table IX, the change in static deflection is inversely proportional to a change in DAVI weight.

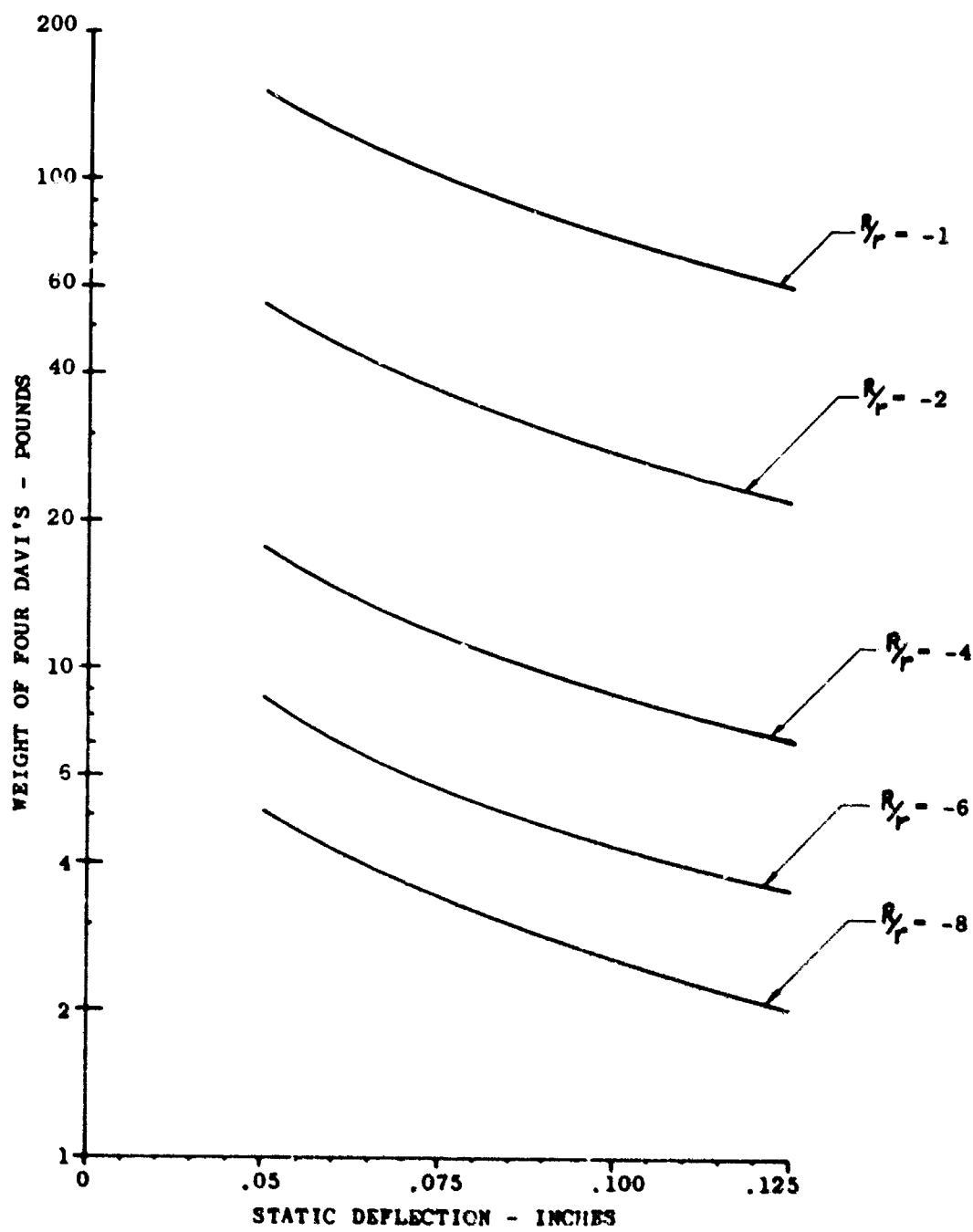


Figure 6. Variation of DAVI Weight With Static Deflection For Four-Bladed, 2300-Pound Helicopter.

TABLE I. CASE AND CONFIGURATION IDENTIFICATION					
Case No.	Gross Weight (lb)	No. of Blades	Rotor rpm	RT	RET
1 HS	2,000	2	413	X	-
2 HS	2,000	3	413	X	-
3 HS	2,000	4	413	X	-
4 HS	6,500	2	297	X	-
5 HS	6,500	3	297	X	-
6 HS	6,500	4	297	X	-
7 HS	10,000	3	262	X	-
8 HS	10,000	4	262	X	-
9 HS	10,000	5	262	X	-
10 HS	40,000	6	177	X	-
11 HS	40,000	7	177	X	-
12 HS	100,000	6	136	X	-
13 HS	100,000	7	136	X	-
14 HS	2,000	2	413	-	X
15 HS	2,000	3	413	-	X
16 HS	2,000	4	413	-	X
17 HS	6,500	2	297	-	X
18 HS	6,500	3	297	-	X
19 HS	6,500	4	297	-	X
20 HS	10,000	3	262	-	X
21 HS	10,000	4	262	-	X
22 HS	10,000	5	262	-	X
23 HS	40,000	6	177	-	X
24 HS	40,000	7	177	-	X
25 HS	100,000	6	136	-	X
26 HS	100,000	7	136	-	X
27 CS	20,000	4	210	X	-
28 CS	20,000	5	210	X	-
29 CS	20,000	6	210	X	-
30 CS	20,000	4	210	-	X
31 CS	20,000	5	210	-	X
32 CS	20,000	6	210	-	X
33 HT	2,000	2	413	X	-
34 HT	6,500	2	297	X	-
35 HT	10,000	3	262	X	-
36 HT	40,000	6	177	X	-
37 HT	100,000	6	136	X	-
38 CT	20,000	4	210	X	-

TABLE II. DAVI DESIGN DETAILS AND STATIC DEFLECTION VERSUS CONFIGURATIONS

Case	Total DAVI Weight (lb)	R/r	P/P_s	Total DAVI Spring Rate (lb/ft)	Total Long. Spring Rate (lb/ft)	Hel. Gr Wt (lb)	DAVI Weight in % of Gr Wt (%)	Static Deflec. (in.)
1 HS	16.6796	-8.0	27.000	383,985.5	20,000,000	2,000	.833	.050
2 HS	12.5800	-8.0	16.333	383,985.5	20,000,000	3,000	.629	.050
3 HS	14.5800	-4.0	8.333	383,985.5	20,000,000	2,000	.729	.050
4 HS	104.7910	-8.0	27.000	1,247,967.0	40,000,000	6,500	1.812	.050
5 HS	79.1089	-8.0	16.333	1,247,976.0	40,000,000	6,500	1.217	.050
6 HS	91.6020	-4.0	8.333	1,247,976.0	40,000,000	6,500	1.409	.050
7 HS	104.2500	-8.0	16.333	1,279,962.7	800,000	10,000	1.042	.075
8 HS	120.7500	-4.0	8.333	1,279,962.7	1,000,000	10,000	1.207	.075
9 HS	77.2800	-4.0	8.333	1,279,962.7	1,200,000	10,000	.728	.075
10 HS	132.7280	-8.0	16.333	3,839,888.0	4,000,000	40,000	.331	.100
11 HS	259.1840	-4.0	8.333	3,839,888.0	6,000,000	40,000	.647	.100
12 HS	724.8470	-8.0	16.333	9,599,720.0	6,000,000	100,000	.724	.100
13 HS	533.0510	-8.0	16.333	9,599,720.0	8,000,000	100,000	.633	.100
14 HS	15.7000	-8.0	27.000	361,348.0	20,000,000	2,000	.785	.050
15 HS	11.8620	-8.0	16.333	361,348.0	20,000,000	2,000	.583	.050
16 HS	13.7300	-4.0	8.333	361,348.0	20,000,000	2,000	.688	.050
17 HS	98.6210	-8.0	27.000	1,174,652.0	40,000,000	6,500	1.510	.050
18 HS	74.4720	-8.0	16.333	1,174,652.0	40,000,000	6,500	1.145	.050
19 HS	86.2310	-4.0	8.333	1,174,652.0	40,000,000	6,500	1.326	.050
20 HS	98.1320	-8.0	16.333	1,204,764.0	800,000	10,000	.980	.075
21 HS	113.8530	-4.0	8.333	1,204,764.0	1,200,000	10,000	1.1385	.075
22 HS	72.7330	-4.0	8.333	1,204,764.0	1,400,000	10,000	.727	.075
23 HS	161.296	-8.0	16.333	3,614,392.0	1,000,000	40,000	.403	.100
24 HS	243.960	-4.0	8.333	3,614,392.0	1,600,000	40,000	.609	.100
25 HS	682.536	-8.0	16.333	9,035,640.0	1,400,000	100,000	.682	.100
26 HS	501.740	-8.0	16.333	9,035,640.0	2,400,000	100,000	.5017	.100
27 CS	108.836	-8.0	16.333	1,230,648.0	980,000	20,000	.544	.100
28 CS	108.836	-8.0	16.333	1,230,648.0	1,280,000	20,000	.544	.100
29 CS	108.836	-8.0	16.333	2,770,204.0	2,000,000	20,000	.544	.070
30 CS	182.252	-8.0	16.333	2,036,036.0	100,000,000	20,000	.911	.080
31 CS	165.620	-8.0	16.333	2,747,732.0	120,000,000	20,000	.825	.088
32 CS	120.865	-8.0	16.333	3,074,580.0	800,000	20,000	.604	.080

TABLE III. VERTICAL LOCATION OF ISOLATORS FOR FOUR-DAVI INSTALLATION				
Case	z_{R_1} (ft)	z_{R_2} (ft)	z_{R_3} (ft)	z_{R_4} (ft)
1 HS	-1.0	-1.0	-1.0	-1.0
2 HS	-1.0	-1.0	-1.0	-1.0
3 HS	-1.0	-1.0	-1.0	-1.0
4 HS	-1.0	-1.0	-1.0	-1.0
5 HS	-1.0	-1.0	-1.0	-1.0
6 HS	-1.0	-1.0	-1.0	-1.0
7 HS	-2.0	-2.0	-2.0	-2.0
8 HS	-2.0	-2.0	-2.0	-2.0
9 HS	-2.0	-2.0	-2.0	-2.0
10 HS	-2.0	-2.0	-2.0	-2.0
11 HS	-2.0	-2.0	-2.0	-2.0
12 HS	-3.0	-3.0	-3.0	-3.0
13 HS	-3.0	-3.0	-3.0	-3.0
14 HS	-1.0	-1.0	-1.0	-1.0
15 HS	-1.0	-1.0	-1.0	-1.0
16 HS	-1.0	-1.0	-1.0	-1.0
17 HS	-1.0	-1.0	-1.0	-1.0
18 HS	-1.0	-1.0	-1.0	-1.0
19 HS	-1.0	-1.0	-1.0	-1.0
20 HS	-2.0	-2.0	-2.0	-2.0
21 HS	-2.0	-2.0	-2.0	-2.0
22 HS	-2.0	-2.0	-2.0	-2.0
23 HS	-2.0	-2.0	-2.0	-2.0
24 HS	-2.0	-2.0	-2.0	-2.0
25 HS	-3.0	-3.0	-3.0	-3.0
26 HS	-3.0	-3.0	-3.0	-3.0
27 CS	-2.0	-2.0	-2.0	-2.0
28 CS	-2.0	-2.0	-2.0	-2.0
29 CS	-2.0	-2.0	-2.0	-2.0
30 CS	-2.0	-2.0	-2.0	-2.0
31 CS	-2.0	-2.0	-2.0	-2.0
32 CS	-2.0	-2.0	-2.0	-2.0
33 NT	-1.0	-1.0	-1.0	-1.0
34 NT	-1.0	-1.0	-1.0	-1.0
35 NT	-2.0	-2.0	-2.0	-2.0
36 NT	-2.0	-2.0	-2.0	-2.0
37 NT	-3.0	-3.0	-3.0	-3.0
38 CT	-2.0	-2.0	-2.0	-2.0

TABLE IV. LONGITUDINAL LOCATION OF ISOLATORS FOR FOUR-DAVI INSTALLATION				
Case	x_{R1} (ft)	x_{R2} (ft)	x_{R3} (ft)	x_{R4} (ft)
1 HS	-1.0	1.0	1.0	-1.0
2 HS	-1.0	1.0	1.0	-1.0
3 HS	-1.0	1.0	1.0	-1.0
4 HS	-1.0	1.0	1.0	-1.0
5 HS	-1.0	1.0	1.0	-1.0
6 HS	-1.0	1.0	1.0	-1.0
7 HS	-2.0	2.0	2.0	-2.0
8 HS	-2.0	2.0	2.0	-2.0
9 HS	-2.0	2.0	2.0	-2.0
10 HS	-2.0	2.0	2.0	-2.0
11 HS	-2.0	2.0	2.0	-2.0
12 HS	-3.0	3.0	3.0	-3.0
13 HS	-3.0	3.0	3.0	-3.0
14 HS	-1.0	3.0	3.0	-1.0
15 HS	-1.0	3.0	3.0	-1.0
16 HS	-1.0	3.0	3.0	-1.0
17 HS	-2.0	2.0	2.0	-2.0
18 HS	-2.0	2.0	2.0	-2.0
19 HS	-2.0	2.0	2.0	-2.0
20 HS	-2.0	4.0	4.0	-2.0
21 HS	-2.0	4.0	4.0	-2.0
22 HS	-2.0	4.0	4.0	-2.0
23 HS	-5.5	1.5	1.5	-5.5
24 HS	-5.5	1.5	1.5	-5.5
25 HS	-8.0	0.0	0.0	-8.0
26 HS	-8.0	0.0	0.0	-8.0
27 CS	-2.0	2.0	2.0	-2.0
28 CS	-2.0	2.0	2.0	-2.0
29 CS	-2.0	2.0	2.0	-2.0
30 CS	-3.0	3.0	3.0	-3.0
31 CS	-3.0	3.0	3.0	-3.0
32 CS	-3.0	3.0	3.0	-3.0
33 NT	-1.0	1.0	1.0	-1.0
34 NT	-1.0	1.0	1.0	-1.0
35 NT	-2.0	2.0	2.0	-2.0
36 NT	-2.0	2.0	2.0	-2.0
37 NT	-3.0	3.0	3.0	-3.0
38 CT	-2.0	2.0	2.0	-2.0

TABLE V. LATERAL LOCATION OF ISOLATORS FOR FOUR-DAVI INSTALLATION				
Case	Y_{R_1} (ft)	Y_{R_2} (ft)	Y_{R_3} (ft)	Y_{R_4} (ft)
1 HS	-1.0	-1.0	1.0	1.0
2 HS	-1.0	-1.0	1.0	1.0
3 HS	-1.0	-1.0	1.0	1.0
4 HS	-1.0	-1.0	1.0	1.0
5 HS	-1.0	-1.0	1.0	1.0
6 HS	-1.0	-1.0	1.0	1.0
7 HS	-2.0	-2.0	2.0	2.0
8 HS	-2.0	-2.0	2.0	2.0
9 HS	-2.0	-2.0	2.0	2.0
10 HS	-2.0	-2.0	2.0	2.0
11 HS	-2.0	-2.0	2.0	2.0
12 HS	-3.0	-3.0	3.0	3.0
13 HS	-3.0	-3.0	3.0	3.0
14 HS	-1.0	-1.0	1.0	1.0
15 HS	-1.0	-1.0	1.0	1.0
16 HS	-1.0	-1.0	1.0	1.0
17 HS	-1.0	-1.0	1.0	1.0
18 HS	-1.0	-1.0	1.0	1.0
19 HS	-1.0	-1.0	1.0	1.0
20 HS	-2.0	-2.0	2.0	2.0
21 HS	-2.0	-2.0	2.0	2.0
22 HS	-2.0	-2.0	2.0	2.0
23 HS	-2.0	-2.0	2.0	2.0
24 HS	-2.0	-2.0	2.0	2.0
25 HS	-3.0	-3.0	3.0	3.0
26 HS	-3.0	-3.0	3.0	3.0
27 CS	-2.0	-2.0	2.0	2.0
28 CS	-2.0	-2.0	2.0	2.0
29 CS	-2.0	-2.0	2.0	2.0
30 CS	-2.0	-2.0	2.0	2.0
31 CS	-2.0	-2.0	2.0	2.0
32 CS	-2.0	-2.0	2.0	2.0
33 HT	-1.0	-1.0	1.0	1.0
34 HT	-1.0	-1.0	1.0	1.0
35 HT	-2.0	-2.0	2.0	2.0
36 HT	-2.0	-2.0	2.0	2.0
37 HT	-3.0	-3.0	3.0	3.0
38 CT	-2.0	-2.0	2.0	2.0

TABLE VI. LOCATION OF POINT OF EXCITATION FOR ALL CONFIGURATIONS						
Case	X _{SH} (ft)	Y _{SH} (ft)	Z _{SH} (ft)	X _H (ft)	Y _H (ft)	Z _H (ft)
1 HS	0	0	2.0	-	-	.5
2 HS	0	0	2.0	0	0	.5
3 HS	0	0	2.0	0	0	.5
4 HS	0	0	3.0	0	0	.5
5 HS	0	0	3.0	0	0	.5
6 HS	0	0	3.0	0	0	.5
7 HS	0	0	3.0	0	0	.5
8 HS	0	0	3.0	0	0	.5
9 HS	0	0	3.0	0	0	.5
10 HS	0	0	4.0	0	0	.75
11 HS	0	0	4.0	0	0	.75
12 HS	0	0	6.5	0	0	1.5
13 HS	0	0	6.5	0	0	1.5
14 HS	0	0	2.0	1.0	0	.5
15 HS	0	0	2.0	1.0	0	.5
16 HS	0	0	2.0	1.0	0	.5
17 HS	0	0	3.0	1.0	0	.5
18 HS	0	0	3.0	1.0	0	.5
19 HS	0	0	3.0	1.0	0	.5
20 HS	0	0	3.0	1.0	0	.5
21 HS	0	0	3.0	1.0	0	.5
22 HS	0	0	3.0	1.0	0	.5
23 HS	0	0	4.0	-2.0	0	.75
24 HS	0	0	4.0	-2.0	0	.75
25 HS	0	0	6.5	0	0	1.5
26 HS	0	0	6.5	0	0	1.5
27 CS	0	0	3.0	0	0	.5
28 CS	0	0	3.0	0	0	.5
29 CS	0	0	3.0	0	0	.5
30 CS	0	0	3.0	0	0	.5
31 CS	0	0	3.0	-.5	0	.5
32 CS	0	0	3.0	-.5	0	.5
33 NT	0	0	2.0	0	0	.5
34 NT	0	0	3.0	0	0	1.0
35 NT	0	0	3.0	0	0	.5
36 NT	0	0	4.0	0	0	.75
37 NT	0	0	6.5	0	0	1.5
38 CT	0	0	3.0	0	0	.5

TABLE VII. SUMMARY OF GROSS WEIGHT, MASS, AND PREDOMINANT FREQUENCIES VERSUS CONFIGURATIONS									
Case	Gr Wt (lb)	m _S (slugs)	m _R (slugs)	m _P (slugs)	f _{1/rev} (cps)	f _{N/rev} (cps)	f _{2N/rev} (cps)	f _{3N/rev} (cps)	f _{4N/rev} (cps)
1 HS	2,000	62.11	12.42	49.69	6.9	13.8	27.5	41.3	55.1
2 HS	2,000	62.11	12.42	49.69	6.9	20.6	41.3	31.9	82.6
3 HS	2,000	62.11	12.42	49.69	6.9	27.5	51.5	82.6	110.4
4 HS	6,500	201.86	40.37	161.49	4.95	9.9	19.8	29.7	39.6
5 HS	6,500	201.86	40.37	161.49	4.95	14.8	29.7	44.5	59.4
6 HS	6,500	201.86	40.37	161.49	4.95	19.8	39.6	59.4	79.2
7 HS	10,000	310.55	62.11	248.44	4.4	13.1	21.2	39.3	52.4
8 HS	10,000	310.55	62.11	248.44	4.4	17.5	34.9	52.4	69.9
9 HS	10,000	310.55	62.11	248.44	4.4	21.8	43.6	65.5	87.3
10 HS	40,000	1242.20	248.44	993.76	2.95	17.7	35.4	53.1	70.8
11 HS	40,000	1242.20	248.44	993.76	2.95	20.6	41.3	62.0	82.6
12 HS	100,000	3105.50	621.10	2484.4	2.3	13.8	27.6	41.4	55.2
13 HS	100,000	3105.50	621.10	2484.4	2.3	16.1	32.2	48.3	64.4
14 HS	2,000	62.11	15.34	46.77	6.9	73.8	27.5	41.3	55.1
15 HS	2,000	62.11	15.34	46.77	6.9	20.6	41.3	61.9	82.6
16 HS	2,000	62.11	15.34	46.77	6.9	27.5	51.5	82.6	110.4
17 HS	6,500	201.86	49.86	152.00	4.95	9.9	19.8	29.7	39.6
18 HS	6,500	201.86	49.86	152.00	4.95	14.8	29.7	44.5	59.4
19 HS	6,500	201.86	49.86	152.00	4.95	19.8	39.6	59.4	79.2
20 HS	10,000	310.55	76.71	233.84	4.4	13.1	21.2	39.3	52.4
21 HS	10,000	310.55	76.71	233.84	4.4	17.5	34.9	52.4	69.9
22 HS	10,000	310.55	76.71	233.84	4.4	21.8	43.6	65.5	87.3
23 HS	40,000	1242.20	306.82	935.38	2.95	17.7	35.4	53.1	70.8
24 HS	40,000	1242.20	306.82	935.38	2.95	20.6	41.3	62.0	82.6
25 HS	100,000	3105.50	767.10	2338.40	2.3	13.8	27.6	41.4	55.2
26 HS	100,000	3105.50	767.10	2338.40	2.3	16.1	32.2	48.3	64.4
27 CS	20,000	621.10	124.70	496.40	3.7	14.7	29.4	44.1	58.7
28 CS	20,000	621.10	124.70	496.40	3.7	18.4	36.8	55.0	73.5
29 CS	20,000	621.10	124.70	496.40	3.7	22.0	44.1	66.1	88.3
30 CS	20,000	621.10	124.70	496.40	3.7	14.7	29.4	44.1	58.7
31 CS	20,000	621.10	124.70	496.40	3.7	18.4	36.8	55.0	73.5
32 CS	20,000	621.10	124.70	496.40	3.7	22.0	44.0	66.1	88.3
33 HT	2,000	62.11	12.42	49.69	6.9	13.8	27.5	41.3	55.1
34 HT	6,500	201.86	40.37	161.49	4.95	9.9	19.8	29.7	39.6
35 HT	10,000	310.55	62.11	248.44	4.4	13.1	21.2	39.3	52.4
36 HT	40,000	124.22	248.44	993.76	2.95	17.7	35.4	53.1	70.8
37 HT	100,000	3105.50	621.10	2484.40	2.3	13.8	27.6	41.4	55.2
38 CT	20,000	621.10	124.70	496.40	3.7	14.7	29.4	44.1	58.7

TABLE VIII. SUMMARY OF AIRCRAFT AND UPPER BODY INERTIA VERSUS CONFIGURATION						
Case	I_{S_X}	I_{S_Y}	I_{S_Z}	I_{R_X}	I_{R_Y}	I_{R_Z}
1 HS	140.0	5,240.0	492.0	3.56	3.60	.13
2 HS	140.0	5,240.0	492.0	3.56	3.60	.13
3 HS	140.0	5,240.0	492.0	3.56	3.60	.13
4 HS	1,478.8	5,534.8	5,196.8	37.60	38.03	1.37
5 HS	1,478.8	5,534.8	5,196.8	37.60	38.03	1.37
6 HS	1,478.8	5,534.8	5,196.8	37.60	38.03	1.37
7 HS	3,500.0	13,100.0	12,300.0	89.00	90.00	3.24
8 HS	3,500.0	13,100.0	12,300.0	89.00	90.00	3.24
9 HS	3,500.0	13,100.0	12,300.0	89.00	90.00	3.24
10 HS	56,000.0	209,600.0	196,800.0	1,424.00	1,440.00	51.84
11 HS	56,000.0	209,600.0	196,800.0	1,424.00	1,440.00	51.84
12 HS	350,000.0	1,310,000.0	1,230,000.0	8,900.00	9,000.00	324.00
13 HS	350,000.0	1,310,000.0	1,230,000.0	8,900.00	9,000.00	324.00
14 HS	140.0	524.0	492.0	3.40	7.72	5.92
15 HS	140.0	524.0	492.0	3.40	7.72	5.92
16 HS	140.0	524.0	492.0	3.40	7.72	5.92
17 HS	1,478.8	5,534.8	5,196.8	35.91	81.54	62.53
18 HS	1,478.8	5,534.8	5,196.8	35.91	81.54	62.53
19 HS	1,478.8	5,534.8	5,196.8	35.91	81.54	62.53
20 HS	3,500.0	13,100.0	12,300.0	85.00	193.00	148.00
21 HS	3,500.0	13,100.0	12,300.0	85.00	193.00	148.00
22 HS	3,500.0	13,100.0	12,300.0	85.00	193.00	148.00
23 HS	56,000.0	209,600.0	196,800.0	1,360.00	3,088.00	2,368.00
24 HS	56,000.0	209,600.0	196,800.0	1,360.00	3,088.00	2,368.00
25 HS	350,000.0	1,310,000.0	1,230,000.0	8,500.00	19,300.00	14,800.00
26 HS	350,000.0	1,310,000.0	1,230,000.0	8,500.00	19,300.00	14,800.00
27 CS	34,680.0	73,840.0	72,000.0	297.00	3,070.00	39.00
28 CS	34,680.0	73,840.0	72,000.0	297.00	3,070.00	39.00
29 CS	34,680.0	73,840.0	72,000.0	297.00	3,070.00	39.00
30 CS	34,680.0	73,840.0	72,000.0	632.00	1,020.00	428.00
31 CS	34,680.0	73,840.0	72,000.0	632.00	1,020.00	428.00
32 CS	34,680.0	73,840.0	72,000.0	632.00	1,020.00	428.00
33 HT	140.0	5,240.0	492.0	3.56	3.60	.13
34 HT	1,478.8	5,534.8	5,196.8	37.60	38.03	1.37
35 HT	3,500.0	13,100.0	12,300.0	89.00	90.00	3.24
36 HT	56,000.0	209,600.0	196,800.0	1,424.00	1,440.00	51.84
37 HT	350,000.0	1,310,000.0	1,230,000.0	8,900.00	9,000.00	324.00
38 CT	34,680.0	73,840.0	72,000.0	297.00	307.00	39.00

TABLE IX. VARIATION OF DAVI WEIGHT WITH STATIC DEFLECTION					
m_{oi} (slugs)	$\sum m_{oi}$ (lb)	K_{oi} (lb/ft)	$\sum K_{oi}$ (lb/ft)	$\left(\frac{\sum m_{oi}}{m_s}\right) 100$ (%)	δ_{st} (in.)
.7112	91.602	311,994	1,247,976	1.409	.050
.4742	61.077	207,997	831,988	.939	.075
.3556	45.800	155,997	623,988	.704	.100
.2845	36.640	124,797	499,188	.563	.125

Table X summarizes the natural frequencies of the coupled system. Using the mode shape as a guide, each natural frequency was associated with a predominant response and was thus identified.

Certain goals were established as the objectives of this feasibility study:

1. Isolation of the fuselage.
2. Design for minimum static deflection at a minimum weight penalty.
3. Antiresonant isolation at the predominant excitation frequency.
4. Isolation at all multiples of N/rev frequencies up to 4N/rev.
5. Minimum amplification at 1/rev. Effectivity should be $\geq .90$.
6. All natural frequencies above 1/rev.

Having set forth these goals, the results will be divided into two groups:

1. Rotor isolation of helicopters, and
2. Rotor isolation of compound helicopters.

TABLE X. NATURAL FREQUENCIES OF COUPLED
DAVI ROTOR ISOLATION SYSTEM

Case	$f_{1/\text{rev}}$ (cps)	f_{n_x} (cps)	f_{n_y} (cps)	f_{n_z} (cps)	f_{n_α} (cps)	f_{n_β} (cps)	f_{n_ψ} (cps)
1 HS	6.883	250.2738	12.1500	12.3579	12.0300	13.0547	96.0133
2 HS	6.883	267.0095	15.8779	16.5407	16.0134	18.9939	141.8710
3 HS	6.883	284.2272	18.3960	20.1040	19.2624	24.2346	184.2538
4 HS	4.950	188.8716	9.4741	9.2660	8.7093	8.8346	54.4310
5 HS	4.950	193.4519	12.9000	13.0837	12.9500	13.6406	80.3538
6 HS	4.950	201.2303	14.5344	16.1877	14.0498	17.4183	104.2435
7 HS	4.367	20.2875	10.7097	11.3995	10.3899	12.2229	14.9819
8 HS	4.367	26.6078	12.5244	13.9633	12.3793	15.6116	21.4375
9 HS	4.367	32.3704	13.9738	16.1337	13.8737	19.0939	27.8912
10 HS	2.950	26.3047	10.2490	13.5378	10.1711	14.7155	23.4685
11 HS	2.950	34.4522	16.2342	14.7005	10.9800	11.0600	29.7846
12 HS	2.767	19.7581	11.8946	11.3190	8.8640	9.0319	16.1959
13 HS	2.267	23.1331	9.6620	12.6126	9.5261	13.4888	19.9745
14 HS	6.883	221.9752	11.9300	12.2100	12.8547	13.0487	49.5878
15 HS	6.883	226.9735	15.7097	15.6839	18.3809	18.9709	71.5144
16 HS	6.883	232.2015	18.1731	18.2485	22.9968	24.1985	90.6590
17 HS	4.950	171.8750	9.4813	8.9298	9.3251	8.8540	28.4116
18 HS	4.950	174.3491	10.8900	13.2900	12.8800	13.6898	41.3006
19 HS	4.950	175.7760	14.1018	14.6971	16.7819	17.3755	51.0184
20 HS	4.367	17.9721	10.3333	11.3568	10.6162	12.1533	13.1423
21 HS	4.367	26.0508	12.1406	14.0491	12.7793	15.5801	18.0849
22 HS	4.367	29.5324	13.4104	14.3765	16.2539	19.0360	22.4112
23 HS	2.950	14.6036	9.6839	12.1133	9.4918	15.0939	13.2725
24 HS	2.950	10.7081	10.1018	13.7661	16.6542	16.8062	14.5108
25 HS	2.267	20.3506	8.2342	10.5884	8.2532	11.4268	12.0525
26 HS	2.267	11.1032	8.7210	13.4756	8.2390	13.8137	11.2894
27 CS	3.500	18.9930	8.3580	10.0240	8.4820	11.2020	15.5160
28 CS	3.500	22.1550	9.2400	12.5310	9.8600	14.0020	18.7630
29 CS	3.500	27.5420	12.5290	15.0390	12.8600	16.8050	22.8950
30 CS	3.500	158.4510	8.7970	10.5740	9.8960	11.1600	53.1740
31 CS	3.500	174.1900	10.4830	12.7410	11.8920	13.5240	60.9970
32 CS	3.500	10.8090	11.9330	15.0400	16.1060	14.2930	17.0200

ROTOR ISOLATION OF HELICOPTER

Using the computer program, calculations were done for five statistical helicopters with varying numbers of blades and upper body weights. Effectivities were obtained for each of the coupled responses as a function of frequency. Included in this frequency sweep were the effectivities at 1/rev, N/rev, 2N/rev, 3N/rev, and 4N/rev. All data presented hereafter, unless specified otherwise, include no damping either across the DAVI or across the conventional isolator.

Table XI summarizes the effectiveness for the steady-state cases at 1/rev and shows that in nearly all cases, the effectivity (E) was kept above .90. Of the 130 effectivities shown in this table, 68 were above .95 while only 4 were below .90. The effectivity at 1/rev can be modified in either direction, that is, above .90 or below .90, by modifying the requirements of static deflection. However, by doing this, the DAVI weight enters into the compromise. Thus, (E) at 1/rev can be increased, bringing about weight penalties of the DAVI.

This study, so far, has indicated that 1/rev amplification can be held to a minimum. Although compromises were made in weight tradeoffs to obtain the desired low static deflections, as shown in Table X, another desirable feature was obtained, namely, increasing the 1/rev effectivity. By no means is the tradeoff study optimum; it merely reflects the feasibility and flexibility of passive DAVI-type isolation.

There appeared to be no significant difference between the first 13 cases, which had no offset cg, and the next 13 cases, which had the offset cg.

Table XII summarizes the effectivities at N/rev or the predominant excitation frequency. Although, theoretically, the effectivity in the vertical, lateral, and roll mode should be infinity at N/rev, since there is no damping included, the computer results present a finite value which offers excellent isolation at N/rev. Review of these data shows, however, that better isolation or effectivity is obtained for the first 13 cases (1 HS through 13 HS), which have no horizontal cg offset, than for the remaining 13 cases, which include the horizontal cg offset. More precise tuning, of course, would help to increase the effectivity. This does not yet explain the difference between the effectivity of the first 13 cases and that of the remaining 13 cases.

TABLE XI. EFFECTIVITY AT 1/REV					
Case	E_x	E_x	E_z	E_y	E_θ
1 HS	.90	.90	.93	.89	.90
2 HS	.92	.92	.94	.91	.91
3 HS	.92	.92	.95	.91	.92
4 HS	.93	.95	.97	.96	.94
5 HS	.93	.94	.98	.94	.93
6 HS	.95	.96	.98	.97	.95
7 HS	.90	.90	.97	.94	.94
8 HS	.92	.93	.97	.95	.94
9 HS	.93	.93	.97	.94	.94
10 HS	.94	.96	.98	.96	.95
11 HS	.95	.96	.99	.96	.95
12 HS	.96	.97	.99	.98	.97
13 HS	.96	.97	.99	.98	.97
14 HS	.99	.97	.92	.88	.88
15 HS	.99	.98	.89	.90	.94
16 HS	.99	.98	.94	.90	.90
17 HS	.99	.98	.96	.95	.93
18 HS	.98	.99	.97	.95	.94
19 HS	.99	.99	.98	.96	.95
20 HS	.92	.91	.96	.93	.93
21 HS	.95	.94	.97	.94	.94
22 HS	.95	.95	.97	.94	.94
23 HS	.92	.91	.98	.95	.94
24 HS	.94	.94	.98	.96	.94
25 HS	.92	.91	.99	.98	.97
26 HS	.94	.94	.99	.98	.97

TABLE XII. EFFECTIVITY AT N/REV					
Case	E_{α}	E_x	E_z	E_y	E_{θ}
1 HS	25.3	8.9	223.4	488.9	314.3
2 HS	398.0	131.7	1,860.3	7,239.2	2,785.1
3 HS	116.6	43.6	3,170.1	16,883.7	4,817.5
4 HS	3.6	2.1	131.5	150.3	175.4
5 HS	14.2	5.8	1,411.2	4,226.2	3,176.1
6 HS	4.4	2.5	1,313.6	1,847.9	2,079.5
7 HS	7.5	2.3	1,066.6	1,796.0	1,748.5
8 HS	8.2	2.5	1,730.8	3,023.3	2,853.9
9 HS	9.6	3.0	3,917.5	7,433.8	6,713.0
10 HS	2.7	1.1	7,331.2	9,913.6	15,880.4
11 HS	2.9	1.2	4,702.8	6,324.1	10,159.3
12 HS	2.8	1.1	379.3	545.8	836.5
13 HS	2.8	1.1	2,731.2	3,915.1	6,069.4
14 HS	4.9	1.9	130.8	20.3	258.3
15 HS	6.0	2.4	63.1	21.0	2,772.1
16 HS	6.6	2.7	62.4	21.0	1,203.8
17 HS	2.2	1.3	196.8	48.0	124.1
18 HS	1.3	1.4	119.4	47.1	189.0
19 HS	2.4	1.4	210.3	72.1	920.0
20 HS	3.2	1.1	491.1	4.4	164.8
21 HS	3.8	1.3	399.5	27.1	963.8
22 HS	3.7	1.3	276.7	18.5	1,159.2
23 HS	4.0	1.8	650.8	1,117.6	15,488.5
24 HS	2.9	1.3	480.3	988.5	9,766.0
25 HS	4.8	2.1	162.5	418.3	447.2
26 HS	3.1	1.3	187.3	3,739.5	824.2

To establish the cause for variations in effectivity, an effort was made to change the vertical distance between the upper-body cg and the isolators, thus varying the inertia-coupling effect for Case 20 HS. The results and change in vertical effectivity versus the variation in vertical distance are plotted in Figure 7. The change in effectivity is substantial and points out that inertia coupling has a significant impact on effectivity; therefore, an optimum installation must include these inertia effects.

Figure 8 also shows the variation in vertical effectivity versus longitudinal distance between rigid-body cg and upper-body cg for Case 20 HS. Here, again, the inertia coupling enters into the picture and affects the effectivity substantially.

Tables XIII, XIV, and XV present the effectivities at 2N/rev, 3N/rev, and 4N/rev respectively. As will be noted, the DAVI rotor isolation system provides isolation up to and including 4N/rev in the vertical and lateral directions and conventional isolation in the longitudinal direction.

One of the problems in analyzing this system was the placement of natural frequencies so that the 1/rev amplification was a minimum with no amplification evident at N/rev, 2N/rev, 3N/rev, and 4N/rev. Although it was fairly routine when dealing with the DAVI natural frequencies, the longitudinal spring of conventional isolator inclusion became the problem. Therefore, parametric studies were conducted to select a conventional isolator spring that would meet the foregoing requirements. These natural frequencies are placed over the entire frequency sweep depending on configuration; as a result, they show their influence on the erratic behavior of the effectivities in longitudinal displacement (E_x) and in pitch (E_α).

Table XVI presents the normalized accelerations at the 1/rev, N/rev, 2N/rev, 3N/rev, and 4N/rev frequencies for vertical excitation. Using the excitation criterion shown in Figure 93(c) and multiplying it by the inverse of effectivity ($1/E_z$) for the various configurations, the result is the response in g's at the various frequencies normalized on the g level at N/rev.

Figures 9, 10, 11, 12, and 13 are typical curves of effectivity versus frequency for the 2000-pound helicopter with rotor plus transmission upper body (Case 1 HS), while Figures 14 through 18 present the various effectivities for the 100,000-pound helicopter (Case 12 HS). The natural frequencies, as discussed earlier, are evident in these frequency sweeps and, as mentioned, are such that none give amplification.

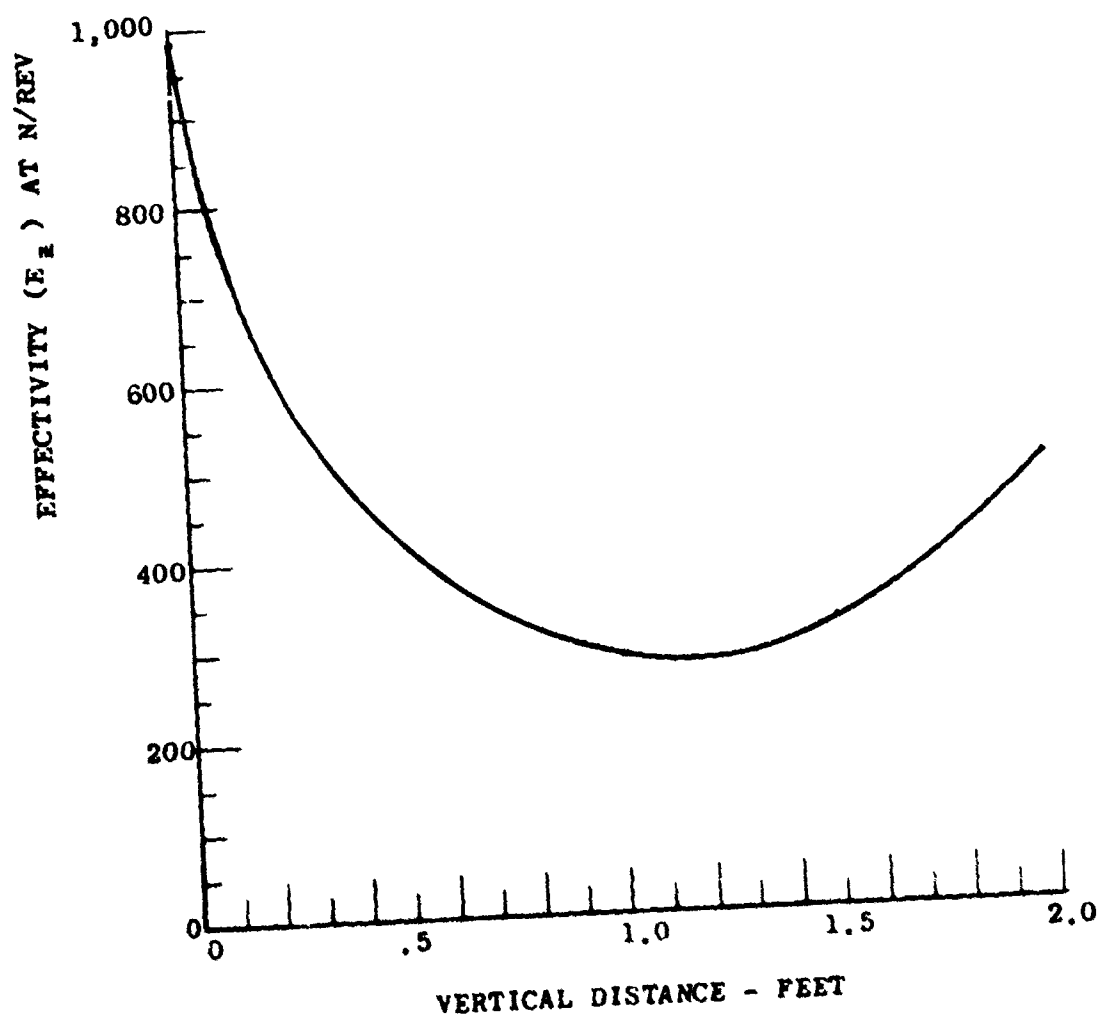


Figure 7. Vertical Effectivity at N/rev Versus Vertical Distance From DAVI Isolator to Upper-Body Center of Gravity for Case 20 HS.

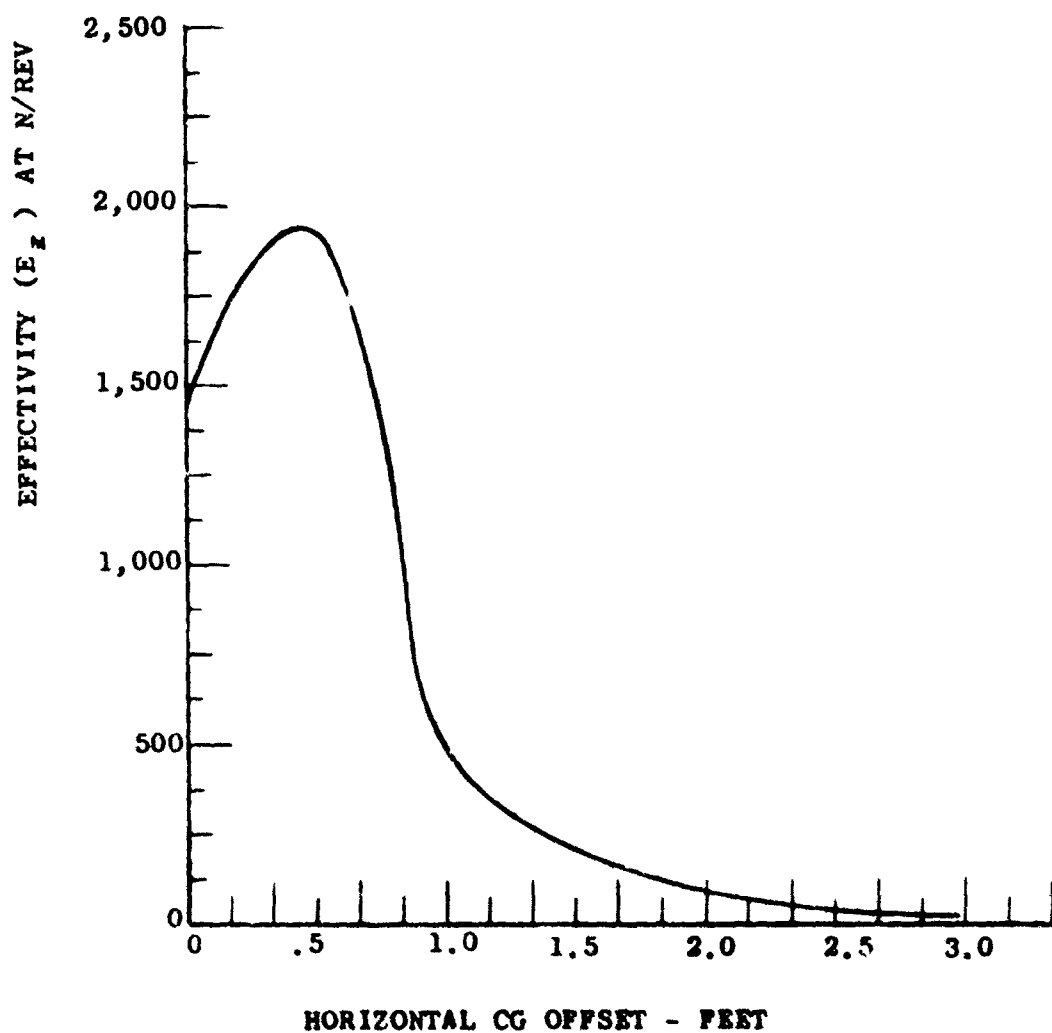


Figure 8. Vertical Effectivity at N/rev Versus Horizontal Distance From Upper-Body Center of Gravity to Rigid-Body Center of Gravity for Case 20 HS.

TABLE XIII. EFFECTIVITY AT 2N/REV					
Case	E_y	E_x	E_z	E_y	E_θ
1 HS	1.4	1.4	1.3	1.5	1.5
2 HS	1.9	1.8	1.7	2.3	2.0
3 HS	2.5	2.5	2.2	3.4	2.8
4 HS	1.2	1.2	1.2	1.3	1.3
5 HS	1.7	1.6	1.4	1.9	1.8
6 HS	1.7	1.5	1.7	2.1	2.2
7 HS	1.7	1.0	1.5	1.7	1.7
8 HS	2.0	1.1	1.8	2.3	2.3
9 HS	4.1	1.8	2.1	3.0	2.9
10 HS	2.8	1.3	2.0	2.6	3.3
11 HS	2.2	1.0	2.3	3.1	4.1
12 HS	3.2	1.3	1.6	2.1	2.5
13 HS	3.4	1.4	1.8	2.4	3.0
14 HS	1.3	1.1	1.3	1.6	1.5
15 HS	1.4	1.2	1.7	2.7	2.1
16 HS	1.6	1.3	2.1	5.4	3.1
17 HS	1.2	1.0	1.2	1.3	1.3
18 HS	5.0	2.9	1.4	1.7	1.7
19 HS	1.3	1.0	1.7	2.7	2.6
20 HS	2.8	1.5	1.5	1.8	1.8
21 HS	2.1	1.1	1.8	2.4	2.3
22 HS	4.4	1.9	2.2	3.1	2.9
23 HS	51.7	11.1	1.9	2.6	3.2
24 HS	730.1	9.3	2.3	3.0	3.9
25 HS	37.5	12.0	1.5	1.8	2.2
26 HS	355.5	9.3	1.6	2.1	2.6

TABLE XIV. EFFECTIVITY AT 3N/REV					
Case	E_{α}	E_x	E_z	E_y	E_{θ}
1 HS	1.3	1.3	1.3	1.4	1.4
2 HS	1.7	1.6	1.6	2.0	1.8
3 HS	2.2	2.2	2.0	3.0	2.5
4 HS	1.2	1.1	1.2	1.3	1.3
5 HS	1.5	1.4	1.3	1.8	1.7
6 HS	1.6	1.4	1.6	1.9	2.0
7 HS	21.9	4.0	1.4	1.6	1.6
8 HS	30.0	4.5	1.6	2.1	2.1
9 HS	110.3	6.6	2.0	2.7	2.6
10 HS	24.2	4.9	1.8	2.3	2.9
11 HS	15.7	4.3	2.1	2.8	3.6
12 HS	239.9	4.9	1.8	2.3	2.9
13 HS	104.0	5.1	1.7	2.2	2.7
14 HS	1.3	1.0	1.3	1.7	1.5
15 HS	1.3	1.1	1.6	4.0	2.4
16 HS	1.4	1.1	2.0	6.2	8.2
17 HS	1.2	1.0	1.2	1.0	1.1
18 HS	1.1	1.0	1.4	1.6	1.6
19 HS	1.2	1.0	1.6	1.5	1.6
20 HS	55.0	4.0	1.4	1.7	1.6
21 HS	21.4	4.2	1.7	2.2	2.1
22 HS	1,441.5	6.3	2.0	2.8	2.6
23 HS	17.4	27.3	1.8	2.4	2.9
24 HS	24.4	22.9	2.1	2.8	3.5
25 HS	16.4	29.4	1.4	1.8	2.1
26 HS	23.3	22.9	1.5	2.0	2.4

TABLE XV. EFFECTIVITY AT 4N/REV

Case	E_{α}	E_x	E_z	E_y	E_{θ}
1 HS	1.2	1.2	1.3	1.4	1.4
2 HS	1.6	1.5	1.5	2.0	1.8
3 HS	2.0	1.9	1.9	2.9	2.4
4 HS	1.2	1.1	1.2	1.2	1.2
5 HS	1.5	1.3	1.3	1.7	1.7
6 HS	1.4	1.2	1.6	1.9	1.9
7 HS	20.9	8.5	1.4	1.6	1.6
8 HS	21.5	9.4	1.6	2.0	2.0
9 HS	16.3	13.6	1.9	2.6	2.5
10 HS	52.2	9.6	1.7	2.3	2.9
11 HS	722.9	8.3	2.1	2.8	3.5
12 HS	16.4	10.1	2.8	1.9	1.4
13 HS	24.6	9.0	1.6	2.2	2.6
14 HS	1.2	1.0	1.3	1.2	1.2
15 HS	1.2	1.0	1.6	1.4	1.4
16 HS	-	-	-	-	-
17 HS	1.1	1.0	1.2	1.2	1.2
18 HS	1.0	1.0	1.4	1.6	1.6
19 HS	1.1	.9	1.6	1.7	1.8
20 HS	15.4	11.3	1.4	1.6	1.6
21 HS	27.0	8.8	1.7	2.1	2.0
22 HS	17.7	13.7	2.0	2.7	2.6
23 HS	14.3	50.6	1.8	2.3	2.8
24 HS	18.6	40.1	2.0	2.7	3.4
25 HS	13.7	57.5	1.4	1.7	2.0
26 HS	18.5	38.0	1.5	1.9	2.3

TABLE XVI. NORMALIZED ACCELERATION FOR THE VERTICAL EXCITATION ONLY					
Case	$\frac{1/\text{rev g's}}{\text{g's N/rev}}$	$\frac{\text{N/rev g's}}{\text{g's N/rev}}$	$\frac{2\text{N/rev g's}}{\text{g's N/rev}}$	$\frac{3\text{N/rev g's}}{\text{g's N/rev}}$	$\frac{4\text{N/rev g's}}{\text{g's N/rev}}$
1 HS	.1075	.004470	.3078	.07692	.07692
2 HS	.1084	.000537	.2353	.0625	.06666
3 HS	.1053	.000315	.1818	.0500	.05263
4 HS	.1031	.00780	.3333	.08333	.08333
5 HS	.1020	.000709	.2857	.07692	.07692
6 HS	.1020	.000761	.2353	.0625	.0625
7 HS	.1031	.000937	.26667	.07142	.07142
8 HS	.1031	.000578	.2222	.0625	.0625
9 HS	.1031	.000255	.1904	.0500	.05263
10 HS	.1020	.000138	.2000	.05555	.05882
11 HS	.1010	.000213	.1739	.04762	.04762
12 HS	.1010	.002638	.2500	.05555	.03571
13 HS	.1010	.000366	.2222	.05882	.0625
14 HS	.1087	.00769	.3077	.07692	.07692
15 HS	.1121	.0158	.2353	.0625	.0625
16 HS	.1064	.01602	.1904	.0500	-
17 HS	.1042	.005081	.3333	.08333	.08333
18 HS	.1031	.0084	.2857	.07142	.07142
19 HS	.1020	.00476	.2353	.0625	.0625
20 HS	.1042	.002038	.2667	.07142	.07142
21 HS	.1031	.002506	.2222	.05882	.05882
22 HS	.1031	.00361	.1818	.0500	.0500
23 HS	.1020	.001536	.2105	.05555	.05555
24 HS	.1020	.002084	.1739	.04762	.0500
25 HS	.1000	.006153	.2667	.07142	.07142
26 HS	.1010	.00533	.2500	.06666	.06666

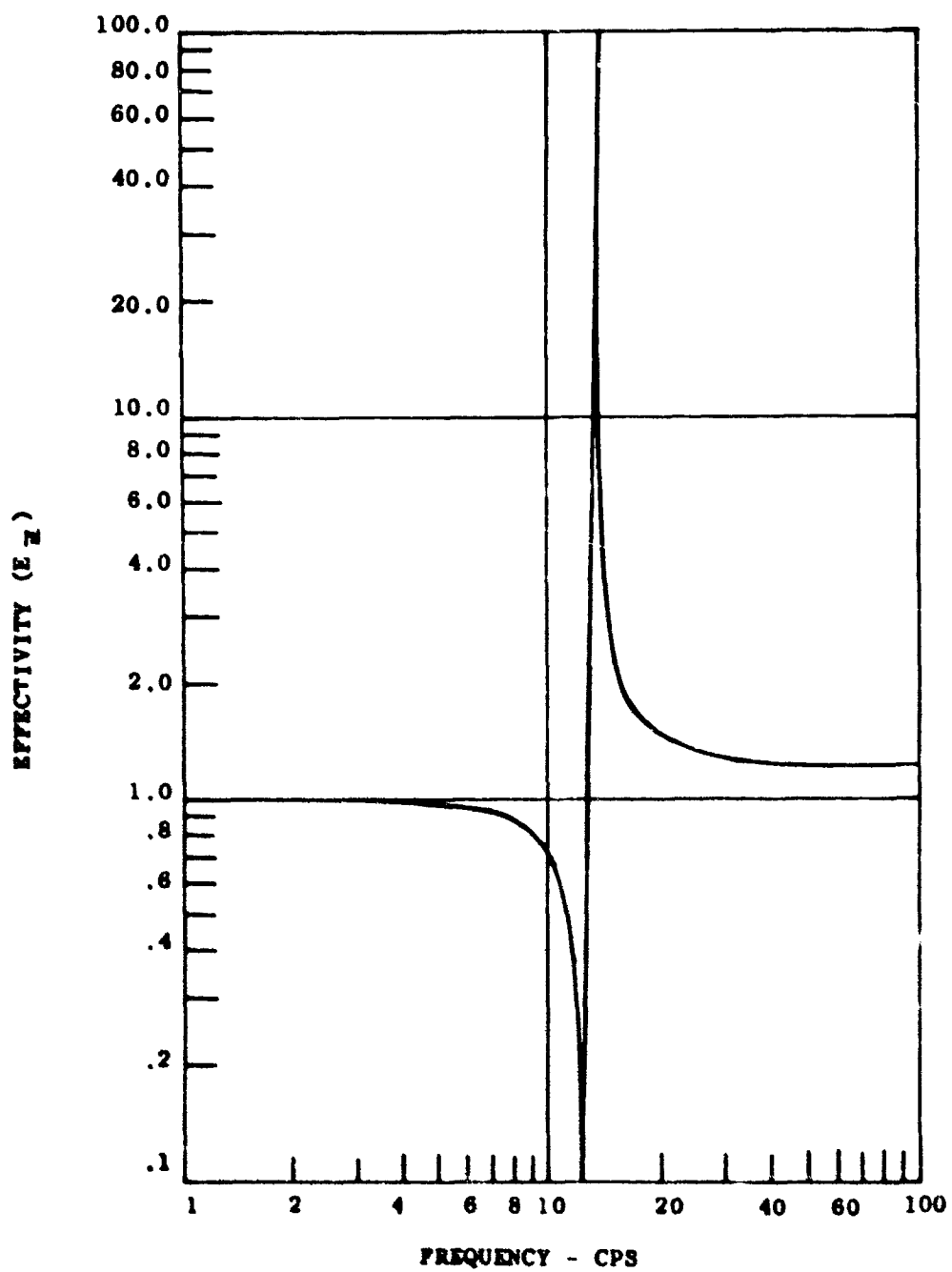


Figure 9. Vertical Effectivity for Case 1 HS Versus Frequency.

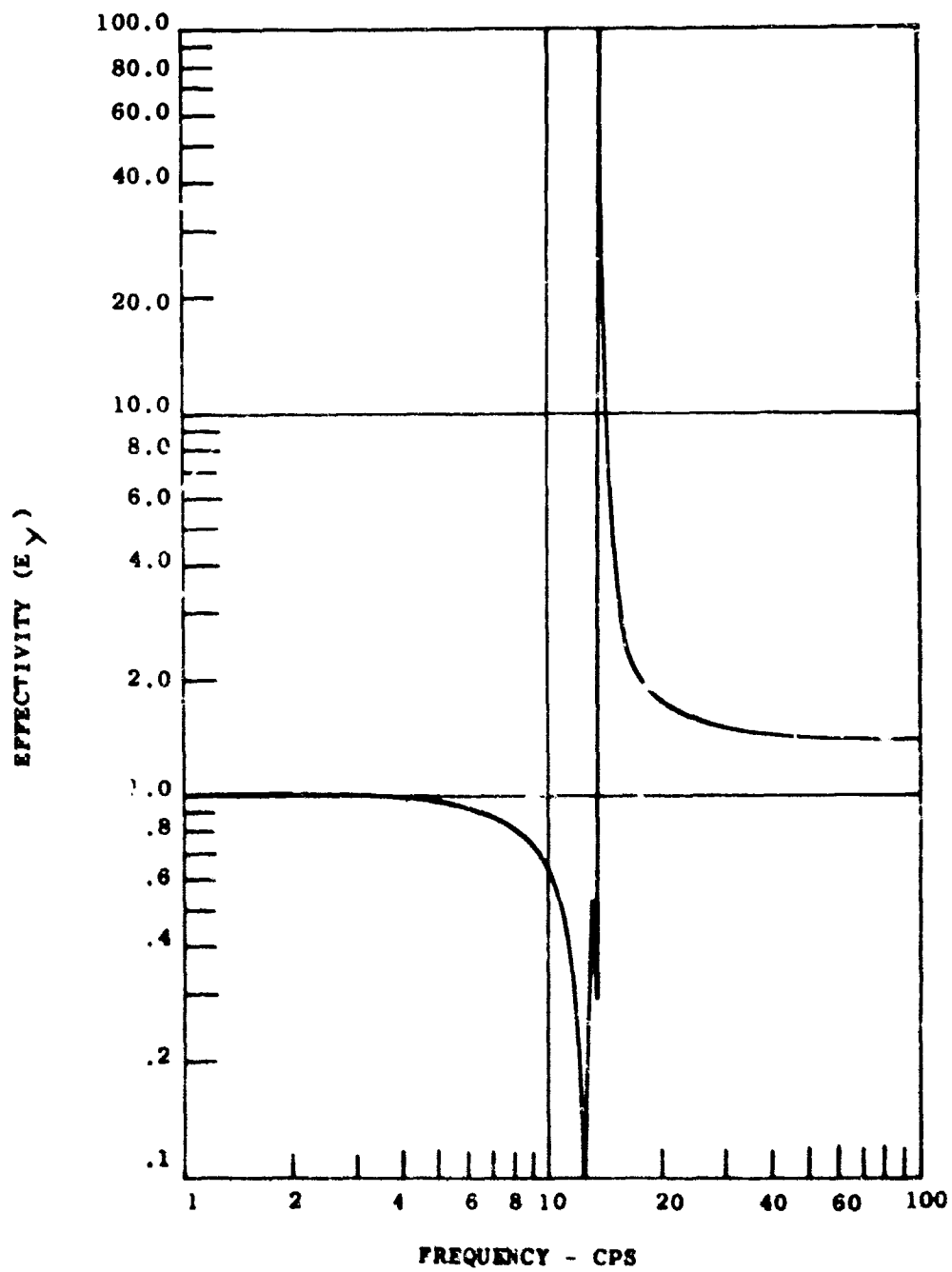


Figure 10. Lateral Effectivity for Case 1 HS Versus Frequency.

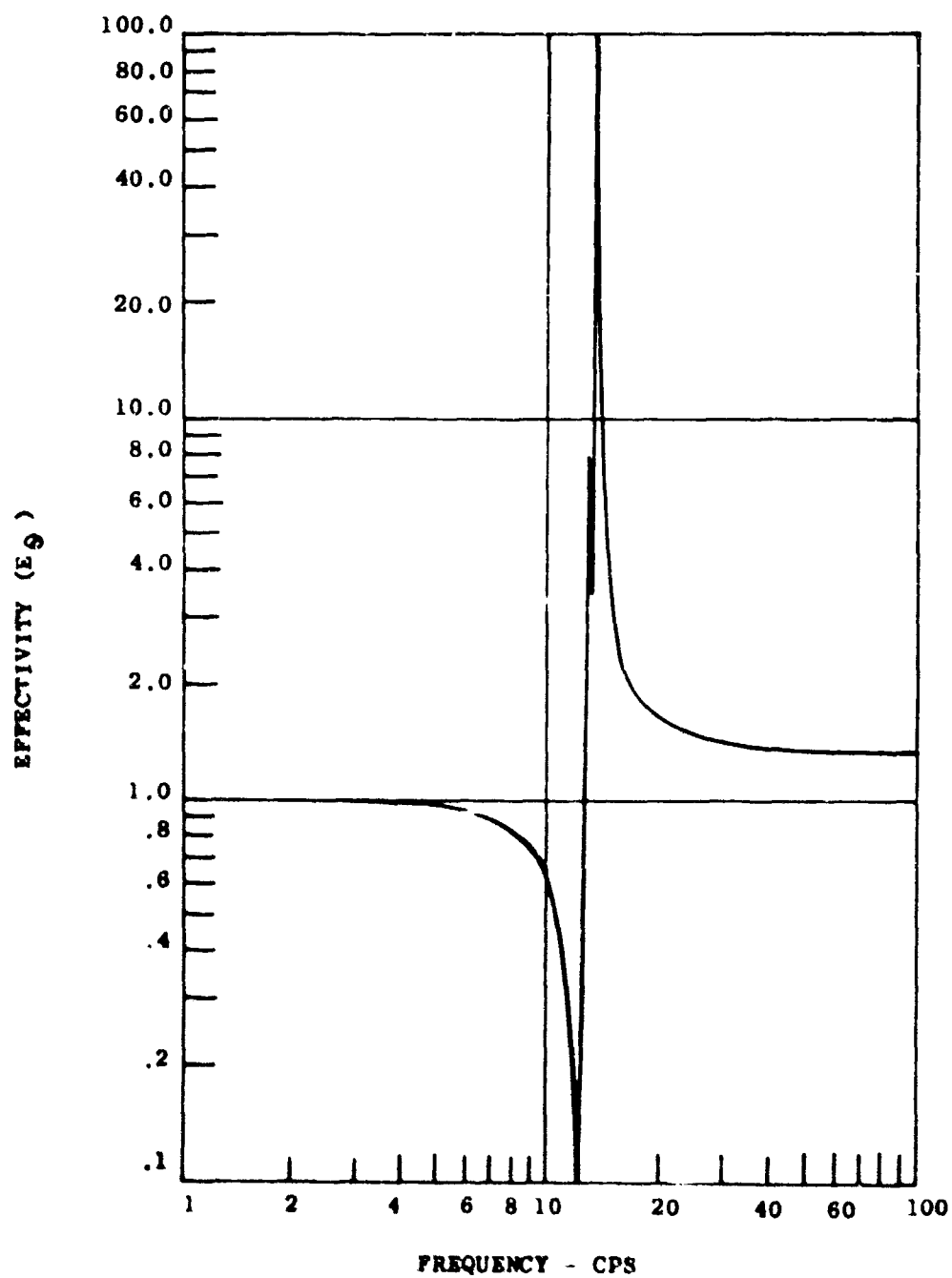


Figure 11. Roll Effectivity for Case 1 HS Versus Frequency.

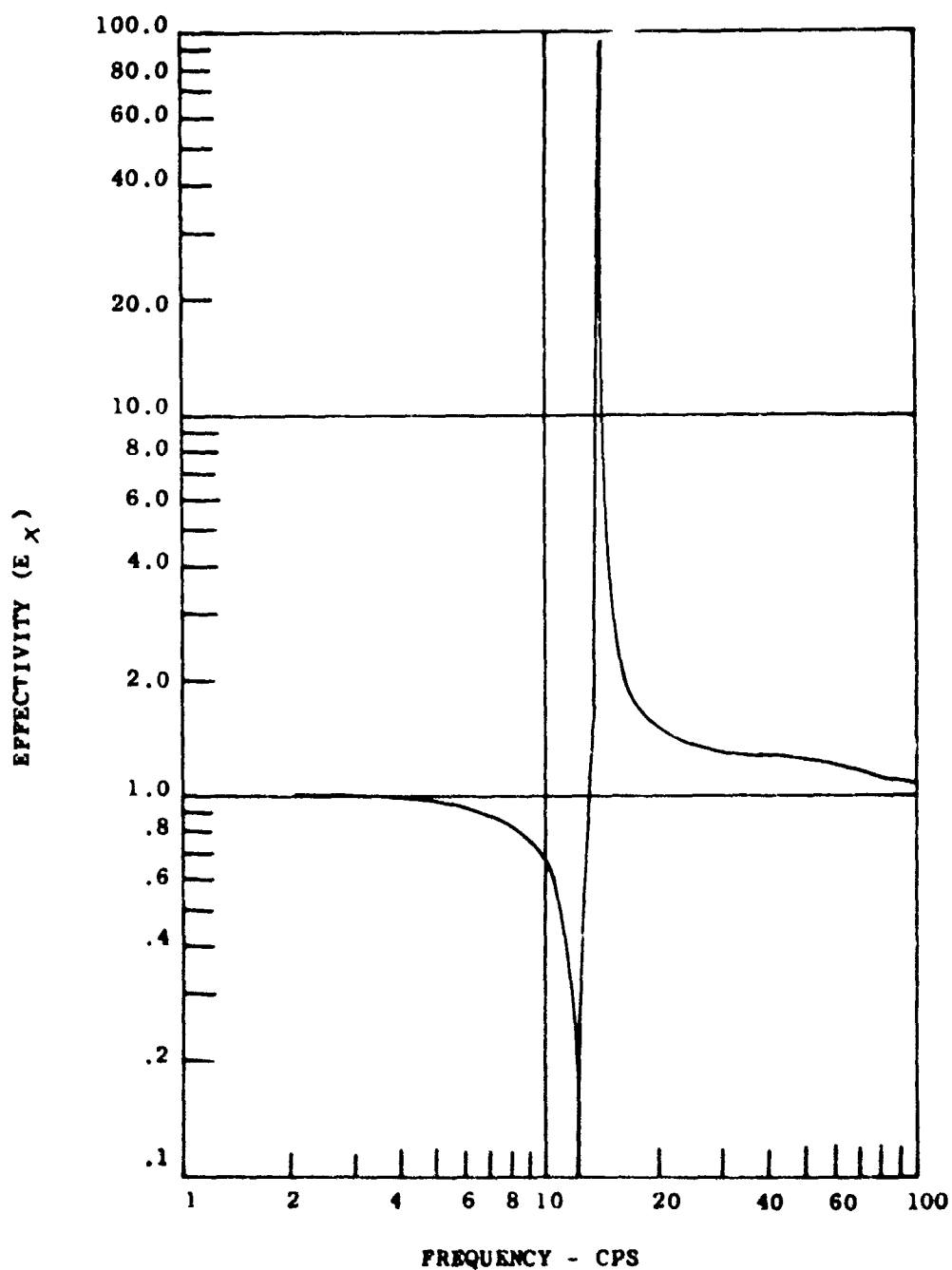


Figure 12. Longitudinal Effectivity for Case 1 HS Versus Frequency.

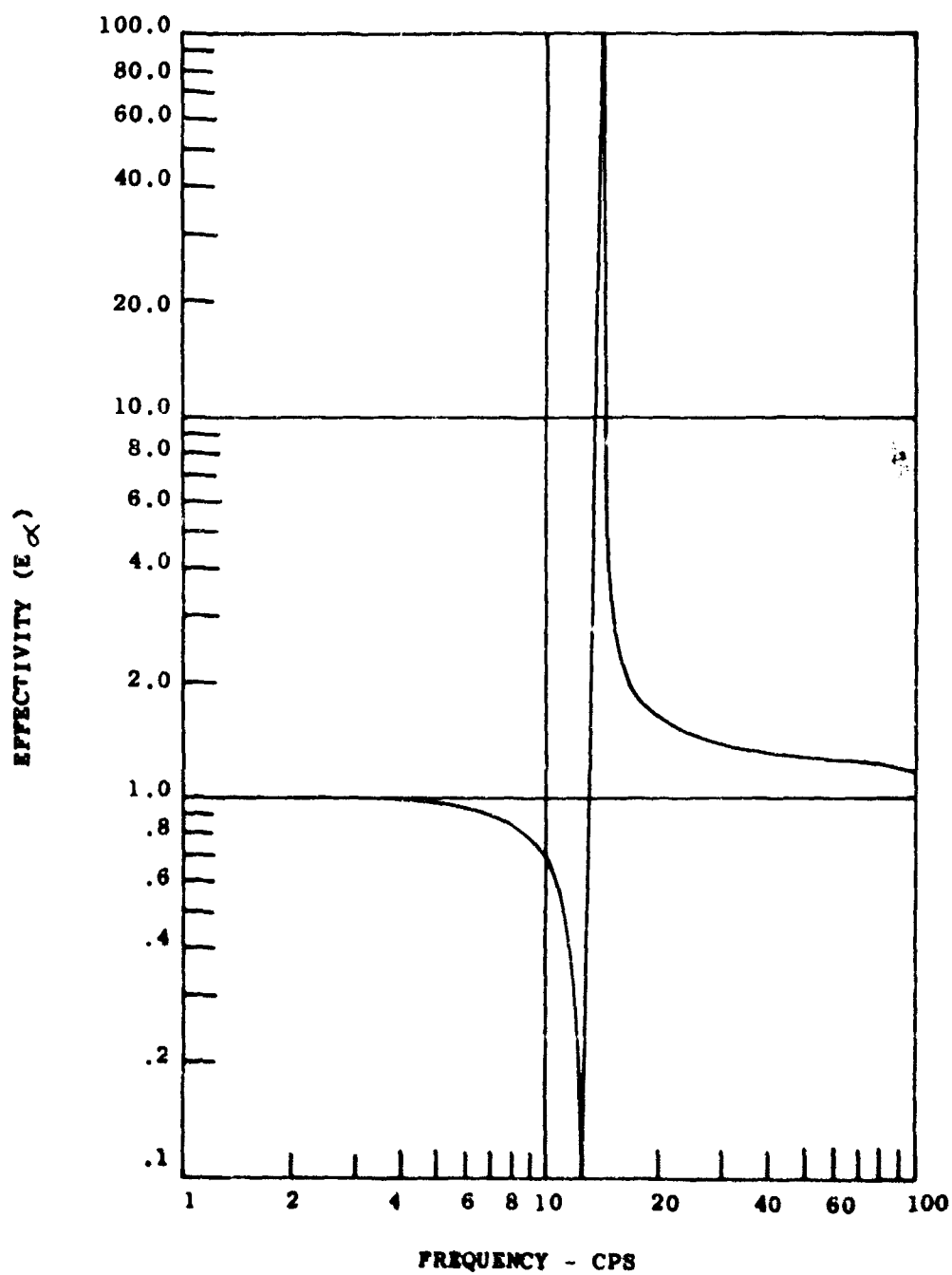


Figure 13. Pitch Effectivity for Case 1 HS Versus Frequency.

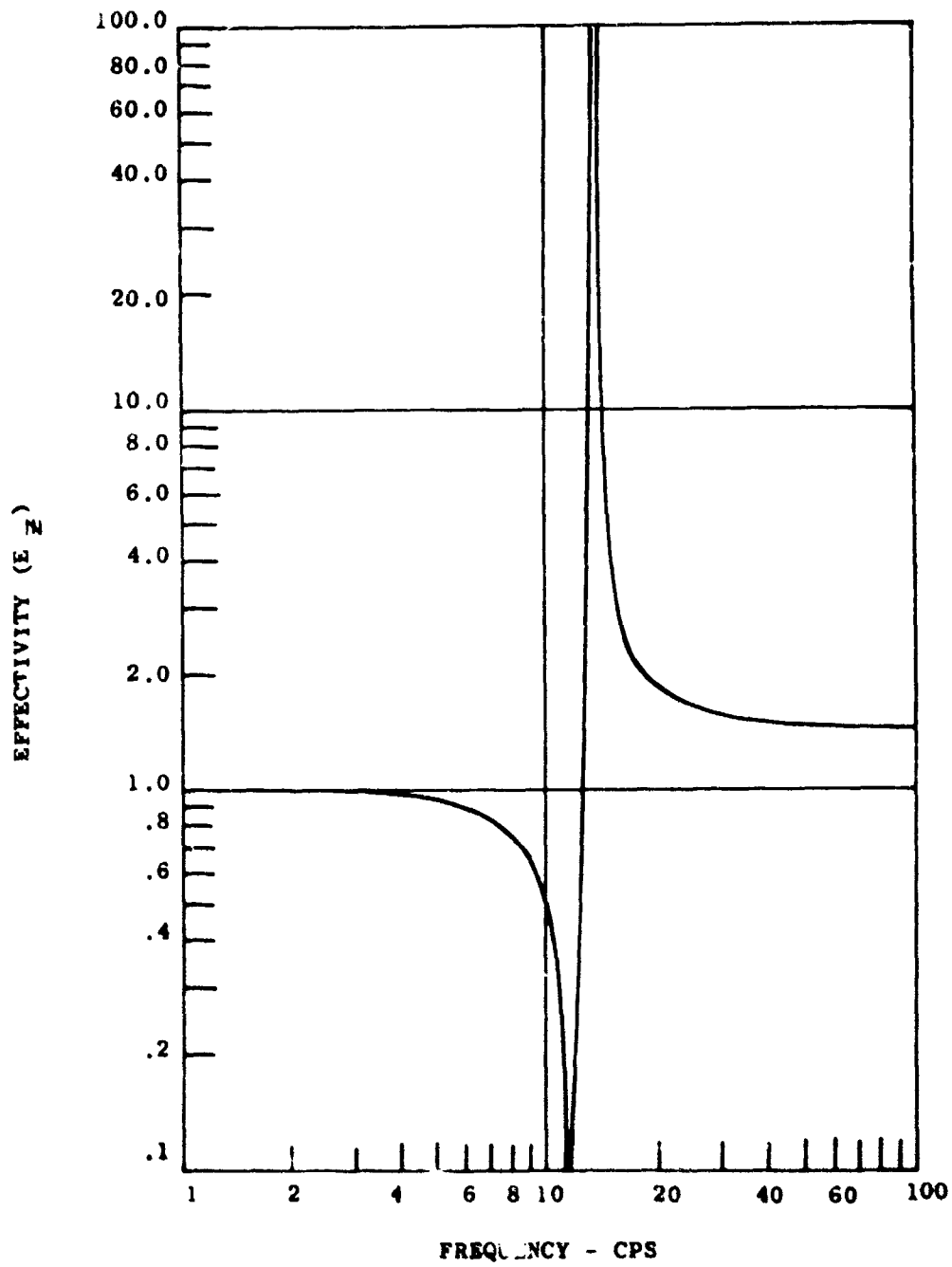


Figure 14. Vertical Effectivity for Case 12 HS Versus Frequency.

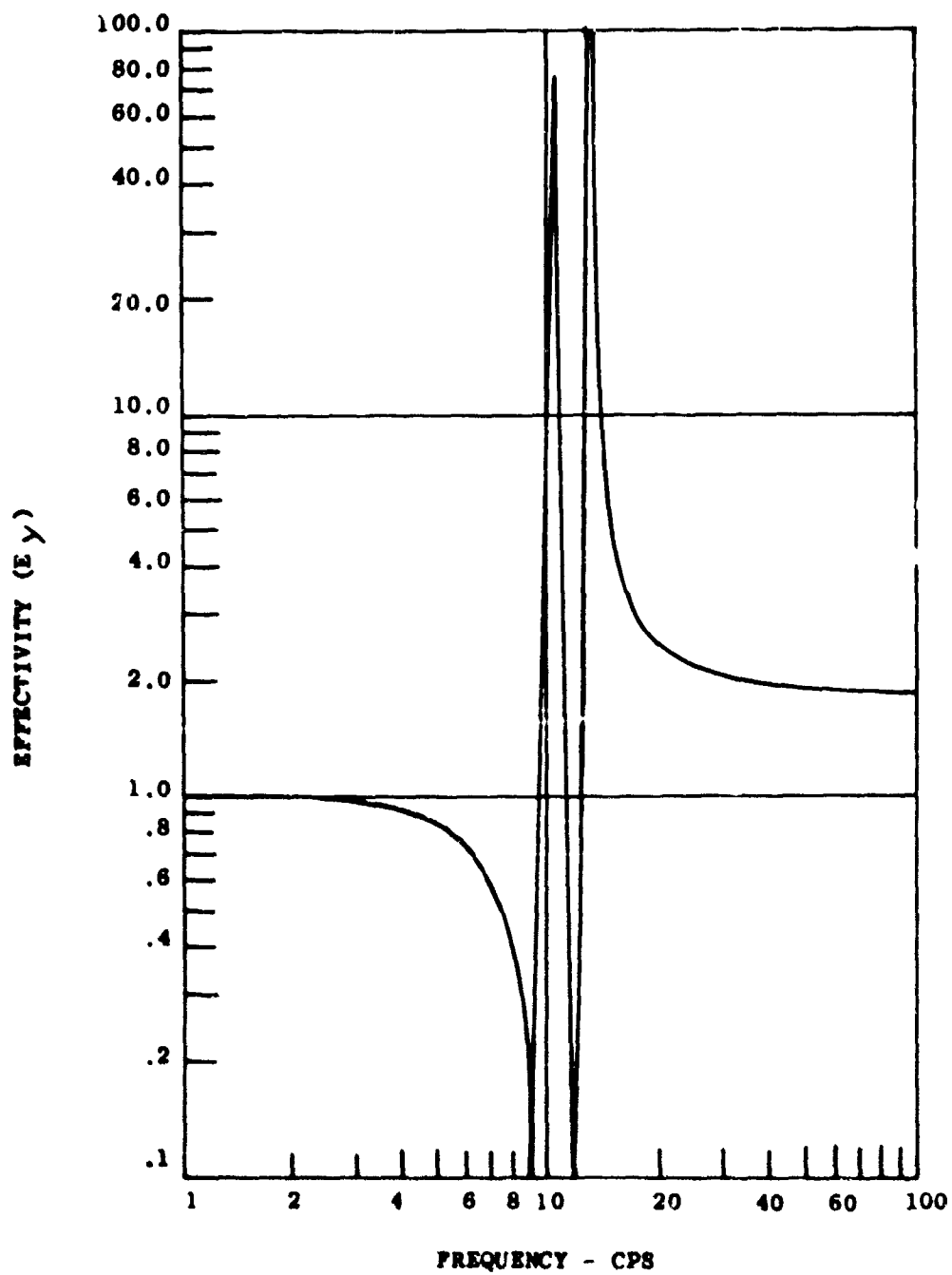


Figure 15. Lateral Effectivity for Case 12 HS Versus Frequency.

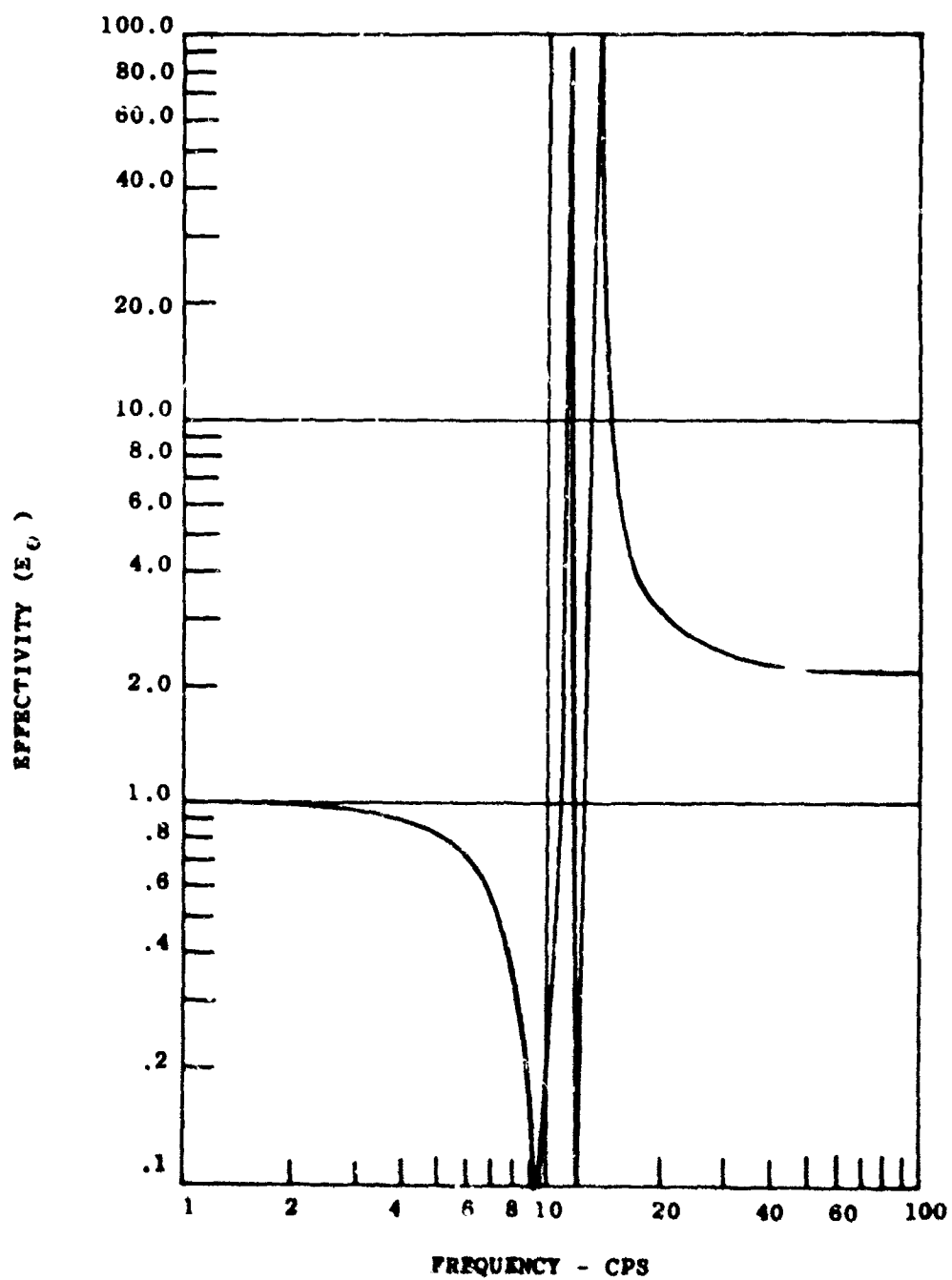


Figure 16. Roll Effectivity for Case 12 HS Versus Frequency.

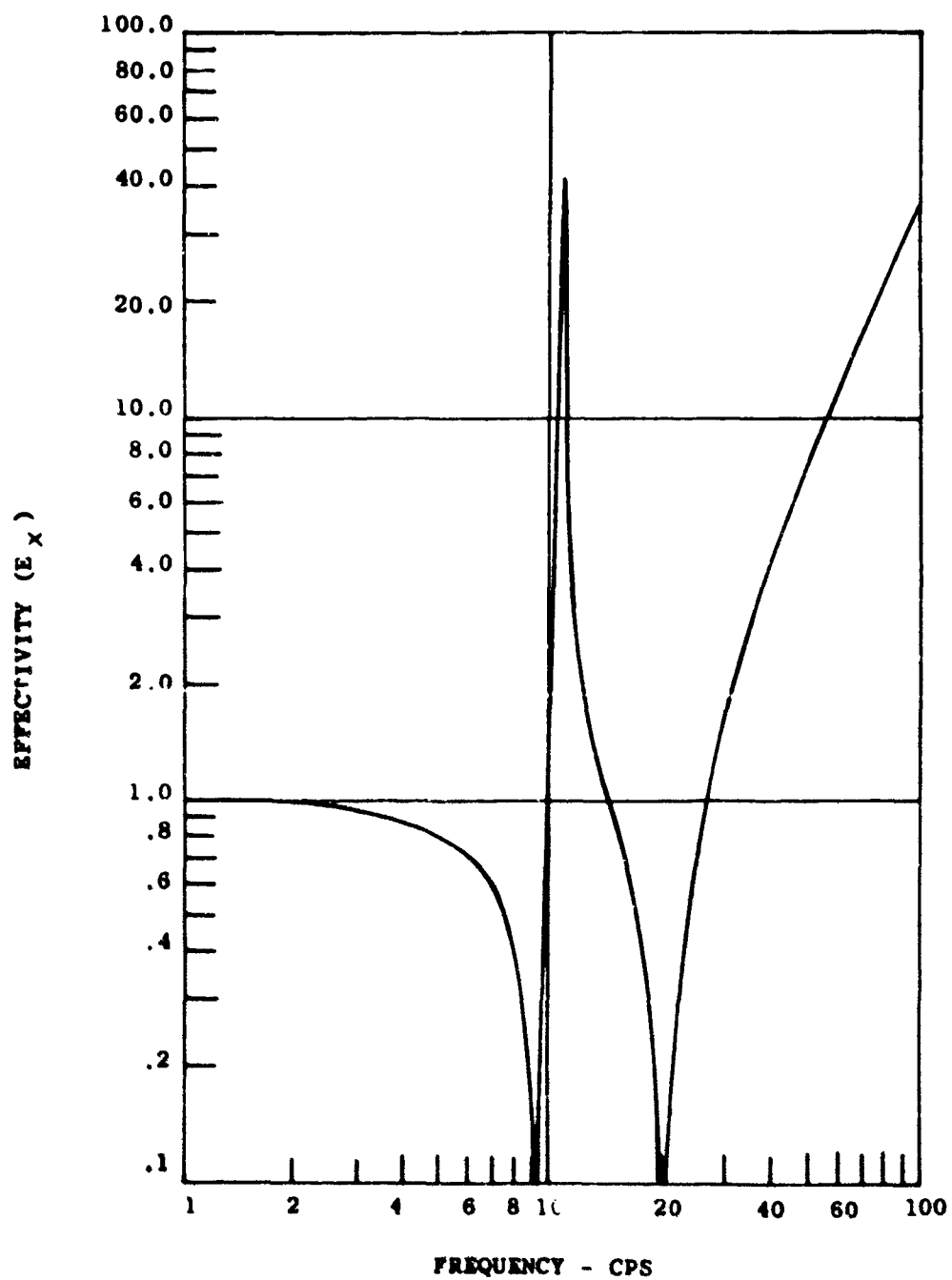


Figure 17. Longitudinal Effectivity for Case 12 HS Versus Frequency.

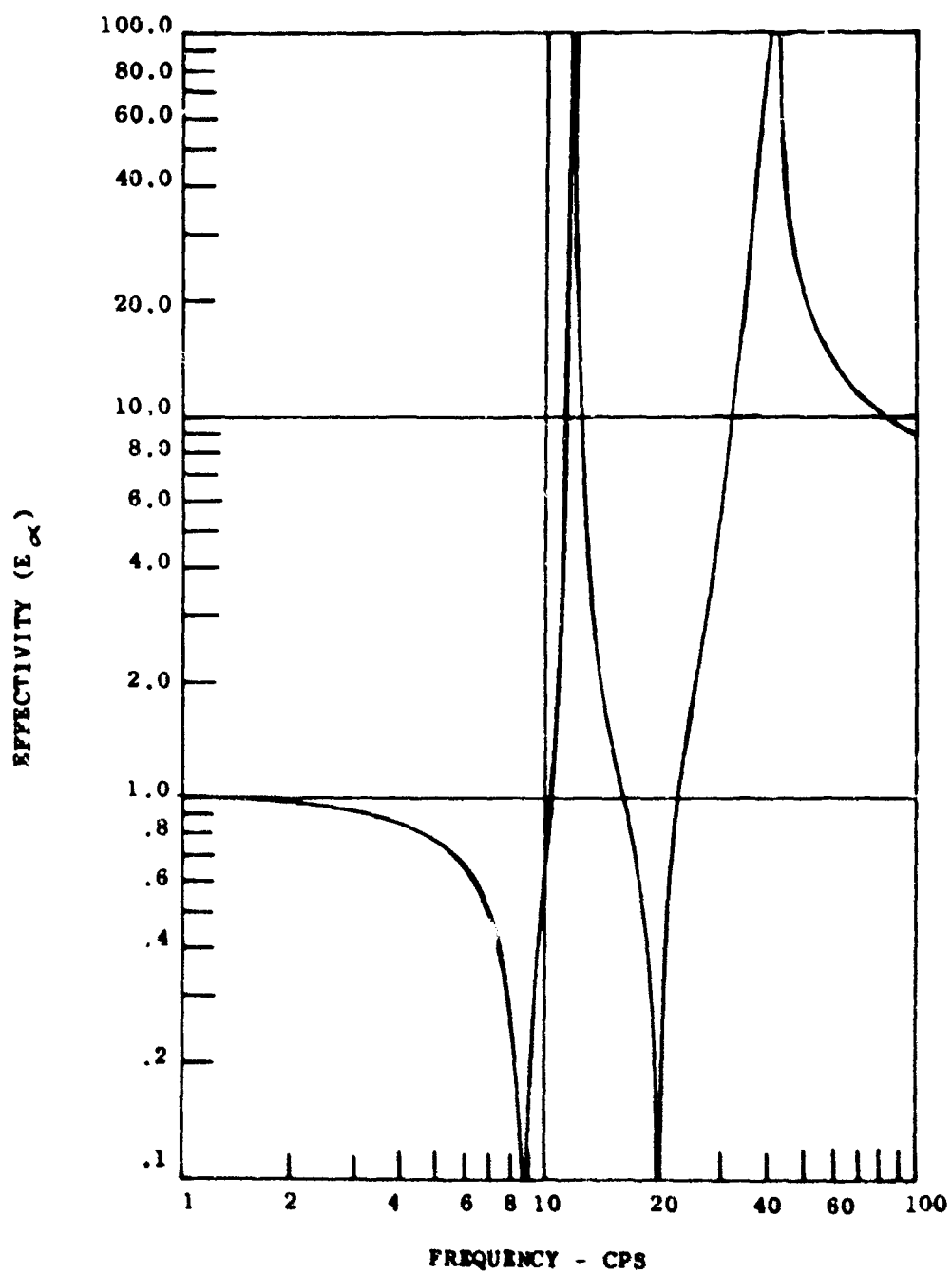


Figure 18. Pitch Effectivity for Case 12 HS Versus Frequency.

Figures 19 through 23 show the various effectivities for the 2000-pound, horizontally offset cg case, and Figures 24 through 28 present the effectivities for the 100,000-pound helicopter for the rotor plus engine plus transmission configuration.

Damping across the DAVI in the rotor isolation analysis has the conventional effect of lowering the resonant peak or increasing effectivity; at the same time, it has the additional characteristic of reducing the degree of isolation at the antiresonance at the tuned or predominant frequency. This reduction in isolation is shown in Figure 29, which illustrates the vertical effectivity at the tuned frequency for several damping rates for Case 14 HS versus frequency.

Figure 29 also gives a good indication of the bandwidth which is obtainable with DAVI isolation at the tuned or predominant frequency. Case 14 HS illustrated here is typical and offers a bandwidth of isolation of $\pm 4\%$ minimum.

Figure 30 shows the variation in lower-body mass at the tuned or predominant frequency. Since the system is not perfectly tuned, there will be some variation, as is indicated. The change in effectivity, due to a plus or minus change of 40 slugs in lower-body mass, is small and provides better than 99% isolation even though it was not perfectly tuned.

Figure 31 presents the vertical effectivities for Case 17 HS for several arrangements of DAVI's, ranging from a 3-DAVI installation to an 8-DAVI installation. The vertical effectivity at the tuned frequency (N/rev) varies as the installation arrangement varies. The effectivity is not directly related to the number of DAVI's used; instead, the location of the DAVI's affects the results through inertia coupling of the system. The effectivity obtained for the DAVI arrangements shown is excellent, even though it varies. Proper design and location of such an installation would produce an optimum result.

Thus far, it has been demonstrated that it is feasible to obtain helicopter isolation with a tuned antiresonance at the predominant frequency using the unique features of the DAVI. In addition, all multiples of N/rev up to 4N/rev give isolation in all directions. Amplification at 1/rev was held to a minimum while static deflection was held to .10 inch or less. Therefore, helicopter isolation is feasible.

It is seen from these calculations that the results obtained for vertical and lateral isolation were excellent. The static deflection of the mounts was well within the design criteria imposed. Thus, for all maneuver loads, minimum deflection will occur and is easily in the realm of spring design, thus requiring no bottoming devices. Also, because of the stiffness required, the response of the helicopter to a control input will be similar to that of a rigid system.

It is also seen that the effectivities obtained for all helicopter configurations were excellent. Tuning the DAVI to the predominant Nth harmonic will virtually eliminate this critical vibratory problem. Since the isolation of the DAVI at its tuned frequency is not affected by the isolated mass, the vibratory characteristics of the helicopter due to a variation of gross weight will not be changed.

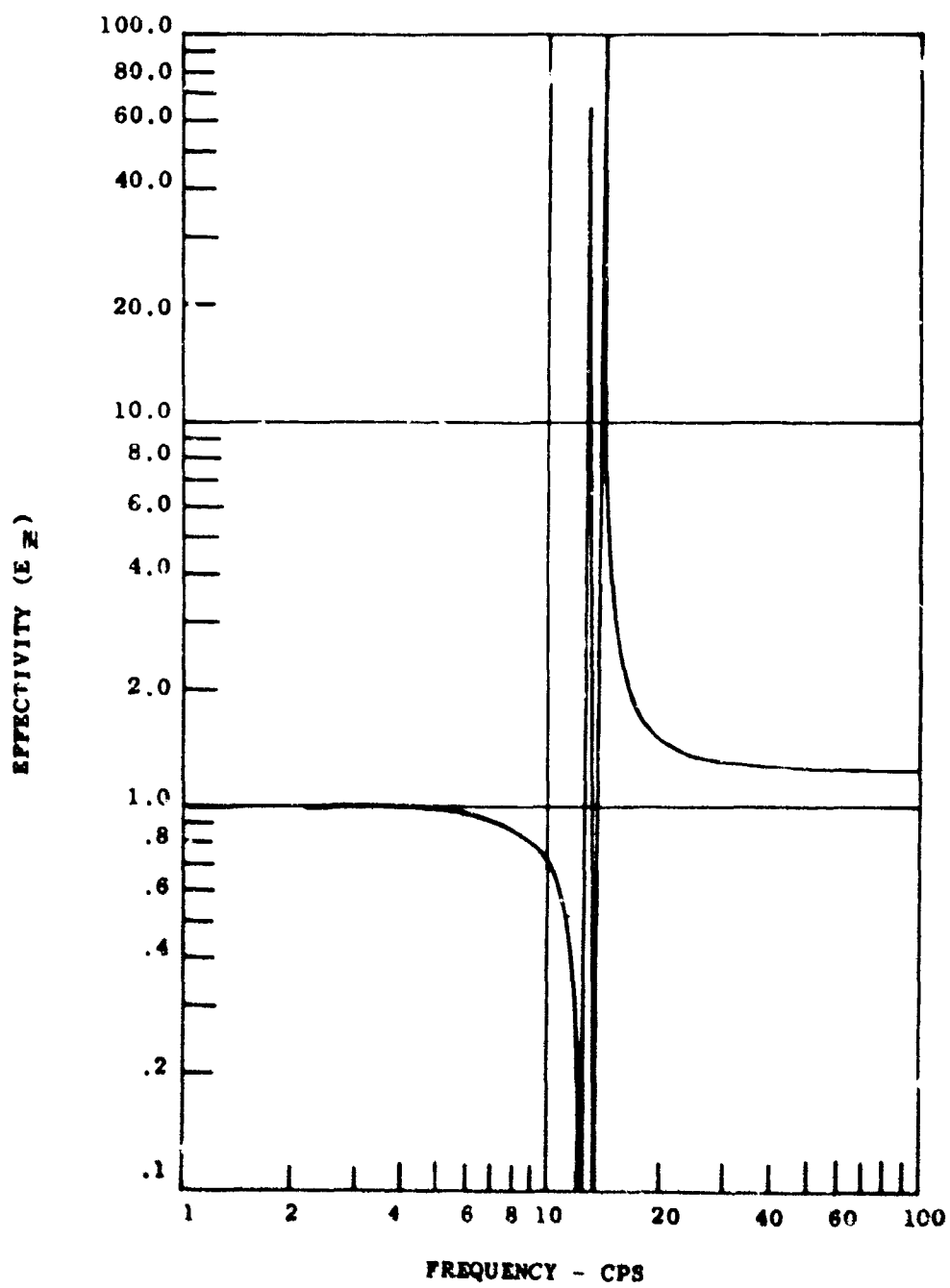


Figure 19. Vertical Effectivity for Case 14 HS Versus Frequency.

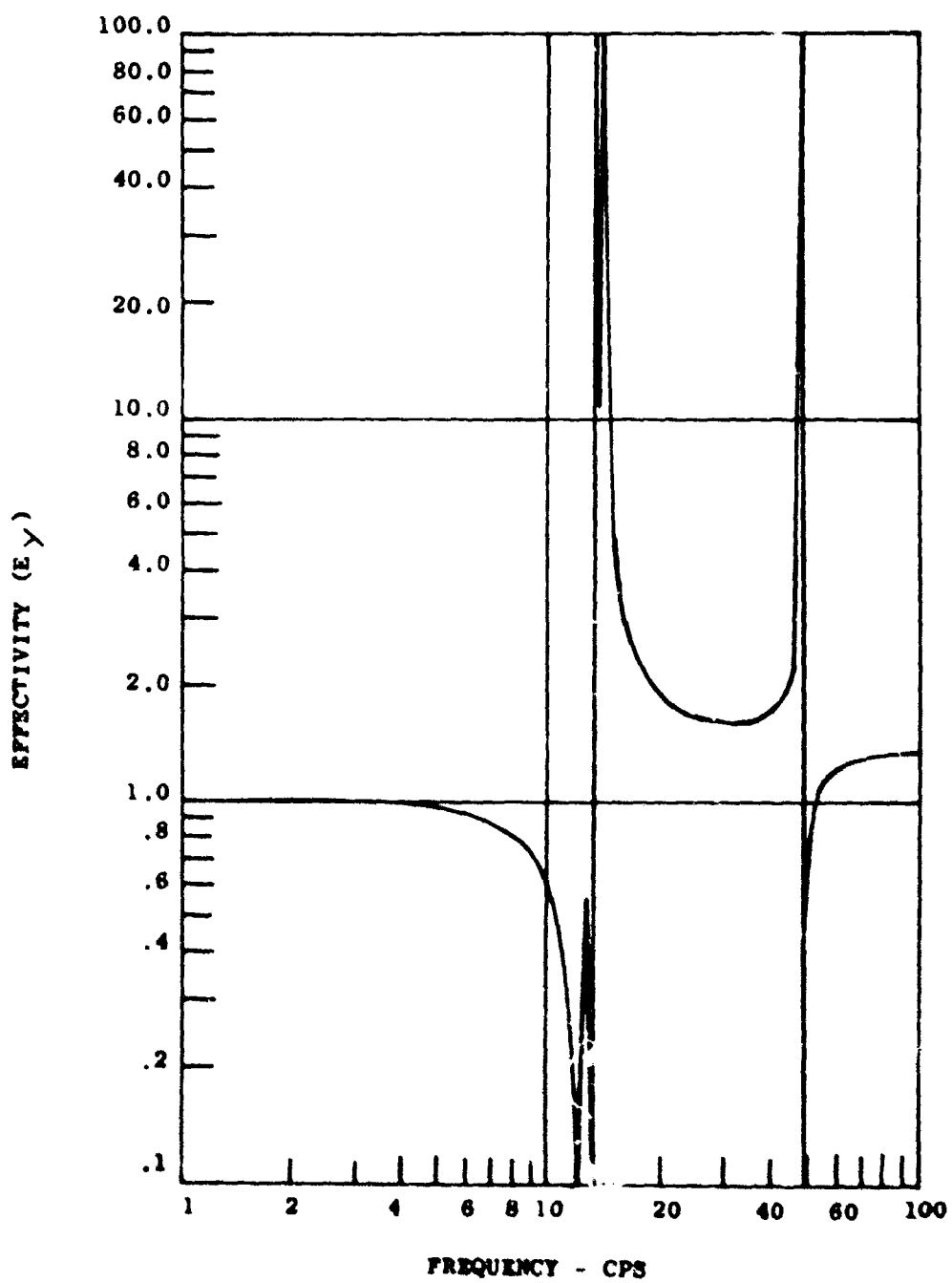


Figure 20. Lateral Effectivity for Case 14 HS Versus Frequency.

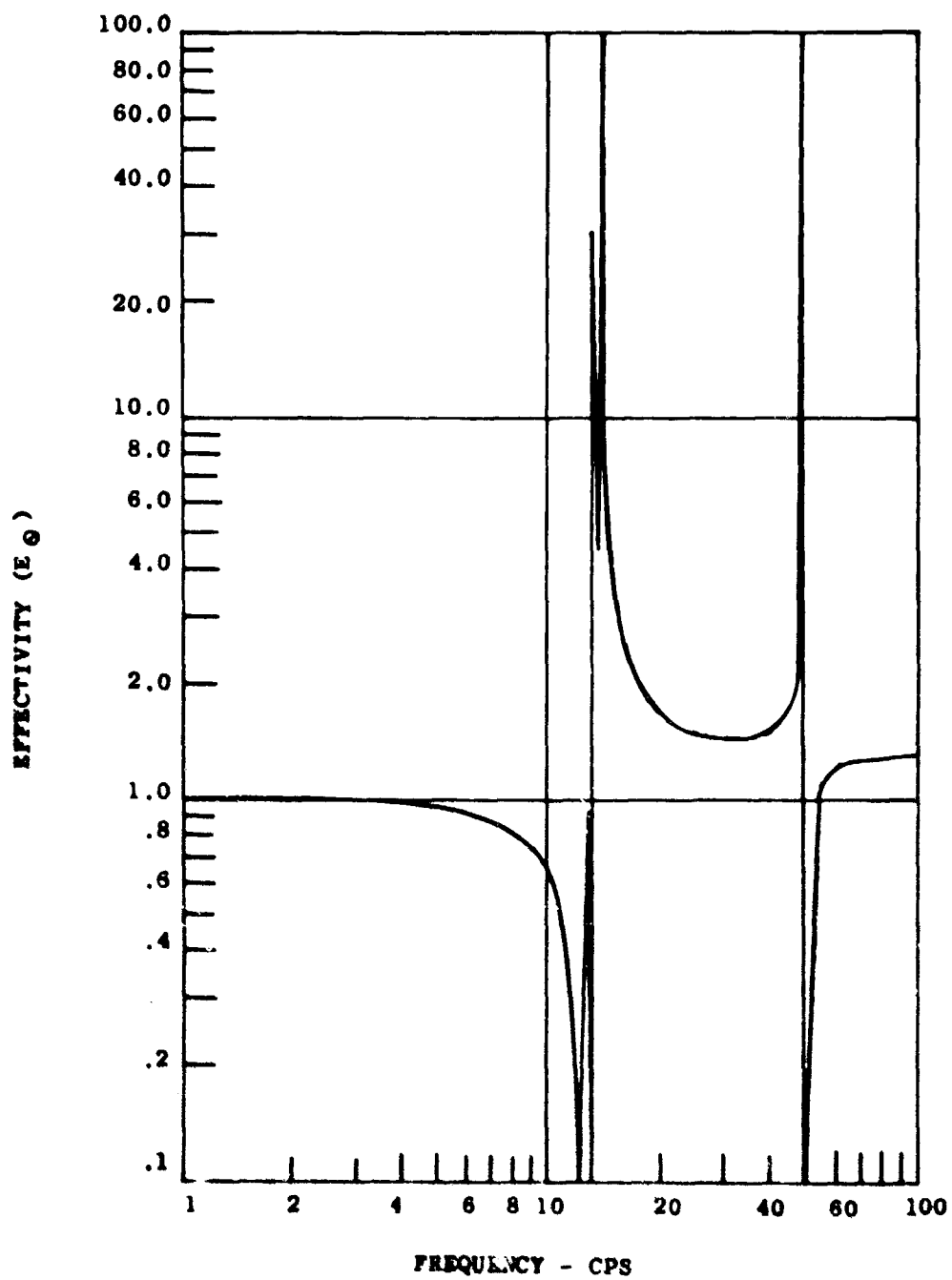


Figure 21. Roll Effectivity for Case 14 HS Versus Frequency.

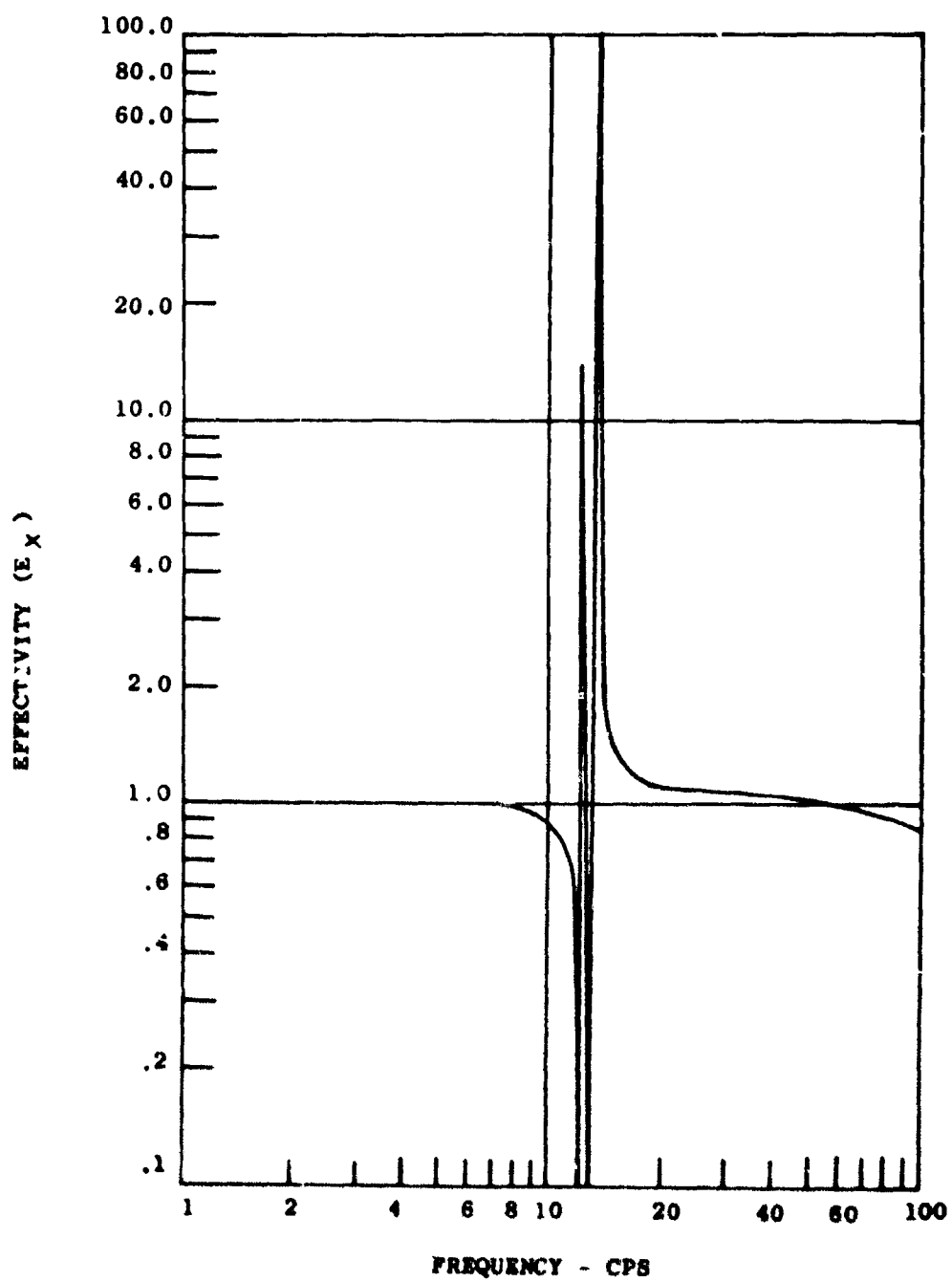


Figure 22 Longitudinal Effectivity for
Case 14 HS Versus Frequency

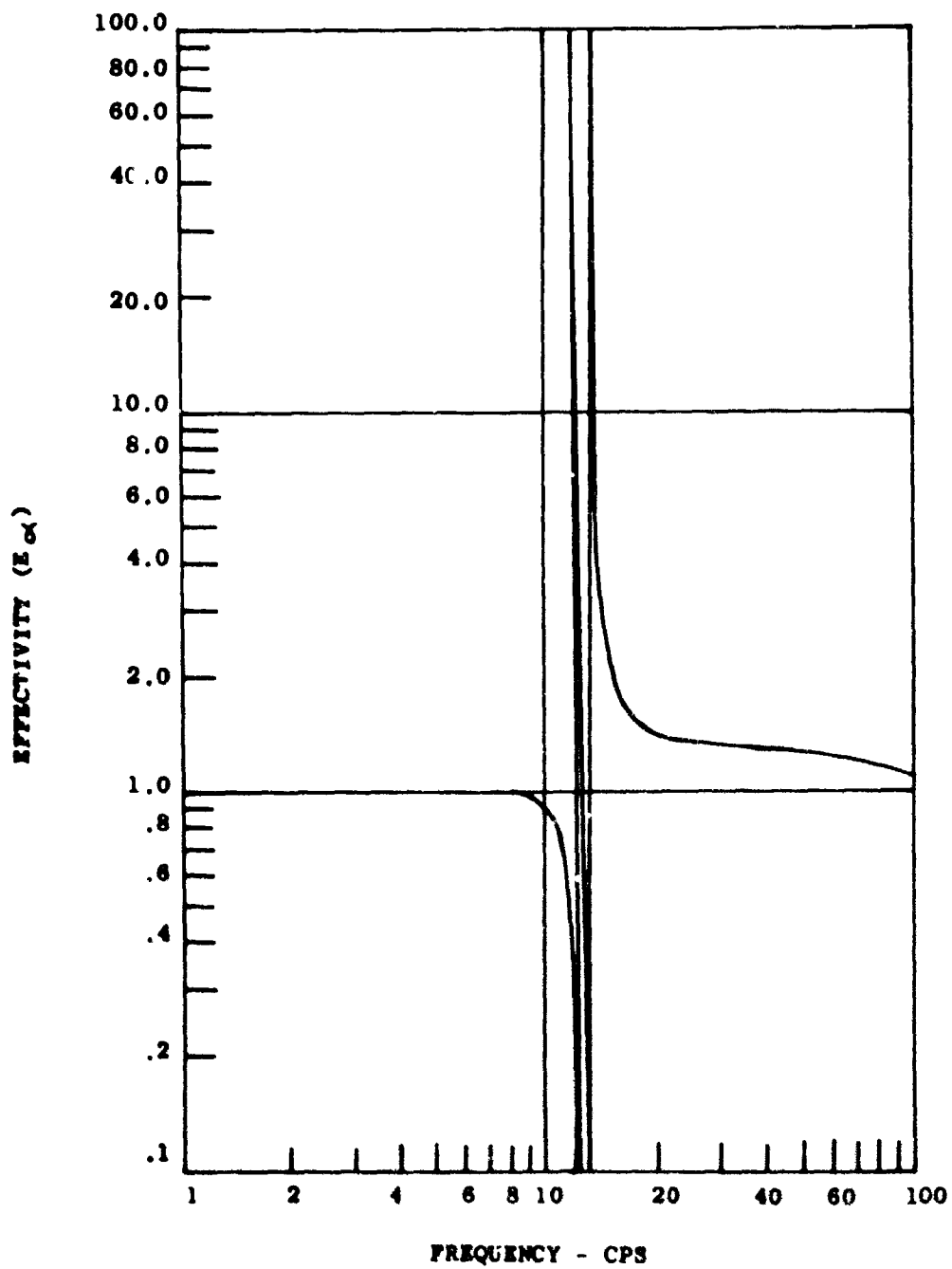


Figure 23. Pitch Effectivity for Case 14 HS Versus Frequency.

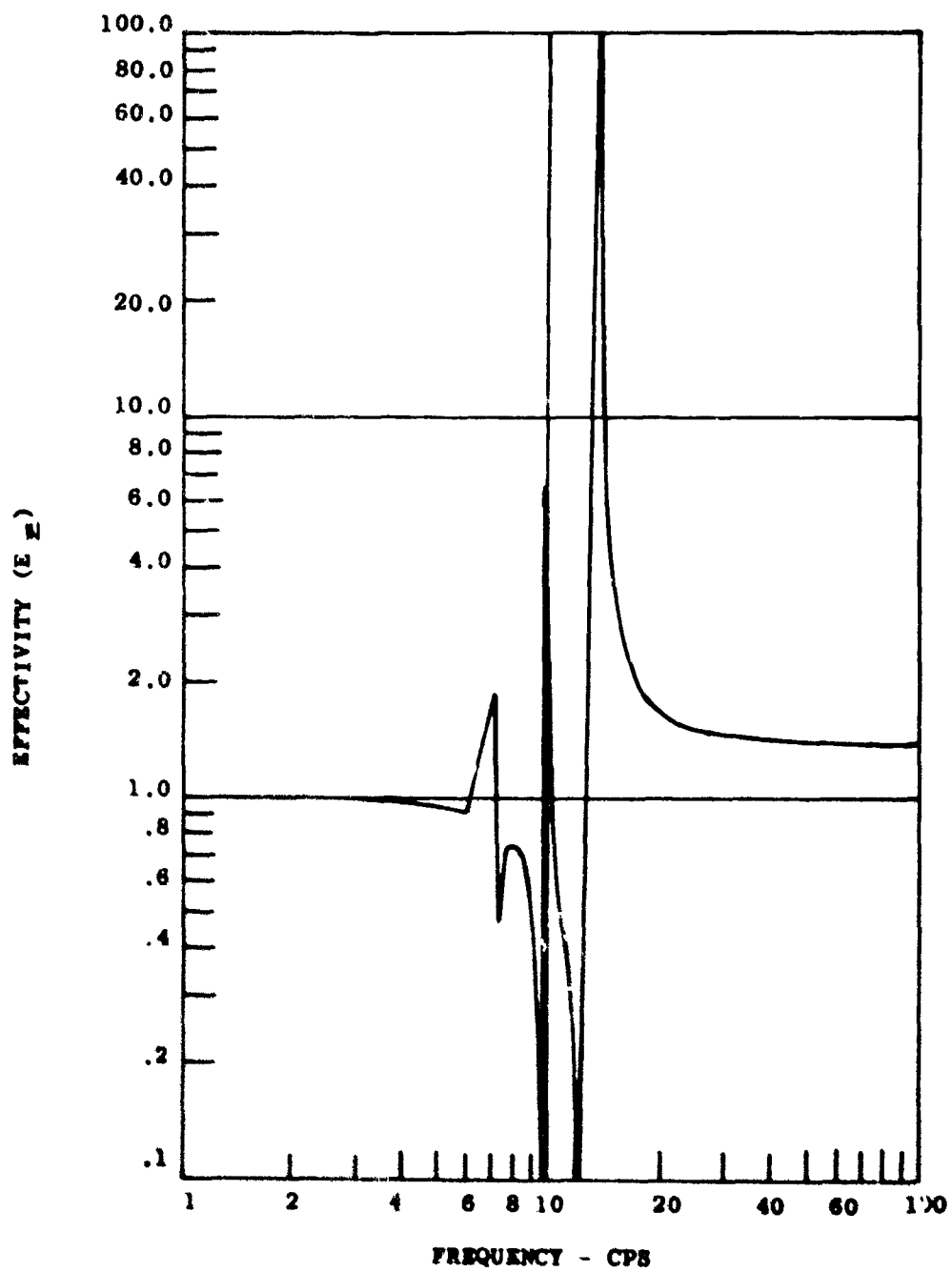


Figure 24. Vertical Effectivity for Case 25 HS Versus Frequency.

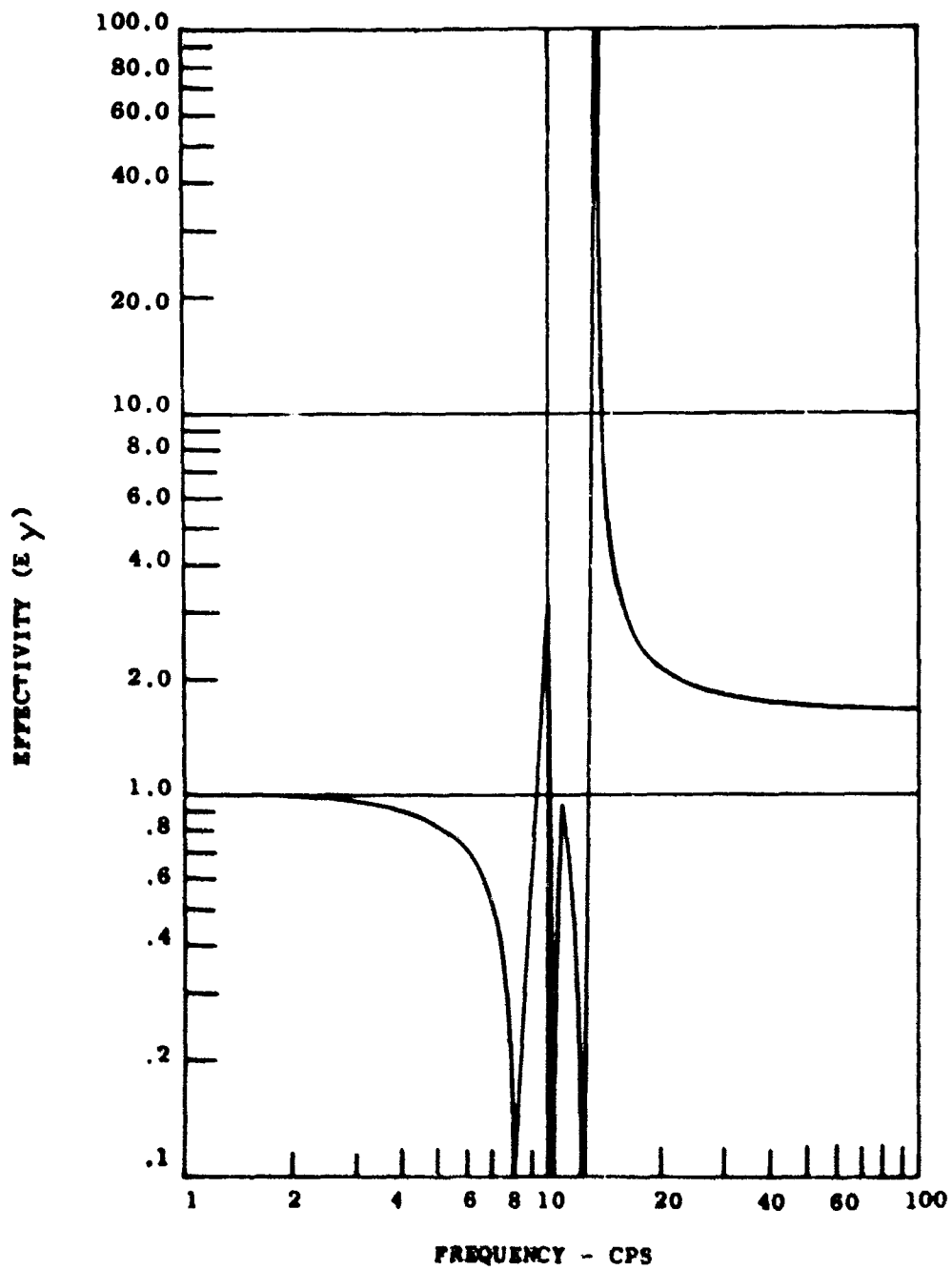


Figure 25. Lateral Effectivity for Case 25 HS Versus Frequency.

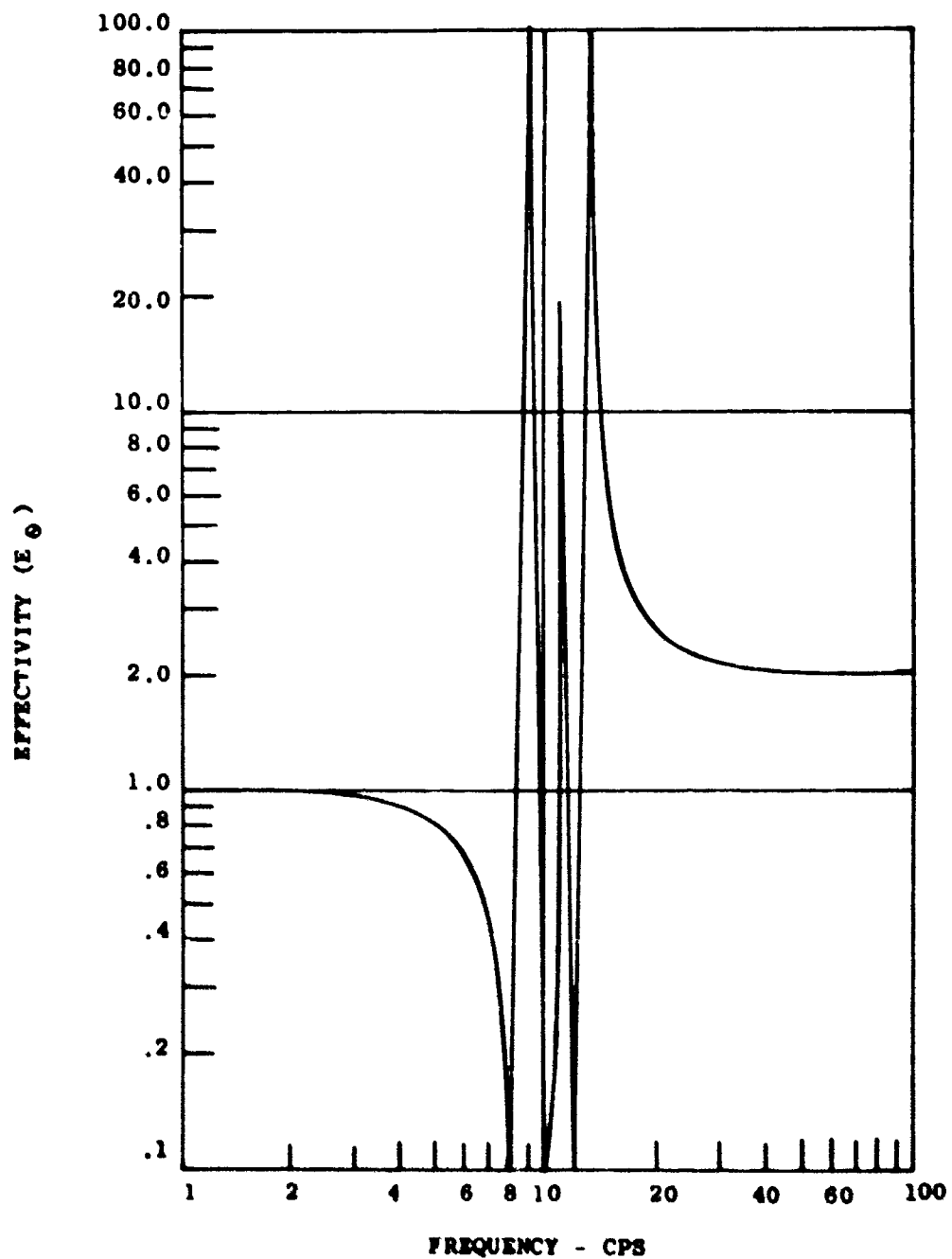


Figure 26. Roll Effectivity for Case 25 HS Versus Frequency.

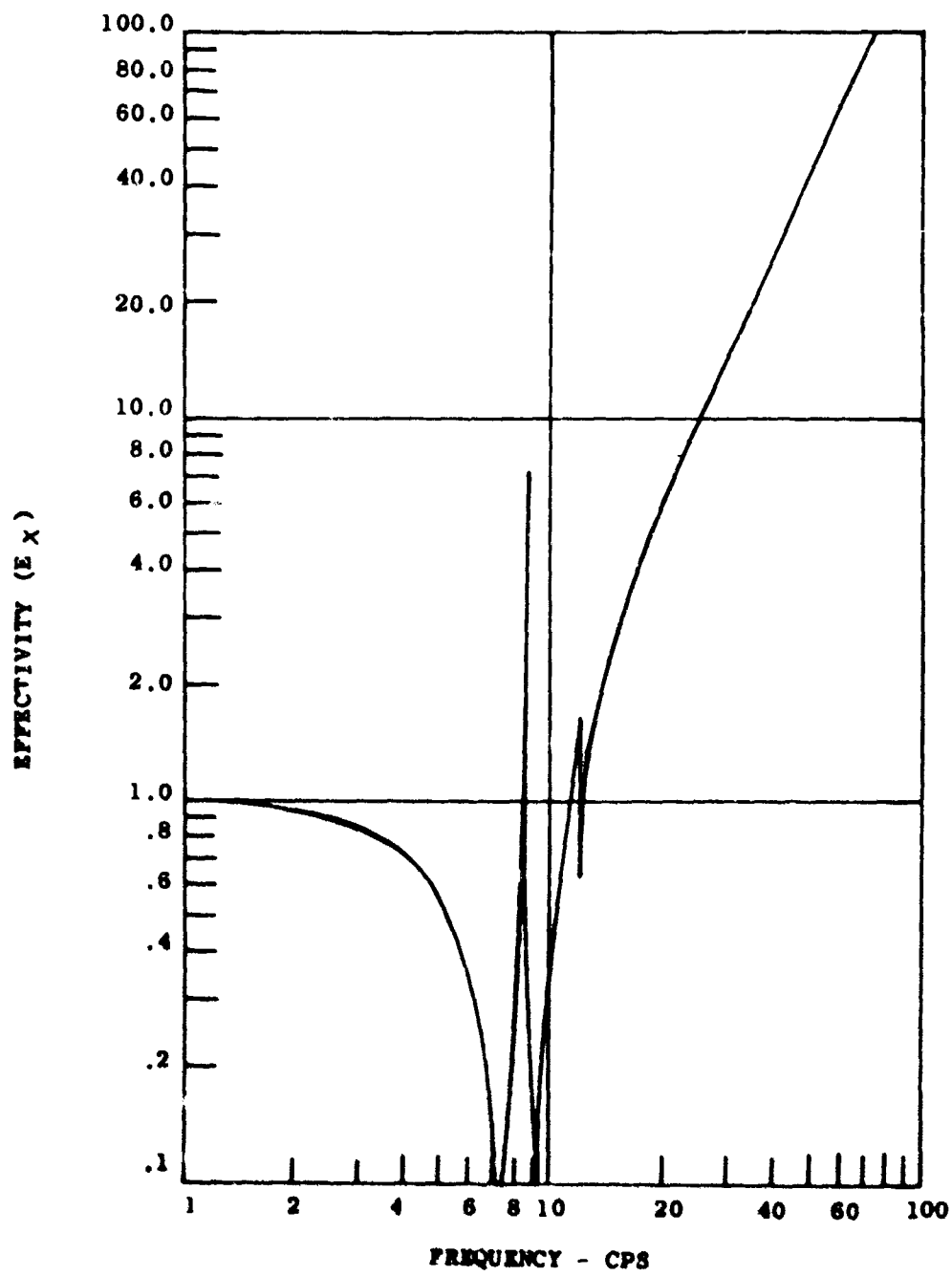


Figure 27. Longitudinal Effectivity for Case 25 HS Versus Frequency.

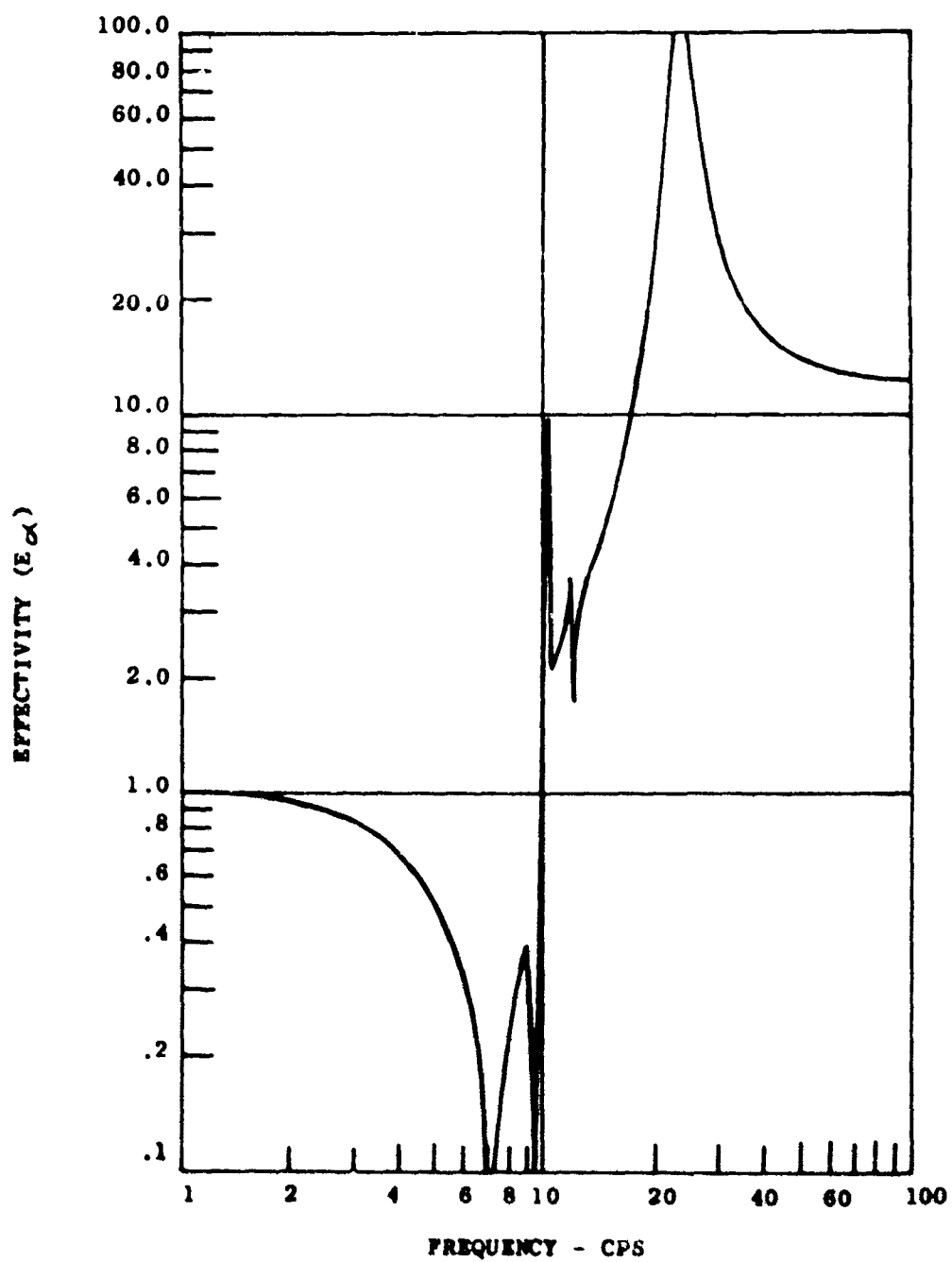


Figure 28. Pitch Effectivity for Case 25 HS Versus Frequency.

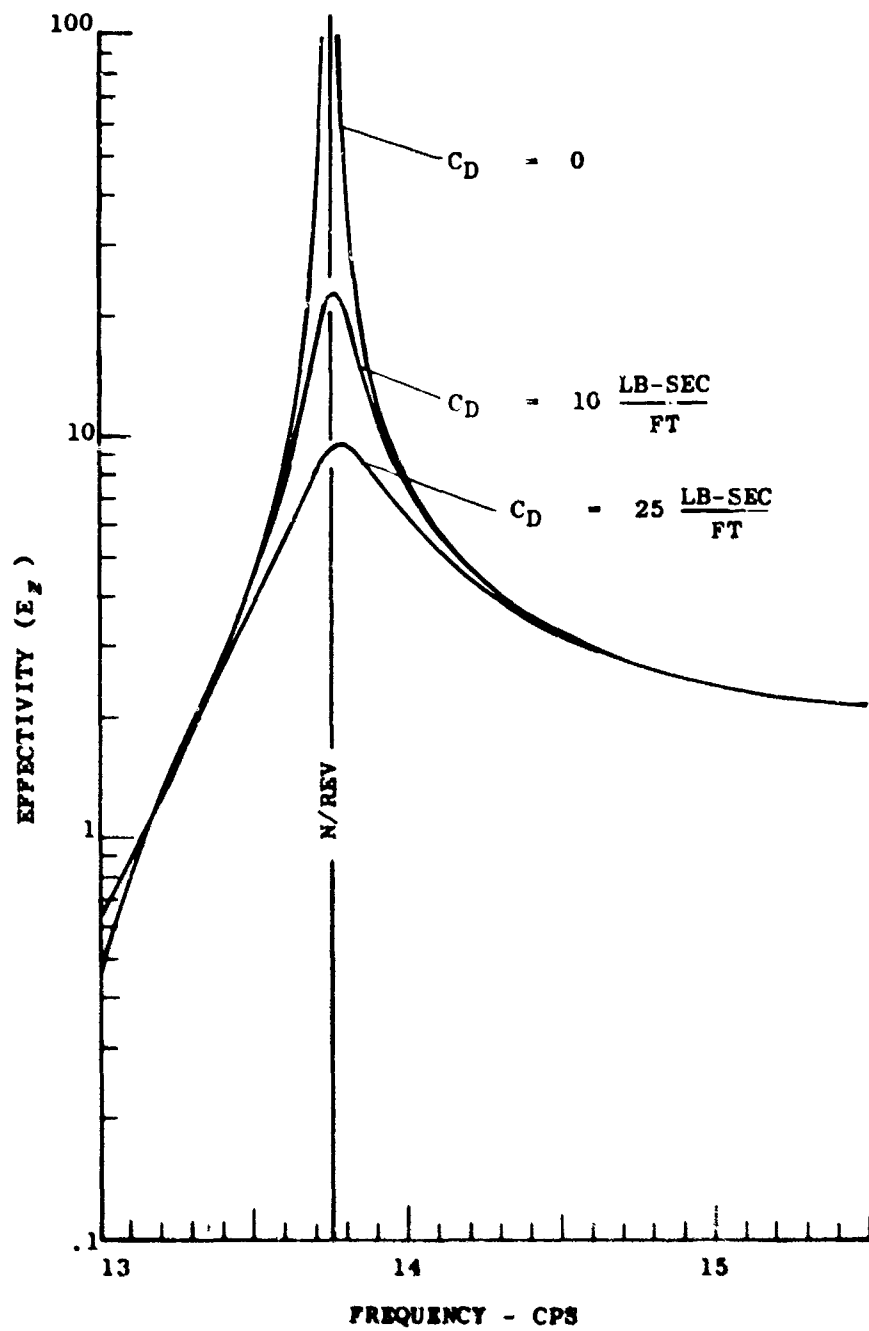


Figure 29. Vertical Effectivity at the Tuned Frequency for Several Damping Rates for Case 14 HS Versus Frequency.

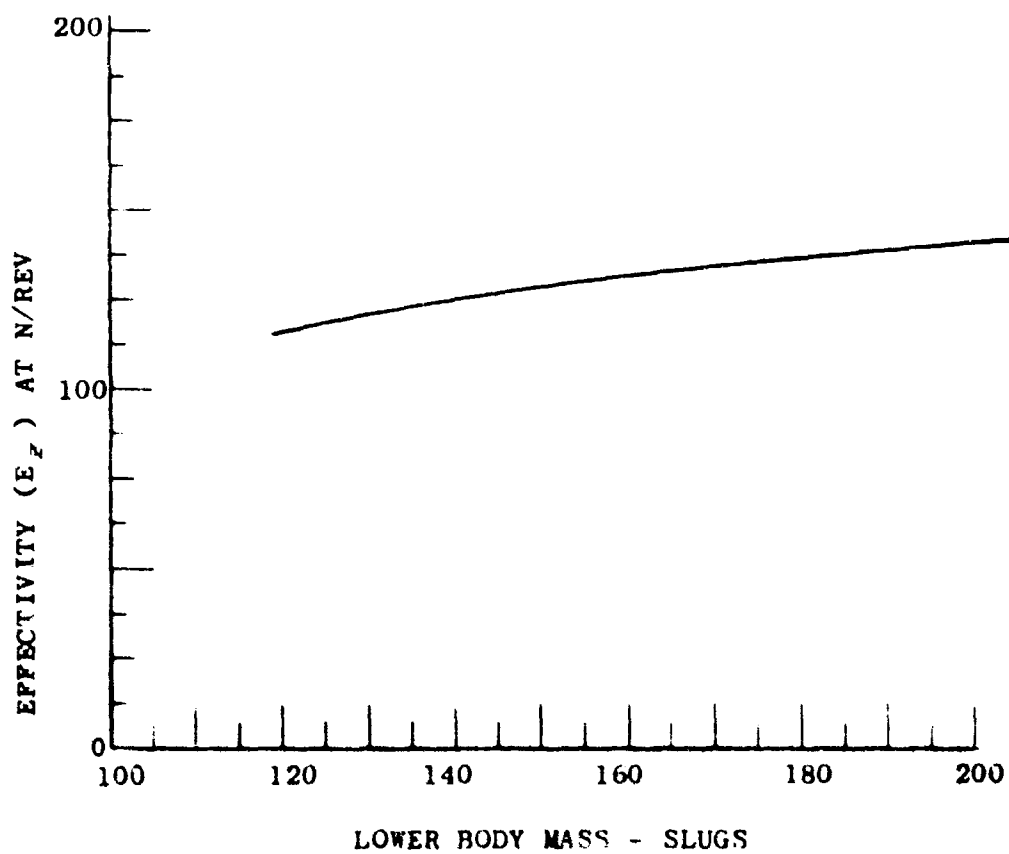


Figure 30. Change in Vertical Effectivity
at Tuned Frequency Versus Change
in Lower Body Mass for Case 4 HS.

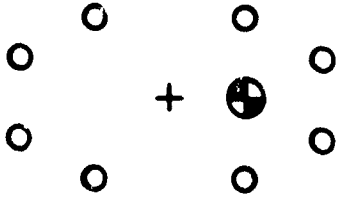
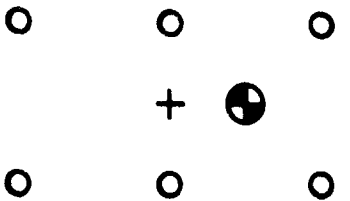
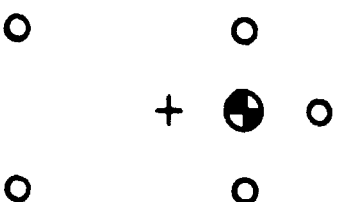

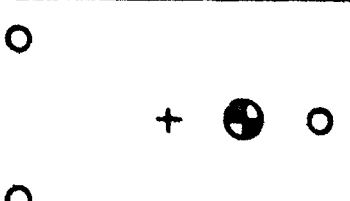


Configuration	No. Of DAVI's	Effectivity (Ez) At N/Rev
	8	95.4
	6	204.0
	5	186.0
	4	198.3
	3	133.5
+ Center line of Motor Hub  - Upper-Body Cg  - DAVI		

Figure 3i. Vertical Effectivities at the Tuned Frequency for Several DAVI Arrangements for Case 17 HS.

ROTOR ISOLATION OF COMPOUND HELICOPTERS

For compound helicopters, reduction in rotor rpm of approximately 15 percent may be required in going from the high thrust condition of the rotor at low airspeed to the unloaded or partially loaded rotor at high airspeed.

To cover this range, the system was designed such that the extreme points have an effectivity in the vertical direction of 3.0 with the maximum effectivity at antiresonance falling somewhere between these extremes. Table XVII presents the effectivities for the six compound helicopter configurations at the extreme range points; that is, at the 85 percent and 100 percent points of the 1/rev, N/rev, 2N/rev, 3N/rev, and 4N/rev frequencies. Practically all effectivities at 1/rev are above .90, with more than 50 percent of these effectivities equal to or above .95. As indicated, the desired effectivities were obtained at N/rev as well as isolation or effectivity above N/rev at multiples of N/rev, up to 4N/rev.

The effectivities at the DAVI antiresonant frequencies for the various compound helicopter configurations for the N/rev range are summarized in Table XVIII. As was the case for the helicopter, the compound cases with the horizontal cg offset present a lower effectivity than the cases where the cg's are lined up. The effectivity for the first three cases (27 CS, 28 CS, and 29 CS), where the cg's are lined up, is excellent and indicates that these cases can be tuned more easily than those where the cg is offset, as is illustrated by the following three cases.

Table XIX presents the normalized accelerations at the extreme range points of the 1/rev, 2N/rev, 3N/rev and 4N/rev frequencies for vertical isolation. Included also are the normalized accelerations at the antiresonant frequency of the DAVI for the N/rev frequency. These data are presented for the various compound configurations studied.

Figures 32 through 36 are typical of the responses of the compound configuration. Shown are the antiresonant effectivity, the placement of natural frequencies, and the effectivity at the multiples of N/rev.

This study has shown that it is feasible to effectively isolate a compound helicopter for the various configurations studied. In addition, it is possible to obtain not only antiresonant isolation but also effective isolation over a 15 percent rpm range.

TABLE XVII. RANGE EFFECTIVITIES FOR THE VARIOUS COMPOUND HELICOPTER CONFIGURATIONS

Case	/rev	R_x		R_x		R_z		R_y		R_0	
		85%	100%	85%	100%	85%	100%	85%	100%	85%	100%
27 CS	1	.92	.88	.93	.90	.97	.96	.93	.90	.93	.89
	N	25668.00	2.30	2.90	1.20	3.90	4.00	6.50	6.50	10.00	7.60
	2N	1.90	4.90	1.00	2.10	1.80	1.70	2.60	2.40	2.80	2.60
	3N	24.00	101.20	4.30	6.60	1.60	1.60	2.30	2.30	2.50	2.40
	4N	27.80	16.90	9.00	13.10	1.60	1.60	2.30	2.20	2.40	2.30
28 CS	1	.94	.92	.95	.93	.98	.98	.96	.94	.95	.94
	N	303.00	2.00	2.70	1.00	3.90	4.00	6.50	6.50	10.00	7.60
	2N	3.20	7.60	1.50	2.70	1.80	1.70	2.60	2.40	2.80	2.60
	3N	73.80	36.90	5.40	8.00	1.70	1.60	2.30	2.30	2.40	2.40
	4N	20.70	14.80	10.80	15.60	1.60	1.60	2.20	2.20	2.40	2.30
29 CS	1	.96	.95	.97	.95	.99	.98	.98	.96	.97	.96
	N	887.50	2.10	2.70	1.10	3.90	4.00	6.50	6.50	10.00	7.60
	2N	2.50	6.00	1.20	2.40	1.80	1.70	2.60	2.40	2.80	2.60
	3N	36.90	53.40	4.80	7.30	1.70	1.60	2.30	2.30	2.50	2.40
	4N	23.70	15.70	9.80	14.30	1.60	1.60	2.20	2.20	2.40	2.30
30 CS	1	.97	.96	.99	.98	.99	.98	.96	.94	.94	.92
	N	15.50	2.30	1.60	1.30	2.90	2.80	3.70	4.10	7.60	5.70
	2N	1.50	1.50	1.10	1.10	1.60	1.50	2.00	1.80	2.40	2.20
	3N	1.40	1.40	1.10	1.10	1.50	1.50	1.80	1.80	2.10	2.10
	4N	1.30	1.30	1.00	1.00	1.40	1.40	1.80	1.70	2.10	2.10
31 CS	1	.98	.97	.99	.99	.99	.98	.97	.96	.96	.94
	N	6.30	2.30	1.50	1.30	7.60	2.80	10.00	3.90	18.60	5.40
	2N	1.50	1.50	1.10	1.10	1.60	1.50	2.10	2.00	2.50	2.30
	3N	1.40	1.40	1.10	1.00	1.50	1.50	1.80	1.80	2.30	2.20
	4N	1.30	1.20	1.00	.97	1.50	1.50	1.80	1.80	2.10	2.10
32 CS	1	.90	.90	.93	.90	.98	.99	.98	.96	.96	.95
	N	4.10	5.90	1.10	2.20	3.90	4.00	5.00	5.60	10.50	8.30
	2N	47.70	22.00	8.80	12.70	1.80	1.70	2.40	2.30	3.00	2.80
	3N	14.50	12.70	21.80	31.10	1.70	1.60	2.30	2.20	2.60	2.60
	4N	11.80	11.10	4.10	59.30	1.60	1.60	2.10	2.10	2.60	2.50

TABLE XVIII. ANTIRESONANT EFFECTIVITIES AT N/REV FOR THE COMPOUND HELICOPTER CASES					
Case	E_x	E_y	E_z	E_y	E_z
27 CS	6.4	2.0	3,547.9	6,086.0	7,837.2
28 CS	5.6	1.8	126.6	217.0	278.8
29 CS	5.8	1.8	75.0	128.5	164.8
30 CS	4.1	1.5	34.5	50.2	79.6
31 CS	4.9	1.5	24.0	31.7	56.6
32 CS	4.3	1.5	70.4	93.1	164.7

TABLE XIX. NORMALIZED ACCELERATION FOR COMPOUND HELICOPTER (VERTICAL ONLY)							
Frequency		27 CS	28 CS	29 CS	30 CS	31 CS	32 CS
1/rev	85%	.1031	.1020	.1010	.1010	.1010	.1111
	100%	.1042	.1020	.1020	.1020	.1010	.1010
N/rev	85%	.2564	.2564	.2564	.3448	.1316	.2564
	f_n *	.0003	.0079	.0143	.0290	.0417	.0143
	100%	.2500	.2500	.2500	.3448	.35714	.2500
2N/rev	85%	.2222	.2222	.2222	.2500	.2500	.2222
	100%	.2353	.2353	.2353	.2666	.2666	.2353
3N/rev	85%	.0625	.05882	.05882	.06666	.06666	.05882
	100%	.0625	.0625	.0625	.06666	.06666	.0625
4N/rev	85%	.0625	.0625	.0625	.07142	.06666	.0625
	100%	.0625	.0625	.0625	.07142	.06666	.0625
* Percentage where DAVI antiresonance occurs; it varies with configuration							

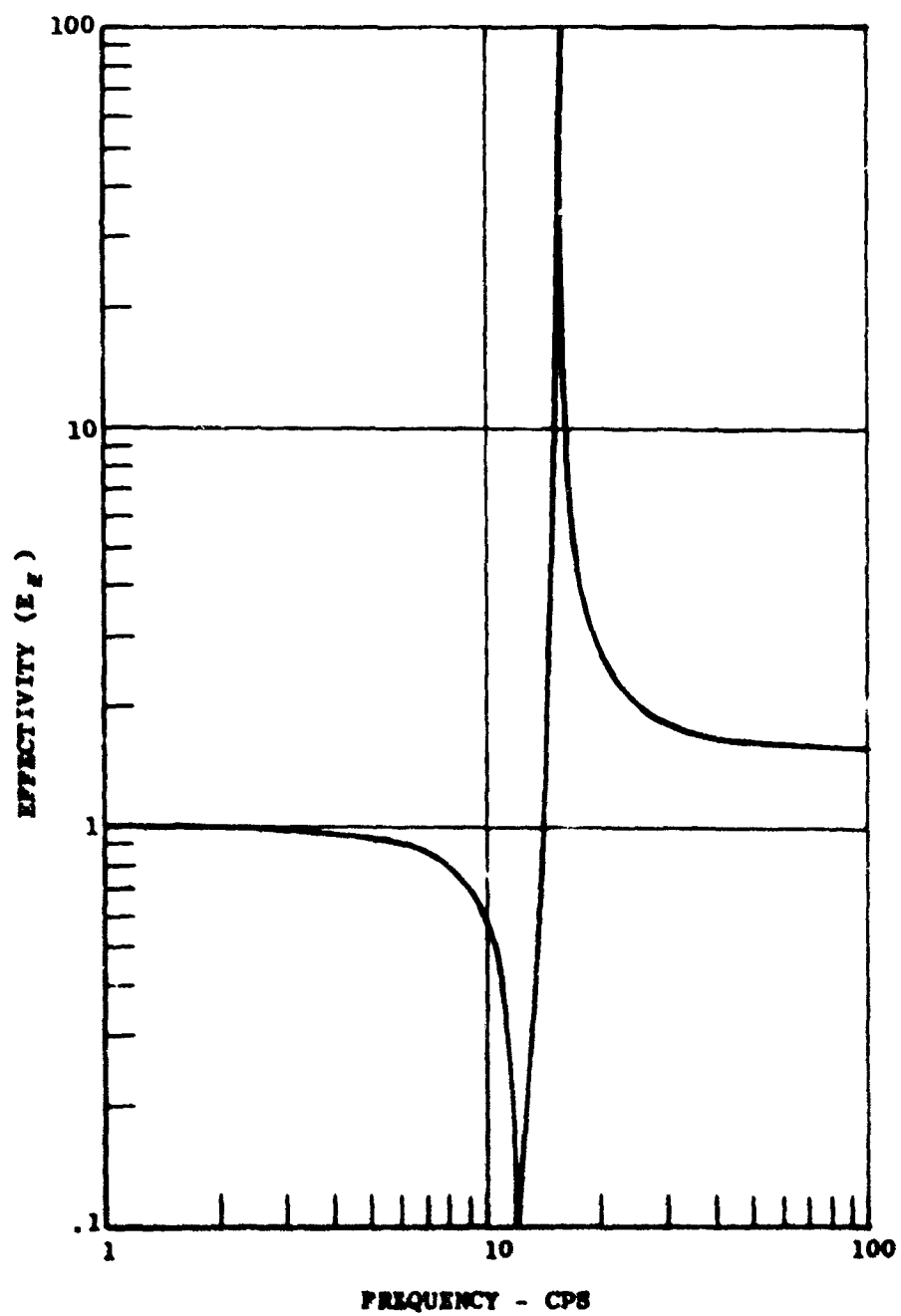


Figure 32. Vertical Effectivity for the Compound Helicopter for Case 28 CS Versus Frequency.

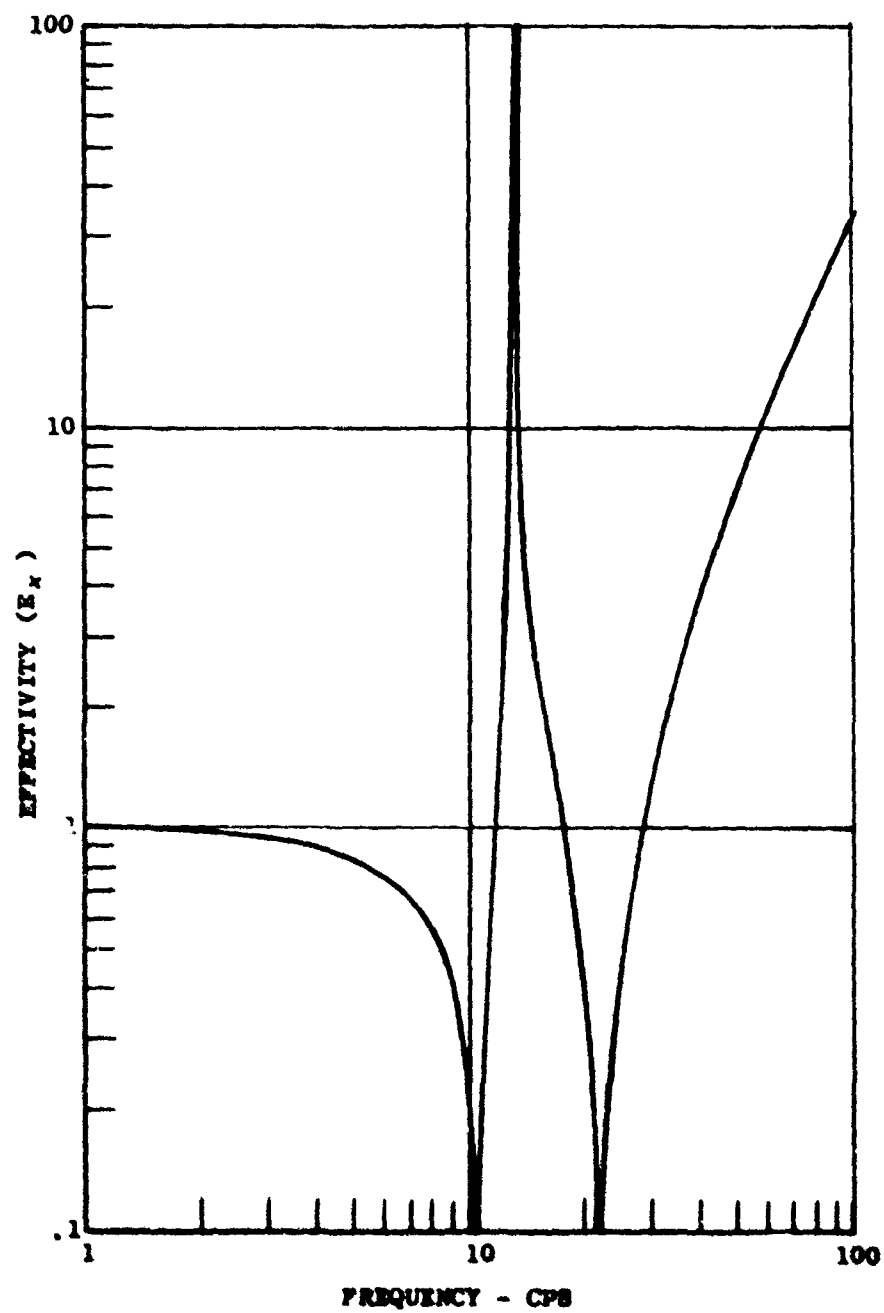


Figure 33. Longitudinal Effectivity for the Compound Helicopter for Case 28 CS Versus Frequency.

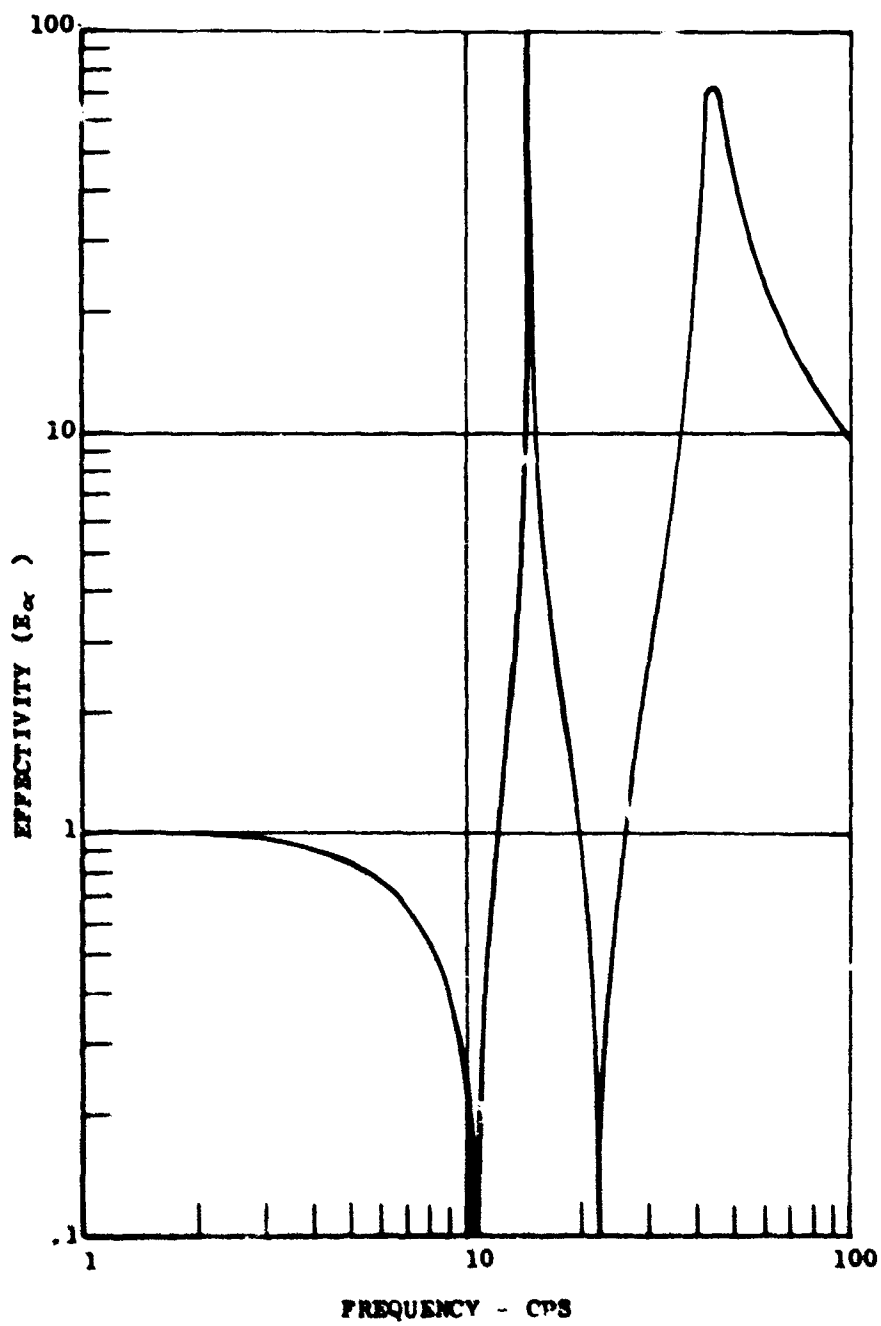


Figure 34. Pitch Effectivity for the Compound Helicopter for Case 28 CS Versus Frequency.

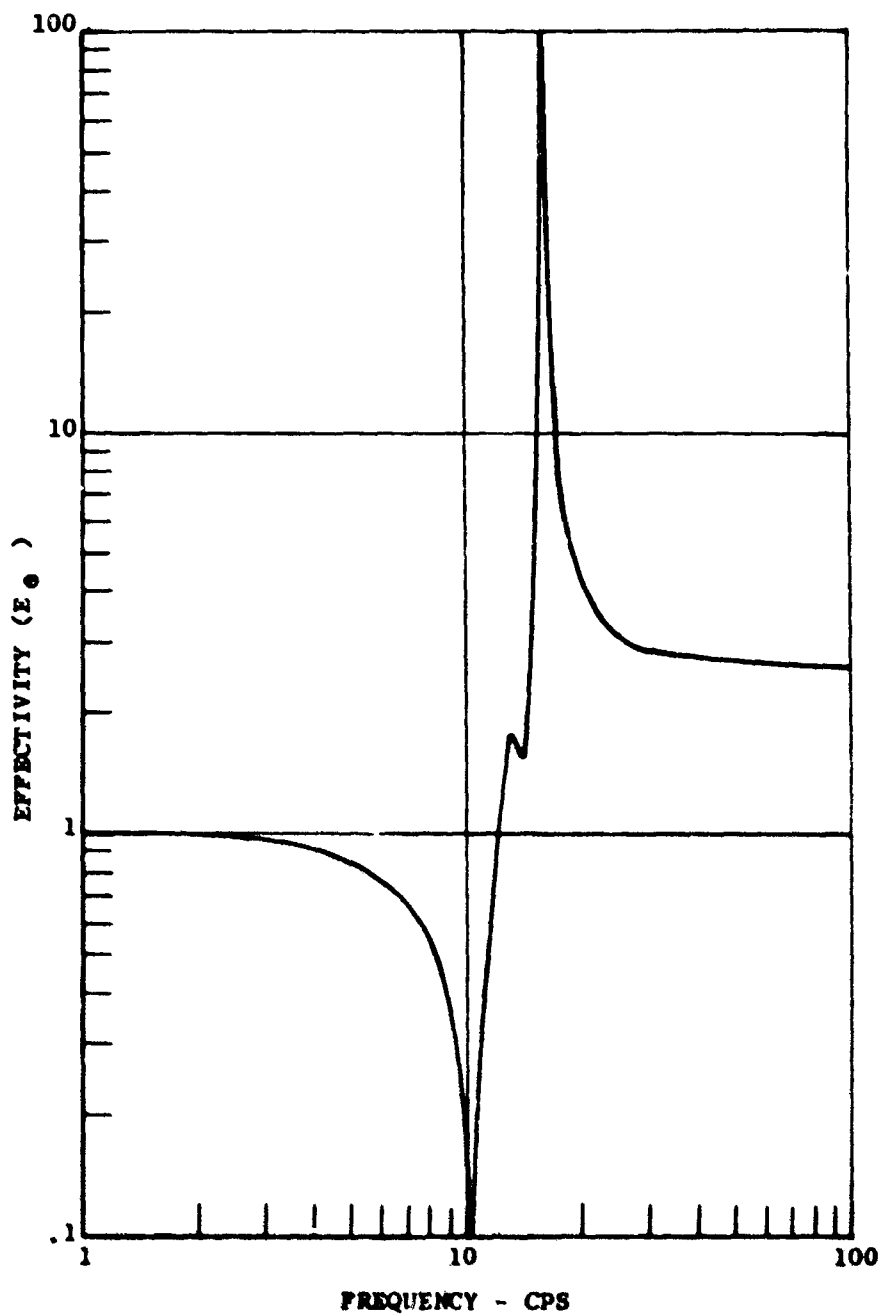


Figure 35. Roll Effectivity for the Compound Helicopter for Case 28 CS Versus Frequency.

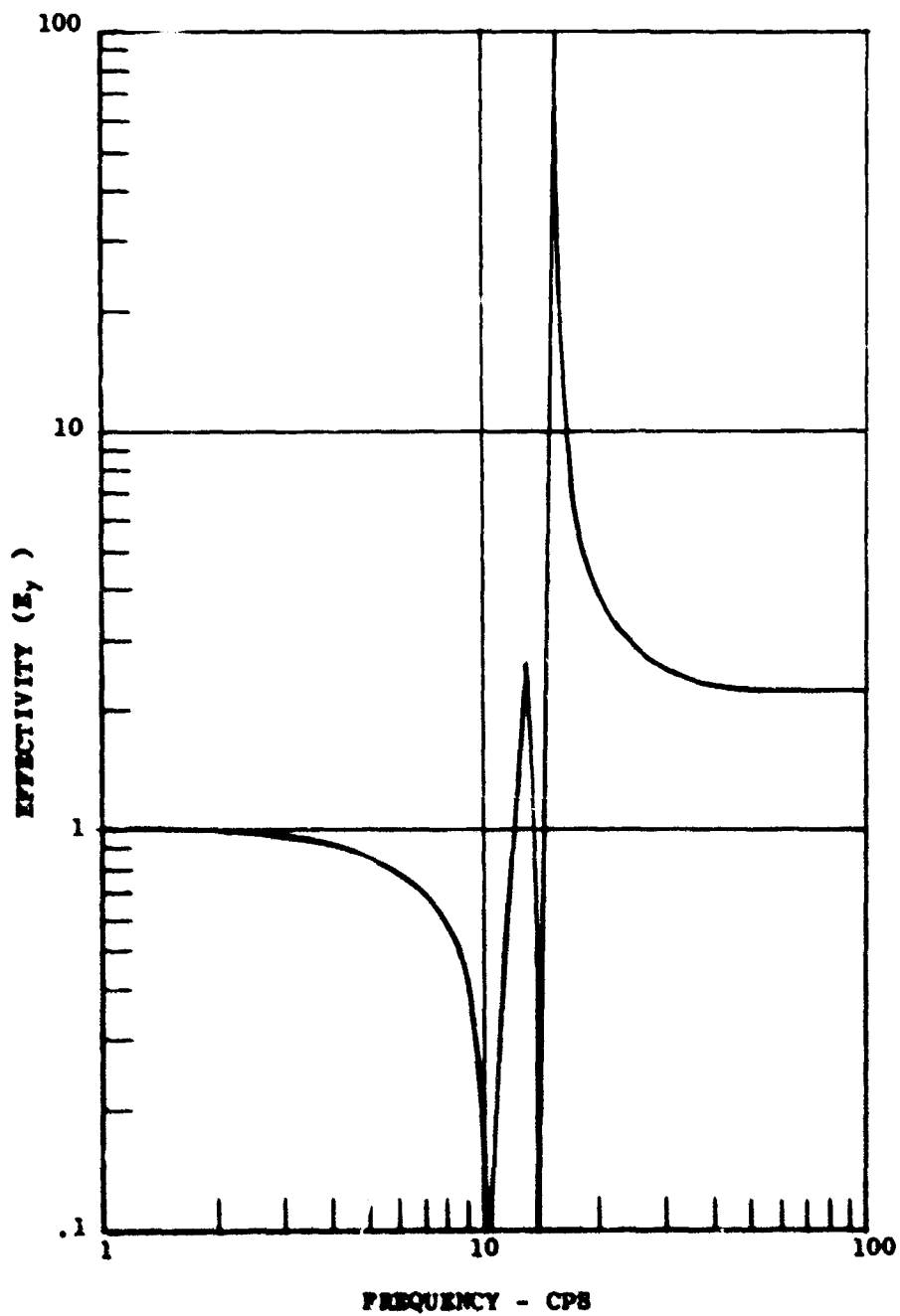


Figure 36. Lateral Effectivity for the Compound Helicopter for Case 28 CS Versus Frequency.

TRANSIENT EQUATIONS

Since the transient excitation scheduled is in the vertical direction only, the system was decoupled to include only the vertical and pitch degrees of freedom. From Figure 37, the equations can be written.

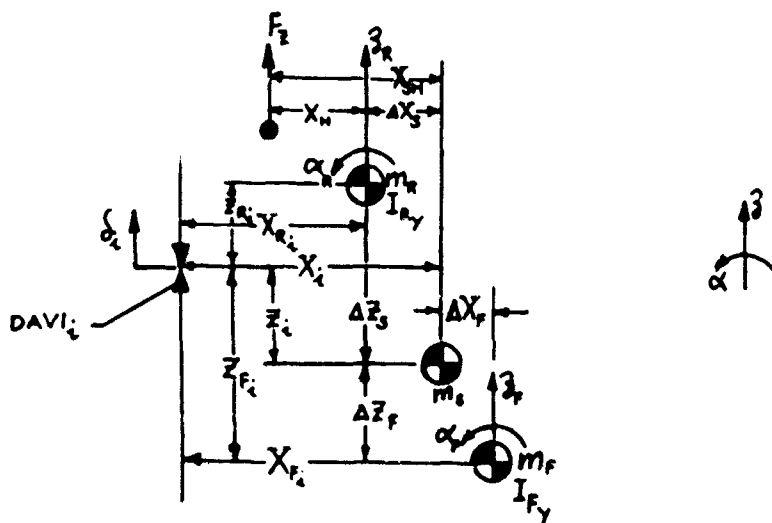


Figure 37. Schematic of DAVI Installation for Transient Analysis.

Defining the geometry of the configuration,

$$m_f = m_s - m_r \quad (41)$$

$$\Delta X_f = \frac{m_r \Delta X_s}{m_s - m_r} = \bar{\mu} \Delta X_s \quad (42)$$

$$\Delta z_f = \frac{m_r \Delta z_s}{m_s - m_r} = \bar{\mu} \Delta z_s \quad (43)$$

where

$$\bar{\mu} = \frac{m_r}{m_s - m_r}$$

Also,

$$X_{R_i} = X_i - \Delta X_s \quad (44)$$

$$X_{F_i} = X_i + \bar{\mu} \Delta X_s \quad (45)$$

Defining the motion across the DAVI at point (1),

$$\delta_i = \ddot{z}_R - \ddot{z}_F - \alpha_R X_{R_i} + \alpha_F X_{F_i}$$

$$\delta_i = \ddot{z}_R - \ddot{z}_F - \alpha_R (X_i - \Delta X_s) + \alpha_F (X_i + \bar{\mu} \Delta X_s) \quad (46)$$

Defining the motion across the rigid body cg,

$$\lambda = \ddot{z}_R - \ddot{z}_F + (\alpha_R + \alpha_F \bar{\mu}) \Delta X_s \quad (47)$$

$$\lambda = \ddot{z}_R - \ddot{z}_F + (1 + \bar{\mu}) \alpha_R \Delta X_s - \bar{\mu} \Delta \alpha \Delta X_s \quad (48)$$

Also,

$$\Delta \alpha = \alpha_R - \alpha_F \quad (49)$$

Then the motion across DAVI (1) is

$$\delta_i = \lambda - \Delta \alpha X_i \quad (50)$$

Therefore, the DAVI spring and damping forces at (1) are

$$F_{\delta_i} = f_{k_i}(\delta_i) + f_{c_i}(\dot{\delta}_i) \quad (51)$$

The equations of motion are

\ddot{z}_R Equation

$$\ddot{z}_R (m_R + \sum_{i=1}^n M_{R_i}) + \ddot{z}_F \sum_{i=1}^n M_{A_i} - \ddot{\alpha}_R \sum_{i=1}^n M_{R_i} X_{R_i} - \ddot{\alpha}_F \sum_{i=1}^n M_{A_i} X_{F_i} + \sum_{i=1}^n F_{\delta_i} = F_R(t) \quad (52)$$

\ddot{z}_F Equation

$$\ddot{z}_R \sum_{i=1}^n M_{A_i} + \ddot{z}_F (m_F + \sum_{i=1}^n M_{C_i}) - \ddot{\alpha}_R \sum_{i=1}^n M_{A_i} X_{R_i} - \ddot{\alpha}_F \sum_{i=1}^n M_{C_i} X_{F_i} - \sum_{i=1}^n F_{\delta_i} = 0 \quad (53)$$

α_R Equation

$$-\ddot{\sum}_{i=1}^n M_{R_i} X_{R_i} - \ddot{\sum}_{i=1}^n M_{A_i} X_{R_i} + \ddot{\alpha}_R (I_{R_y} + \ddot{\sum}_{i=1}^n M_{R_i} X_{R_i}^2) + \ddot{\alpha}_F \sum_{i=1}^n M_{A_i} X_{F_i} X_{R_i} - \ddot{\sum}_{i=1}^n F_{R_i} X_{R_i} = -F_z(t) X_H \quad (54)$$

α_F Equation

$$-\ddot{\sum}_{i=1}^n M_{A_i} X_{F_i} - \ddot{\sum}_{i=1}^n M_{C_i} X_{F_i} + \ddot{\alpha}_R \sum_{i=1}^n M_{A_i} X_{F_i} X_{R_i} + \ddot{\alpha}_F (I_{F_y} + \ddot{\sum}_{i=1}^n M_{C_i} X_{F_i}^2) + \ddot{\sum}_{i=1}^n F_{F_i} X_{F_i} = 0 \quad (55)$$

The forcing function was represented for either a gust loading as $\frac{1}{2} \sin^2$ or a control input with a ramp as a function of time. Each of the six configurations considered was analyzed for two load factors and three time periods of input.

The transient configurations were analyzed for a 3.0 g and a -0.5 g input for periods of input of .6, .8, and 1.0 second. Cases 33 HT through 37 HT represent helicopter configurations, while Case 38 CT represents the compound helicopter. All cases are fully defined in Tables I through VI.

All results shown were obtained from the transient analysis using no damping. The maximum deflections were realized for Case 38 CT (compound configuration at a gross weight of 20,000 pounds), where, because of the 15% rpm range, a compromise was made in static deflection, DAVI weight, and effectiveness at range end points.

For the vertical transient excitations of Tables XX and XXI, the configurations are restricted to an upper body consisting of the rotor and transmission with zero cg offset - that is, the upper body, total aircraft, and lower body centers of gravity are vertically aligned. Since the cg offset is zero and the four (4) DAVI's are symmetrically located about the upper body cg, there are no pitching or rolling moments and the deflections reported are identical for each of the four (4) DAVI's. However, in an effort to determine the angular pitching motions for an offset cg configuration, the two-bladed, 6500 pound, rotor plus engine plus transmission upper body configuration was analyzed.

Table XXII is a summary of the maximum steady transient deflections for a $\frac{1}{2} \sin^2$ and ramp input for a 3.0 g and a -0.5 g input for periods of input of .6, .8, and 1.0 second. In addition, the maximum relative angular pitching motions

TABLE XX. SUMMARY OF STEADY AND VIBRATORY TRANSIENT DEFLECTIONS FOR A $1/2 \sin^2$ INPUT

t	g	Ampl.	Deflection - Inches					
			33 HT	34 HT	35 HT	36 HT	37 HT	38 CT
.6	3.0	Steady	.137760	.126960	.206400	.293400	.282360	.4587600
.6	3.0	Vibr.	.002380	.004029	.002409	.001577	.003846	.0004009
.6	-.5	Steady	-.022968	-.021036	-.034404	-.048900	-.047244	-.0764500
.6	-.5	Vibr.	.000399	.000673	.000403	.000256	.000642	.0000680
.8	3.0	Steady	.137640	.125160	.205320	.289680	.281640	.4351200
.8	3.0	Vibr.	.000511	.002137	.000687	.001272	.000519	.0002860
.8	-.5	Steady	-.022956	-.020772	-.034260	-.048280	-.046908	-.0755100
.8	-.5	Vibr.	.000083	.000362	.000113	.000209	.000087	.0000490
1.0	3.0	Steady	.137160	.124320	.206040	.290280	.282600	.4504800
1.0	3.0	Vibr.	.000755	.001042	.001027	.001528	.001744	.0002220
1.0	-.5	Steady	-.022840	-.020676	-.033914	-.048336	-.047100	-.0750840
1.0	-.5	Vibr.	.000130	.000171	.000237	.000257	.000295	.0000370

TABLE XXI. SUMMARY OF STEADY AND VIBRATORY TRANSIENT DEFLECTIONS FOR A RAMP INPUT

t	g	Ampl.	Deflection - Inches					
			33 HT	34 HT	35 HT	36 HT	37 HT	38 CT
.6	3.0	Steady	.135300	.123720	.205260	.289200	.281700	.446040
.6	3.0	Vibr.	.006540	.006640	.005100	.003960	.008100	.000730
.6	-.5	Steady	-.023490	-.020622	-.034212	-.048288	-.046950	-.074340
.6	-.5	Vibr.	.000912	.001134	.000852	.000564	.001380	.000126
.8	3.0	Steady	.137838	.123906	.205320	.289140	.281640	.446040
.8	3.0	Vibr.	.000162	.004974	.001920	.004500	.001440	.000730
.8	-.5	Steady	-.022460	-.020646	-.034212	.048108	.046940	.074340
.8	-.5	Vibr.	.000328	.000622	.000324	.000794	.000240	.000120
1.0	3.0	Steady	.136320	.123860	.205770	.289090	.281580	.446100
1.0	3.0	Vibr.	.003000	.002940	.004880	.006360	.006300	.000680
1.0	-.5	Steady	-.022304	-.020646	-.034212	-.048180	-.046932	-.074348
1.0	-.5	Vibr.	.000916	.000498	.000828	.001068	.001056	.000114

are shown. The results indicate that these pitching motions are small and, in general, 0.1 degree. This configuration included a one-foot longitudinal cg offset of the upper-body and the system cg.

TABLE XXII. SUMMARY OF MAXIMUM STEADY DEFLECTIONS AND PITCHING MOTIONS FOR A $1/2 \sin^2$ AND RAMP INPUT

t	g	$1/2 \sin^2$ Input		Ramp Input	
		Deflection (Inches)	Pitching Motion (Degrees)	Deflection (Inches)	Pitching Motion (Degrees)
.6	3.0	.152	.0612	.152	.0615
.6	-0.5	-.025	.0102	-.025	.0103
.8	3.0	.150	.0597	.150	.0593
.8	-0.5	-.025	.00997	-.025	.00988
1.0	3.0	.149	.0591	.149	.0587
1.0	-0.5	-.025	.00986	-.024	.00988

Figures 38 through 44 present transient responses versus time for the compound helicopter for the various time periods of input at the 3.0 g and -0.5 g level for the $1/2 \sin^2$ and ramp functions. Figure 43 shows a typical enlargement of the vibration deflections across the DAVI under a transient loading.

Figures 45 through 51 present the transient responses of Case 34 HT, which represents a 6500-pound helicopter. These data shown are typical of the transient envelopes obtained for the other cases.

The transient responses presented show that the DAVI isolation system analyzed herein has a minimum of overshoot and should cause no concern during transient conditions.

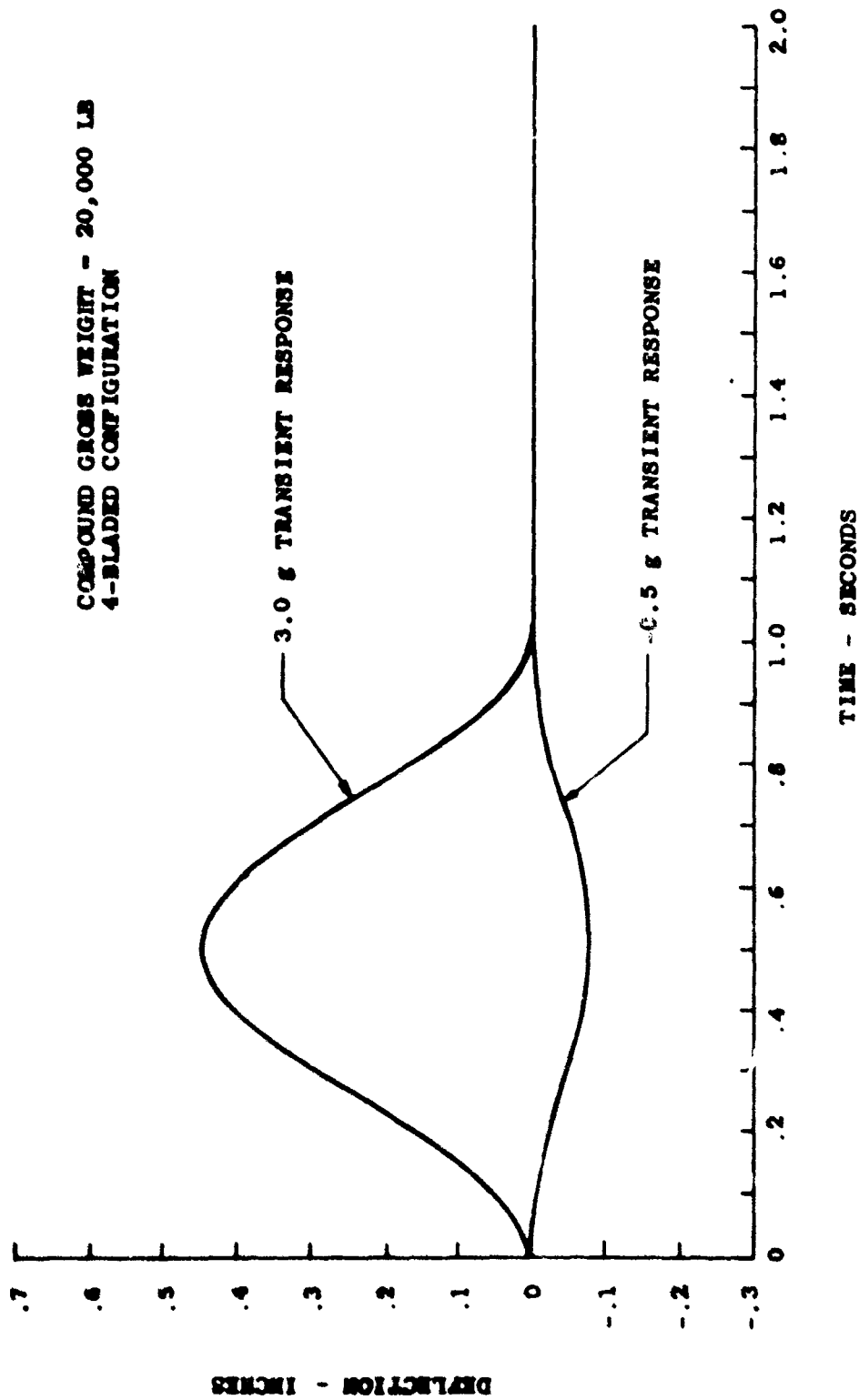


Figure 38. Transient Deflection Envelope for a 1-Second $\frac{1}{2} \sin^2$ Input for Case 38 CT Versus Time.

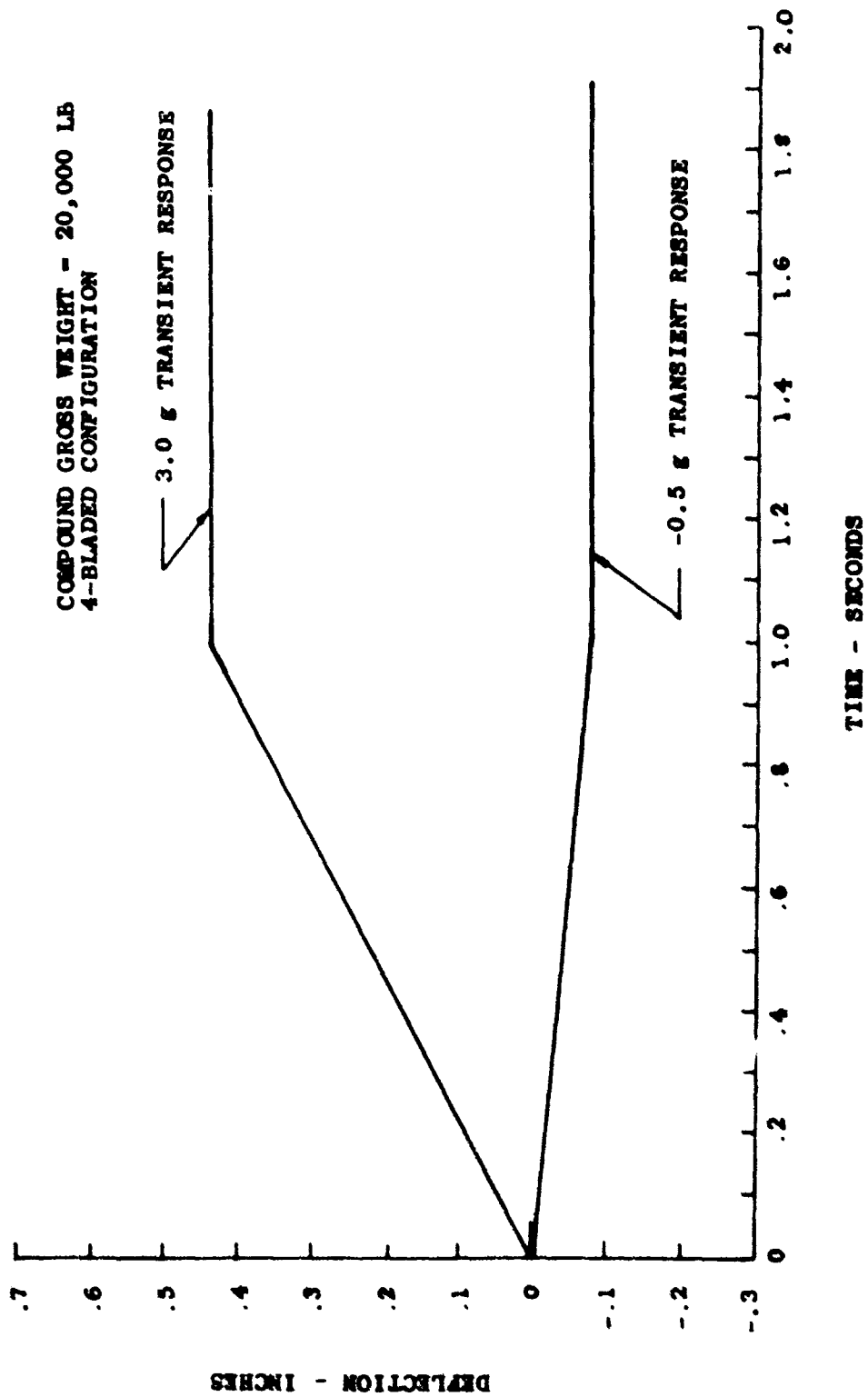


Figure 39. Transient Deflection Envelope for a 1-Second Ramp Input for Case 38 CT Versus Time.

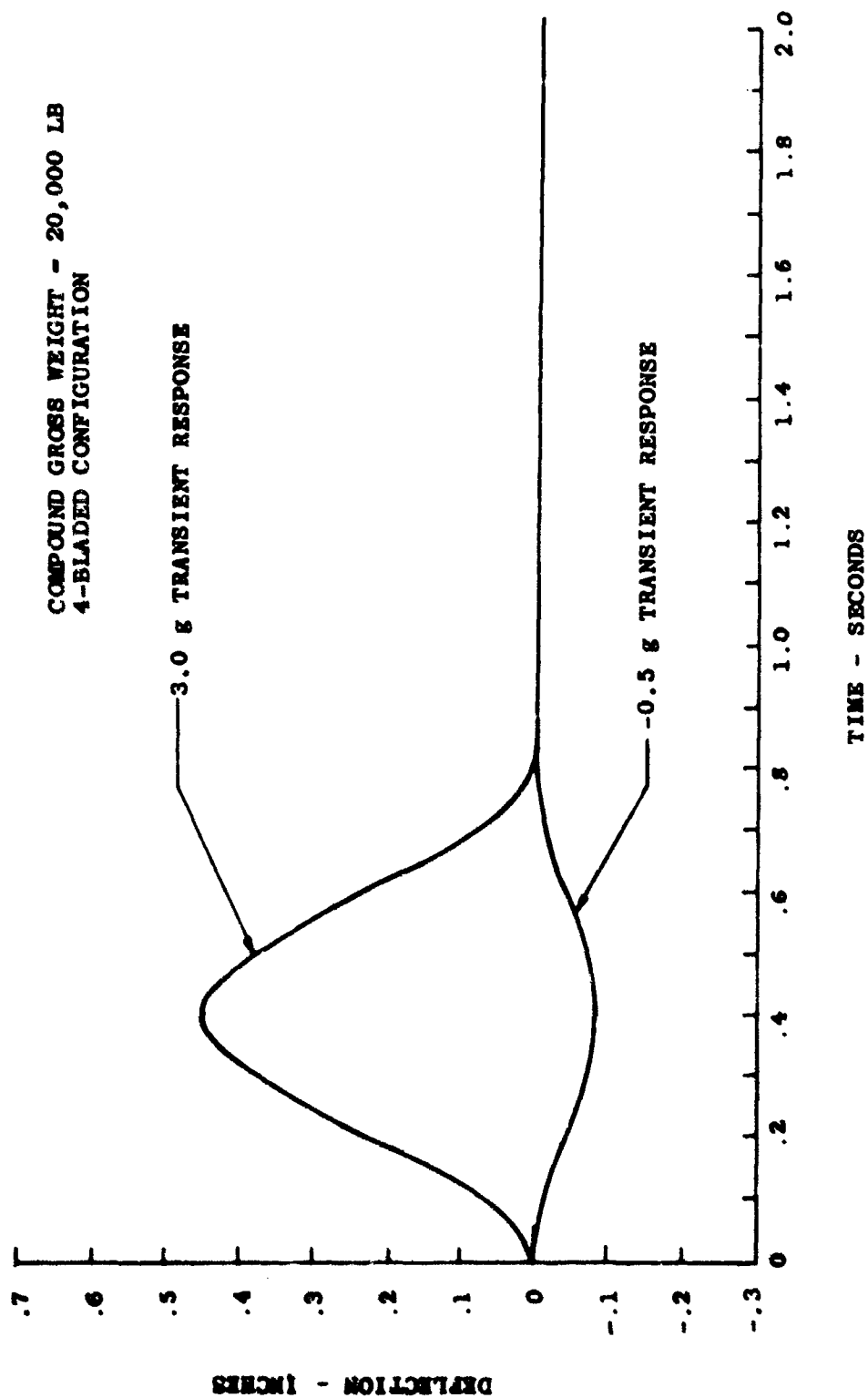


Figure 40. Transient Deflection Envelope for a 0.8-Second $\frac{1}{2} \text{Sin}^2$ Input for Case 38 CT Versus Time.

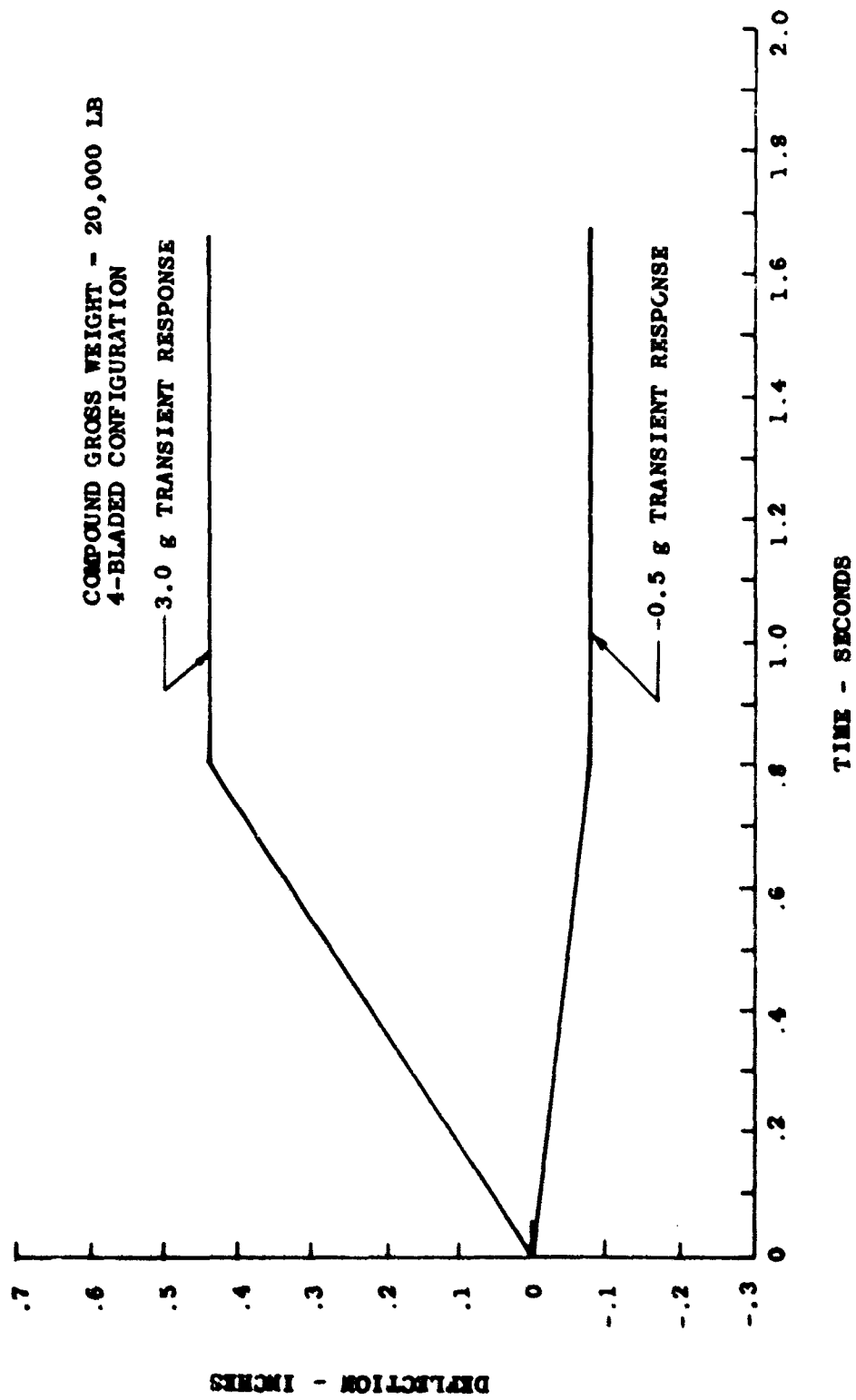


Figure 41. Transient Deflection Envelope for a 0.8-Second Ramp Input for Case 38 CT Versus Time.

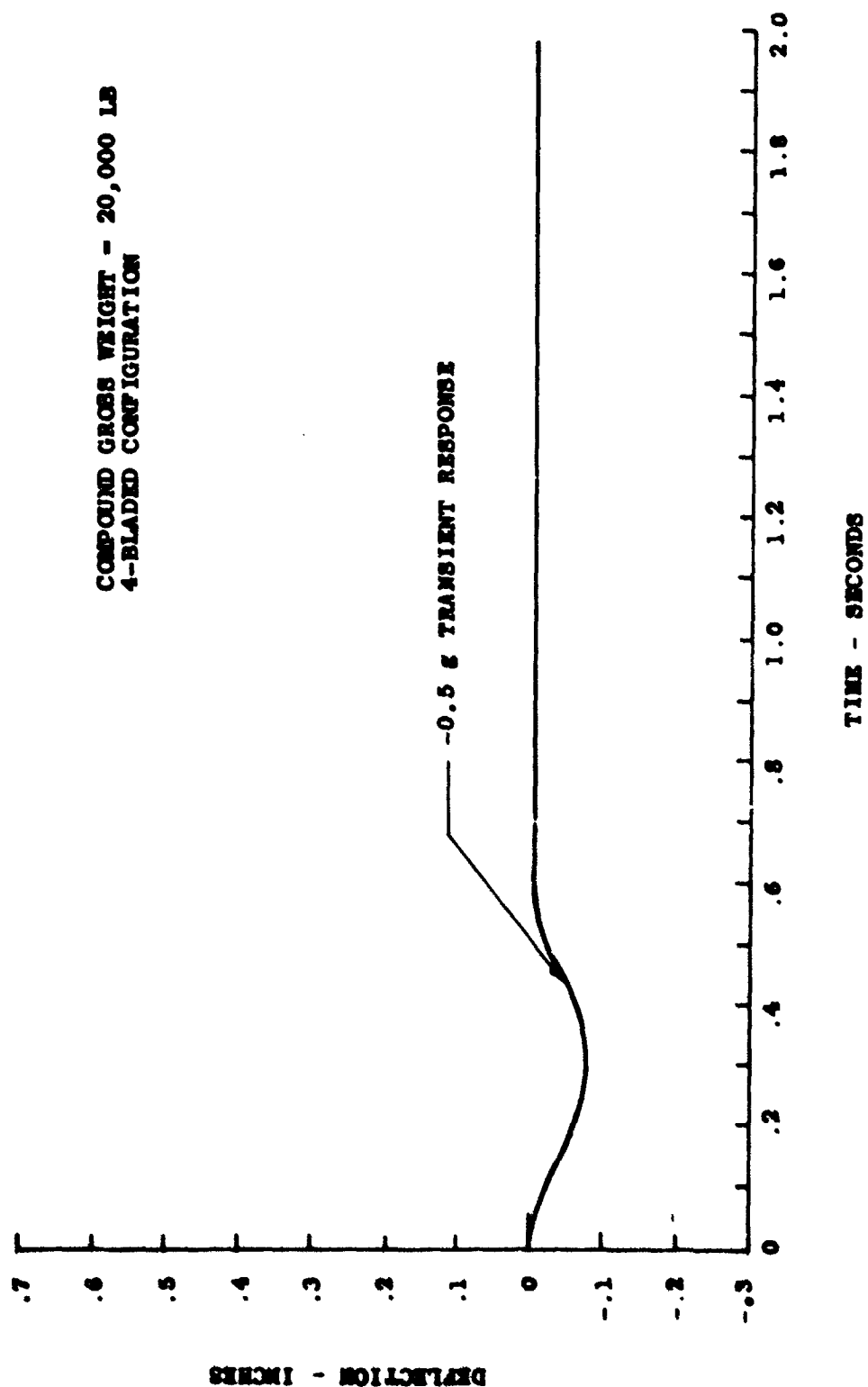


Figure 42. Transient Response to a $-0.5 \text{ g } \frac{1}{2} \sin^2$, 0.6-Second Input for Case 38 CT Versus Time.

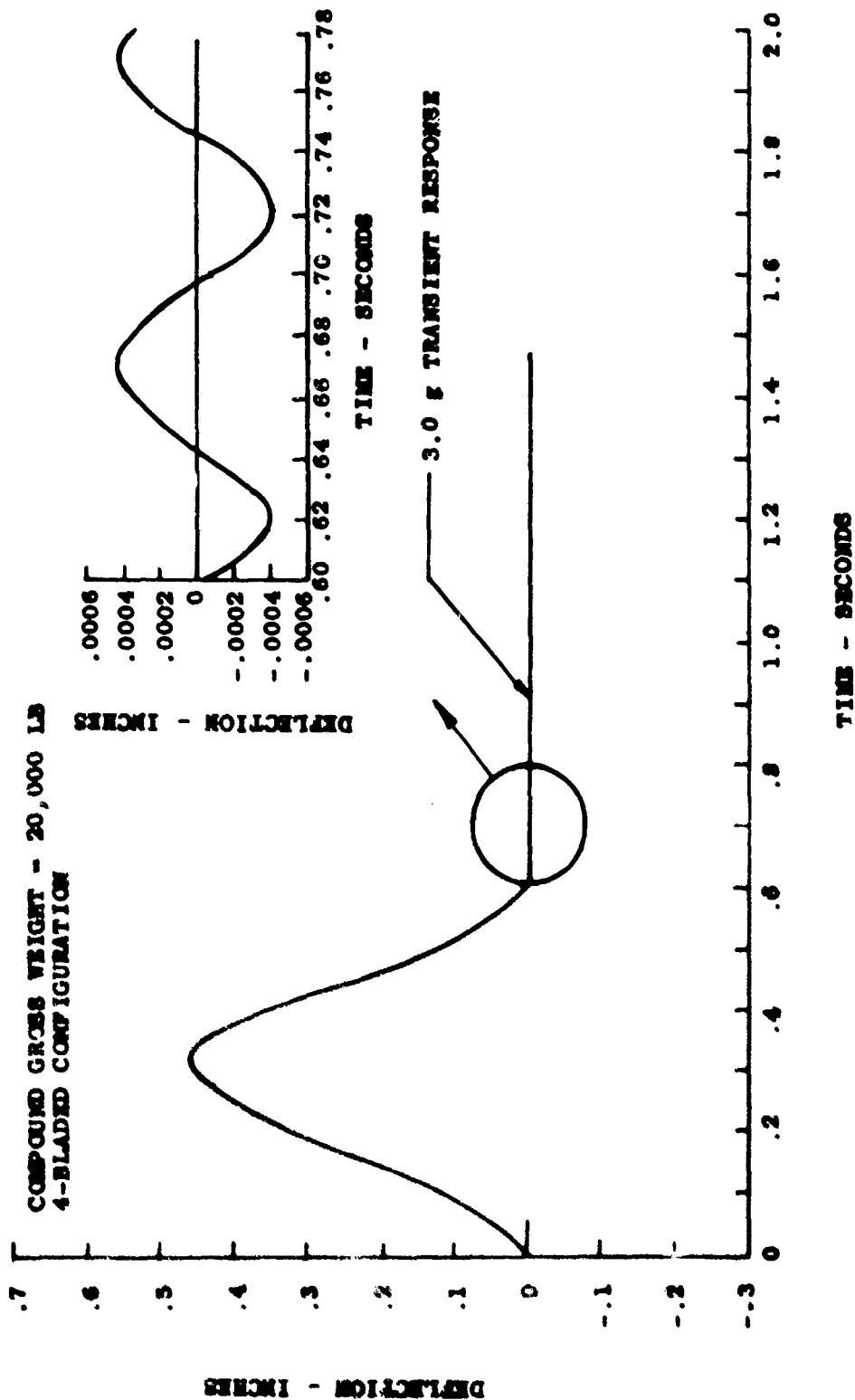


Figure 43. Transient Response to a $3.0 \text{ g } \frac{1}{2} \sin^2$, 0.6-Second Input for Case 38 CT Versus Time.

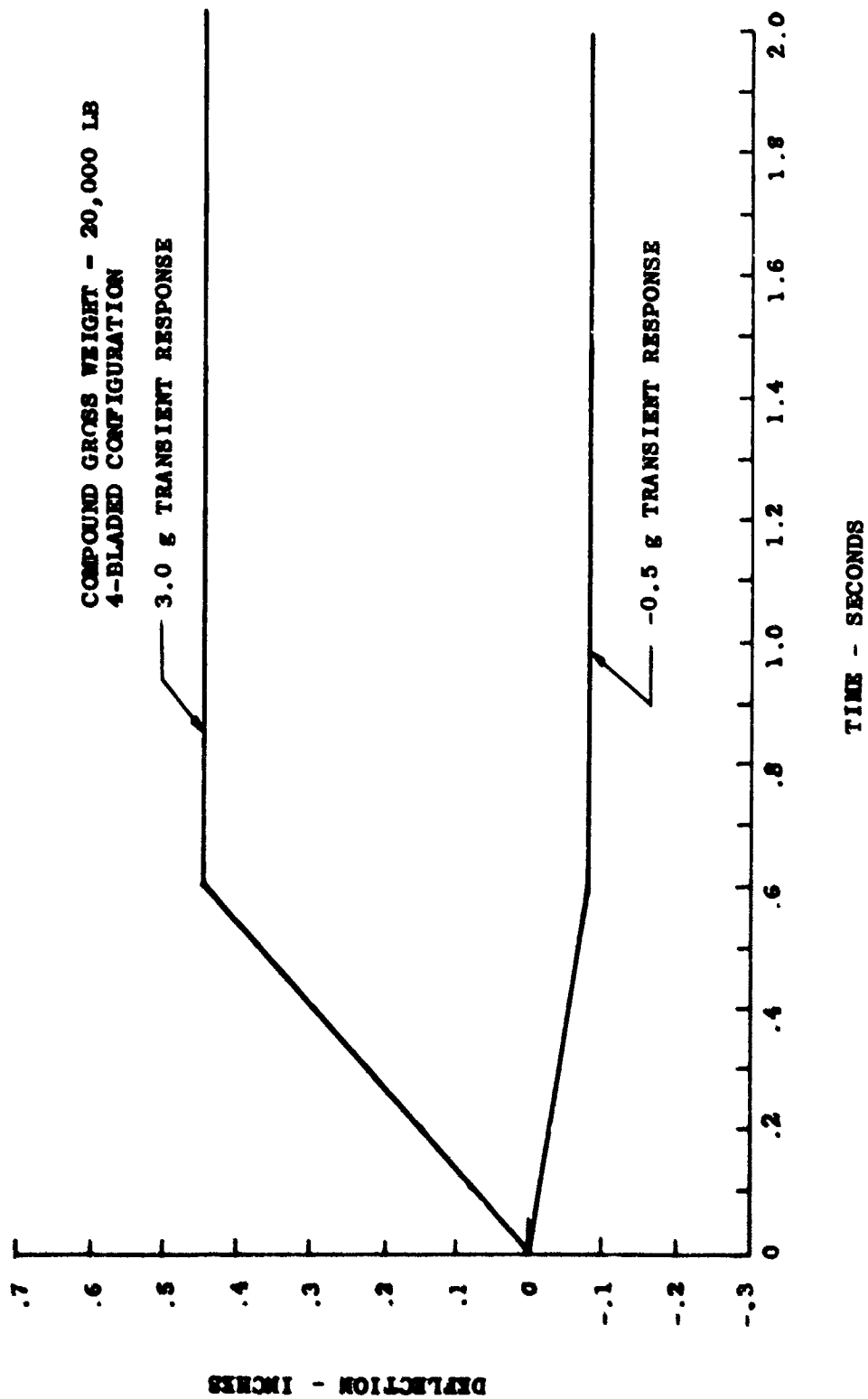


Figure 44. Transient Response Envelope for a 0.6-Second Ramp Input for Case 38 CT Versus Time.

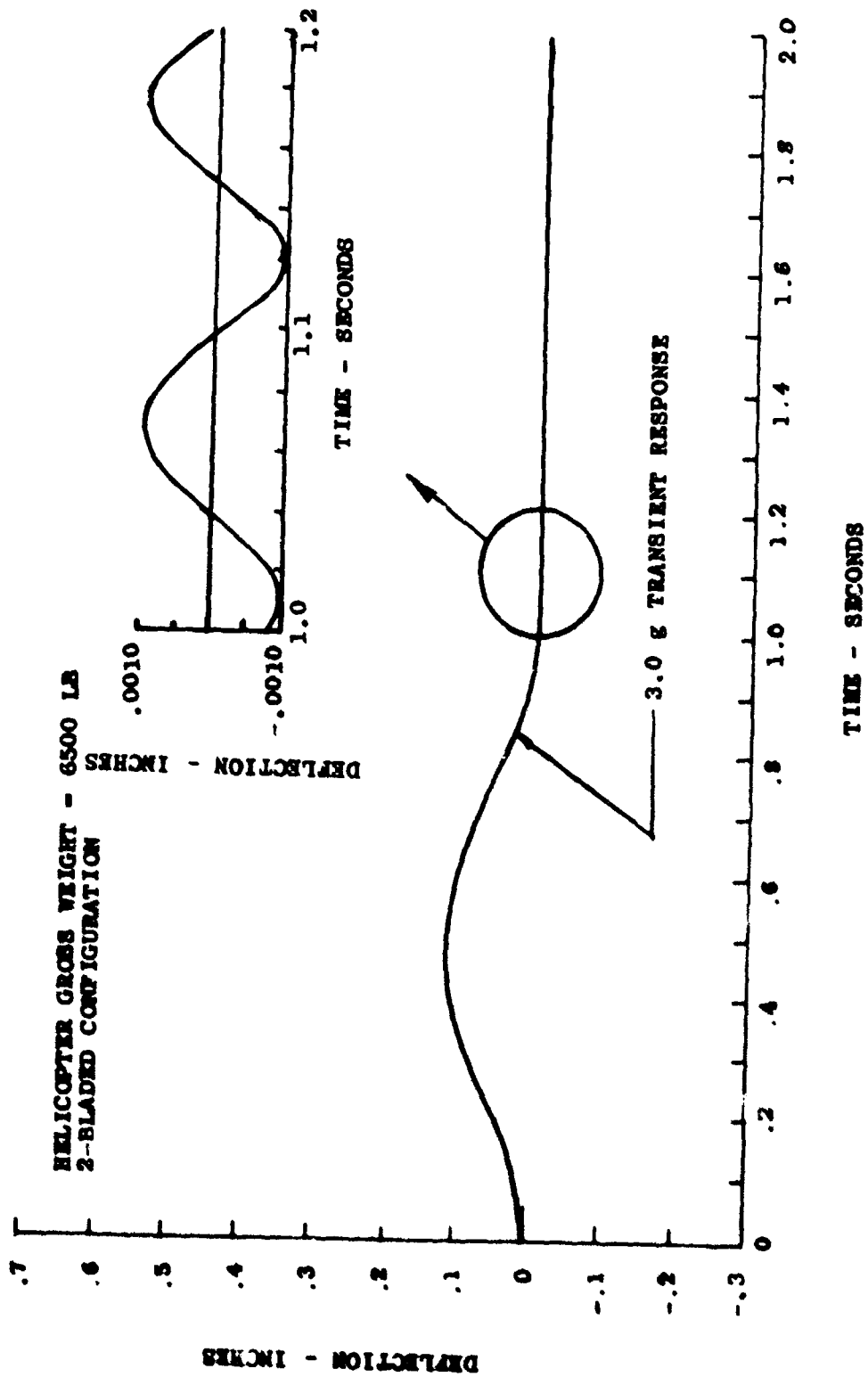


Figure 45. Transient Response to $3.0 \text{ g } \frac{1}{2} \sin^2$, 1.0-Second Input for Case 34 HT Versus Time.

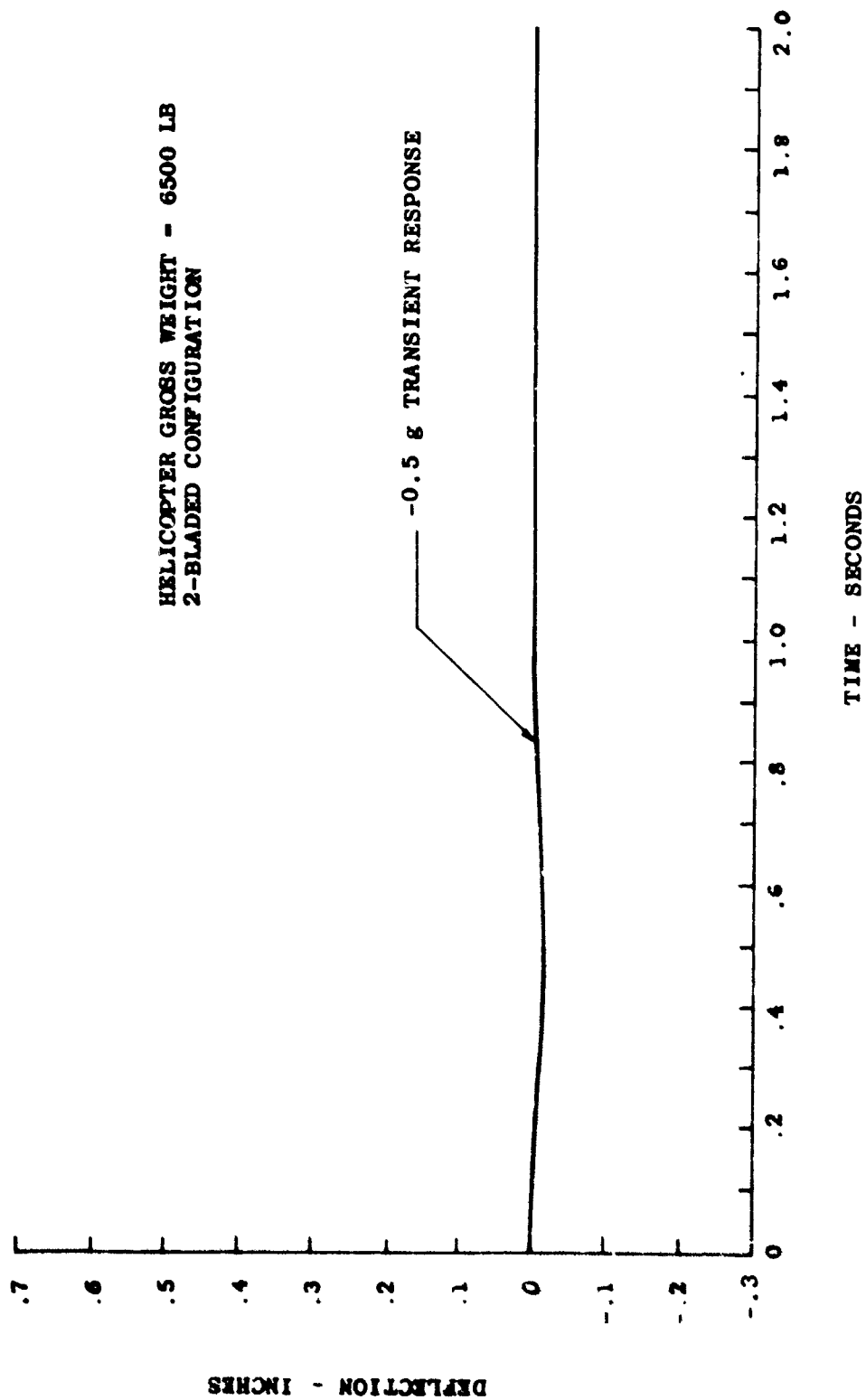


Figure 46. Transient Response to a -0.5 g , $\frac{1}{2} \sin^2$, 1.0-Second Input for Case 34 HT Versus Time.

HELICOPTER GROSS WEIGHT - 6500 LB
2-BLADED CONFIGURATION

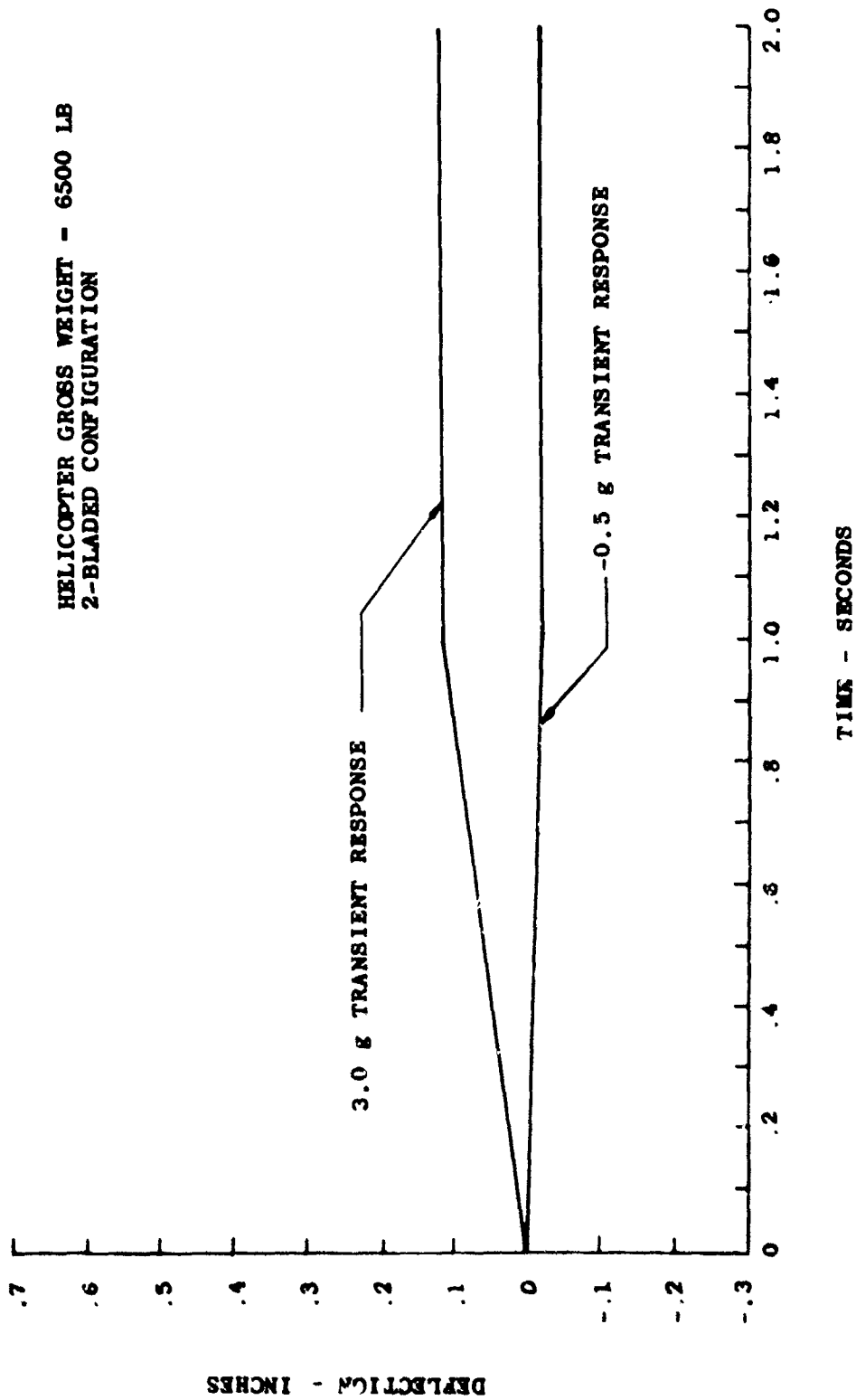


Figure 47. Transient Response Envelope for a 1.0-Second Ramp Input for Case 34 HT Versus Time.

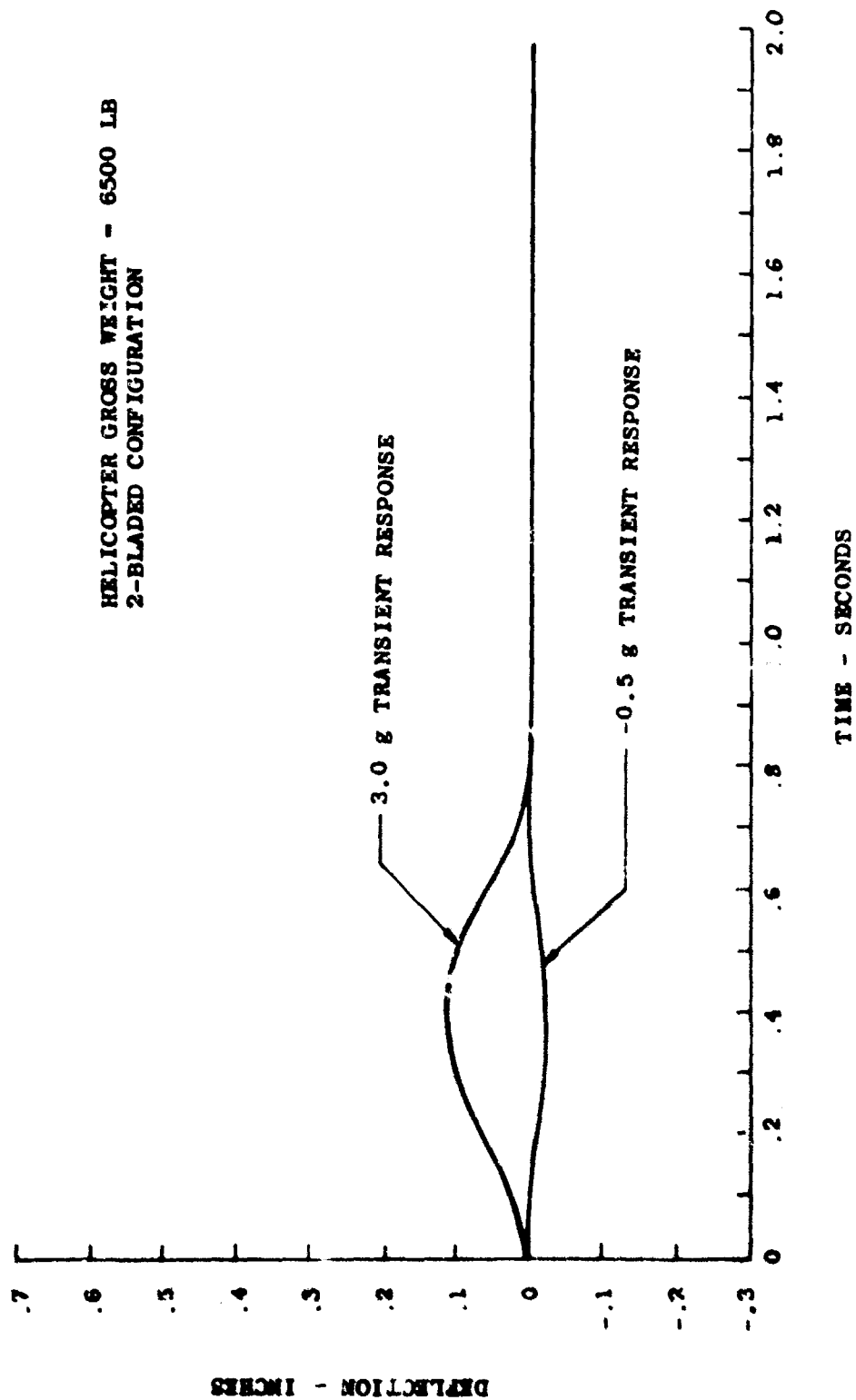


Figure 48. Transient Response Envelope for a 0.8-Second $\frac{1}{2} \sin^2$ Input for Case 34 HT Versus Time.

HELICOPTER GROSS WEIGHT - 6500 LB
2-BLADED CONFIGURATION

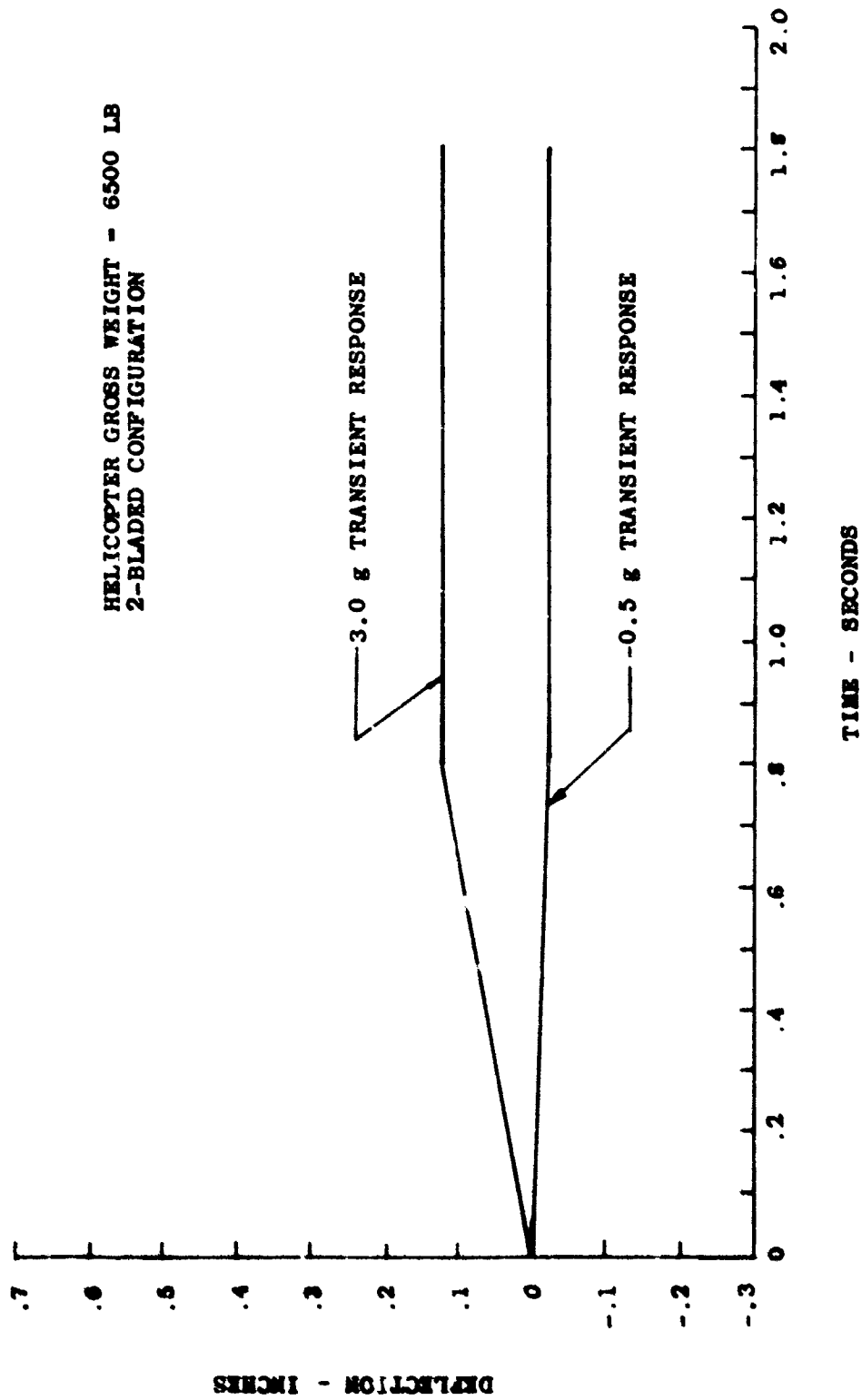


Figure 49. Transient Response Envelope for a 0.8-Second Ramp Input for Case 34 HT Versus Time.

HELICOPTER GROSS WEIGHT - 6500 LB
2-BLADED CONFIGURATION

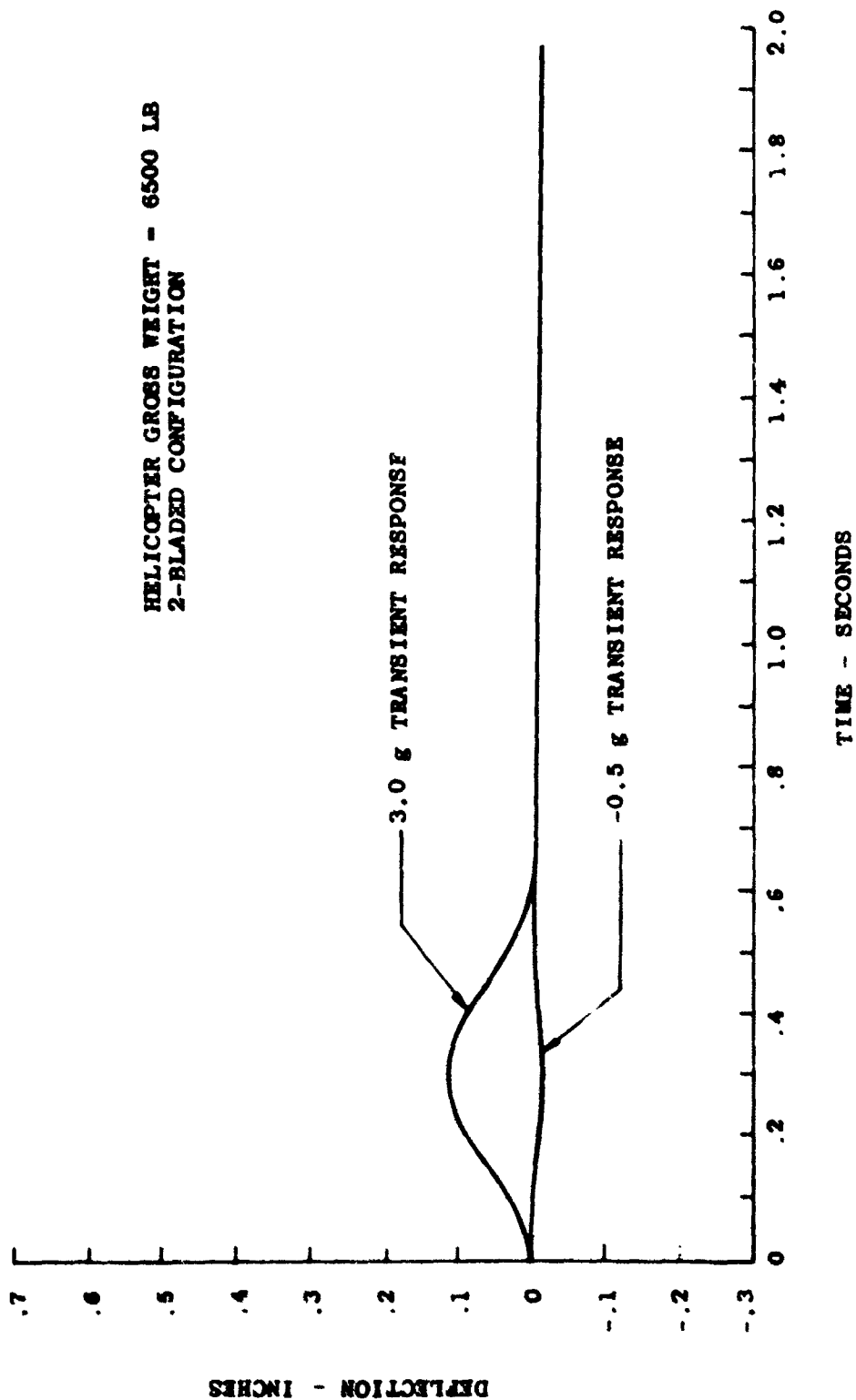


Figure 50. Transient Response Envelope for a 0.6-Second $\frac{1}{2} \sin^2$ Input for Case 34 HT Versus Time.

HELICOPTER GROSS WEIGHT - 6500 LB
2-BLADED CONFIGURATION

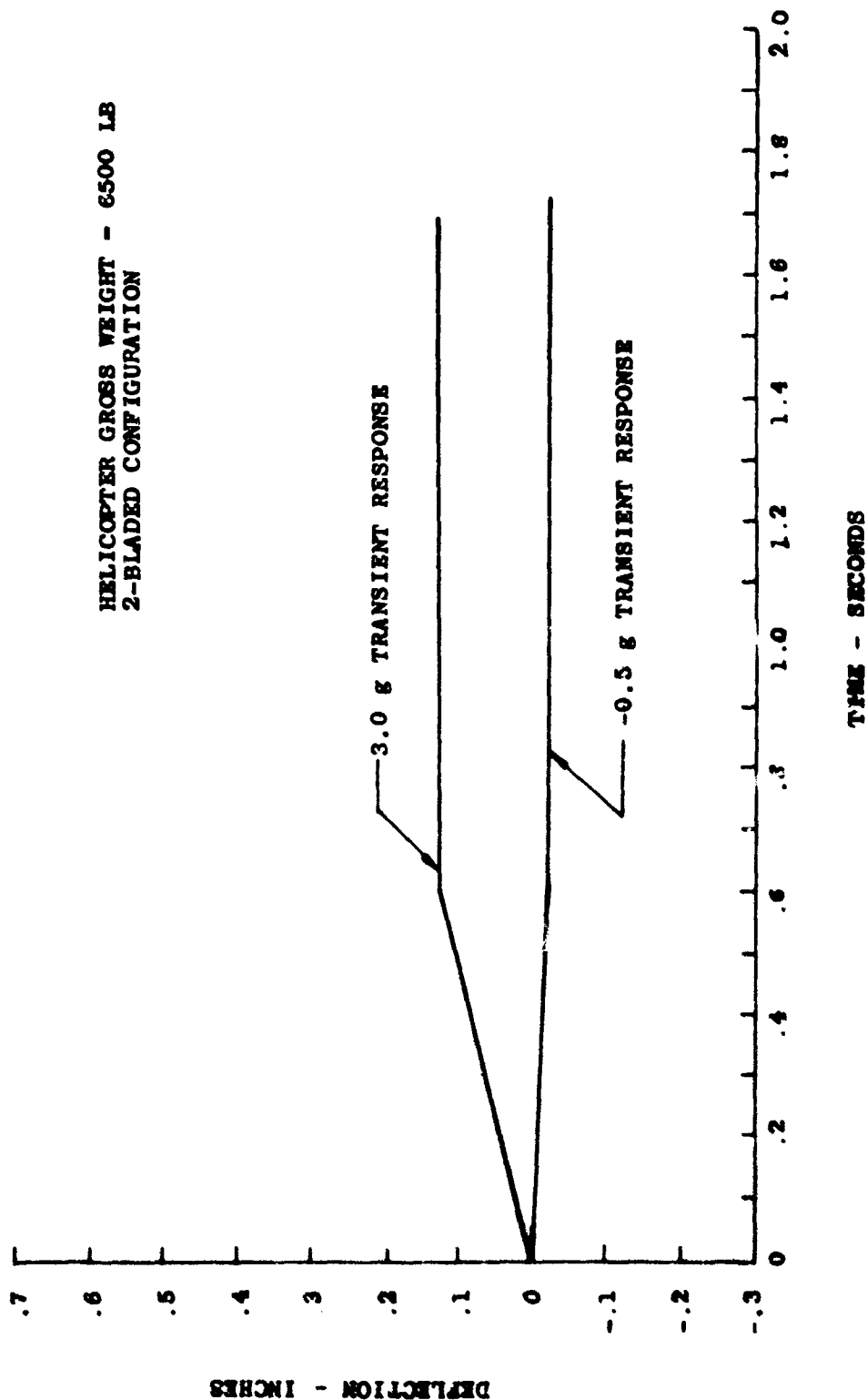


Figure 51. Transient Response Envelope for a 0.6-Second Ramp Input for Case 34 HT Versus Time.

MECHANICAL INSTABILITY

Mechanical instability is caused by the coupling between the in-plane hub motion and in-plane blade motions. The center of mechanical instability, which is the point at which the instability is most critical, is given by the following relationship:

$$\omega_n + \omega_b = \Omega_{M.I.} \quad (56)$$

in which

- ω_n - in-plane natural frequencies;
- ω_b - in-plane blade natural frequency;
- $\Omega_{M.I.}$ - rotor speed for center of mechanical instability.

It is seen from the above equation that, depending upon the natural frequency of the in-plane isolation system, mechanical instability could occur in flight.

For semirigid rotor systems, in which the in-plane natural frequencies of the blade are usually above 1/rev of the rotor, mechanical instability is not a problem. However, for articulated rotor systems, in which the natural frequency of the rigid-body mode of the blade due to lag hinge offset is well below 1/rev, the natural frequency of the blade is

$$\omega_b^2 = \frac{m_b a b \Omega^2}{I_b} \quad (57)$$

where

- m_b - mass of the blade;
- a - the distance from the center of the hub to the lag hinge;
- b - the distance from the lag hinge to the center of gravity of the blade;
- I_b - the moment of inertia of the blade about the lag hinge.

For a uniform blade with a 3.5-percent offset, the blade natural frequency is $.2\Omega$. This frequency is not affected to any great extent by a nonuniform blade distribution. Therefore, by knowing the hub natural frequencies and the blade natural frequency, the center of mechanical instability can be determined. Table XXIII gives the results of these calculations. This table is nondimensionalized on the operating rpm of the configurations considered. Also, only the lowest in-plane natural frequency is shown, since this is the most critical.

TABLE XXIII. CENTERS OF MECHANICAL INSTABILITY		
Case	In-Plane Hub Natural Freq. (ω_n/Ω)	Center of Mechanical Instability (Ω_{nz}/Ω)
1 HS	1.745	1.945
2 HS	2.310	2.510
3 HS	2.670	2.870
4 HS	1.759	1.959
5 HS	2.610	2.810
6 HS	2.840	3.040
7 HS	2.380	2.580
8 HS	2.835	3.035
9 HS	3.180	3.380
10 HS	3.480	3.680
11 HS	3.720	3.920
12 HS	3.775	3.975
13 HS	4.200	4.400
14 HS	1.735	1.935
15 HS	2.285	2.485
16 HS	2.640	2.840
17 HS	1.825	2.025
18 HS	2.196	2.396
19 HS	2.850	3.050
20 HS	2.350	2.550
21 HS	2.785	2.985
22 HS	3.060	3.260
23 HS	3.215	3.415
24 HS	3.430	3.630
25 HS	3.630	3.830
26 HS	3.630	3.830
27 CS	2.380	2.580
28 CS	2.640	2.840
29 CS	3.578	3.780
30 CS	2.510	2.710
31 CS	2.995	3.195
32 CS	3.410	3.610

It is seen from Table XXIII that the DAVI system is designed to have a natural frequency well above 1/rev; thus the center of mechanical instability occurs well above the operating range of the helicopter, and therefore, the possibility of mechanical instability occurring in flight is eliminated.

CRASH LOADS

In a crash condition, the DAVI rotor isolation system can be idealized structurally as a rigid mass, consisting of the rotor head, transmission, etc., which is supported at three, four, or more points. These support points in the vertical and lateral directions will be the DAVI isolators, while conventional isolation will be provided in the third direction. Therefore, combining the DAVI and the conventional isolator as an effective isolation point, the isolation system can be so designed that it can resist a force vector in any direction.

The study, as presented herein, deals with statistical aircraft; as such, all pertinent data represent rotary-wing aircraft in a particular gross weight range. Important factors which would influence the design of such an isolation system, and therefore the crash load analysis, are the locations of the centers of gravity of the upper body and lower body, the locations and numbers of mounting points relative to the centers of gravity of either body, the DAVI configurations, and the material selection. The locations of the DAVI's will determine the wheel base for load reactions when these units are bottomed out under crash conditions.

The DAVI rotor isolation system can be designed to exhibit ultimate strength and rigidity sufficient to withstand load factors of 20 forward, 20 downward, and 10 laterally, acting alternately in either lateral direction, and independent of each other as set forth in the requirements of Reference 24.

The concept of DAVI rotor isolation is feasible. The installation of such a system could be between the main transmission and the transmission mount between the transmission mount and the fuselage structure, or between a palletized upper-body package of rotor, engine, and transmission and the fuselage structure. The DAVI system will be designed to allow for freedom of motion and operation during all steady-state and maneuver flight conditions. The system, in addition, will incorporate at each isolator a bottoming or fail-safe provision which will only become effective outside all normal and maneuver flight conditions and during the buildup of loads resulting from crash accelerations.

CONTROL MOTIONS

When a rotor isolation system is designed, consideration must be given to subsystems, where relative motion could affect their performance. The passive-type DAVI rotor isolation for the cases studied and analyzed in this report resulted in static deflections ranging from .05 inch to .10 inch for the helicopter configurations and up to .155 inch for the compound configurations. Because of these small deflections, the effect on control motions and control inputs is small.

One of the features of the DAVI isolation system is its in-plane isolation above the antiresonant or predominant frequency. Thus, the DAVI isolation discussed herein will retain the magnitude of control input, being a function of relative motion, to a minimum.

Transient deflections, due to maneuver or gust conditions, can introduce control motions. Proper design of the system, however, can either eliminate these effects or produce a stabilizing feedback into the control system.

Maneuver conditions will impart vertical displacements onto the isolation system. Depending on the geometric arrangements of the isolators and the relationship of hub to center of gravity as well as the relationship between upper- and lower-body cg's, there will be either a pure collective or a collective coupled with cyclic input to the control system. The response of the control system to these inputs can also vary depending on the sensitivity of the control system, the geometry and location of the control system, and the magnitude of the control input.

Control motion input resulting from the isolation system installed can be rigged to provide a stabilizing feedback to the rotor itself. Relative control motion inputs fed through the linkages can also be sensed and eliminated by means of compensating linkages, so that no feedback of these relative motions would be present at the pilot's stick. Variations of these methods have been flown on Kaman's HTK, HOK, and K-17 helicopters, where the feasibility has been successfully established.

Therefore, because of the low static deflection of the DAVI isolation system, its excellent transient response, and its in-plane isolation, the DAVI offers unique features beneficial in the design of the control system for an isolated helicopter.

MISALIGNMENT CONSIDERATIONS AND ROTOR RESPONSES

When the upper body is defined as the rotor plus transmission, the engine will be part of the lower body or fuselage package. For this arrangement, misalignment between the two bodies and therefore between the engine and transmission is of great concern. This misalignment can be due to translation or rotation of both upper and lower body.

When taking a typical configuration, such as Case 4 HS, which illustrates a 6500-pound helicopter, and applying a 1000-pound vibratory force at the hub in all three directions, the deflections and angular motions are small. The pitching motion is .191 degree, the rolling motion is .163 degree and the maximum translation occurred in the vertical direction where the displacement was .119 inch.

Although the 1000-pound vibratory forces are conservative, both the angular and translational deflections are small. Both angular and translational deflections are small and should present no problems to couplings and shafting between the engine and the transmission. The relative motions encountered here are well within the conventional coupling and shaft design limitations now in use.

At the tuned or N/rev frequency where the isolated body or fuselage experiences maximum isolation, the upper body or rotor and transmission, as defined in typical case 4HS, will not be isolated. For this two-bladed, 6500-pound helicopter, the upper body response is defined by the effectivity of the upper body. The effectivity of the upper body is the non-dimensional ratio of the response of the rigid system over the response of the unisolated upper body. The vertical effectivity of the upper body for this case is .343 at the tuned frequency. As the frequency increases, this effectivity will increase so that at $2N/\text{rev}$, $3N/\text{rev}$, and $4N/\text{rev}$, the effectivity is .774, .80, and .808, respectively.

RELIABILITY ANALYSIS

ASSUMPTIONS AND DEFINITIONS

The DAVI Rotor Isolation System under analysis is assumed to be that of Figure 52, where fail-safe features such as the two bumper bars are provided. An additional assumption is that four DAVI's are required to adequately isolate main rotor vibration from the aircraft structure. The following definitions apply to the ensuing analysis:

System - A group of four DAVI's.

Mission - The provisions of adequate main rotor to aircraft structure isolation and attachment.

Reliability - The probability of successful operation of the DAVI system under specified conditions for the specified length of time.

Failure - Any event peculiar to the DAVI system (or a subordinate part within it) which causes its performance to deviate from that specified.

Failure Mode - The manner in which a component, assembly, subsystem, system, etc., can fail.

Failure Effect - The manner of DAVI misbehavior resulting from the occurrence of one or more of the component failure modes.

Failure Mode Probability - That proportion of total inherent failure tendencies which can be substituted to a kind, mode, or manner of failure. It is evaluated as a portion of the failure rate of the particular application at each component, assembly, subsystem, system, etc., level.

Catastrophic Loss of Vehicle - That failure occurrence that results in catastrophic loss of the total system or vehicle.

Mandatory Abort - That failure occurrence that results in the execution of an abort procedure immediately upon failure detection.

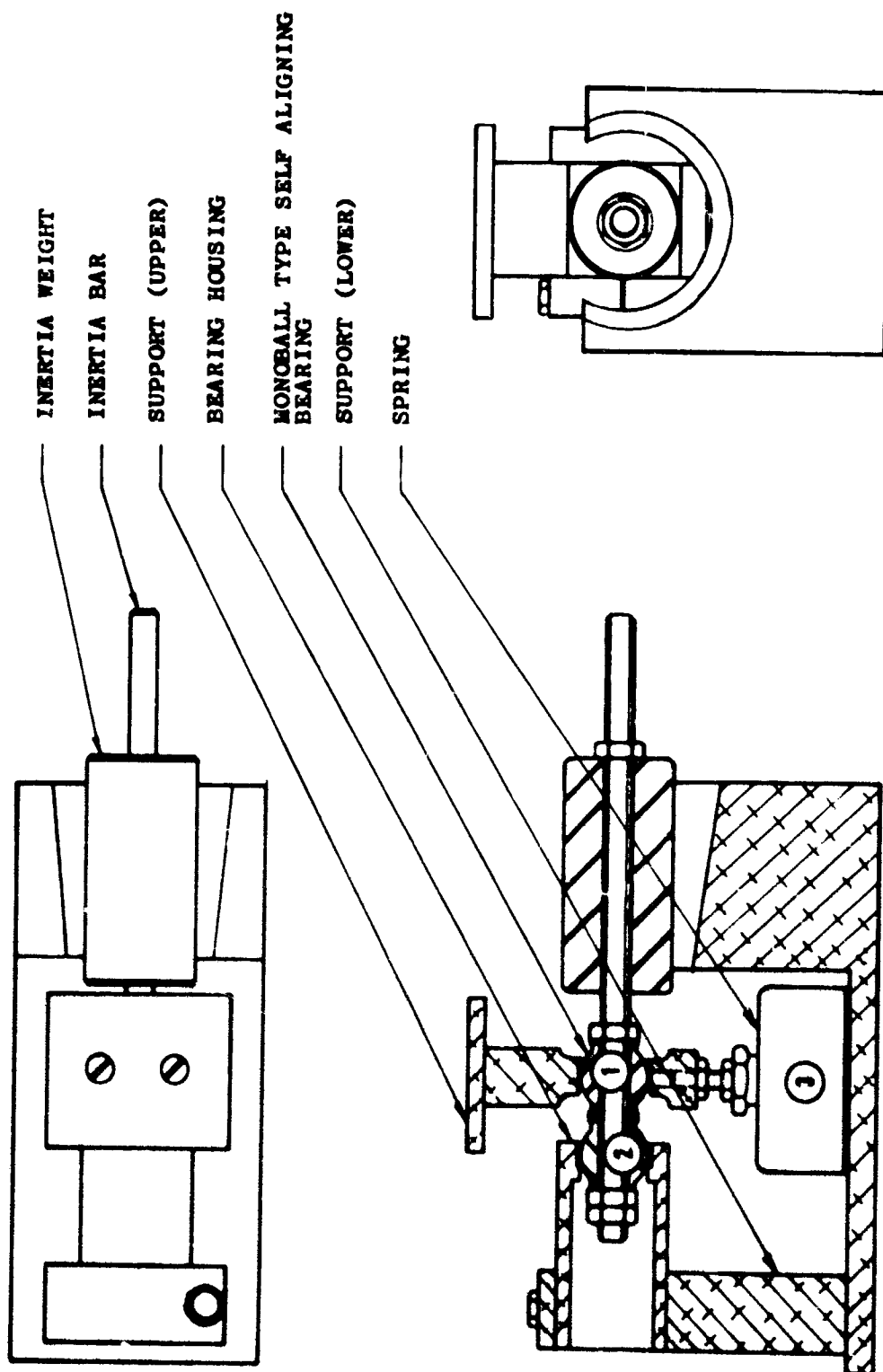


Figure 52. Two-Dimensional DAVI.

Precautionary Abort - That failure occurrence that results in the execution of an abort procedure sometime prior to the end of a mission.

Performance Degradation - That failure occurrence that has little effect on mission accomplishment; however, the system or vehicle does operate at reduced performance.

FAILURE MODES AND EFFECTS ANALYSIS

Component level failure mode analysis indicates the way in which component failures affect total system operation. The following guidelines are generally followed in such an analysis:

1. A detailed explanation of each component failure, its most probable modes of failure, and corresponding effects of each failure on system performance.
2. A determination of whether the system can tolerate these failures.
3. A determination of possible correction measures to minimize or eliminate these potential failure effects.
4. Normally, a verification of the analytical results by performing stress and design verification tests; however, this effort is beyond the scope of this contract.

Failure rates and probabilities derived from various indicated sources are used in the quantitative portion of this analysis.

To effectively organize the analysis process, Kaman Form Failure Modes and Effects Analysis Work Sheet, Table XXIV, is used to catalogue the modes and failure rates of each component of the DAVI rotor isolation system. Each component is itemized, a reference symbol is assigned corresponding to that of Figure 52, failure modes and possible causes of failure are indicated, effects of failure are listed, and possible correction and control measures are established. The section of the form entitled FAILURE RATE ALLOCATION indicating the quantitative reliability estimate of system and malperformance is divided into as many categories as are described by the analyst. Each coded alphabetical letter column is totaled to obtain resultant probabilities. These are used in the analysis of DAVI rotor isolation system function and mission performance.

TABLE XXIV FAILURE MODES AND EVENTS ANALYSIS

NAME SHEET									
ENGINEER S. Pratt			DATE 7-18-67						
CODE: A Catastrophic Loss of Vehicle			D Performance Degrad.						
B MODALITY ANAL.									
C DISCUSSIONARY MODEL									

Table XXV summarizes the expected resultant probabilities of the DAVI rotor isolation system. It is interesting to note that relative to the system configured in Figure 52 and considering worst-case possibilities, in the event of a failure (whose likelihood is extremely small), the predominant mode of failure is the B mode (Mandatory Abort). The A mode (Catastrophic Loss of Vehicle) is much less likely to occur.

RELIABILITY ANALYSIS

The total failure rate of one DAVI rotor isolator shown in Column 8 of Table XXIV is 45 failures per million hours. Since the system consists of four DAVI's in a serial configuration, the system total is 180 failures per million hours. However, these estimates are considered to be extremely conservative, since the data taken from FARADA and Martin-Avco upon which they are made include many types of bearings and springs. Through optimum selection of DAVI components, as well as maintenance and inspection schedules, the failure rate could be reduced considerably with the elimination of the catastrophic mode.

Reliability of the DAVI rotor isolation system, assuming experimentality and considering a mission length of, say, 3 hours and a failure rate of 180 failures/10⁶ hours, is

$$R = e^{-\lambda t} = e^{-(.000180)3} \quad (58)$$

$$= 0.99946$$

where

λ - system failure rate (failures/hours)

t - mission length (hours)

R - system reliability

Based on this reliability analysis and considering 100,000 3-hour-long missions, the mode of failure would be distributed as shown in Table XXIV.

TABLE XXV. EFFECTS SUMMARY			
Failures Per 100,000 3-Hour-Long Missions			
Code	Mode Of Failure	Failure Distribution Probability	Number Of Failures
A	Catastrophic Loss of Vehicle	.005	0.3
B	Mandatory Abort	.89	48.0
C	Precautionary Abort	-	-
D	Performance Degradation	.105	5.7

These figures may be interpreted to mean that one would expect 54 failure occurrences (of which 0.5% or less than 1 would result in catastrophic form, 89% or 48 would result in mandatory abort, and 10.5% or better than 5 would result in performance degradation) in 100,000 3-hour-long missions.

The catastrophic rate (less than 1 in 100,000 missions or 1 in 1 million hours) compares favorably to the reliability of critical components in helicopter systems. Control and rotor components are designed with 0.9999 reliability over the duration of their respective service lives (average of 500 hours). The DAVI system possesses 0.9995 at 500 hours against catastrophic failure, since its catastrophic failure rate is 1 failure per 1 million hours.

Judicious choice of components together with proper maintenance and inspection procedures will further enhance the reliability of the above system.

CONCLUSIONS

This study has accomplished the goals set forth and, thus, has demonstrated that rotor isolation of rotary-wing aircraft is analytically feasible by employing a passive isolation system, the Kaman DAVI. The following conclusions, based on the results of this study, can be made:

1. Rotor isolation with the Kaman DAVI is feasible.
2. Using the analytical model of this study, antiresonant isolation was proven feasible at the N/rev or predominant excitation frequency as well as at its multiples at $2N/\text{rev}$, $3N/\text{rev}$, and $4N/\text{rev}$.
3. This isolation was made feasible with a two-directional DAVI and a conventional isolator in the longitudinal direction. Isolation was achieved in all three translational and rotational modes.
4. Amplification at $1/\text{rev}$ was held at a minimum using an effectivity of 0.90 as a criterion.
5. Rotor isolation is feasible with less than 0.10 inch static deflection in the helicopter isolation system.
6. Rotor isolation is feasible, as exemplified on statistical helicopters ranging from 2000 pounds to 100,000 pounds and on a 20,000-pound compound helicopter.
7. Analytical results showed that for a compound vehicle, isolation can be obtained for a 15% range of rotor speed.
8. Inertia coupling affects the effectivity at the tuned frequency. For maximum isolation, inertia coupling should be minimized with proper selection of isolation system location.
9. Damping across the DAVI system has the conventional effect of reducing the amplification at resonance (increasing effectivity) and reducing isolation at the tuned frequency (reducing the effectivity at N/rev).
10. Changing the mass of the lower body or fuselage has negligible effect on the effectivity at N/rev .

11. For a given condition, the change in static deflection is inversely proportional to a change in DAVI weight, keeping all other geometric relationships of the DAVI design constant.
12. Without damping in the system, the overshoot for the transient conditions analyzed is a minimum.
13. The natural frequencies of the system were well above 1/rev, and therefore the possibility of mechanical instability occurring in flight is eliminated.
14. Changing the number of DAVI's for a given installation varies the effectivity at N/rev due to the change in bandwidth as a result of the coupling effects.

RECOMMENDATIONS

This study dealt with the analytical feasibility of rotor isolation of rotary-wing aircraft. Using a two-body mathematical model employing rigid-body assumptions, the analytical feasibility of rotor isolation has been established utilizing the Kaman DAVI, a passive isolator.

This contractor recommends continued effort using the results of this study as a building block toward the ultimate goal of an operational isolation system for an actual helicopter.

Toward this goal, it is recommended that analytical results be substantiated with test results from a realistic model such as a readily available helicopter which has an existing isolation system. Utilizing mechanical excitation on the model, the effectivity of the existing isolation system can be obtained. An analytical comparison will be made using the geometric, mass, and inertia characteristics of this helicopter. A DAVI rotor isolation system will then be analyzed, an experimental model will be built, and the helicopter will be modified to incorporate the Kaman DAVI. This experimental design would then be tested by the same procedure by which the existing system was evaluated. A comparison will then be made of the DAVI and existing system effectivities for both the analytical and experimental phases of this program.

The experimental hardware should be designed and stress analyzed so that with sufficient test substantiation, this hardware could be employed for a limited flight evaluation.

REFERENCES CITED

1. Theobald, C.E., Jr., and Jones, R., ISOLATION OF HELICOPTER ROTOR VIBRATORY FORCES FROM THE FUSELAGE, Kaman Aircraft; Wright Air Development Center Technical Report 57-404, Wright-Patterson Air Force Base, Ohio, September 1957, AD 130 991.
2. Flannelly, W.G., DYNAMIC ANTIRESONANT VIBRATION ISOLATOR (DAVI), Kaman Aircraft Report RN 63-1, Kaman Aircraft, Bloomfield, Connecticut, November 1963.
3. Anderson, R.C., and Smith, M.F., A STUDY OF THE KAMAN DYNAMIC ANTIRESONANT VIBRATION ISOLATOR (DAVI), Kaman Aircraft; USAAVLABS Technical Report 65-75, U. S. Army Aviation Materiel Laboratories, Fort Eustis, Virginia, January 1966, AD 629 636.
4. Arkin and Colton, STATISTICAL METHODS, Barnes and Noble, Incorporated, New York, New York, 1953, Fourth Edition.
5. Silveria, M.A., AN INVESTIGATION OF PERIODIC FORCES AND MOMENTS TRANSMITTED TO THE HUB OF FOUR LIFTING ROTOR CONFIGURATIONS, NASA TN D-1011, Langley Research Center, Hampton, Virginia, March 1962, AD 272 900.
6. Duvivier, J.F., STUDY OF HELICOPTER ROTOR-ROTOR INTERFERENCE EFFECTS ON HUB VIBRATION, TDR No. ASD-TR-61-601, Wright Patterson Air Force Base, Flight Dynamics Laboratory, Aeronautical Systems Division, Air Force Systems Command, Ohio, June 1962.
7. Scheiman, James, A TABULATION OF HELICOPTER ROTOR-BLADE DIFFERENTIAL PRESSURES, STRESSES, AND MATRICES AS MEASURED IN FLIGHT, NASA TM X-952, Langley Research Center, Hampton, Virginia, March 1961.
8. Smollen, L.E., Marshall, P., and Gabel, R., A SERVO CONTROLLED ROTOR VIBRATION ISOLATION SYSTEM FOR THE REDUCTION OF HELICOPTER VIBRATION, Institute of the Aerospace Sciences, Paper Number 62-34, Institute of the Aerospace Sciences, 2E. 64th Street, New York, New York, January 1962.
9. Gessow, A., and Meyers, G.C., Jr., AERODYNAMICS OF THE HELICOPTER, The Macmillan Company, New York, 1952.

10. Payne, P.R. **HELICOPTER DYNAMICS AND AERODYNAMICS**, The Macmillan Company, New York, 1959.
11. Ham, N.D., and Madden, P.A., **AN EXPERIMENTAL INVESTIGATION OF ROTOR HARMONIC AIRLOADS INCLUDING THE EFFECTS OF ROTOR-ROTOR INTERFERENCE AND BLADE FLEXIBILITY**, Massachusetts Institute of Technology; USAAVLABS Technical Report 65-13, U. S. Army Aviation Materiel Laboratories, Fort Eustis, Virginia, May 1965, AD 615 922.
12. Piziali, R., Daughaday, H., and DuWaldt, F., **ROTOR AIRLOADS**, Cornell Aeronautical Laboratory, Inc.; Cal/TRECOM Symposium on Dynamic Load Problems Associated With Helicopters and V/STOL Aircraft, Buffalo, New York, June 1963.
13. Gabel, R., **IN-FLIGHT MEASUREMENT OF STEADY AND OSCILLATORY ROTOR SHAFT LOADS**, Vertol Division, Boeing Aircraft; Cal/TRECOM Symposium on Dynamic Load Problems Associated With Helicopters and V/STOL Aircraft, Buffalo, New York, June 1963.
14. Foulke, W.K., **EXPLORATION OF HIGH-SPEED FLIGHT WITH THE XH-41A RIGID ROTOR HELICOPTER**, Lockheed-California Company; USAAVLABS Technical Report 65-25, U. S. Army Aviation Materiel Laboratories, Fort Eustis, Virginia, June 1965, AD 617 966.
15. VanWyckhouse, J.F., and Cresap, W.L., **HIGH-PERFORMANCE HELICOPTER PROGRAM**, Bell Helicopter Company; USAAVLABS Technical Report 64-61, U. S. Army Aviation Materiel Laboratories, Fort Eustis, Virginia, October 1964.
16. Whitfield, A.A., and Blackburn, W.E., **UH-2 HELICOPTER HIGH-SPEED FLIGHT RESEARCH PROGRAM UTILIZING JET THRUST AUGMENTATION**, Kaman Aircraft; USAAVLABS Technical Report 65-14, U. S. Army Aviation Materiel Laboratories, Fort Eustis, Virginia, March 1965, AD 616 104.
17. Kelly, B., **HELICOPTER VIBRATION ISOLATION**, SAE Report Preprint, Society of Automotive Engineers, New York, New York, January 1948.
18. Miller, R.H., **ROTOR BLADE HARMONIC AIR LOADING**, Institute of the Aerospace Sciences, Paper Number 62-82, January 1962.
19. Morduchow, M., Yuan, S.W., and Peress, K.E., **HELICOPTER BLADE-FORCES TRANSMITTED TO THE ROTOR HUB IN FLIGHT**; Wright Air Development Center Report 53-355, Wright-Patterson Air Force Base, Ohio, May 1953.

20. Morduchow, M., Yuan, S.W., and Peress, K.E., VIBRATIONS OF A HELICOPTER ROTOR SYSTEM AND FUSELAGE INDUCED BY THE MAIN ROTOR BLADES IN FLIGHT; Wright Air Development Center Report 53-286, Wright-Patterson Air Force Base, Ohio, June 1953, AD 21969.
21. Ricks, R.G., A STUDY OF TANDEM HELICOPTER FUSELAGE VIBRATION, Flight Dynamics Laboratory, Aeronautical Systems Division, ASD-TDR-62-284, Wright-Patterson Air Force Base, Ohio, September 1962.
22. Carter, E.S., Jr., TECHNOLOGICAL CONTRIBUTIONS OF THE CH-53A WEAPONS SYSTEM DEVELOPMENT PROGRAM, AIAA Paper No. 64-784, American Institute of Aeronautics and Astronautics, 1290 Avenue of the Americas, New York, New York, September 1964.
23. Anderson, C.R., HELICOPTER BLADE FORCES TRANSMITTED TO THE ROTOR HUB IN FLIGHT; Wright Air Development Center TR 58-554, Wright-Patterson Air Force Base, Ohio, May 1959, AD 216 297.
24. GENERAL SPECIFICATION OF AIRCRAFT WEAPON SYSTEMS, SD-24J, Volume II, Department of the Navy, Bureau of Naval Weapons, Washington, D.C., June 1963.

APPENDIX STATISTICAL DATA

WEIGHTS AND INERTIA

The scope of this contract required the investigation of rotor isolation and its effects on helicopters ranging in gross weight from 2,000 pounds to 100,000 pounds.

Since there are no operational helicopters (in the free world) near the high gross weight range, it was necessary to estimate the rotor speed, upper and lower body, inertia and weights as well as the ship inertia for the 100,000-pound configuration. These data could then be used for inclusion in the analysis of the rotor isolation system and would thus be a description of a statistical helicopter rather than of any specific contractor vehicle.

The acquisition of data was limited to turbine-powered single-rotor helicopters with the following aircraft included:

Bell	OH-4A, UH-1B, UH-1D, UH-1F, Cobra
Hiller	OH-5A
Hughes	OH-6A, XV-9A
Kaman	UH-2A
Lockheed	XH-51A
Sikorsky	HH-52A, SH-3A, CH-3C, CH-53A, CH-54A

The statistical methods employed are outlined in Reference 4. The relationship of two statistical series may be defined by means of a "least squares" line where the resulting line is known as the line of regression. In the case of rotor speed versus gross weight, the trend is a nonlinear regression curve of the form

$$\log Y = a + b \log X \quad (59)$$

The relationship between gross weight and rotor weight is linear and results in a line of regression of the type

$$Y_c = a X \quad (60)$$

The excellence of the statistical relationship is measured by the coefficient of the correlation; thus, a coefficient of 1.0 presents perfect relationship with no scatter about the line of regression, while a value of zero would be a wholly imperfect relationship. The data presented in this report have a coefficient of .95 and better and are considered to be in excellent agreement with the line of regression.

The rotor weights, engine weight, and transmission weight referred to herein, were obtained, wherever possible, from published data and statistically analyzed to obtain the lines of regression reported in this study. It was assumed by this contractor that the definition of rotor weight, engine weight, and transmission weight were in compliance with the "Weight and Balance Data Reporting Forms for Rotorcraft", Military Standard 451, 2 June 1961. Therefore, the rotor weight includes the blades, retentions, hub and folding mechanism. The swashplate, rotor blade tracking devices and other rotor controls and linkages are excluded from the rotor weight and included in the rotor system controls of the flight controls group. Similar definitions can be made for the transmission and engine weights.

The analysis, presented in another section of this report, requires data for the unisolated helicopter and, therefore, weight and inertia properties of the entire ship. In addition, it is necessary to obtain weight and inertia properties for the isolated vehicle where the isolation system is installed between the upper body and the lower body of the helicopter. The upper body can be either a combination of rotor and transmission weight or rotor plus engine plus transmission weight, while the lower body is the fuselage weight.

Since the analysis includes all six degrees of freedom of both the upper and lower body of the isolated aircraft and all six degrees of freedom of the unisolated helicopter, it is necessary to obtain all weights and inertia for each body, including those of the unisolated aircraft.

Figure 53 shows a plot of rotor rpm versus helicopter gross weight. Presented here is the line of regression obtained from the statistical analysis, which shows a coefficient of correlation of 95.1%.

A plot of the rotor weight versus the gross weight of fourteen single rotor helicopters (varying from 2200 pounds gross weight to 38,000 pounds gross weight) is shown in Figure 54. The line of regression drawn through the data is for a constant ratio of rotor weight equal to 13.3% of gross weight and a statistical analysis of the data shows a coefficient of correlation of 99.0%.

Data for rotor plus transmission weights (W_{RT}) and rotor plus engine plus transmission weights (W_{RET}) are shown in Figures 55 and 56, respectively. These weights are plotted versus helicopter gross weight. The linear lines of regression obtained from the statistical analysis show coefficients of regression of 99% and 99.3%, respectively.

The roll, pitch, and yaw inertias obtained from a statistical analysis for the rotor plus transmission upper body are presented versus a range of helicopter gross weights in Figures 57, 58, and 59. The exponential regression lines have a coefficient of correlation of 98.4%, 98.4%, and 94.5% respectively.

The roll, pitch, and yaw inertias of the rotor plus engine plus transmission upper body are presented versus a range of helicopter gross weights in Figures 60, 61, and 62. This statistical information illustrates exponential regression lines with coefficients of correlation of 94%, 98.3%, and 99.7% respectively.

Figures 63, 64, and 65 present the inertia of the entire helicopter or the unisolated vehicle. The roll, pitch, and yaw inertias are plotted versus helicopter gross weight. The coefficients of correlation for these exponential lines of regression are 94.9%, 98%, and 98.4% respectively.

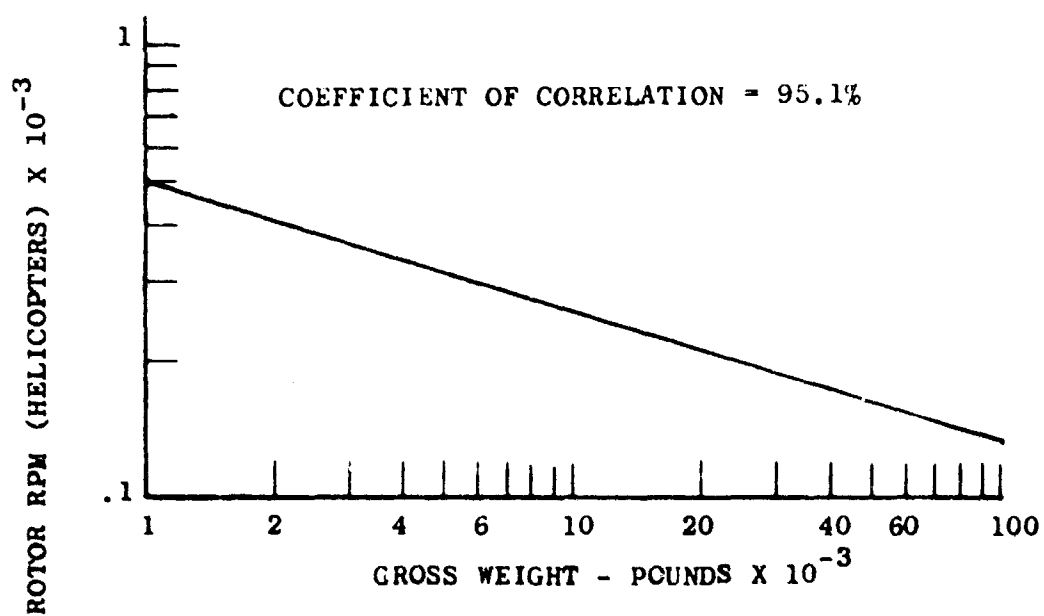


Figure 53. Statistical Rotor RPM for a Range of Helicopter Gross Weights.

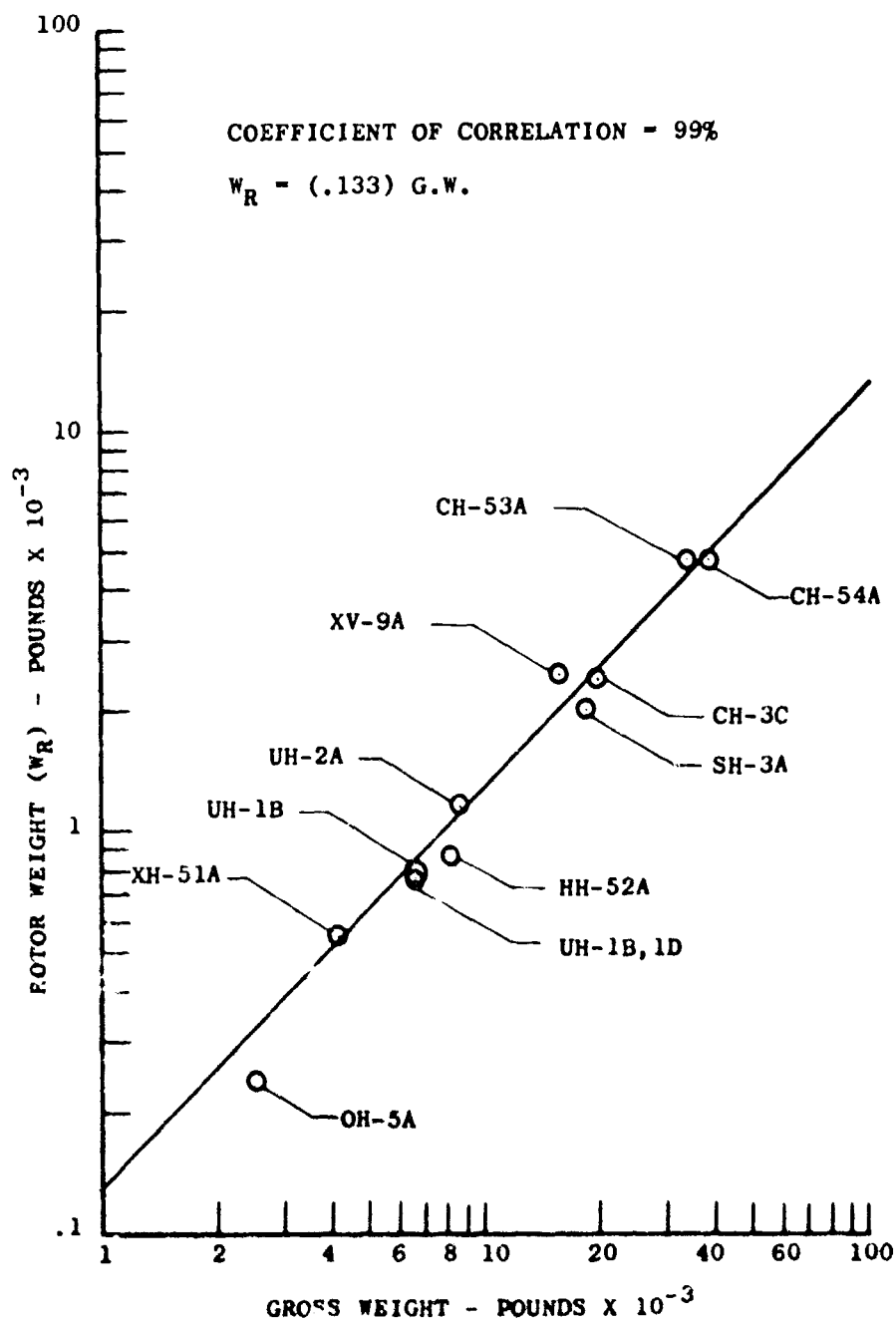


Figure 54. Statistical Rotor Weight for a Range of Helicopter Gross Weights.

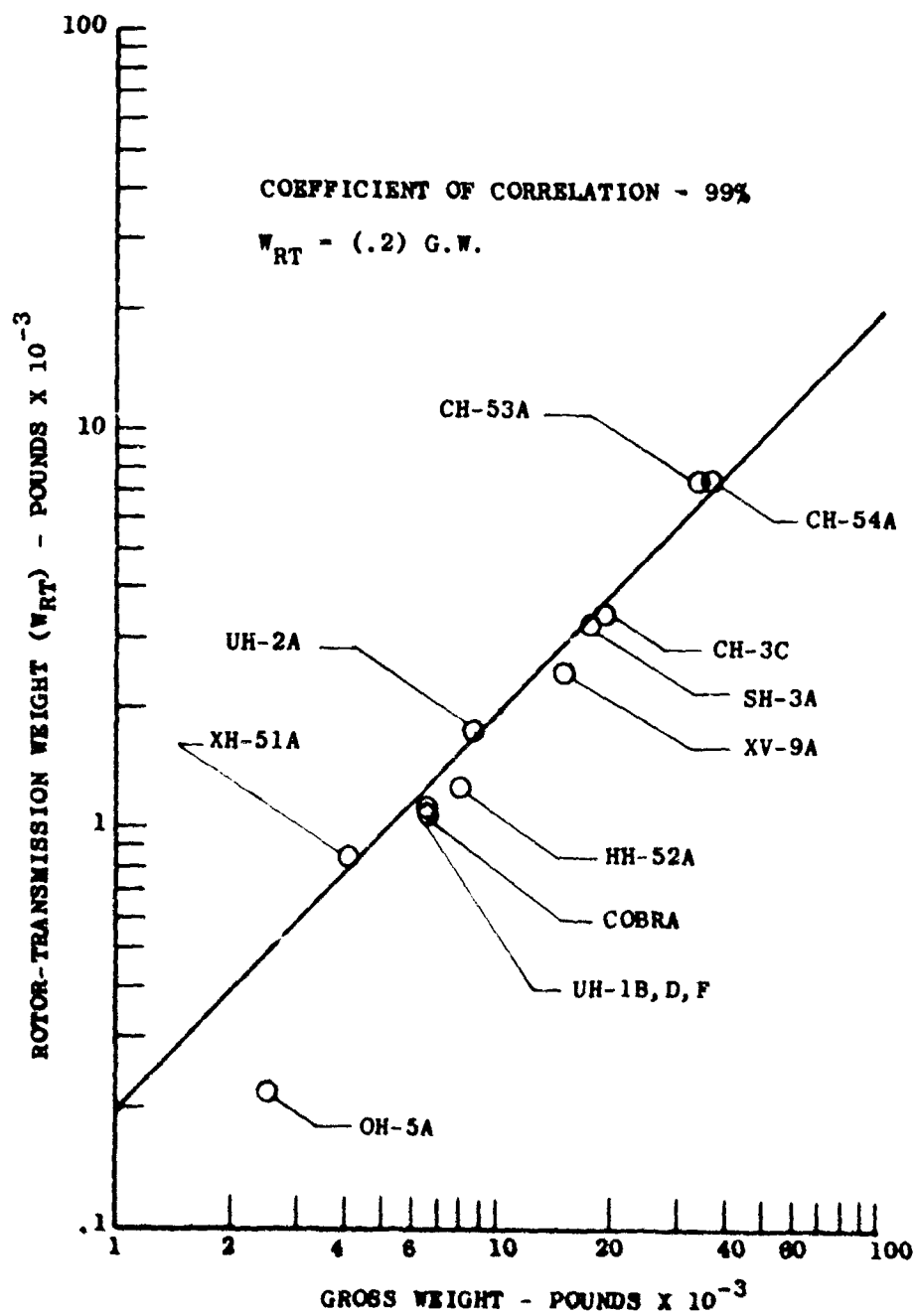


Figure 55. Statistical Rotor-Transmission Weights for a Range of Helicopter Gross Weights.

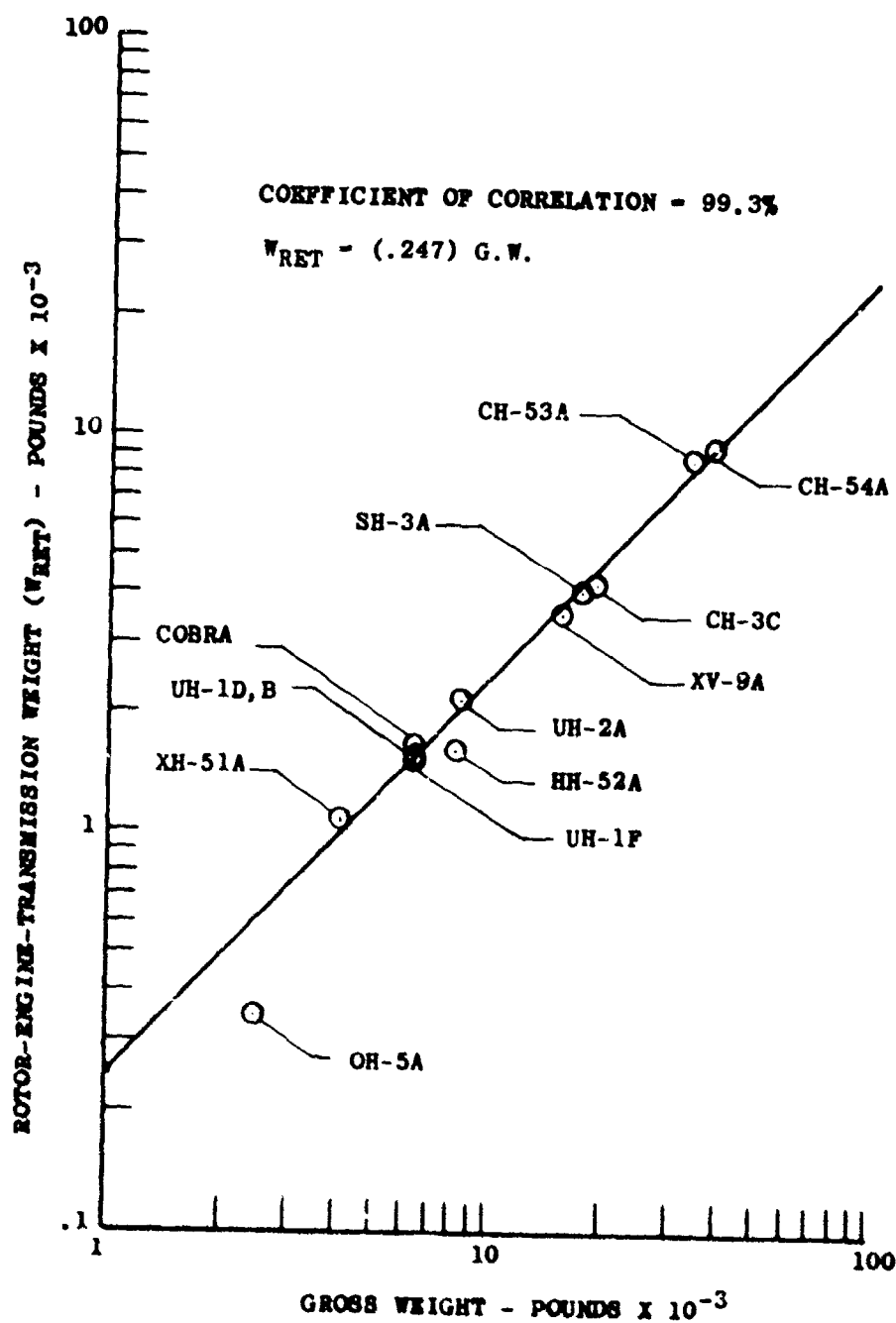


Figure 56. Statistical Rotor-Engine-Transmission Weights for a Range of Helicopter Gross Weights.

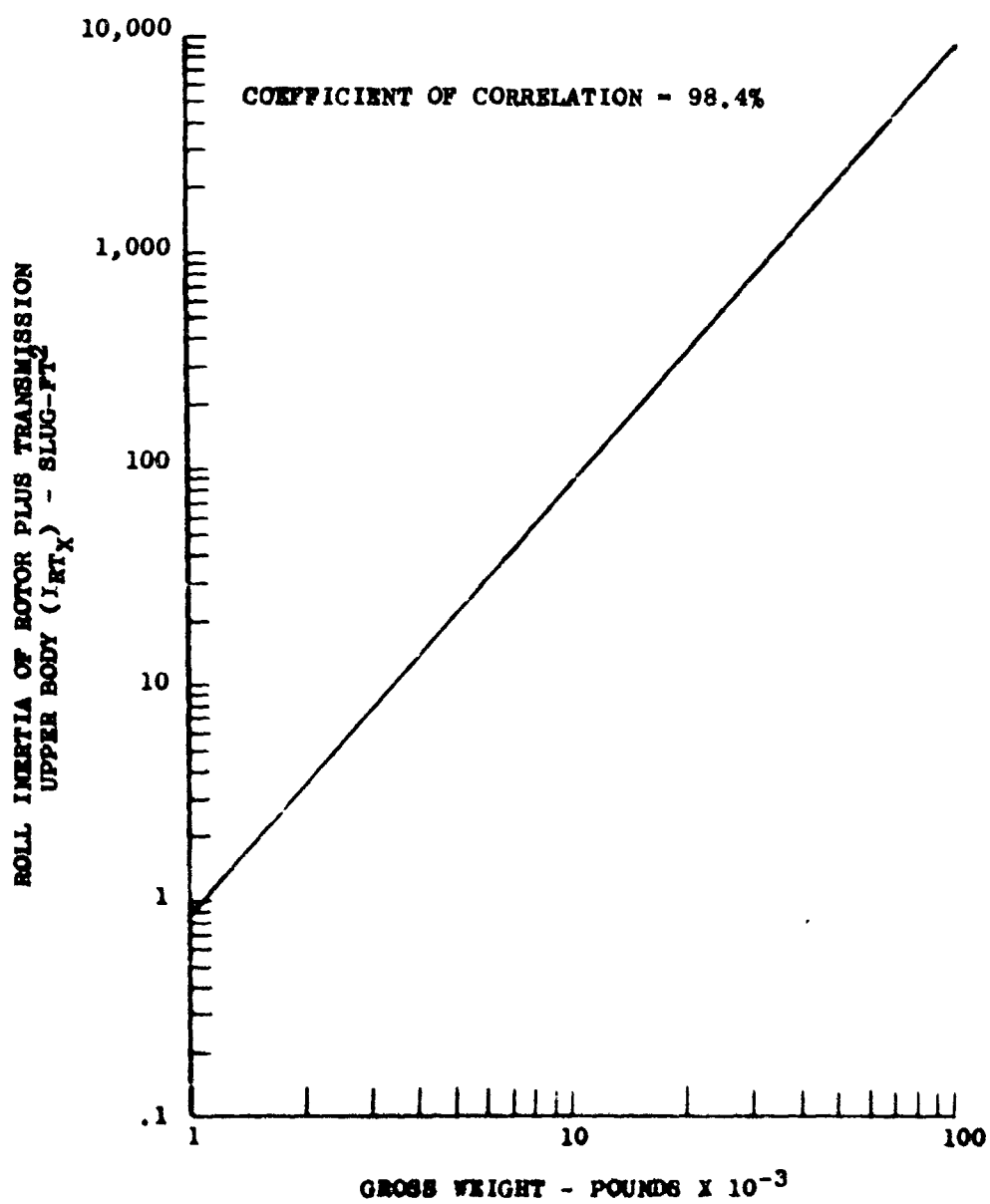


Figure 57. Statistical Roll Inertia of Rotor Plus Transmission Upper Body for a Range of Helicopter Gross Weights.

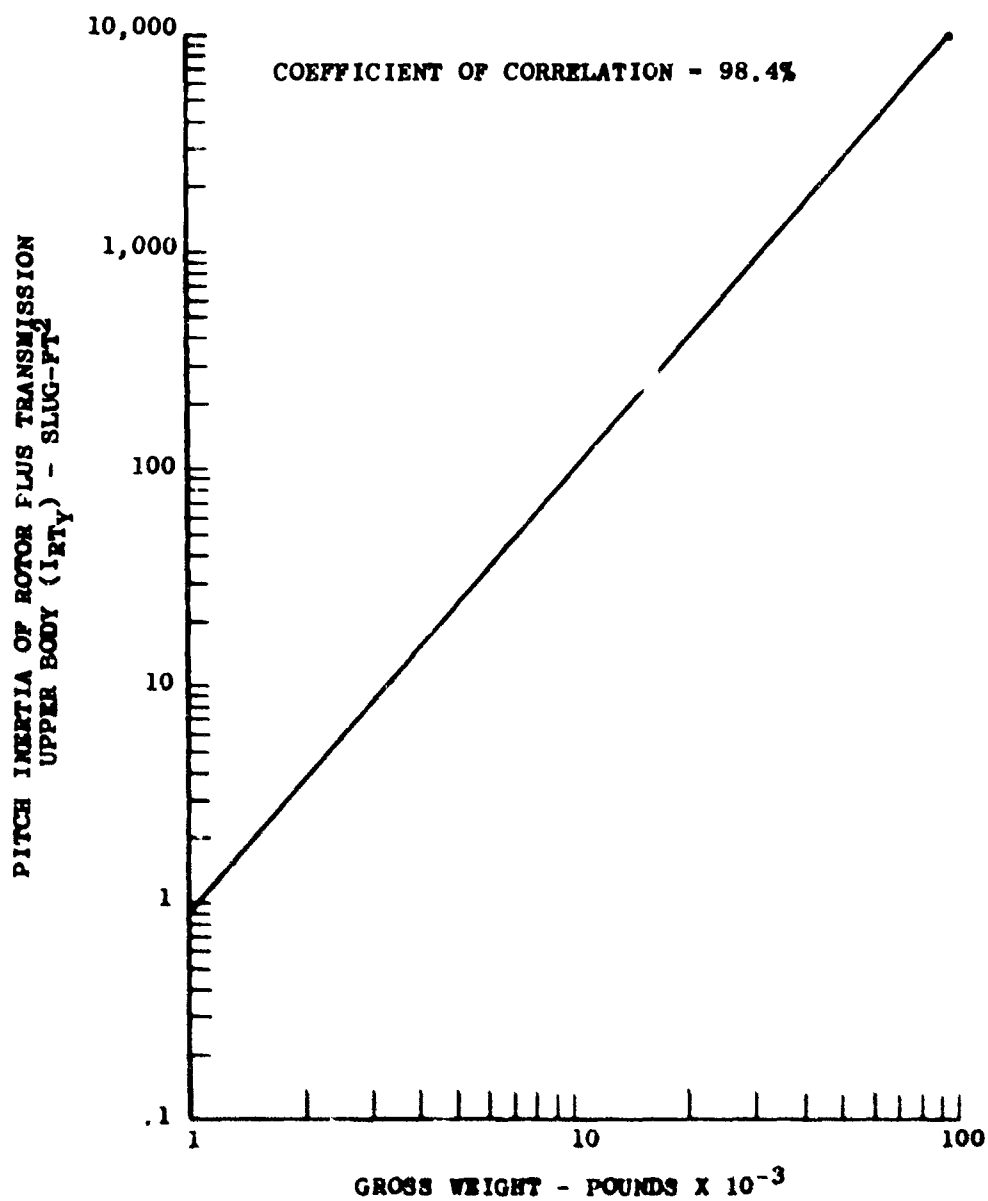


Figure 58. Statistical Pitch Inertia of Rotor Plus Transmission Upper Body for a Range of Helicopter Gross Weights.

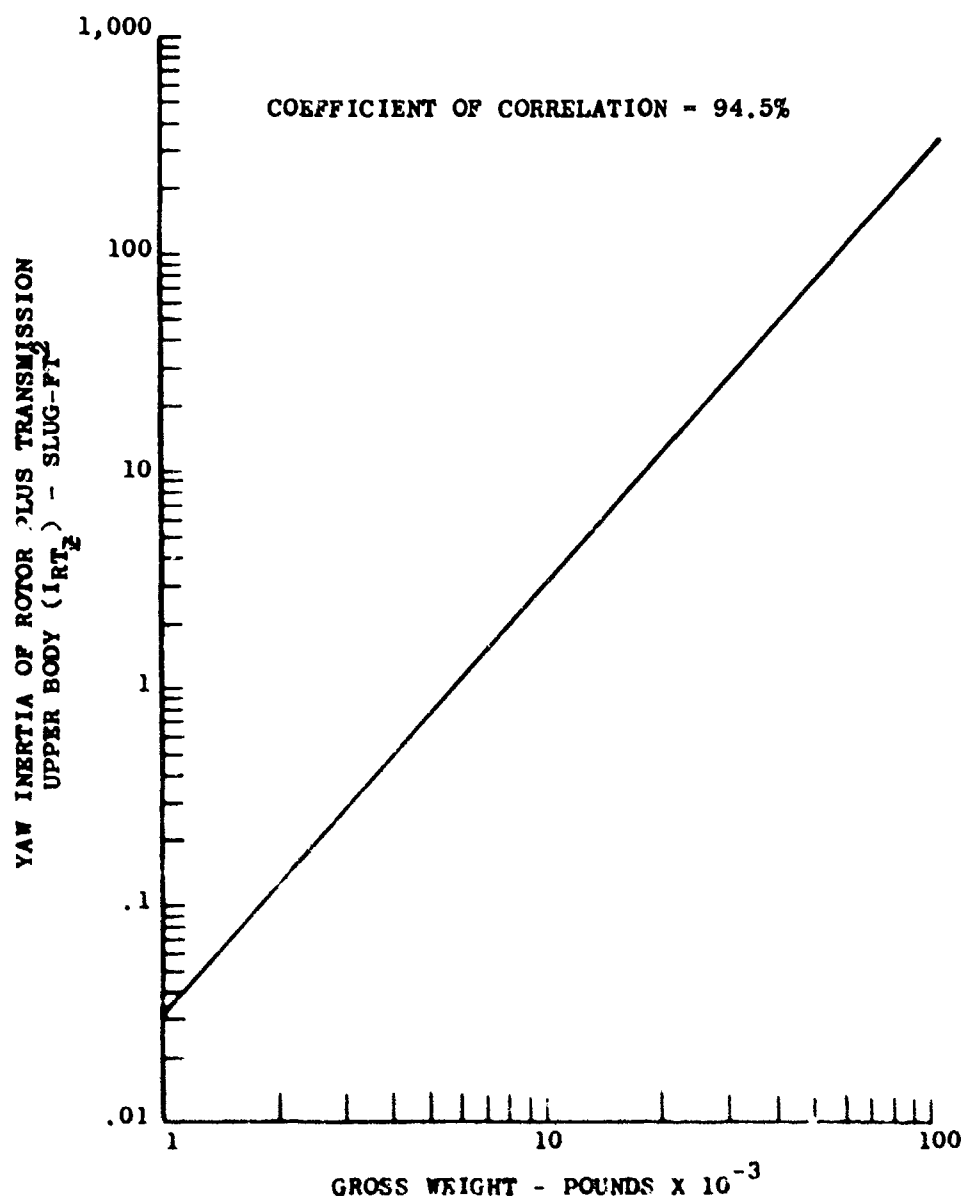


Figure 59. Statistical Yaw Inertia of Rotor Plus Transmission Upper Body for a Range of Helicopter Gross Weights.

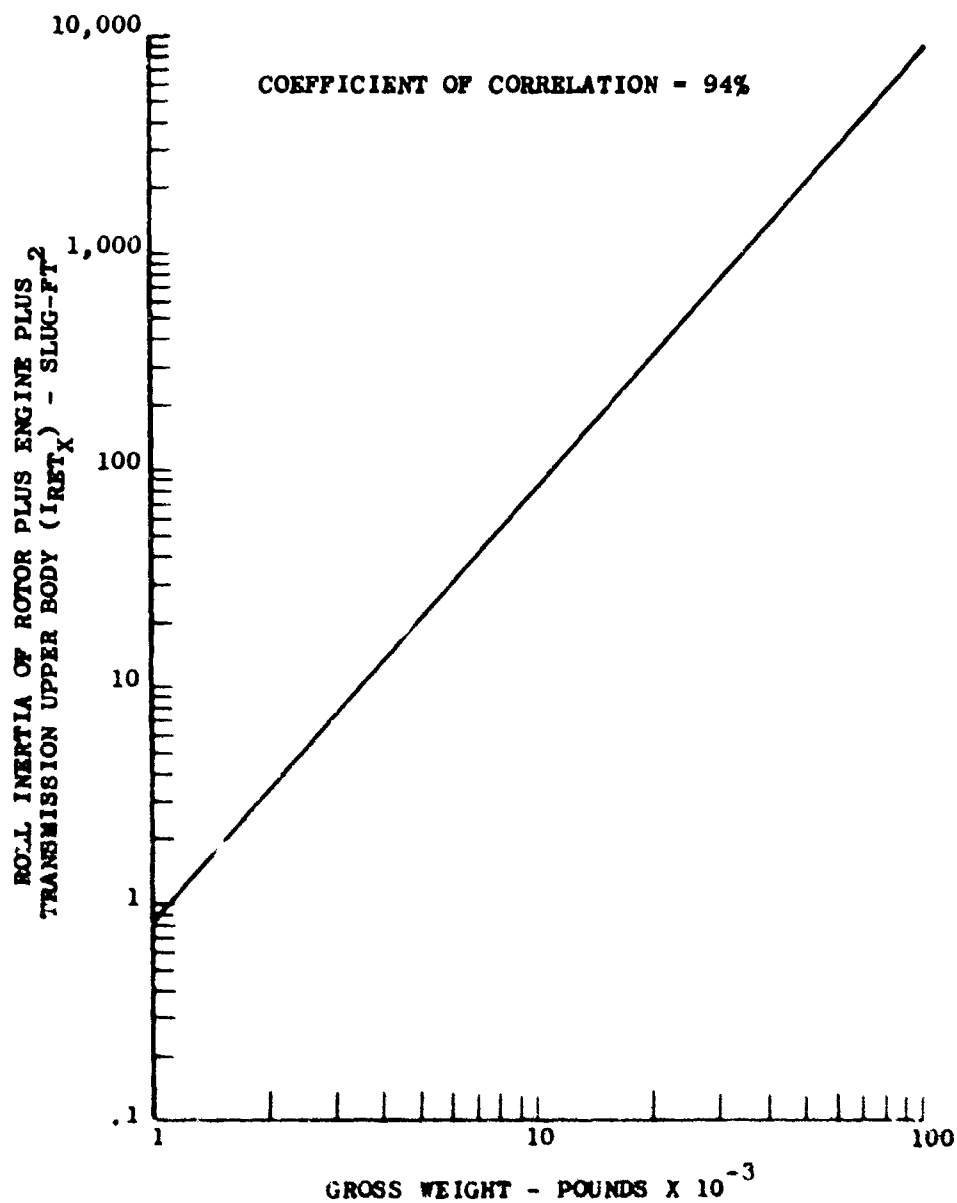


Figure 60. Statistical Roll Inertia of Rotor Plus Engine Plus Transmission Upper Body for a Range of Helicopter Gross Weights.

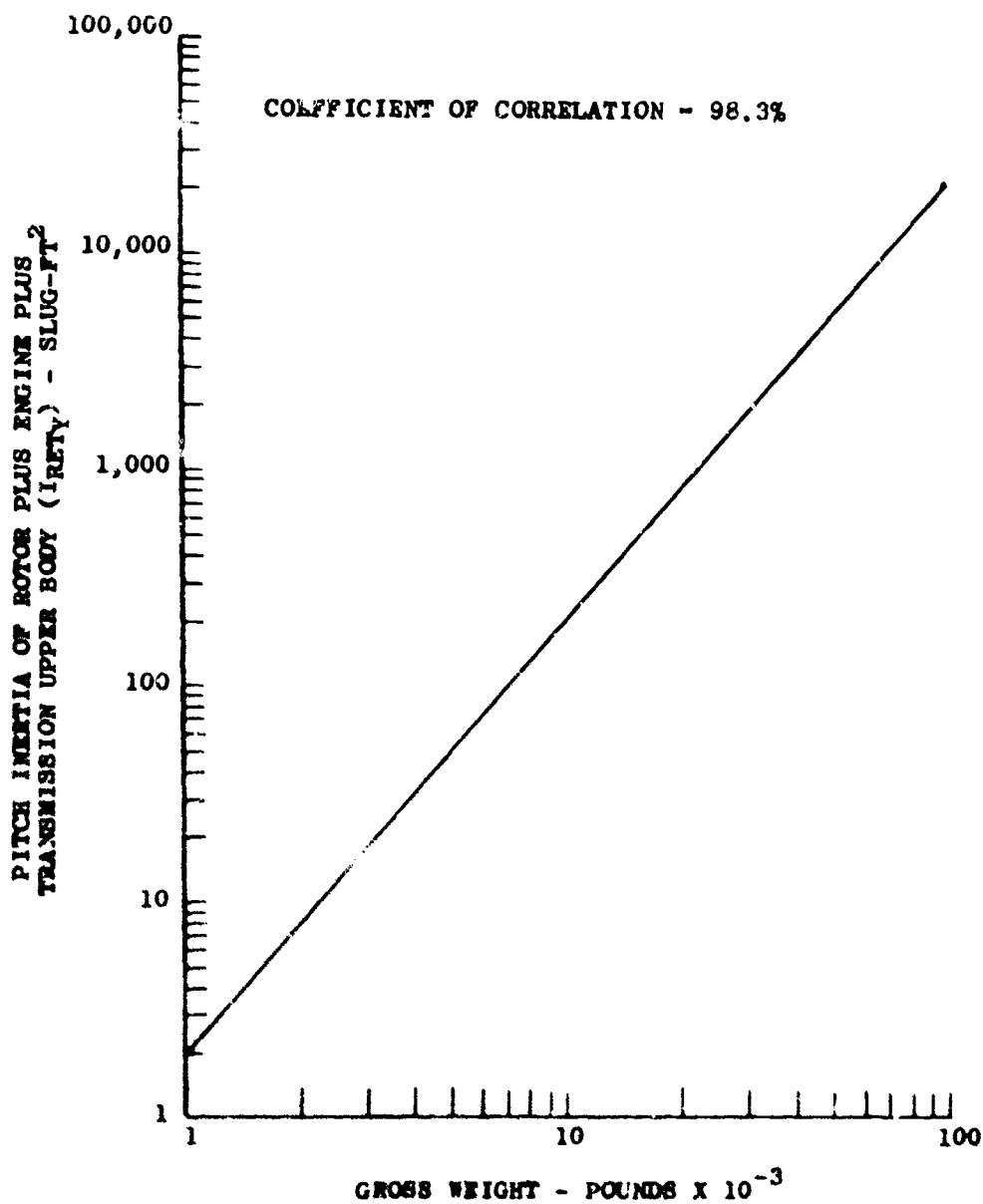


Figure 61. Statistical Pitch Inertia of Rotor Plus Engine Plus Transmission Upper Body for a Range of Helicopter Gross Weights.

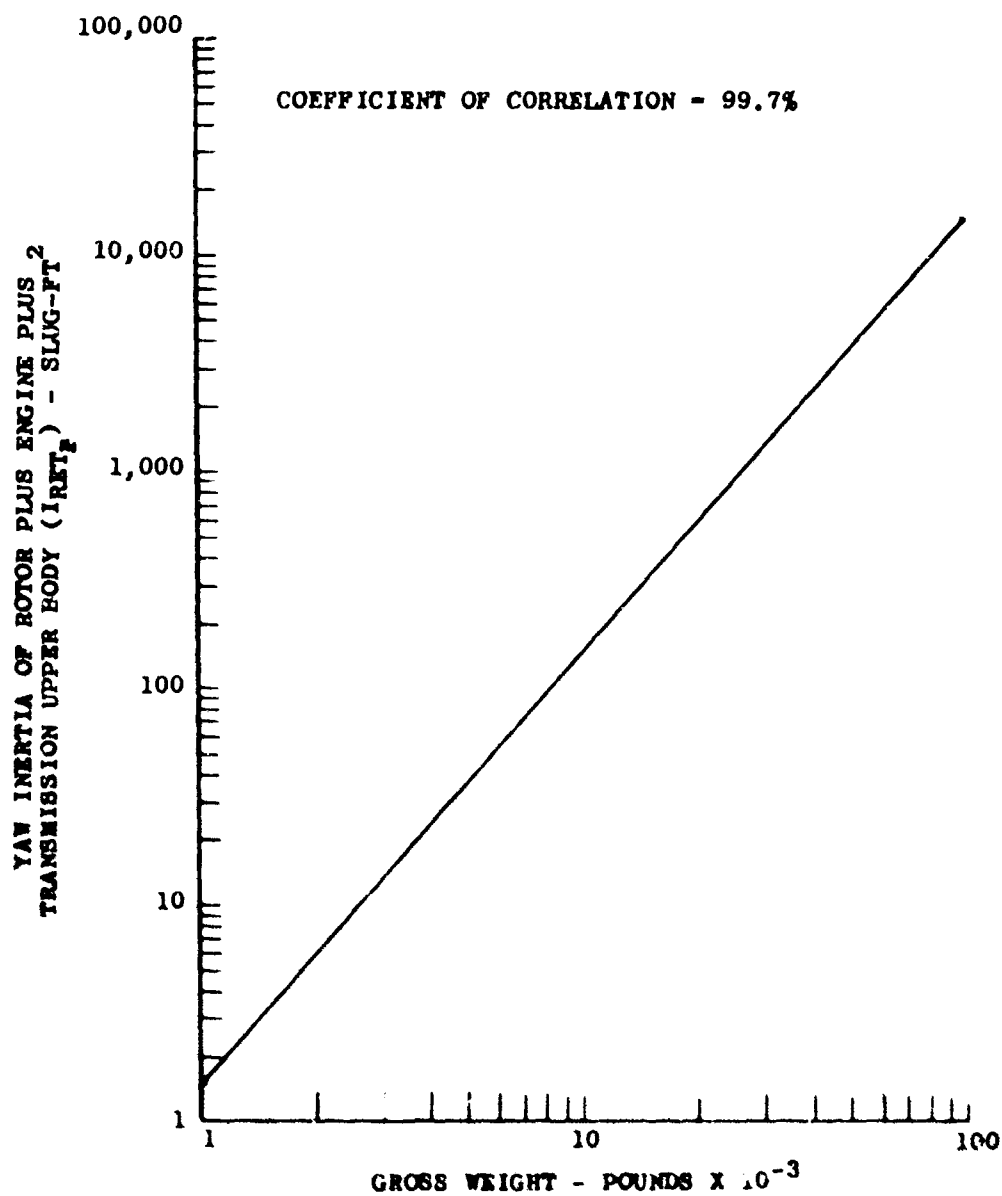


Figure 62. Statistical Yaw Inertia of Rotor Plus Engine Plus Transmission Upper Body for a Range of Helicopter Gross Weights.

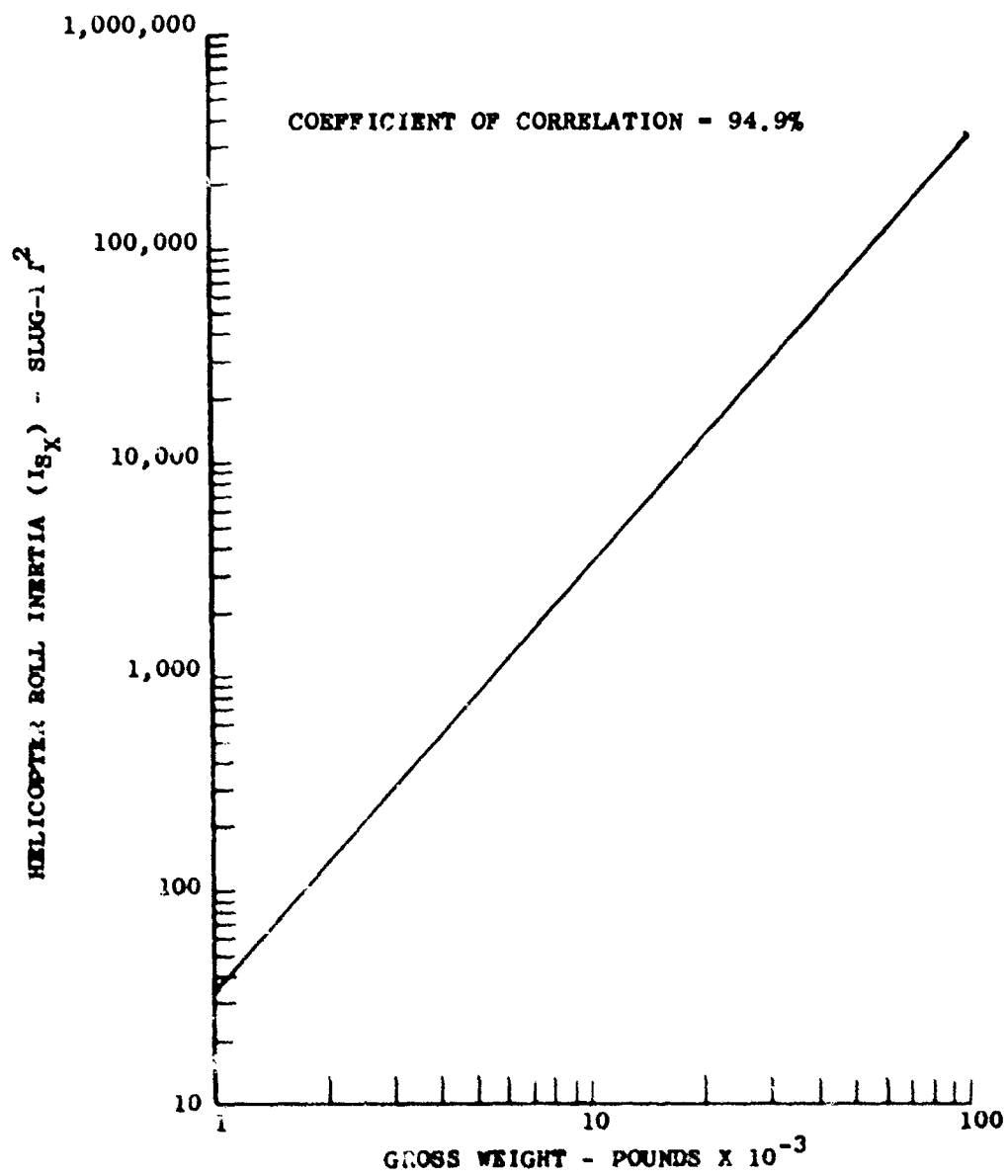


Figure 63. Statistical Roll Inertia of Helicopter for a Range of Helicopter Gross Weights

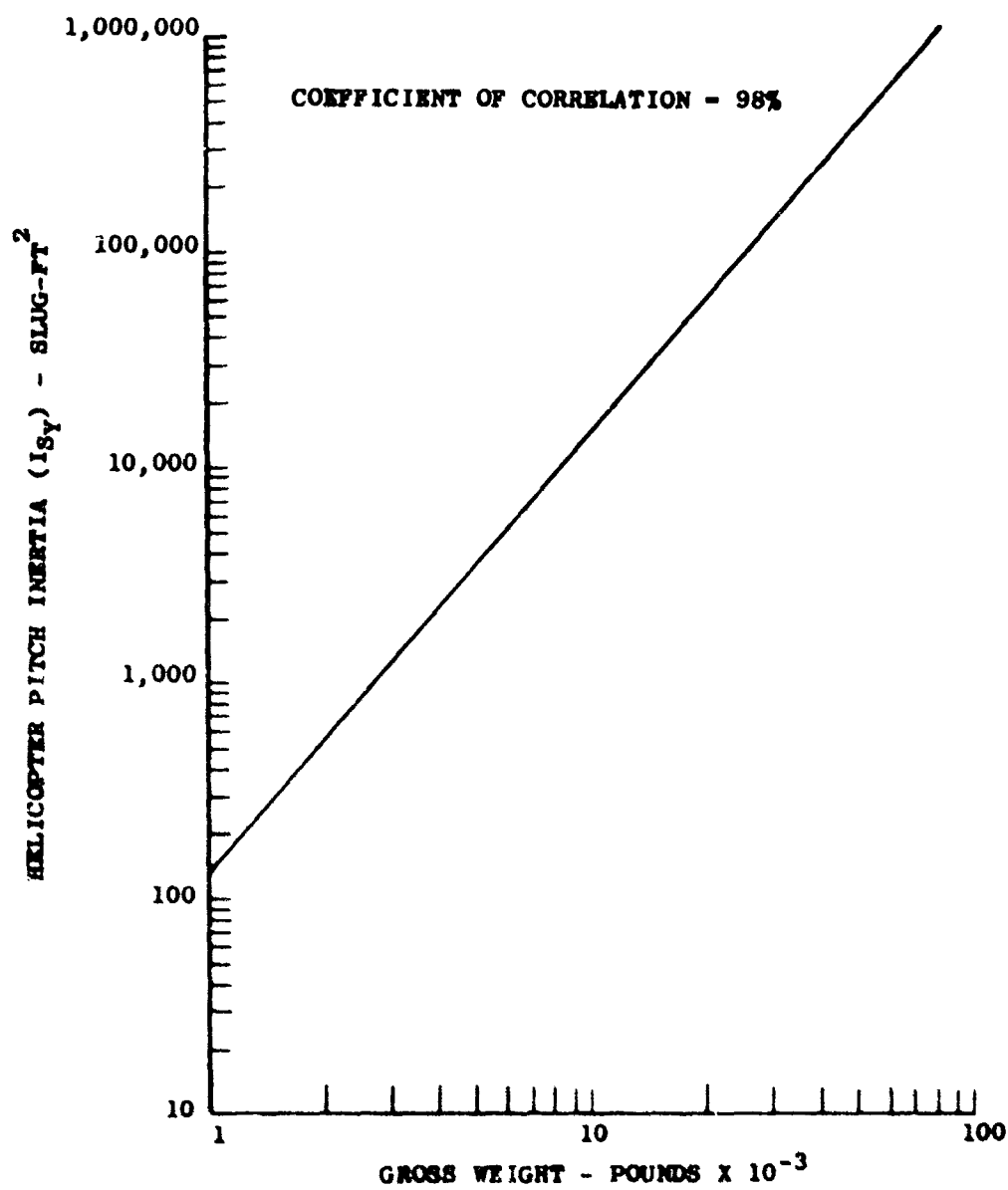


Figure 64. Statistical Pitch Inertia of Helicopter for a Range of Helicopter Gross Weights.

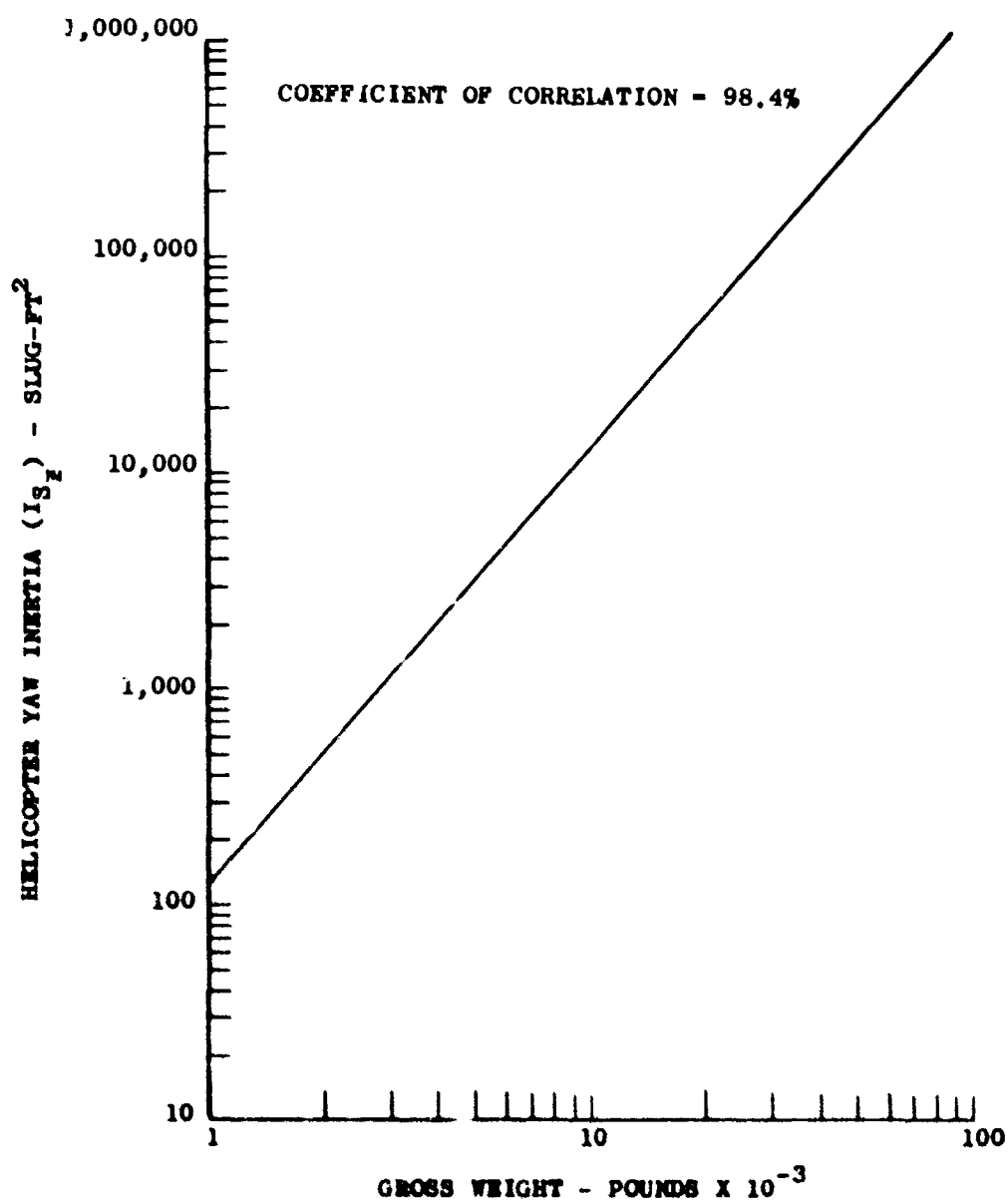


Figure 65. Statistical Yaw Inertia of Helicopter for a Range of Helicopter Gross Weights.

While there were sufficient data available to perform a statistical analysis on the helicopter, the contrary was evident when considering the compound helicopter. Only two such vehicles were sufficiently defined to be considered:

Kaman	UH-2A
Lockheed	XH-51A

Therefore, only two points defined the curves shown in Figures 66 thru 77. These were extrapolated to the gross weight of 20,000 pounds, which was the compound configuration studied in this contract.

Figure 66 presents the extrapolated data of rotor rpm versus a range of compound helicopter gross weights. Figures 67 and 68, respectively, present the compound helicopter upper body weights versus compound helicopter gross weight.

Figures 69, 70 and 71 are plots of roll, pitch, and yaw inertias of the rotor plus transmission upper body of the compound helicopter for a range of gross weights. Figures 72, 73 and 74 are plots of roll, pitch, and yaw inertias of the rotor plus engine plus transmission upper body for a range of compound helicopter gross weights.

Figures 75, 76, and 77 present roll, pitch, and yaw inertias of the unisolated compound helicopter versus a range of gross weights.

The inertias of the upper body (m_R) and of the total vehicle (m_S) have thus far been established. Geometric relationships and the general location of the centers of gravity of the upper body, lower body, and the vehicle have been illustrated in Figure 78.

Because this is a general study, investigating the feasibility of rotor isolation encompassing a range of statistical vehicles, it is difficult to define a specific configuration. Since there is no one location of the center of gravity, some simplifying and general assumptions were made.

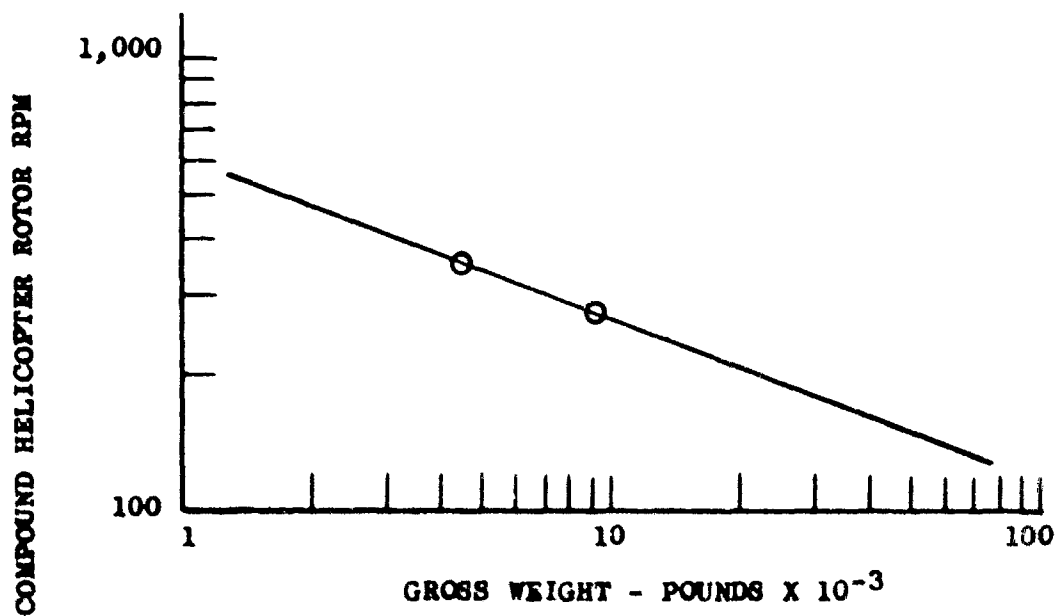


Figure 66. Compound Helicopter Rotor RPM
Versus a Range of Compound
Helicopter Gross Weights.

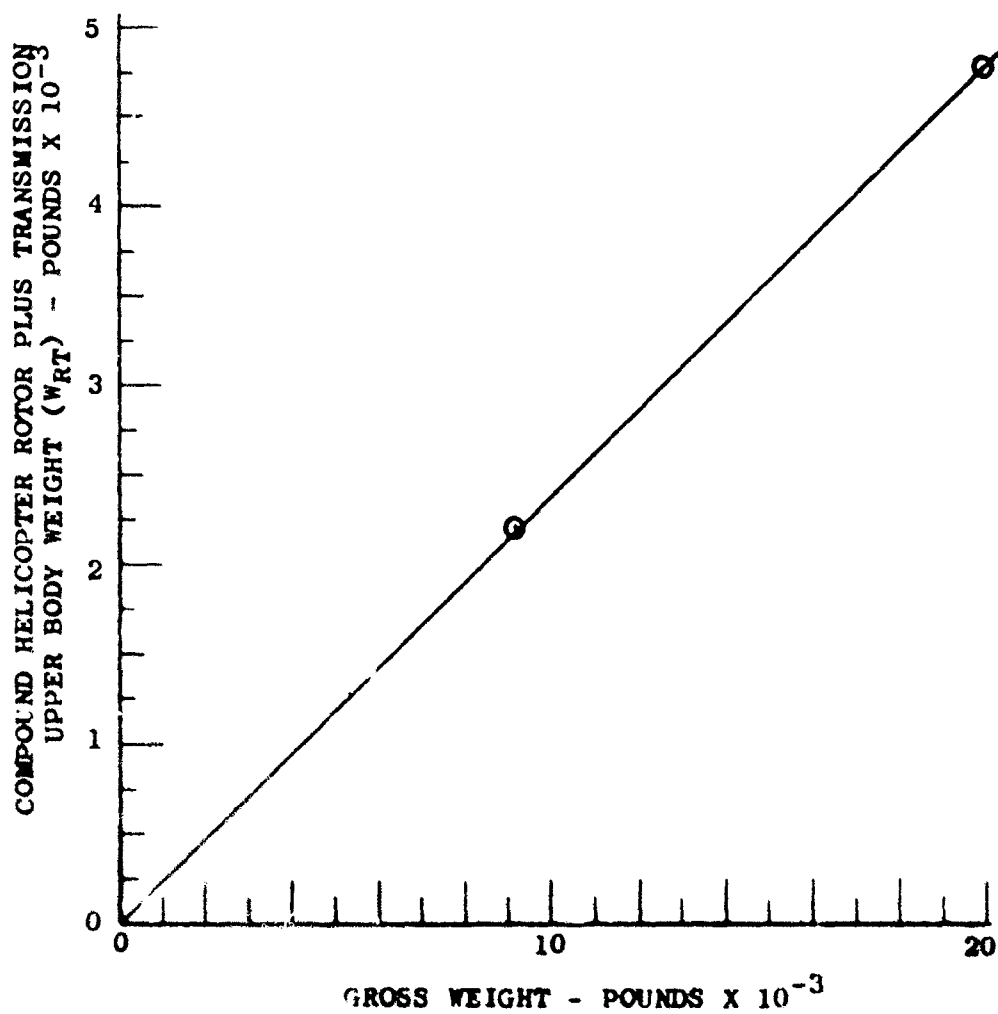


Figure 67. Compound Helicopter Rotor Plus Transmission Upper Body Weight Versus a Range of Compound Helicopter Gross Weights.

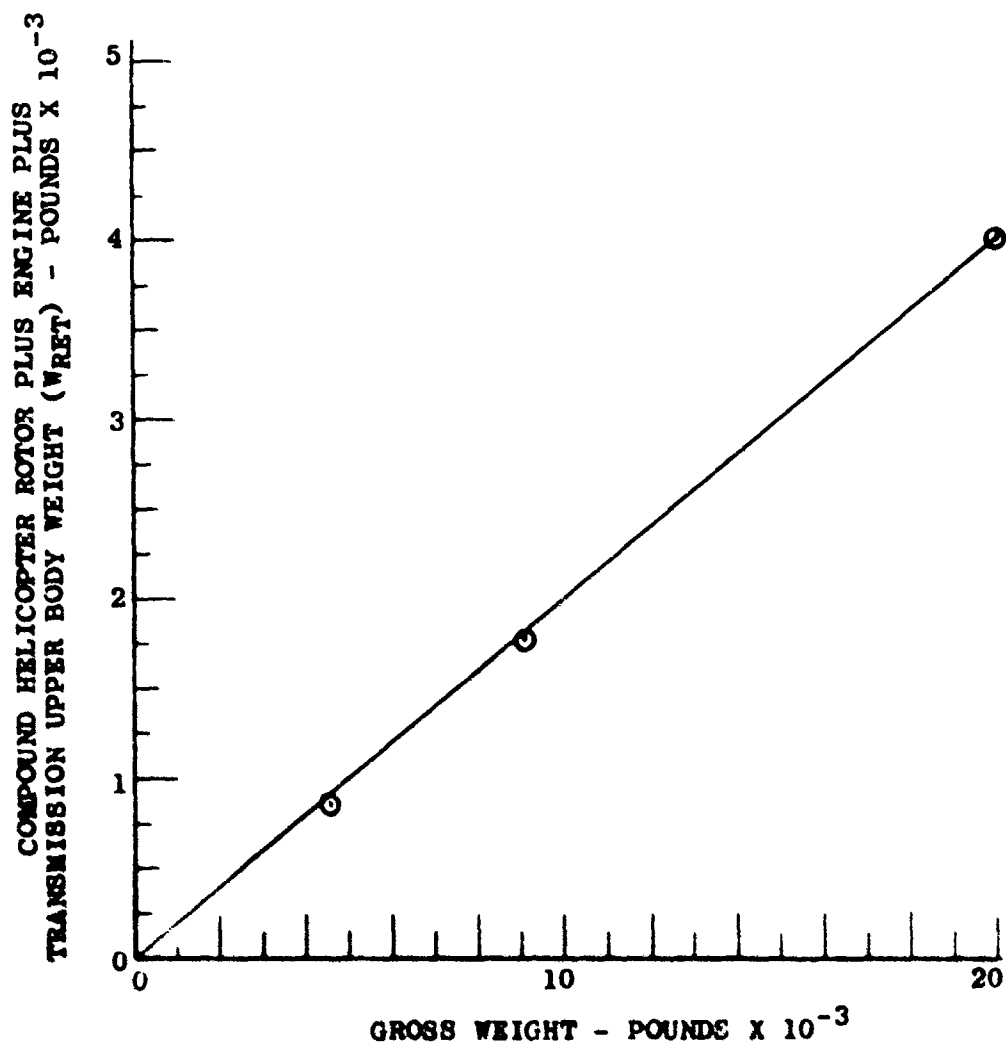


Figure 68. Compound Helicopter Rotor Plus Engine Plus Transmission Upper Body Weight Versus Compound Helicopter Gross Weight.

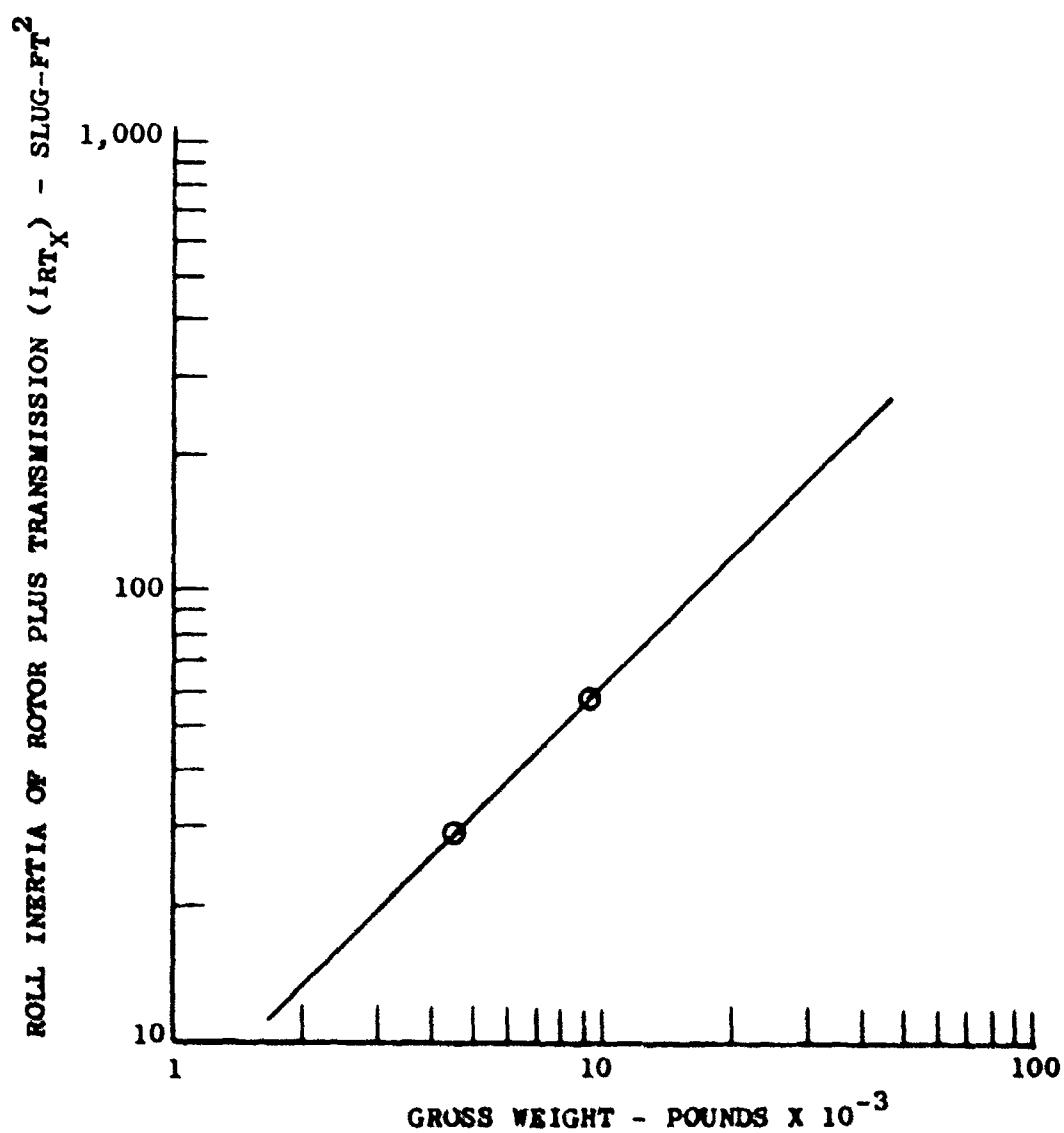


Figure 69. Roll Inertia of Compound Helicopter Rotor Plus Transmission Upper Body for a Range of Compound Helicopter Gross Weights.

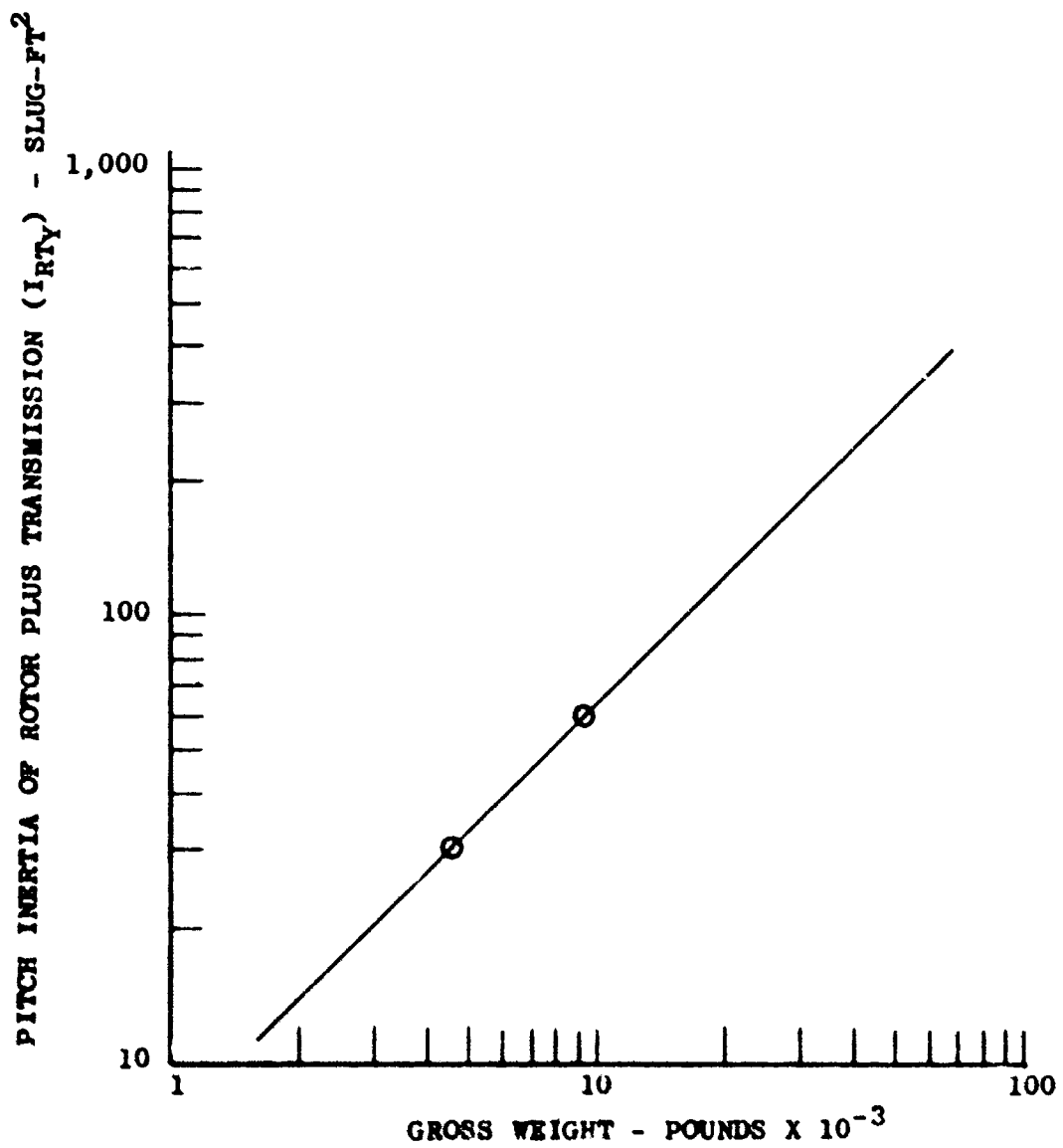


Figure 70. Pitch Inertia of Compound Helicopter Rotor Plus Transmission Upper Body for a Range of Compound Helicopter Gross Weights.

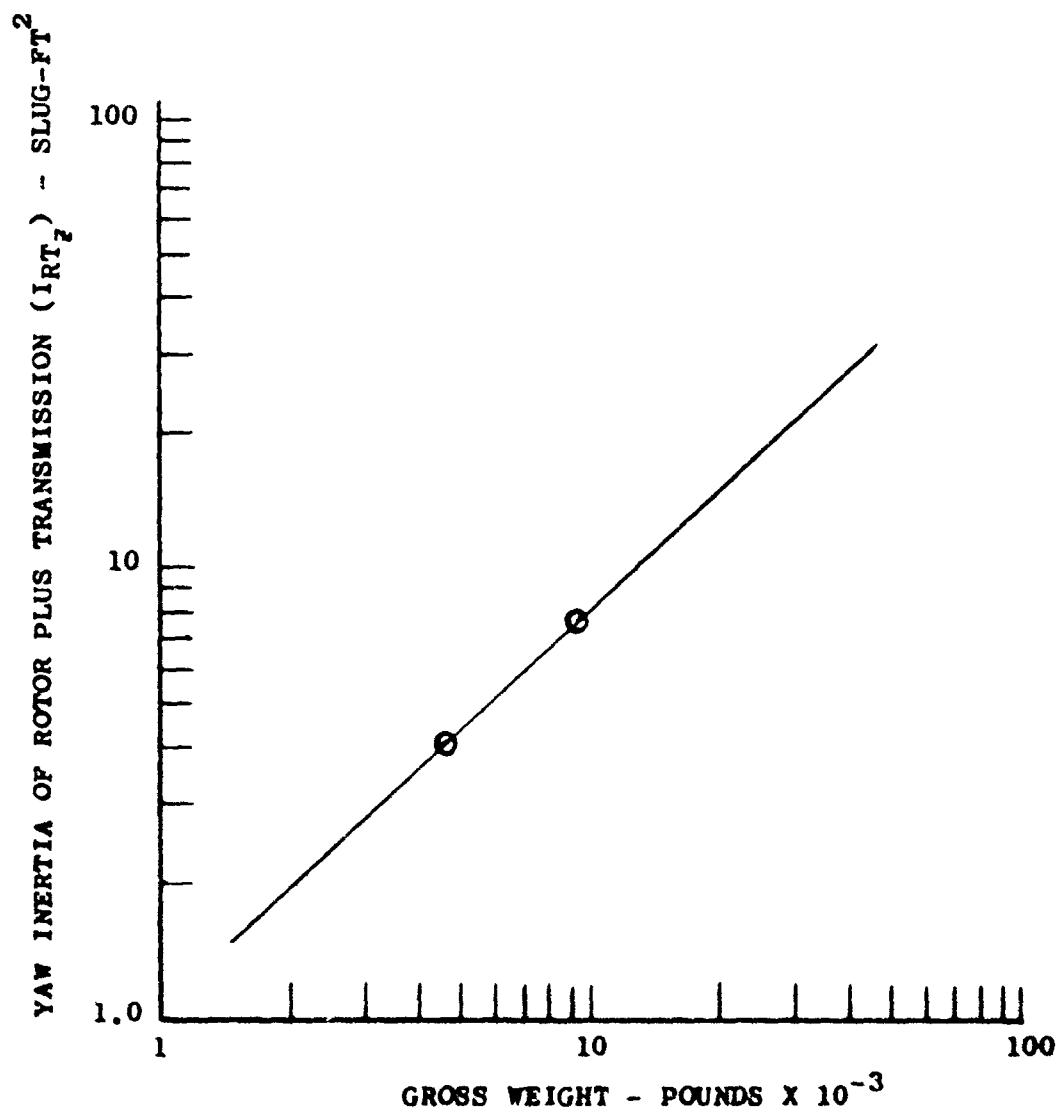


Figure 71. Yaw Inertia of Compound Helicopter Rotor Plus Transmission Upper Body for a Range of Compound Helicopter Gross Weights.

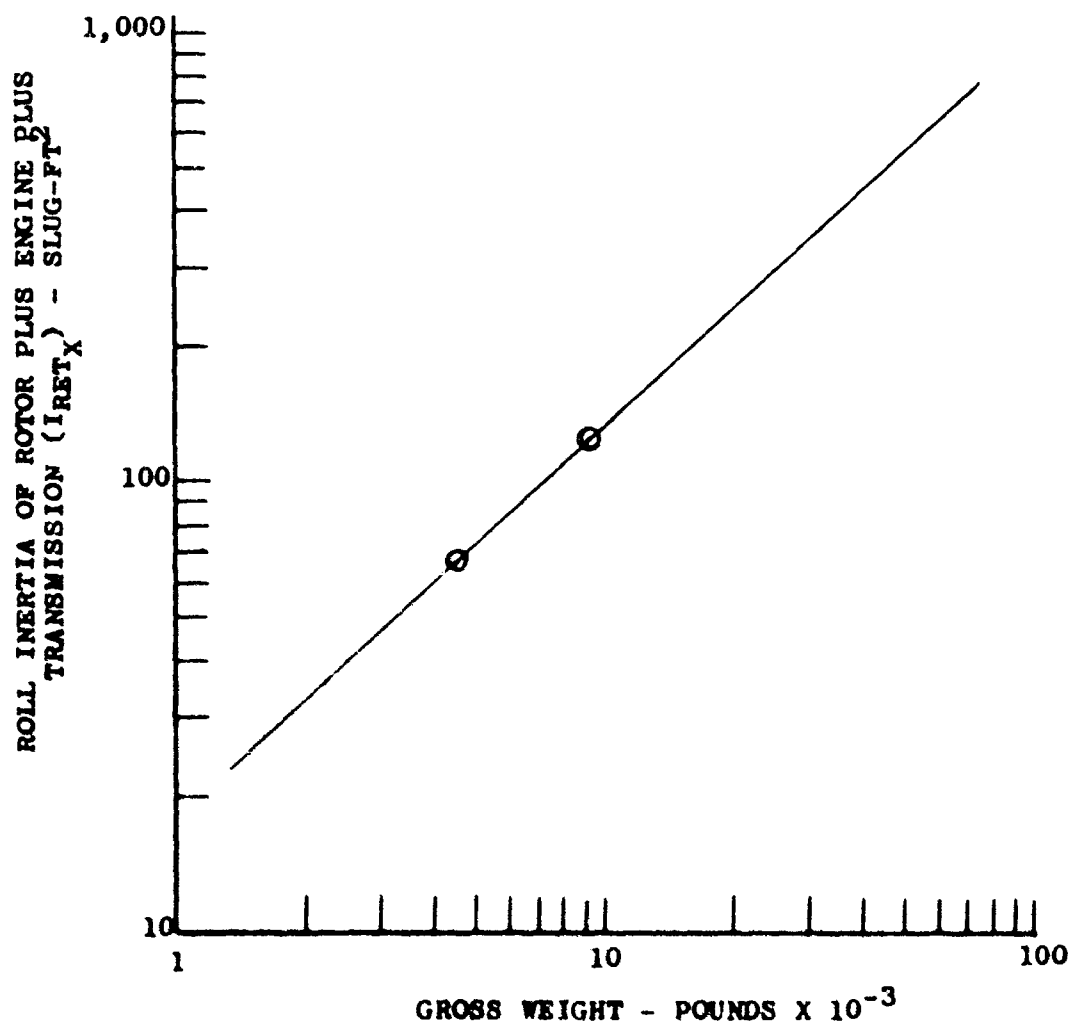


Figure 72. Roll Inertia of Compound Helicopter Rotor Plus Engine Plus Transmission Upper Body for a Range of Gross Weights.

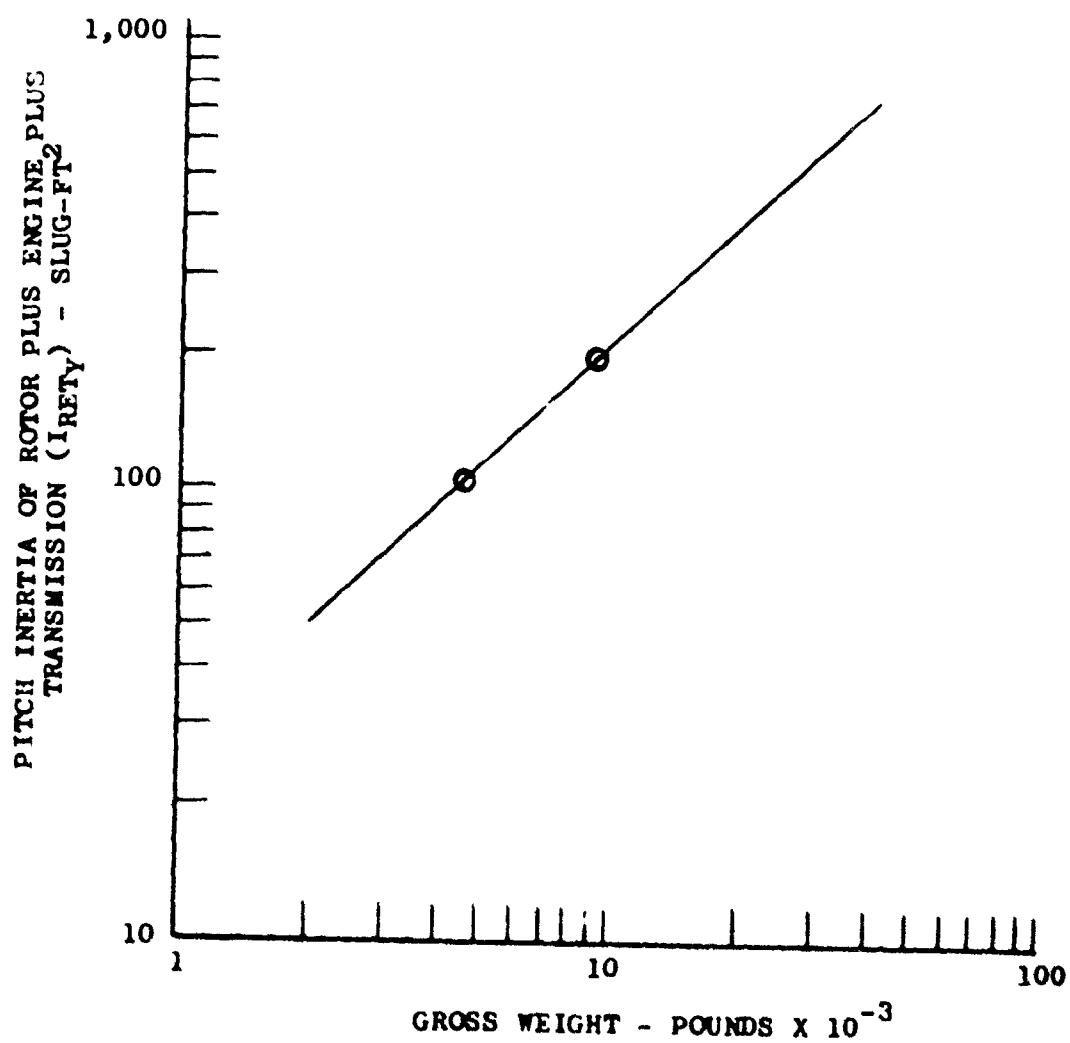


Figure 73. Pitch Inertia of Compound Helicopter Rotor Plus Engine Plus Transmission Upper Body for a Range of Gross Weights.

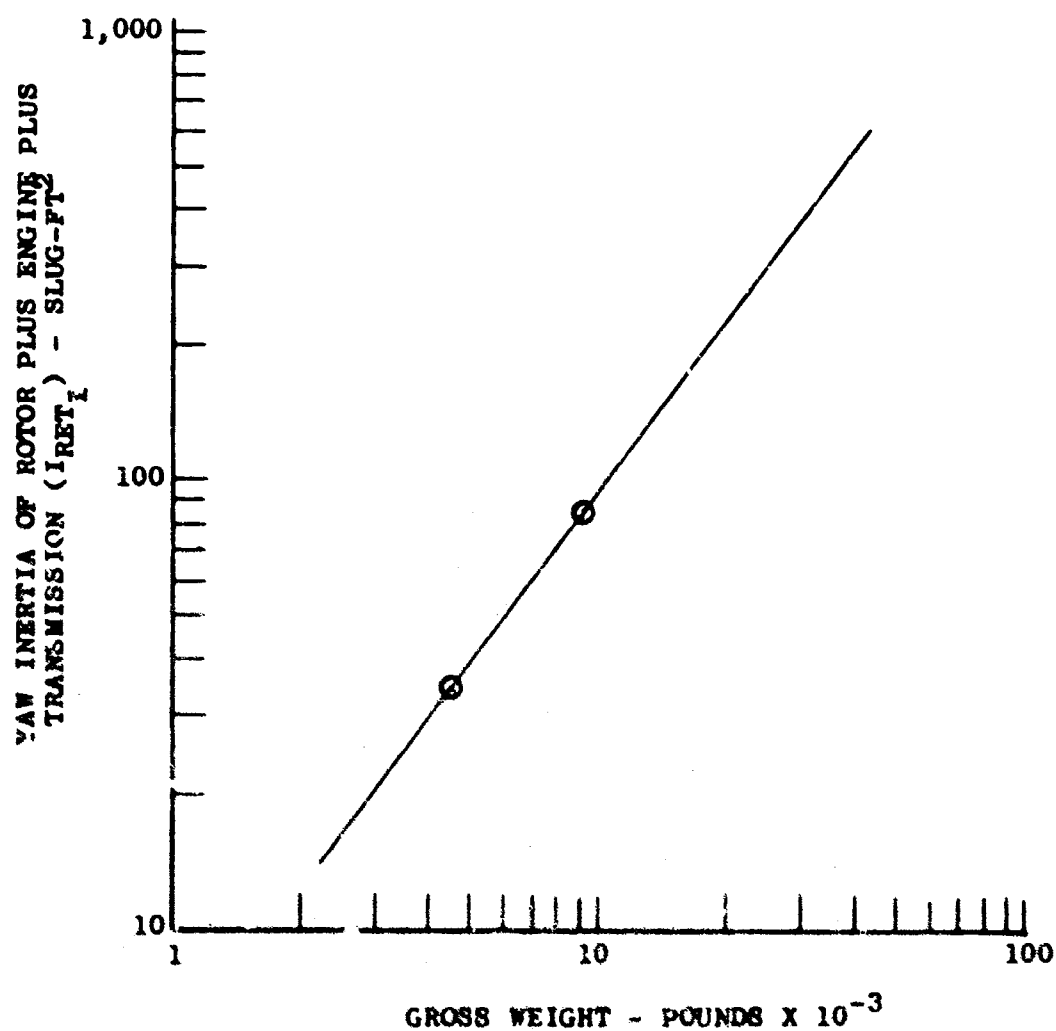


Figure 74. Yaw Inertia of Compound Helicopter Rotor Plus Engine Plus Transmission Upper Body for a Range of Gross Weights.

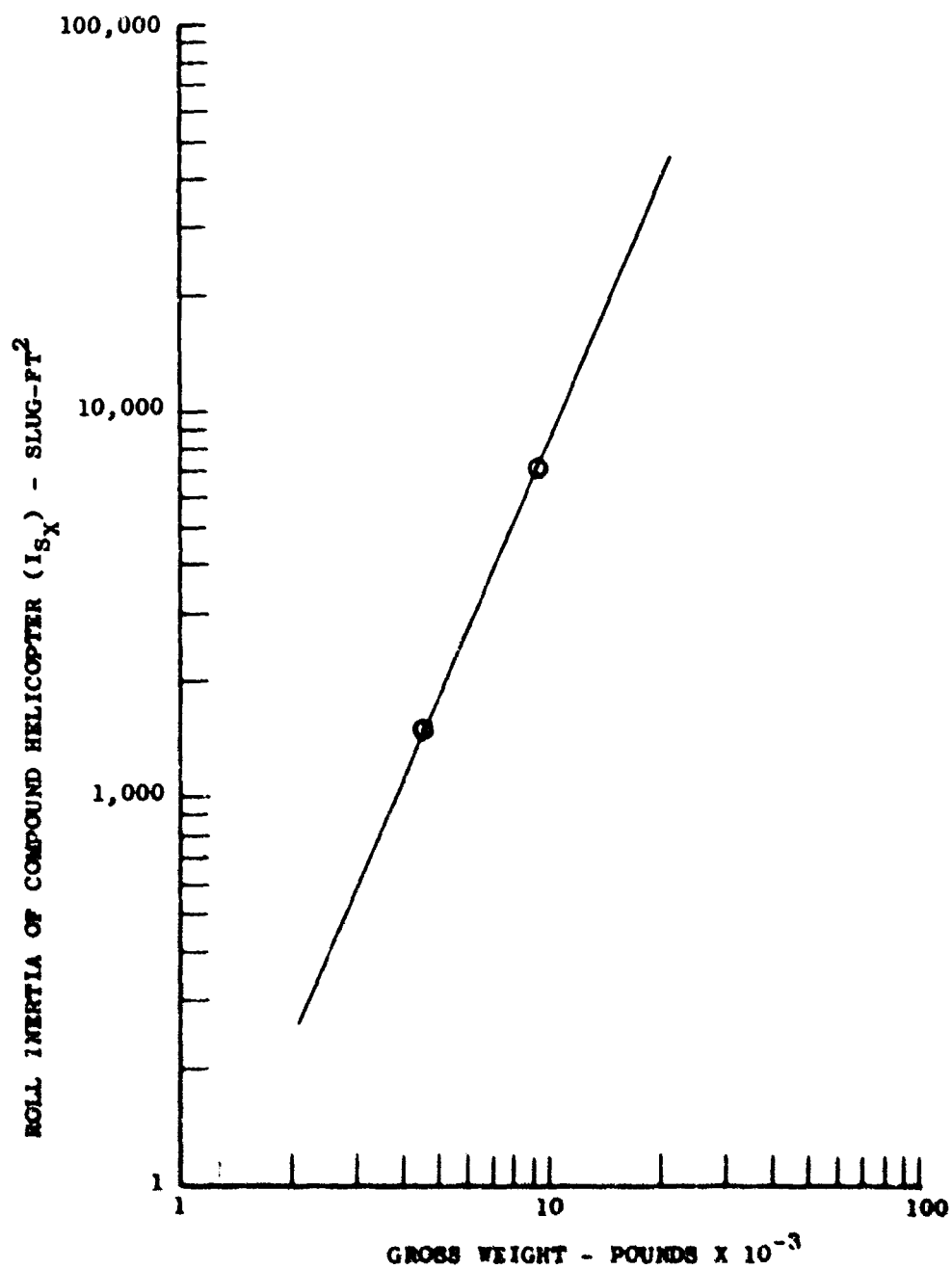


Figure 75. Roll Inertia of Compound Helicopter for a Range of Gross Weights.

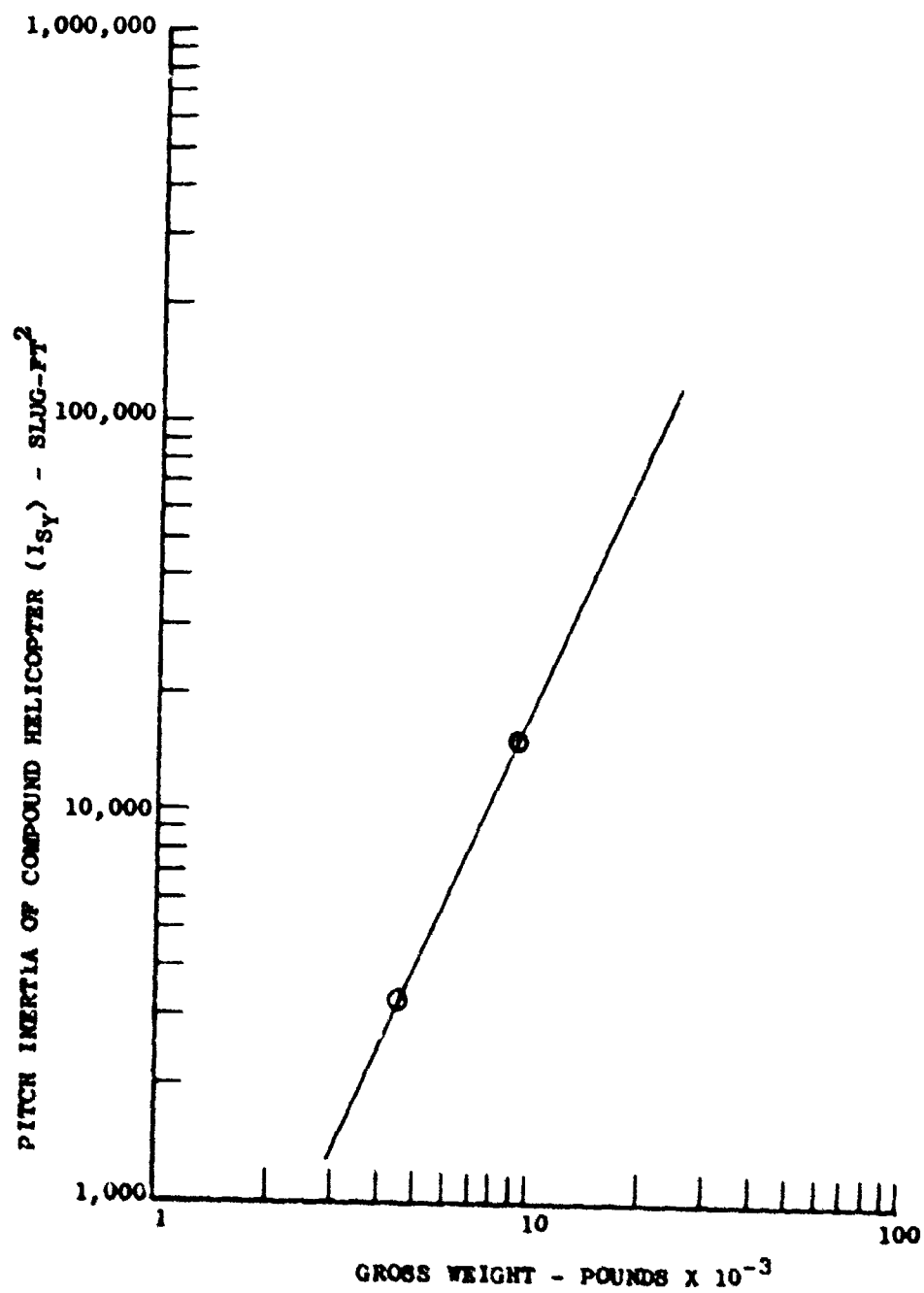


Figure 76. Pitch Inertia of Compound Helicopter for a Range of Gross Weights.

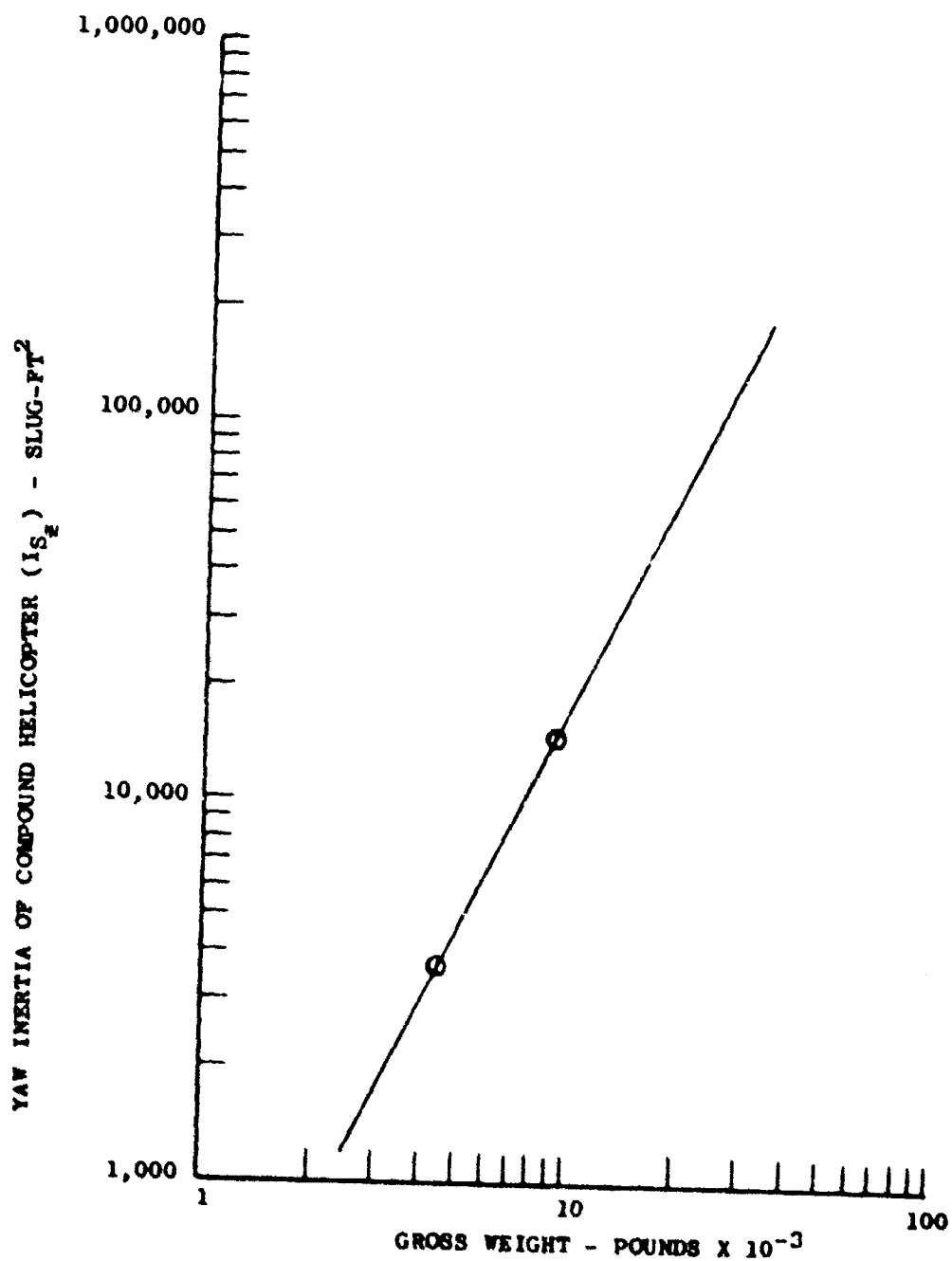


Figure 77. Yaw Inertia of Compound Helicopter for a Range of Gross Weights.

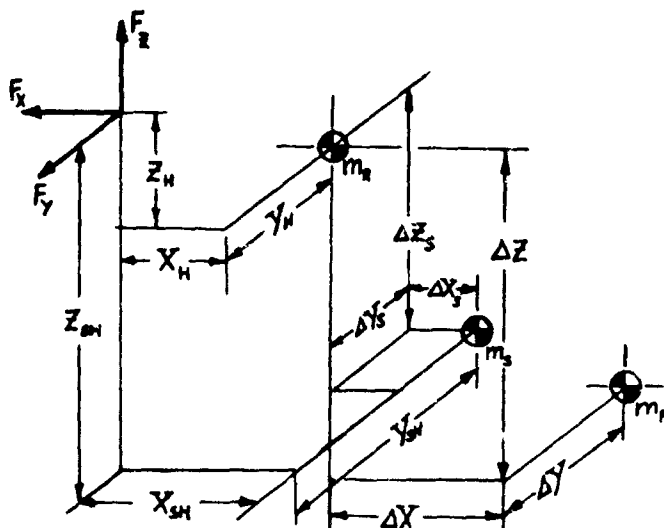


Figure 78. General Location of Centers of Gravity and Point of Excitation.

For the cases where the upper body comprises only the rotor plus transmission, it was assumed that the centers of gravity for the upper-body, vehicle, and the lower body are in line in both the longitudinal and lateral directions. Also, it was assumed that the point of excitation, the hub, is also lined up, with no offset from the vehicle center of gravity. Therefore, referring to Figure 78 $X_u = \Delta X_s = \Delta X = 0$ and $Y_u = \Delta Y_s = \Delta Y = 0$. The assumed vertical distance from the vehicle center of gravity to the upper-body center of gravity and point of excitation has been plotted versus gross weight on Figure 79. Furthermore, it was assumed that the change in configuration from helicopter to compound, as well as the variation in upper-body weight, was small; therefore, the plot of vertical distance as shown in Figure 79 is applicable for all configurations in this study for a given gross weight.

Figure 80 illustrates the schedule of longitudinal distance from the vehicle center of gravity to the rotor plus engine plus transmission upper body cg versus a range of gross weights applicable to helicopter and compound configuration.

Thus, having assumed the vehicle and upper-body center of gravity for all configurations being investigated, it was necessary to determine the relative location of the lower-body center of gravity with respect to the upper-body center of gravity. Figure 78 pictures these distances as ΔX , ΔY , and ΔZ .

$$\Delta X = \frac{(m_s + m_r) \Delta X_s}{m_F} \quad (61)$$

where

$$m_s = m_R + m_F$$

Then

$$\Delta X = \frac{m_s \Delta X_s}{m_F} \quad (62)$$

$$\Delta Y = \frac{m_s \Delta Y_s}{m_F} \quad (63)$$

$$\Delta Z = \frac{m_s \Delta Z_s}{m_F} \quad (64)$$

Also calculated is the distance from the point of excitation to the upper body center of gravity:

$$X_H = X_{SH} - \Delta X_s \quad (65)$$

$$Y_H = Y_{SH} - \Delta Y_s \quad (66)$$

$$Z_H = Z_{SH} - \Delta Z_s \quad (67)$$

The two-body isolated system is now in static equilibrium and has a system center of gravity identical to the total vehicle center of gravity.

Calculated next are the inertias of the lower body, so that the two-body system inertia would be representative of the inertia about the vehicle center of gravity. These equations are general and apply to any lower-body configuration studied in this contract.

$$I_{R_x} = I_{s_x} - I_{R_x} - m_s(\Delta Y_s^2 + \Delta Z_s^2) - m_r(\Delta Y_r^2 + \Delta Z_r^2) \quad (68)$$

$$I_{R_y} = I_{s_y} - I_{R_y} - m_s(\Delta X_s^2 + \Delta Z_s^2) - m_r(\Delta X_r^2 + \Delta Z_r^2) \quad (69)$$

$$I_{R_z} = I_{s_z} - I_{R_z} - m_s(\Delta X_s^2 + \Delta Y_s^2) - m_r(\Delta X_r^2 + \Delta Y_r^2) \quad (70)$$

where

$$\Delta X_p = \Delta X - \Delta X_s \quad (71)$$

$$\Delta Y_p = \Delta Y - \Delta Y_s \quad (72)$$

$$\Delta Z_p = \Delta Z - \Delta Z_s \quad (73)$$

The roll, pitch, and yaw inertias of the lower body, as calculated using Equations (68), (69), and (70) have been plotted versus helicopter gross weights on Figures 81, 82, and 83, respectively. These inertias are for that configuration where the upper body comprises the rotor plus transmission while the lower body is defined as fuselage plus engine.

Figures 84, 85, and 86 are plots of the calculated roll, pitch, and yaw inertias of the lower body versus helicopter gross weight. The lower body is defined as fuselage only, while the upper body comprises the rotor, engine, and transmission.

Based on the upper-body inertia and ship inertia of the two aircraft considered, the lower-body inertia was calculated based on input from these two aircraft, extrapolated and plotted to indicate approximate magnitude. Using the statistical compound helicopter of 20,000 pounds gross weight, the assumed locations of centers of gravity and previously obtained upper-body inertia and vehicle inertia, the lower-body inertia was calculated for one gross weight. This calculated point was also plotted to compare against the two-point extrapolated curve and showed good agreement with previous estimates.

Figures 87, 88, and 89 show the roll, pitch, and yaw inertias of the compound helicopter lower body versus gross weight. The lower body includes the fuselage plus engine, while the upper body includes rotor and transmission.

Figures 90, 91, and 92 present the roll, pitch, and yaw inertias versus compound helicopter gross weight. The lower body includes the fuselage only, while the upper-body configuration includes rotor, engine, and transmission.

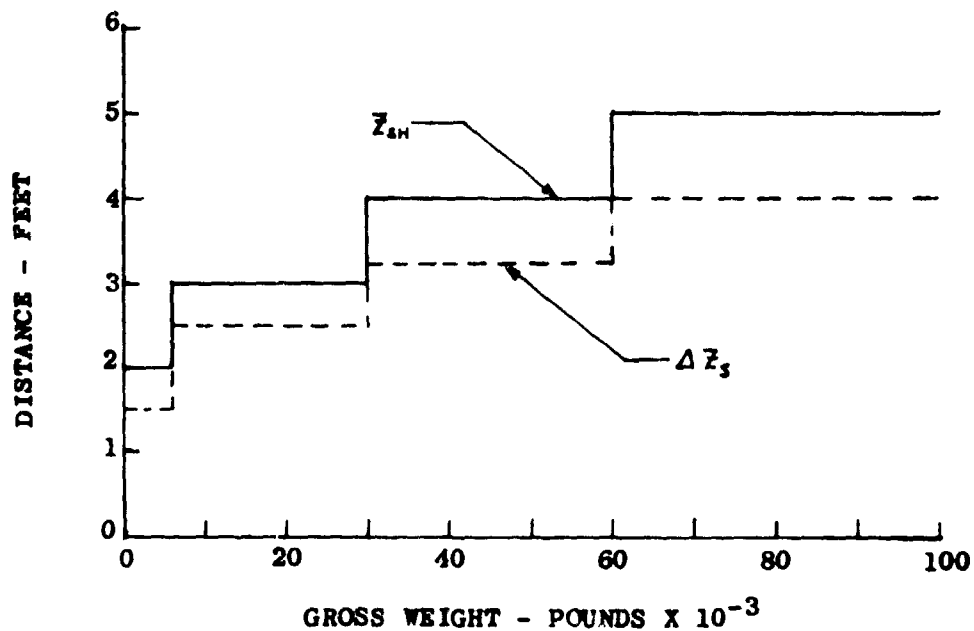


Figure 79. Vertical Distance From Vehicle Center of Gravity to Upper Body Center of Gravity and Point of Excitation for a Range of Gross Weights.

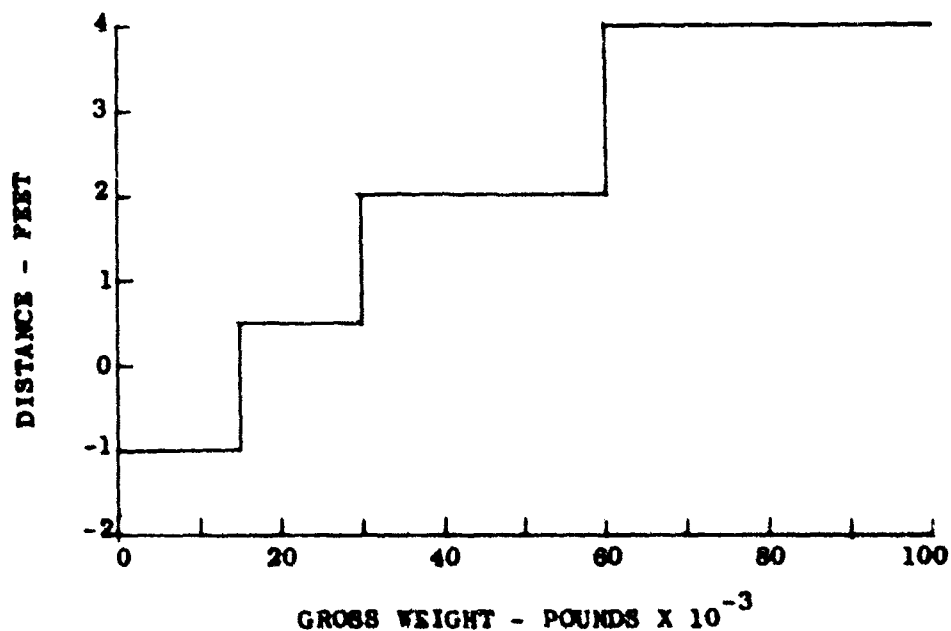


Figure 80. Longitudinal Distance From Vehicle Center of Gravity to Upper Body Center of Gravity for a Range of Gross Weights.

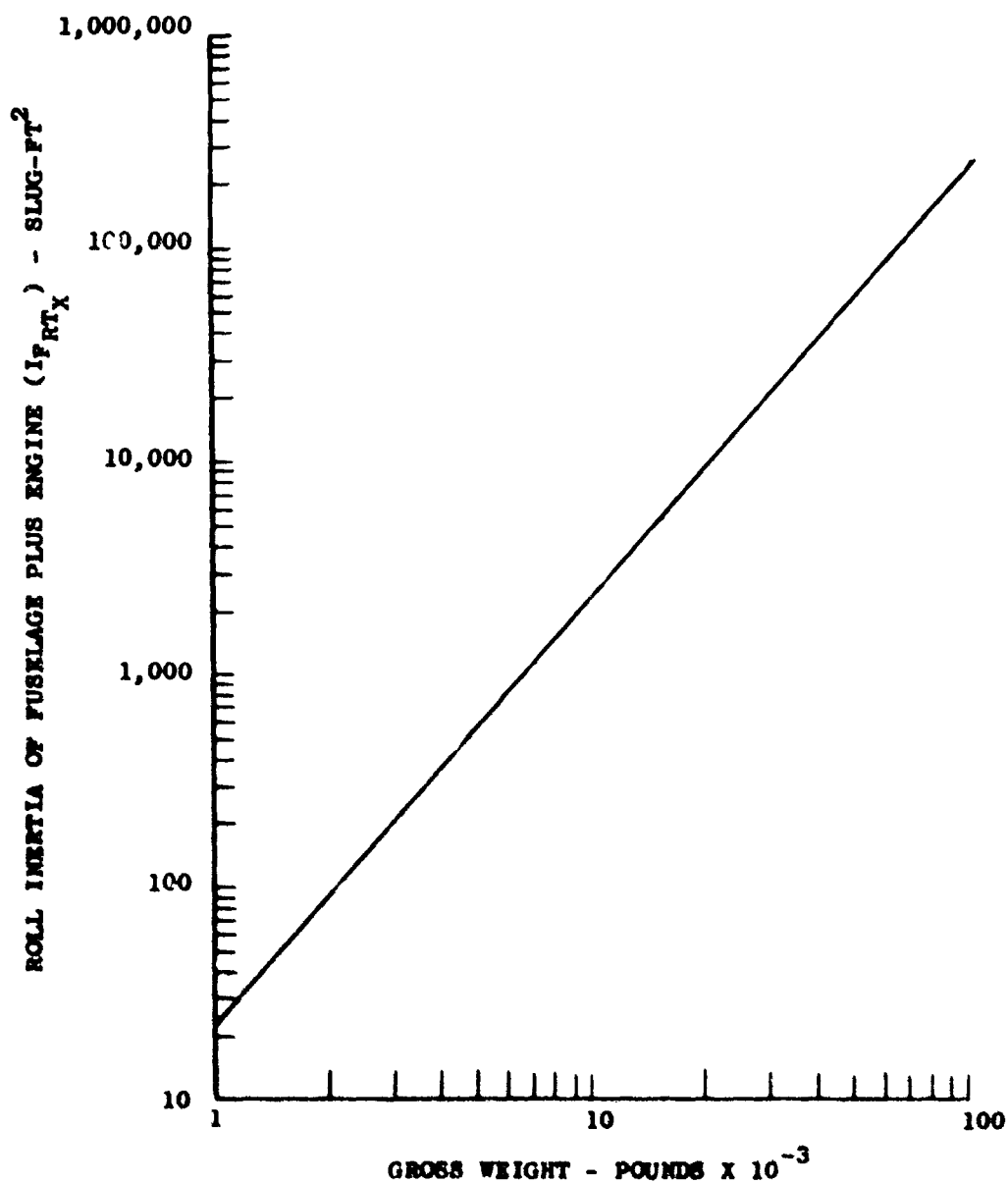


Figure 81. Roll Inertia of Lower Body for Rotor Plus Transmission Configuration for a Range of Helicopter Gross Weights.

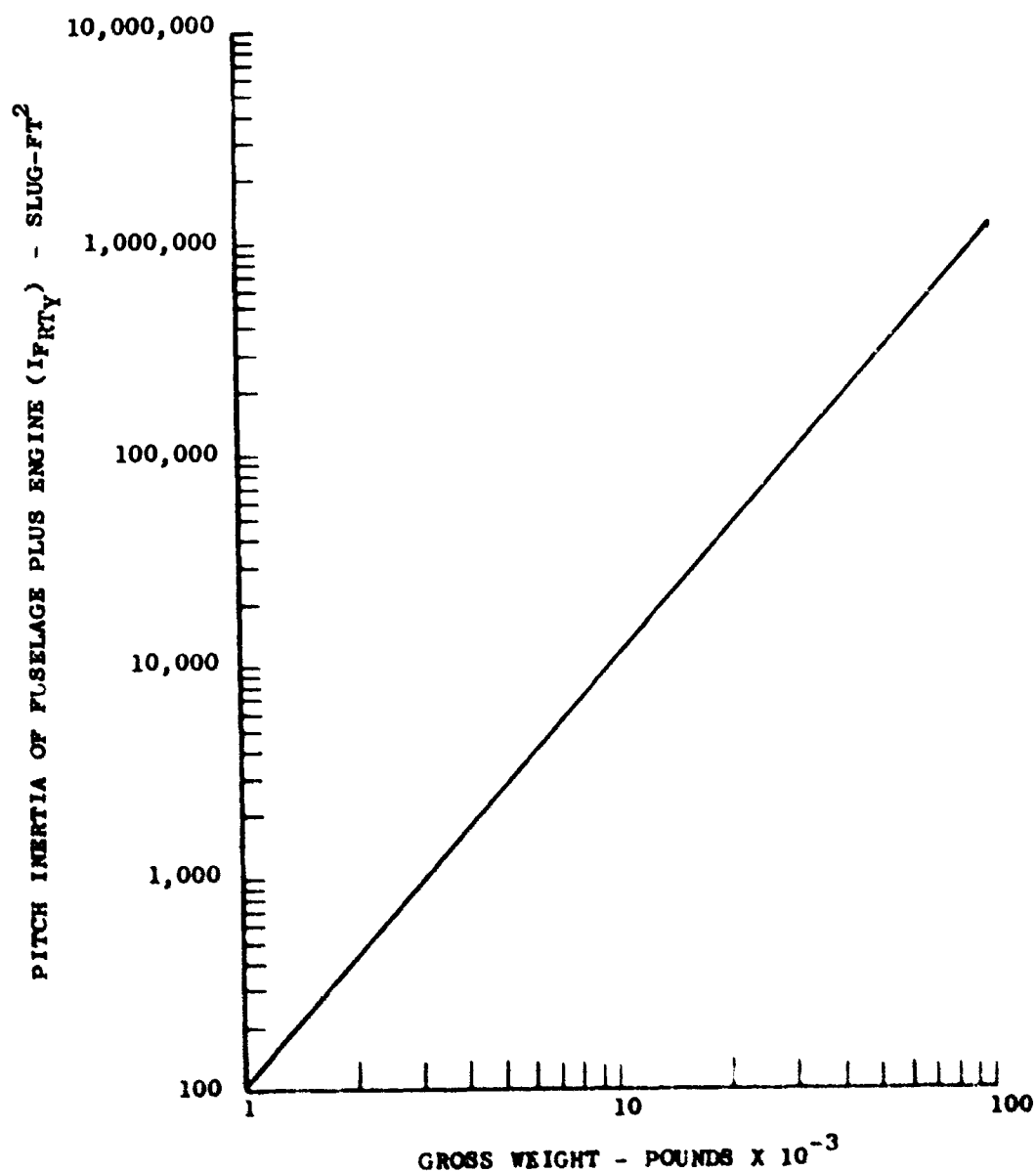


Figure 82. Pitch Inertia of Lower Body for Rotor Plus Transmission Configuration for a Range of Helicopter Gross Weights.

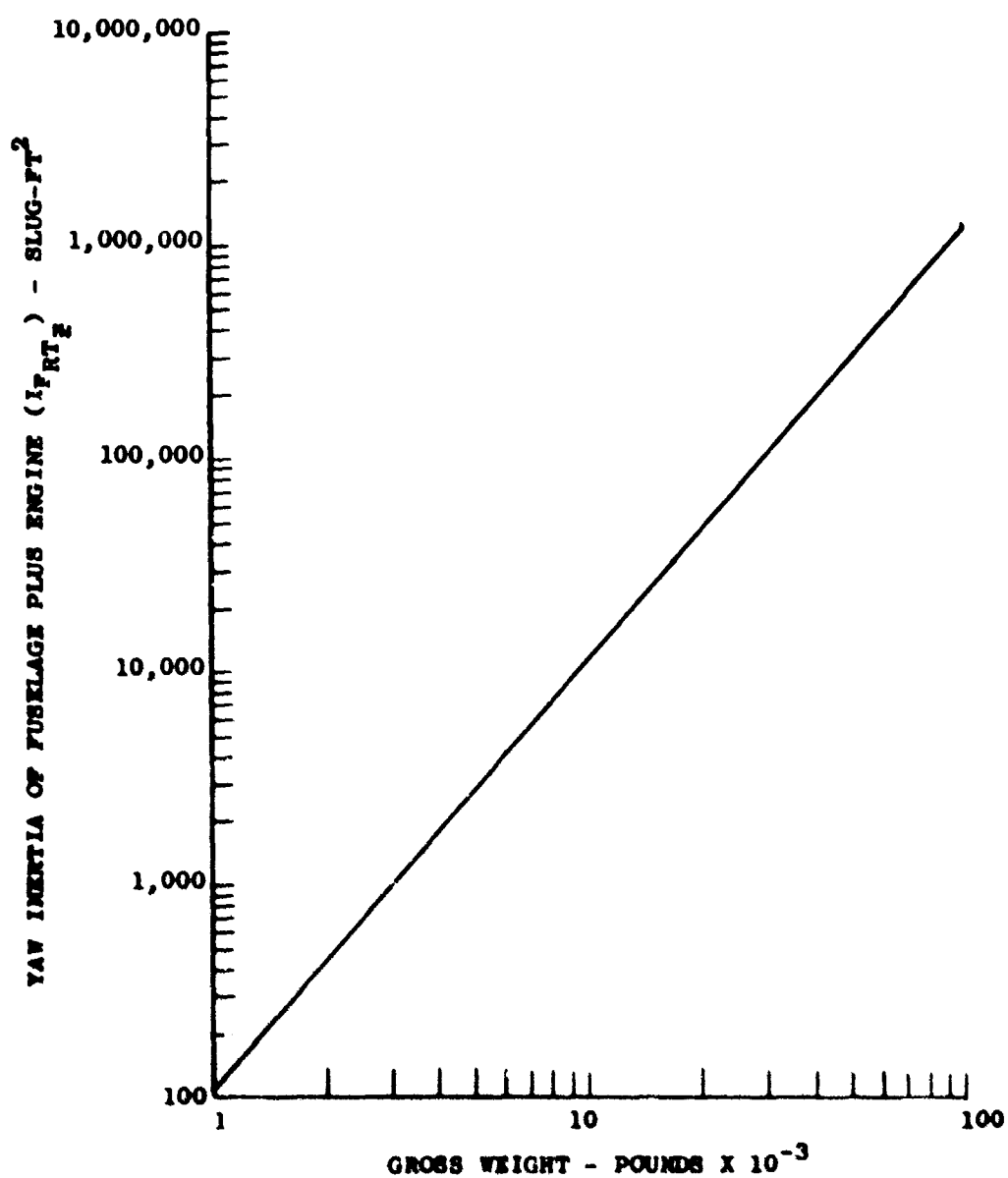


Figure 83. Yaw Inertia of Lower Body for Rotor Plus Transmission Configuration for a Range of Helicopter Gross Weights.

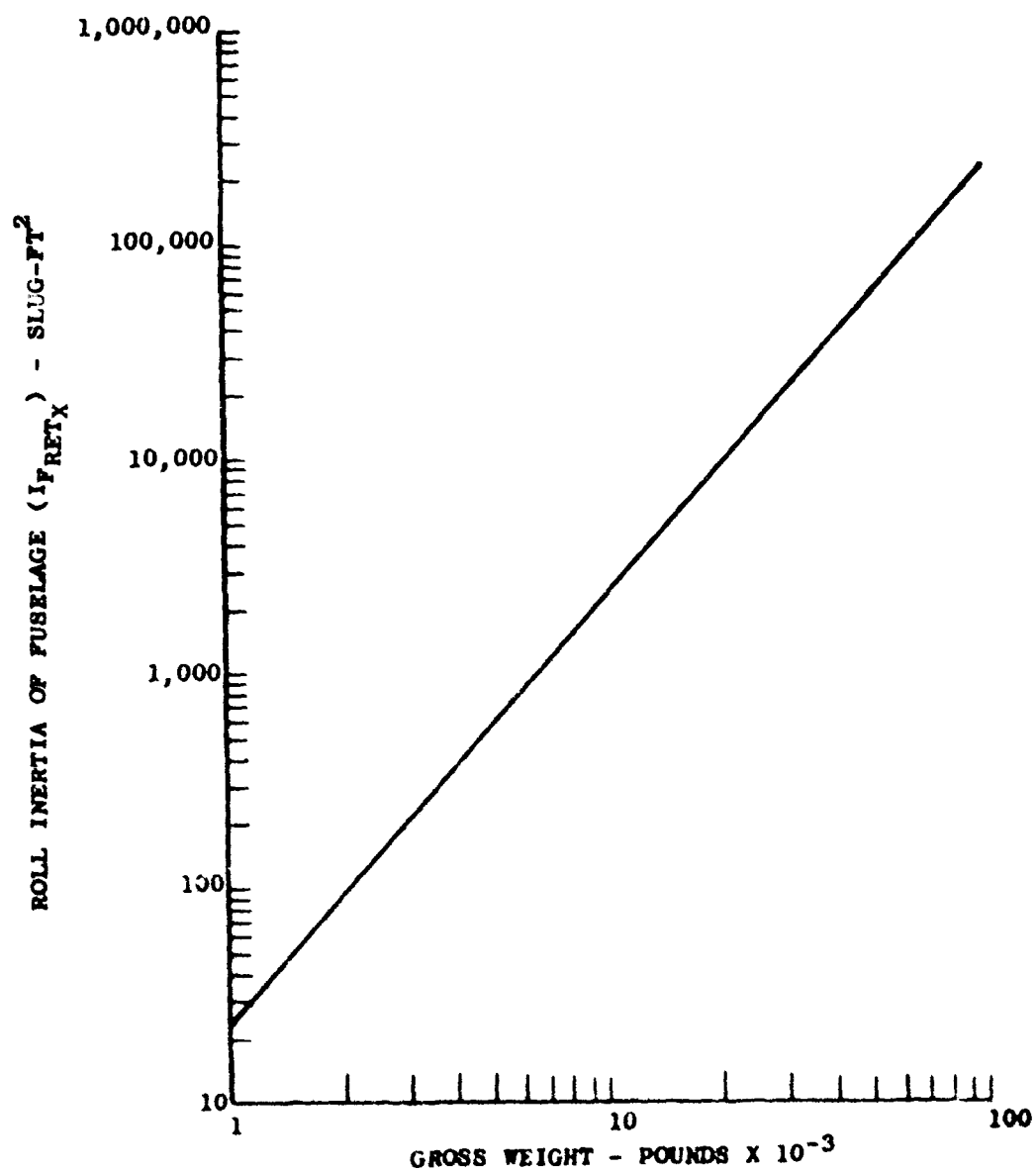


Figure 84. Roll Inertia of Lower Body for Rotor Plus Engine Plus Transmission Configuration for a Range of Helicopter Gross Weights.

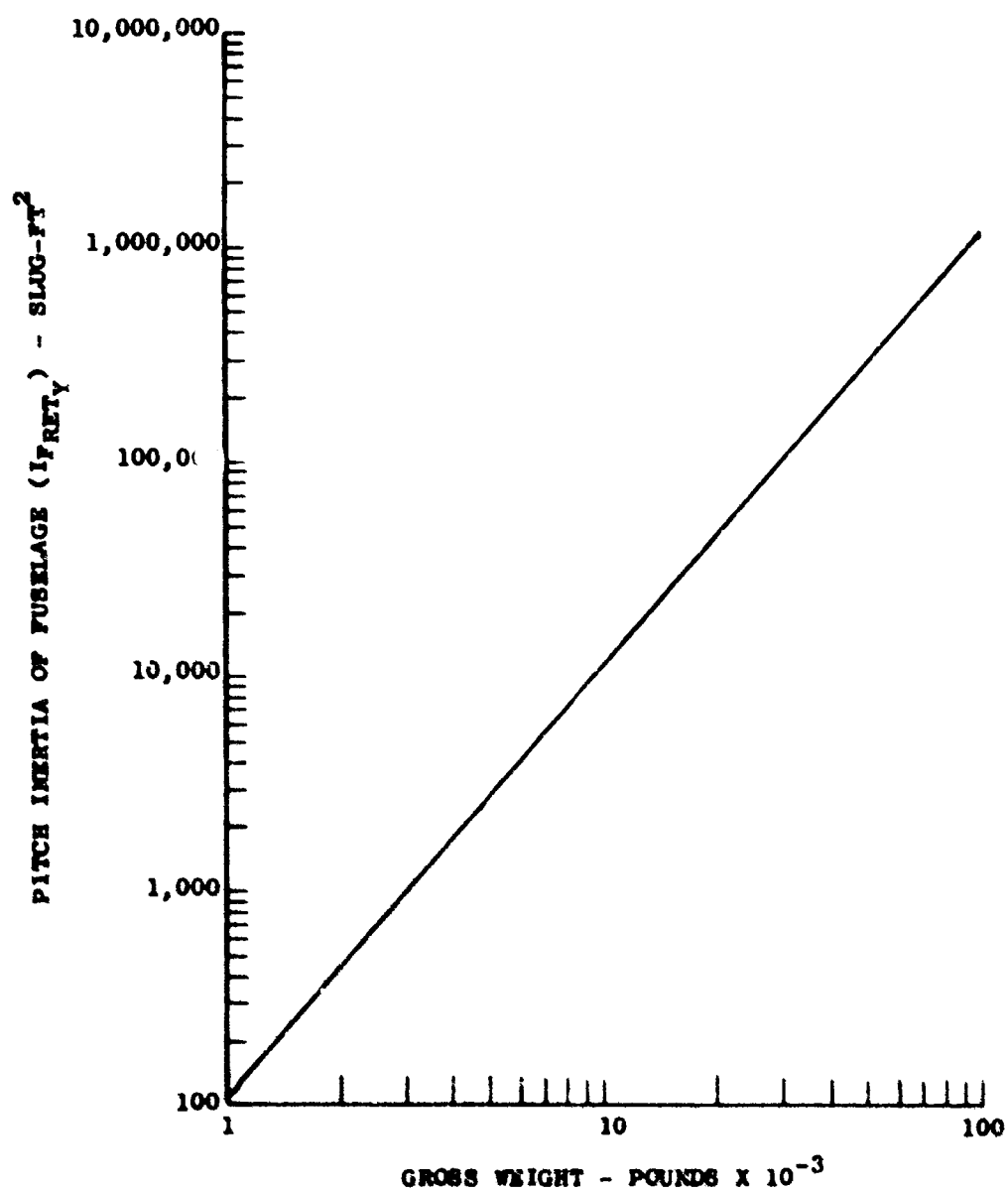


Figure 85. Pitch Inertia of Lower Body for Rotor Plus Engine Plus Transmission Configuration for a Range of Helicopter Gross Weights.

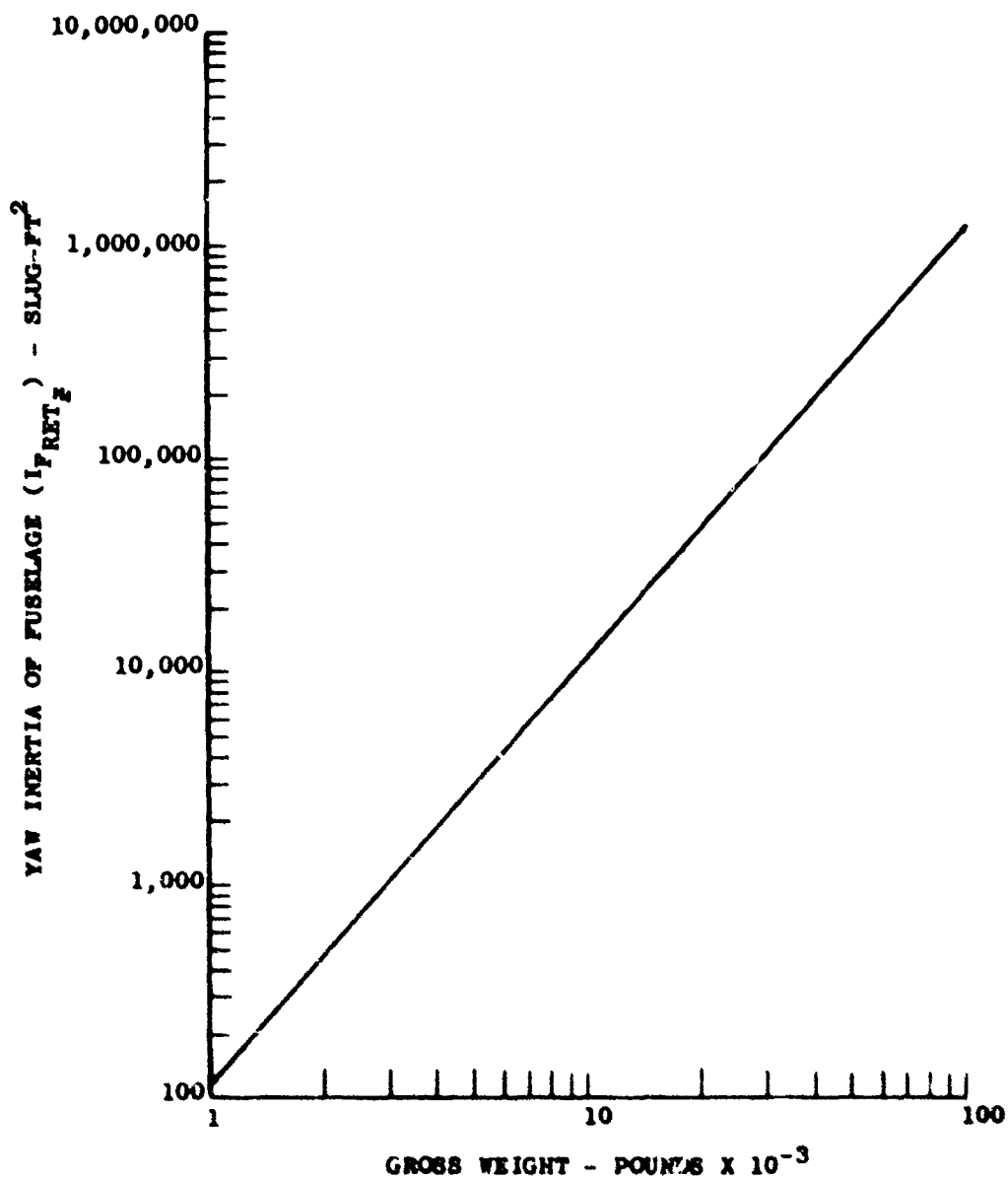


Figure 86. Yaw Inertia of Lower Body for Rotor Plus Engine Plus Transmission Configuration for a Range of Helicopter Gross Weights.

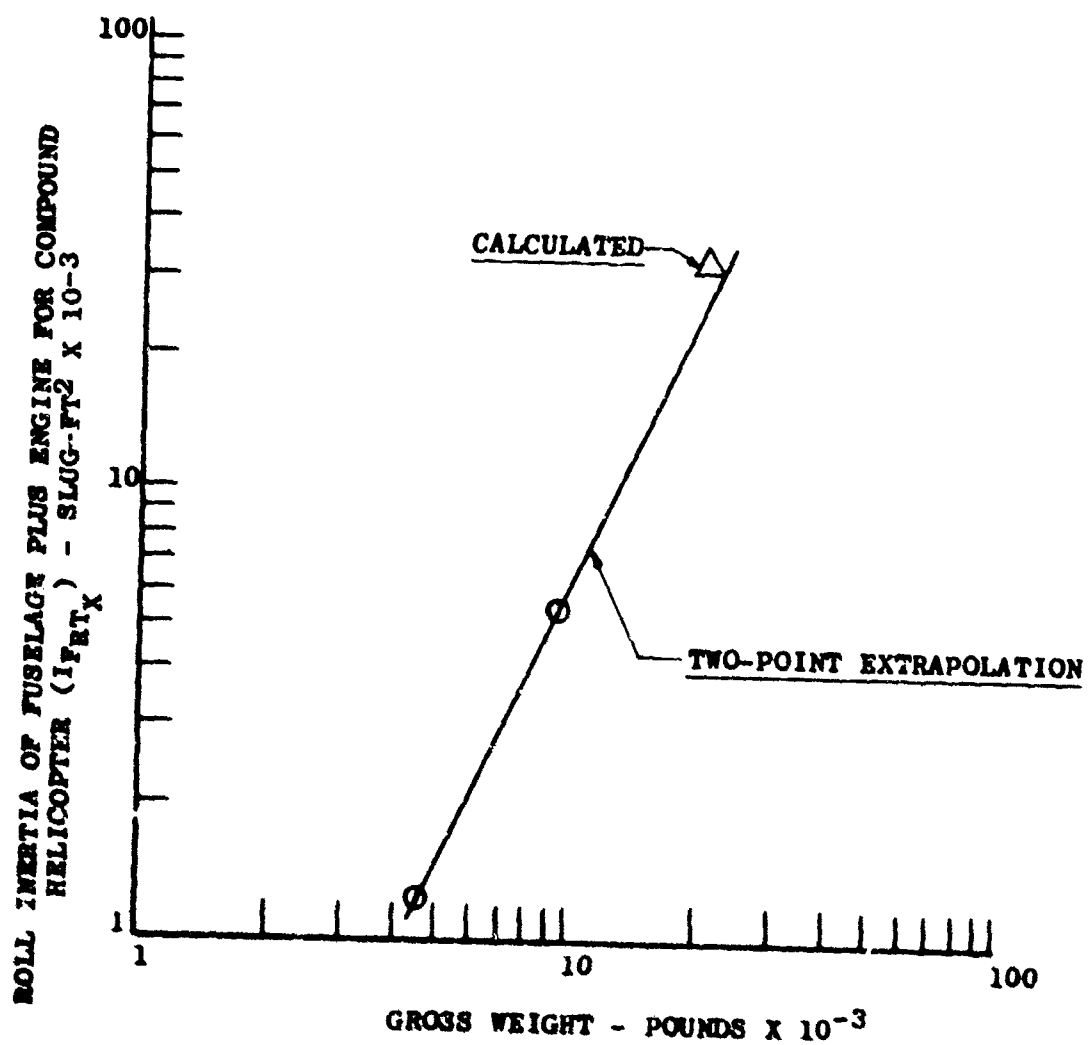


Figure 87. Roll Inertia of Lower Body for Rotor Plus Transmission Configuration for a Range of Compound Helicopter Gross Weights.

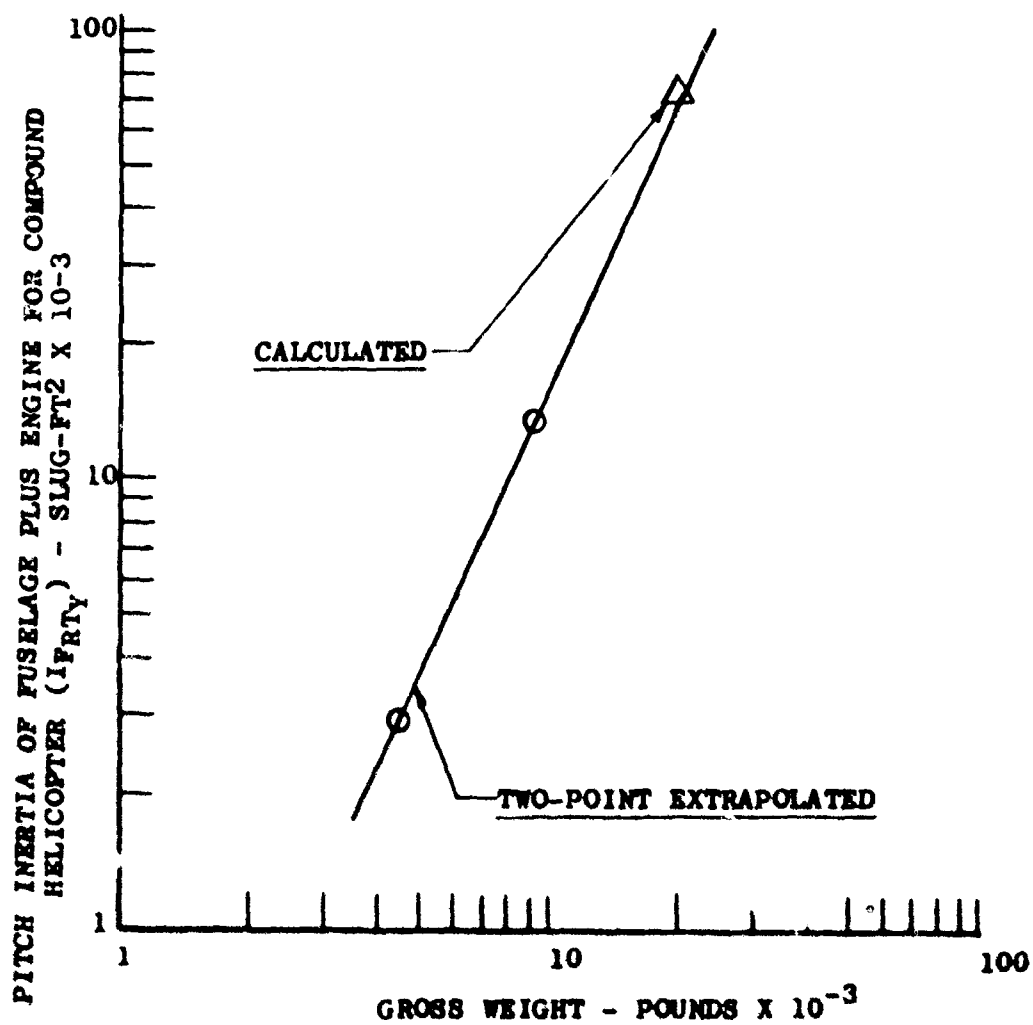


Figure 88. Pitch Inertia of Lower Body for Rotor Plus Engine Configuration for a Range of Compound Helicopter Gross Weights.

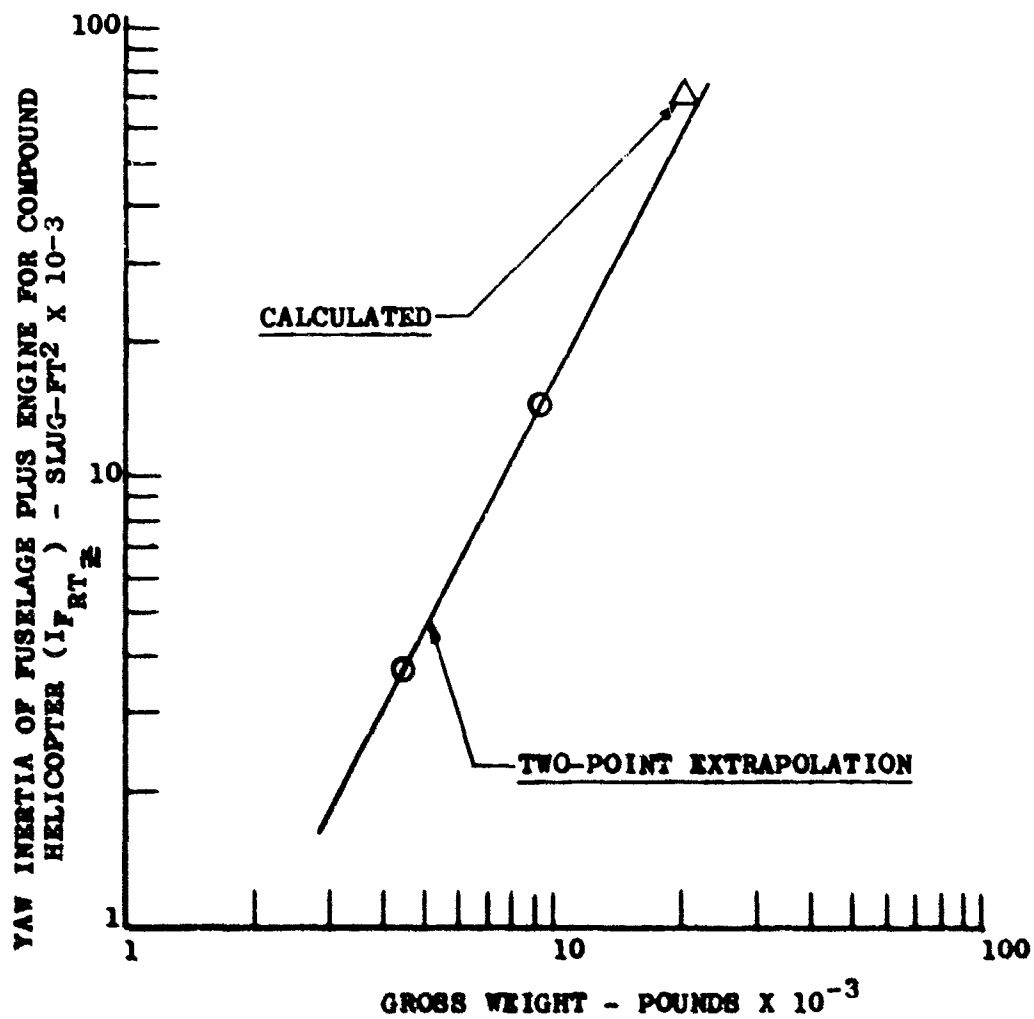


Figure 89 . Yaw Inertia of Lower Body for Rotor Plus Transmission Configuration for a Range of Compound Helicopter Gross Weights.

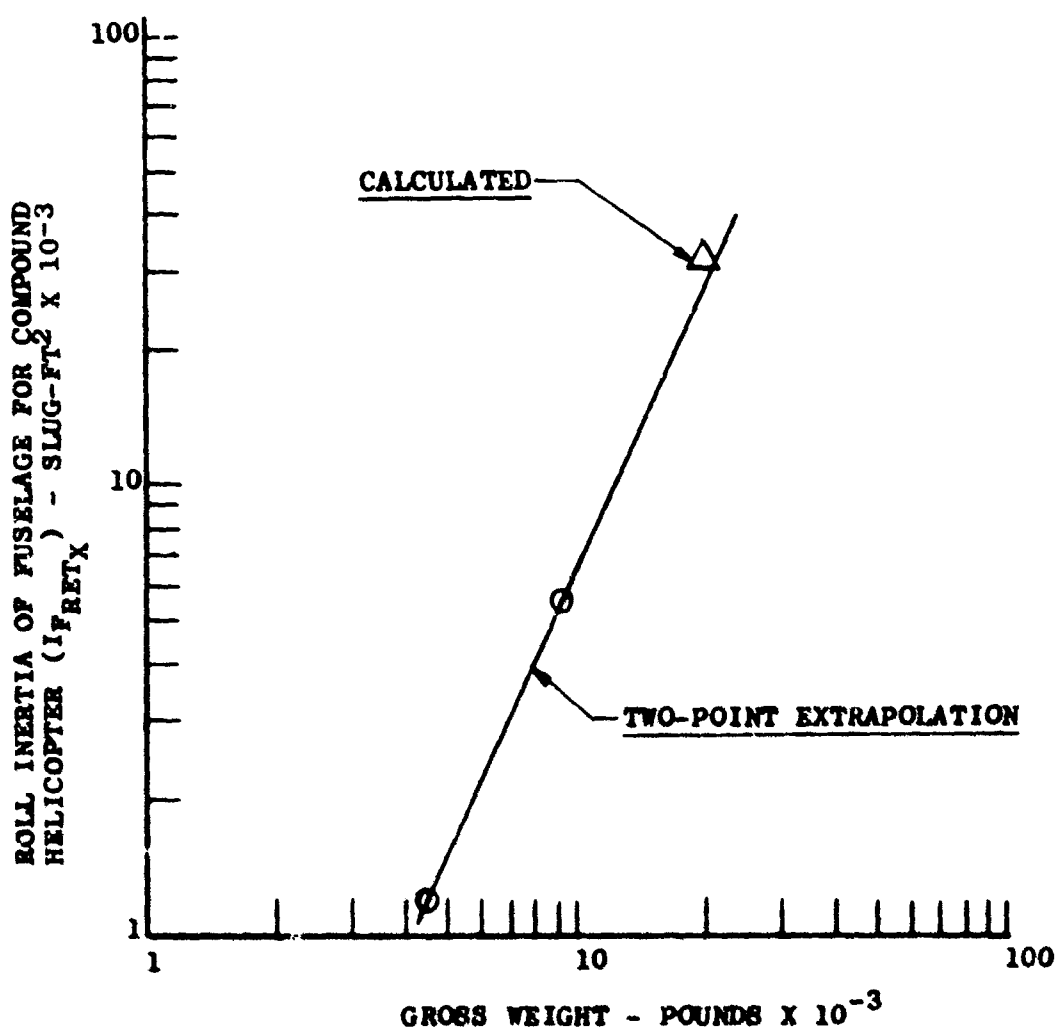


Figure 90. Roll Inertia of Lower Body for Rotor Plus Engine Plus Transmission Configuration for a Range of Compound Helicopter Gross Weights.

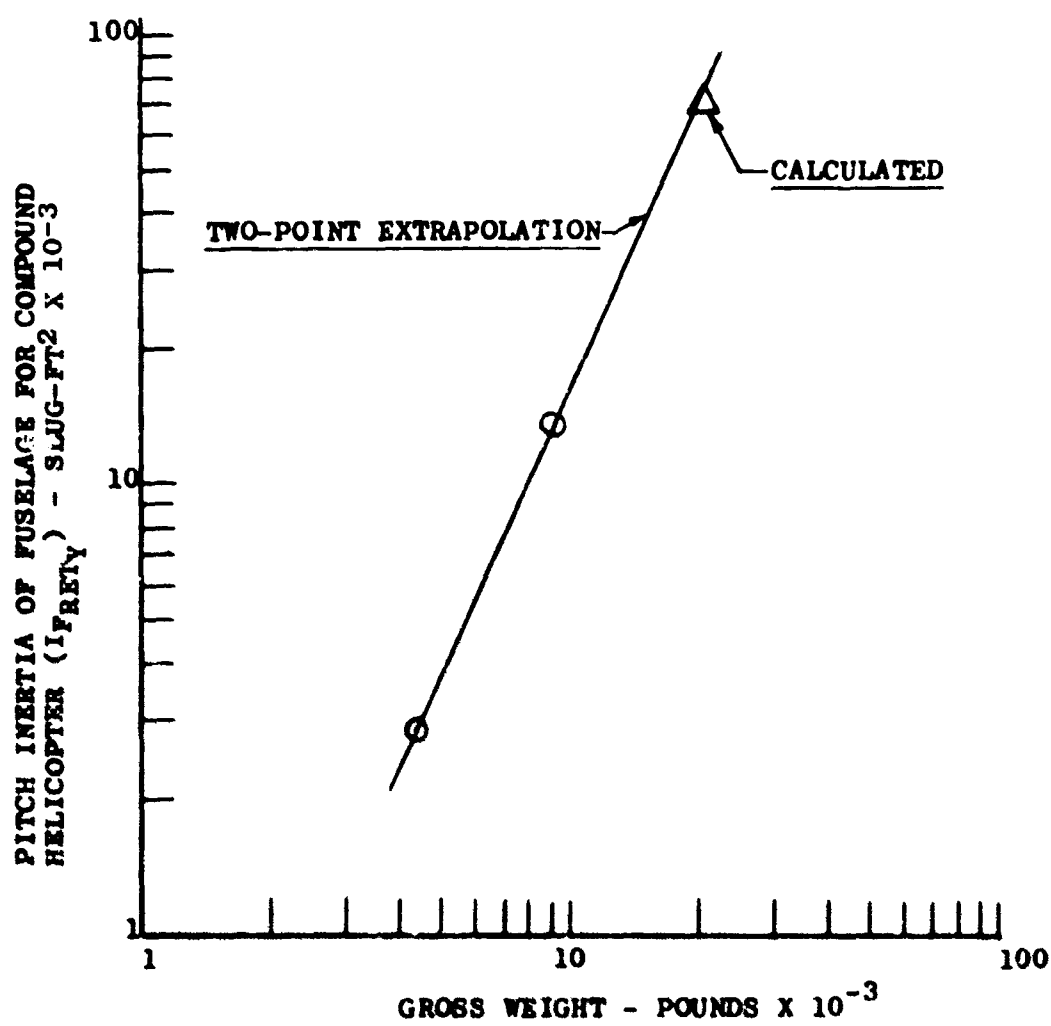


Figure 91. Pitch Inertia of Lower Body for Rotor Plus Engine Plus Transmission Configuration for a Range of Compound Helicopter Gross Weights.

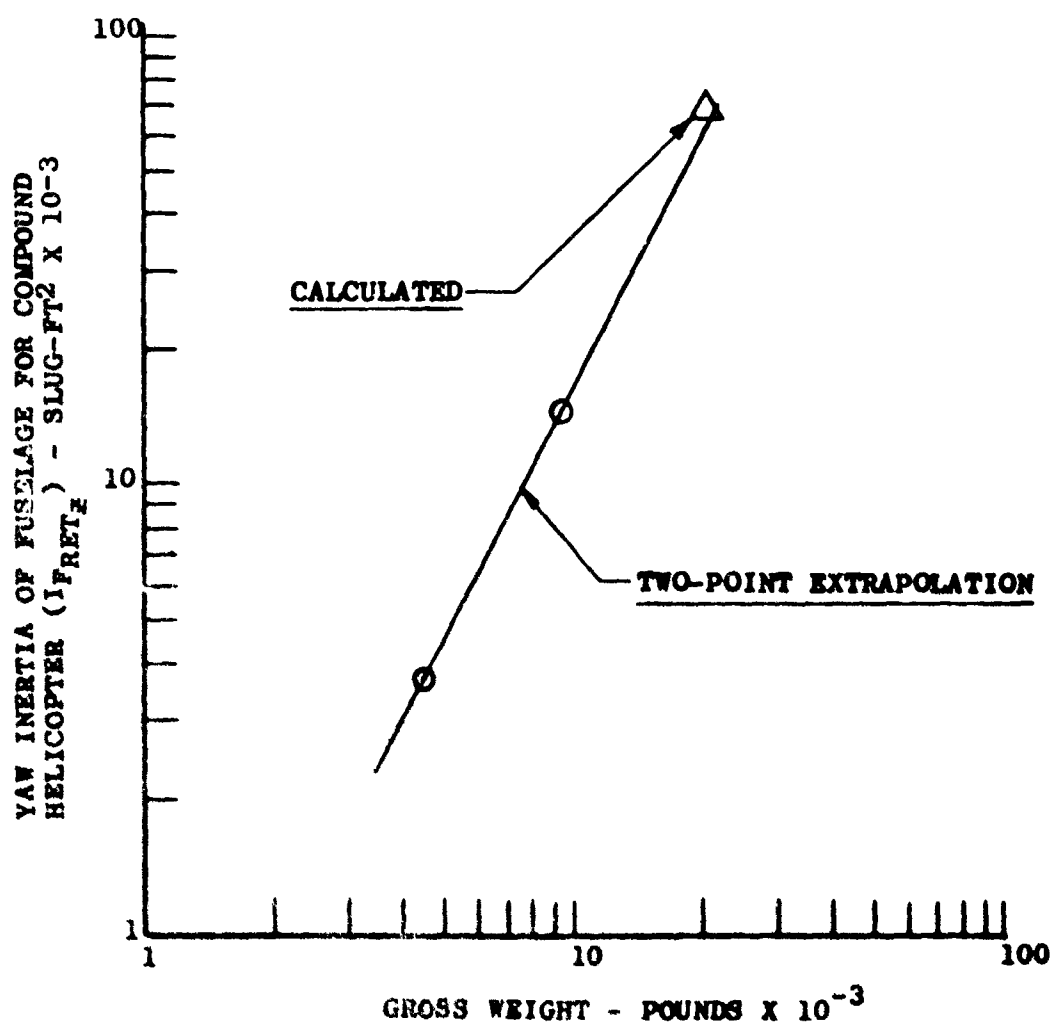


Figure 92. Yaw Inertia of Lower Body for Rotor Plus Engine Plus Transmission Configuration for a Range of Compound Helicopter Gross Weight.

EXCITATION CRITERIA

Excitation criteria were obtained from actual hub shears of flight hardware and of model studies in wind tunnels. These test data were normalized on the predominant N-harmonic. In all cases considered, be it model or flight test data, the effect of advance ratio was averaged, as was the total compilation of all data.

Data presented in Reference 5 are from scaled model rotors which are representative of aerodynamic and dynamic properties of full-scale hardware. These model rotors were configured in the 2-bladed teetering rotor and the 2-, 3-, and 4-bladed flapping rotors and were tested over a range of advance ratios. These data were measured in the fixed system and included the effects of blade bending, inertia shears, and airload shears. These results are included in Table XXVI.

Reference 6 presents model tests of a 3-bladed rotor for single-rotor and tandem-rotor configurations and variations of advance ratio. The single-rotor data were used and are included in Table XXVI.

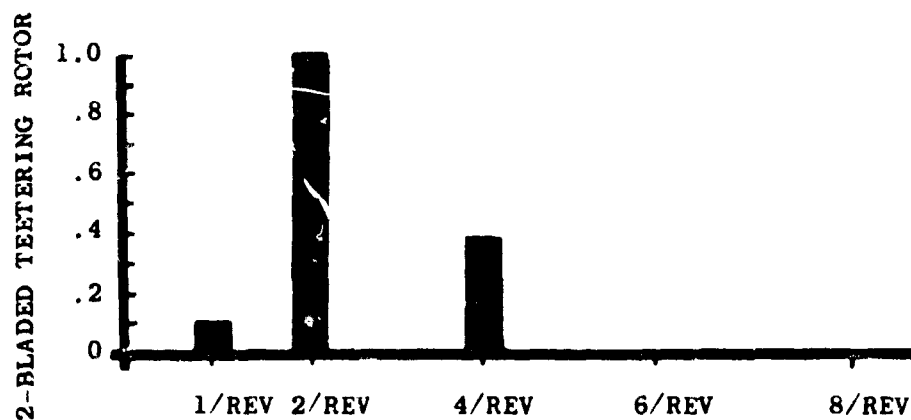
Reference 7 presents data which were presented in section aerodynamic loadings for 10 harmonics and for 7 radial blade stations. This airload information, blade geometry, blade mass distribution, and stiffness distribution were keypunched and introduced into Kaman's Blade Bending Program. Results obtained from the IBM 360-30 computer produced total hub shears in the fixed system which included the inertia shears, airload shears, and shears due to blade bending; therefore, this was a truer representation of hub shears than the airload shears themselves. The total hub shears thus obtained included conditions for trim level flight, out-of-ground effect, ranging in flight speed from hover to 122 knots; and for trim level flight, in-ground effect, over a speed range from 13 knots to 37 knots. For both conditions, in-ground effect and out-of-ground effect, the transition range of the helicopter speed spectrum was analyzed. These data were then included in Table XXVI.

A review of References 8 through 23 added no numerical data on hub shears. These references did, however, indicate that higher harmonics are either small in comparison to the principal excitation frequency (N/rev) or nonexistent.

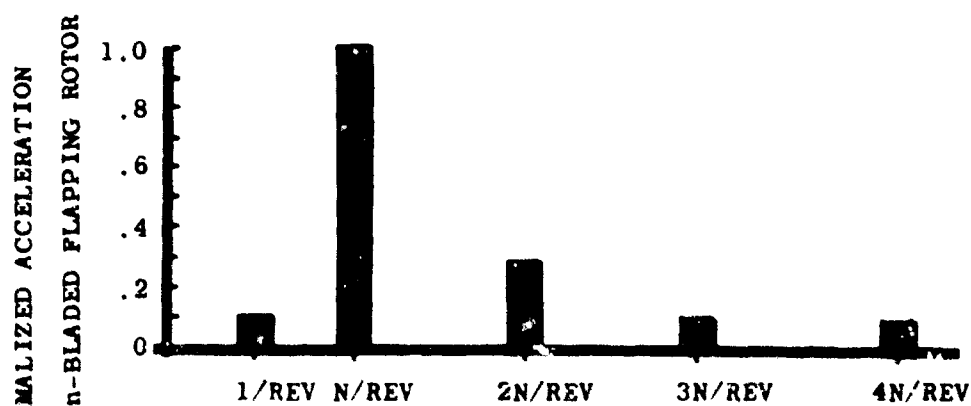
The one-per-rev vibration input at the hub resulting from blade track and/or unbalance can virtually be eliminated. This effect was considered, and in nondimensionalized form, a ratio of .10 was believed to be reasonable. This was plotted in Figure 93.

The averaged results for the teetering rotor in Table XXVI were plotted in Figure 93(a). Then, combining the results of Table XXVI for the 2-, 3-, and 4-bladed flapping rotor into the category of N-bladed flapping rotor (using the highest ratio), these criteria were plotted in Figure 93(b). In an effort to establish only one criterion that encompasses both the teetering and flapping rotor configurations, Figure 93(c) was drawn up. This figure takes the highest ratio of the teetering configuration ($2N/\text{rev} = .373$), uses all others of the N-bladed flapping rotor, and raises these ratios to the nearest tenth, thus establishing new and conservative excitation criteria.

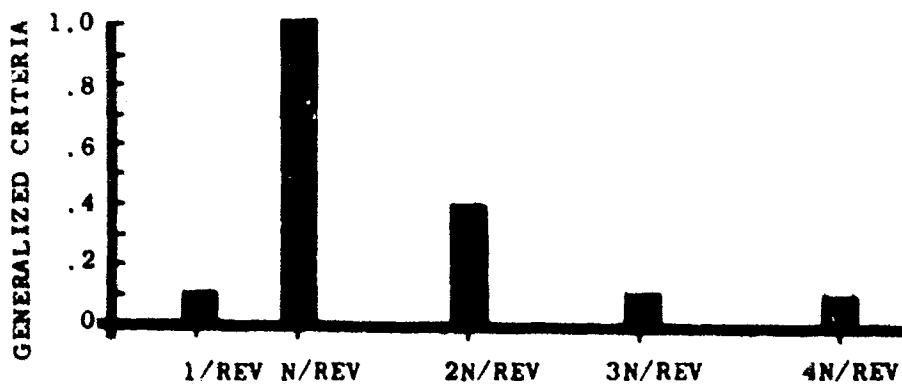
TABLE XXVI. EXCITATION CRITERIA NORMALIZED ON N-HARMONIC					
Rotor Conf	Ref	2N/Rev	3N/Rev	4N/Rev	
2-Bladed Twisting	1	.70	-	-	
	1	.22	-	-	
	1	.26	-	-	
	1	.31	-	-	
		.373	-	-	Avg
2-Bladed Flapping	1	.13	.15	.06	
	1	.35	.12	.13	
	1	.38	.04	.04	
	1	.23	.07	.08	
		.27	.095	.08	Avg
3-Bladed Flapping	1	.18	-	-	
	1	.09	-	-	
	1	.08	-	-	
	1	.09	-	-	
	2	.445	.082	-	
	2	.11	-	-	
	2	.113	.094	-	
	2	.075	.085	-	
	2	.164	.039	-	
	2	.51	.178	-	
		.1857	.0892	-	Avg
4-Bladed Flapping	3	.03	-	-	
	3	.14	-	-	
	3	.282	-	-	
	3	.349	-	-	
	3	.0887	-	-	
	3	.1498	-	-	
	3	.1612	-	-	
	3	.3891	-	-	
	3	.2709	-	-	
	3	.328	-	-	
	3	.5216	-	-	
	3	.1712	-	-	
	3	.1804	-	-	
	3	.1050	-	-	
	3	.0841	-	-	
	3	.1041	-	-	
	3	.1933	-	-	
	3	.0658	-	-	
	3	.2173	-	-	
	3	.2921	-	-	
	3	.3704	-	-	
	3	.1479	-	-	
	3	.4211	-	-	
	3	.8040	-	-	
	1	.03	-	-	
	1	.14	-	-	
		.232	-	-	Avg



(a) FREQUENCY



(b) FREQUENCY



(c) FREQUENCY

Figure 93. Normalized Excitation Criteria.

Unclassified

Security Classification

DOCUMENT CONTROL DATA - R & D		
(Security classification of title, body of abstract and indexing annotation must be entered when the overall report is classified)		
1. ORIGINATING ACTIVITY (Corporate author) Kaman Aircraft Division of Kaman Corporation Bloomfield, Connecticut		2a. REPORT SECURITY CLASSIFICATION Unclassified
		2b. GROUP
3. REPORT TITLE PASSIVE HELICOPTER ROTOR ISOLATION USING THE KAMAN DYNAMIC ANTIRESONANT VIBRATION ISOLATOR (DAVI)		
4. DESCRIPTIVE NOTES (Type of report and inclusive dates) Final Report		
5. AUTHOR(S) (First name, middle initial, last name) Erich P. Schuett		
6. REPORT DATE December 1968	7a. TOTAL NO. OF PAGES 176	7b. NO. OF REFS 24
8a. CONTRACT OR GRANT NO. DA 44-177-AMC-420(T)	9a. ORIGINATOR'S REPORT NUMBER(S) USAAVLABS Technical Report 68-16	
8b. PROJECT NO. Task 1F125901A13903	9b. OTHER REPORT NO(S) (Any other numbers that may be assigned this report) Kaman Aircraft Report R-710	
10. DISTRIBUTION STATEMENT This document has been approved for public release and sale; its distribution is unlimited.		
11. SUPPLEMENTARY NOTES	12. SPONSORING MILITARY ACTIVITY US Army Aviation Materiel Laboratories Fort Eustis, Virginia	
13. ABSTRACT This report contains the analysis and results of a study to determine the feasibility of rotor isolation employing the Dynamic Antiresonant Vibration Isolator (DAVI). The theoretical analysis was conducted employing a two-dimensional DAVI for lateral and vertical isolation with conventional isolation in the longitudinal direction. Steady-state and transient inputs were analyzed. The steady-state analysis includes all six degrees of freedom of the upper body and of the lower isolated body of the helicopter. Statistical data and excitation criteria were established to study the effects and determine the feasibility of rotor isolation for a range of statistical aircraft ranging from 2000 pounds to 100,000 pounds. Also discussed are the effects of rotor isolation on control motions, crash loads, mechanical instability, and system reliability. Results of this feasibility study show that rotor isolation employing the DAVI is feasible. Isolation is feasible at the predominant frequency (N/rev) and all its multiples up to 4N/rev. Low static deflection at a minimum weight penalty are some of the features of the DAVI system.		

DD FORM 1473 1 NOV 68 1473

Unclassified

Security Classification

Unclassified

Security Classification

14. KEY WORDS	LINK A		LINK B		LINK C	
	ROLE	WT	ROLE	WT	ROLE	WT
Rotor Isolation Helicopter Isolation Isolation Vibration Isolation Antiresonant Isolation						

Unclassified

Security Classification

11195-01